**DOC.20080211.0001**

QA: QA

ANL-EBS-NU-000010 REV 00

February 2008

# CSNF Loading Curve Sensitivity Analysis

Prepared for:
U.S. Department of Energy
Office of Civilian Radioactive Waste Management
Office of Repository Development
1551 Hillshire Drive
Las Vegas, Nevada 89134-6321

Prepared by:
Sandia National Laboratories
OCRWM Lead Laboratory for Repository Systems
1180 Town Center Drive
Las Vegas, Nevada 89144

Under Contract Number:
DE-AC04-94AL85000

QA: QA

# CSNF Loading Curve Sensitivity Analysis

# ANL-EBS-NU-000010 REV 00

# February 2008

YMP

# Scientific Analysis/Calculation Signature Page/Change History

1. Total Pages: 176

*Complete only applicable items.*

2. Document Title

CSNF Loading Curve Sensitivity Analysis

3. DI (Including Revision No. and Addendum No.)

ANL-EBS-NU-000010 REV 00

| | Printed Name | Signature | Date |
|---|---|---|---|
| 4. Originator | Charles Henkel | Charles S. Henkel | Feb 7, 2008 |
| 5. Checker | Donald E. Mueller | Donald E. Mueller | Feb. 8, 2008 |
| 6. QCS/Lead Lab QA Reviewer | Charles Beach | Charles Beach | 2-8-08 |
| 7. Responsible Manager/Lead | John Wagner | J. C. Wagner | 2/8/08 |
| 8. Responsible Manager | Cliff Howard | Cliff Howard | 2/8/08 |

9. Remarks

**Change History**

| 10. Revision No. and Addendum No. | 11. Description of Change |
|---|---|
| 00 | Initial Issue |
| | |
| | |
| | |
| | |
| | |

INTENTIONALLY LEFT BLANK

# CONTENTS

**CONTENTS (Continued)**

**Page**

## FIGURES

**Page**

## FIGURES (Continued)

**Page**

# TABLES

## TABLES (Continued)

**Page**

## TABLES (Continued)

**Page**

INTENTIONALLY LEFT BLANK

## ACRONYMS

| | |
|---|---|
| ASTM | American Society of Testing and Materials |
| BSS | borated stainless steel |
| BWR | boiling water reactor |
| CSNF | commercial spent nuclear fuel |
| DPC | dual-purpose canister |
| DTN | data tracking number |
| EALF | energy corresponding to the average neutron lethargy causing fission |
| FBT | fuel basket tube |
| FEPs | features, events, and processes |
| IV | inner vessel |
| MCNP | Monte Carlo N-Particle |
| NRC | U.S. Nuclear Regulatory Commission |
| OCB | outer corrosion barrier |
| PWR | pressurized water reactor |
| QARD | *Quality Assurance Requirements and Description* |
| SNF | spent nuclear fuel |
| SNL | Sandia National Laboratories |
| TAD | transportation, aging, and disposal (canister) |

INTENTIONALLY LEFT BLANK

# 1. PURPOSE

The purpose of this scientific analysis report, *CSNF Loading Curve Sensitivity Analysis*, is to establish the required minimum burnup as a function of initial enrichment for both pressurized water reactor (PWR) and boiling water reactor (BWR) commercial spent nuclear fuel (CSNF) that would allow permanent disposal of these waste forms in the geologic repository at Yucca Mountain. The relationship between the required minimum burnup and fuel assembly initial enrichment forms a *loading curve*. Loading curves, which are functions of burnup and enrichment, are the loci of values delineating the region of acceptable burnup/enrichment combinations for postclosure criticality control. In order to accommodate multiple canister criticality control design configurations, focus is placed on the transportation, aging, and disposal (TAD) canister specification requirements (DOE 2007 [DIRS 181403]) for developing a robust loading curve that is expected to bound all of the potential design variants over the 10,000-year regulatory period. In applying this methodology, the loading curve is generated once and the assigned burnup values of all assemblies considered for loading into the TAD canister are compared directly against this loading curve. Assemblies having burnup values in the unacceptable range must be loaded into waste packages or canisters with additional reactivity control mechanisms (e.g., disposal control rod assemblies). The loading curves generated in this report are intended to enable repository postclosure objectives to be met in accordance with 10 CFR Part 63 [DIRS 180319] and do not necessarily apply to transportation of CSNF.

The scope of this analysis considers the TAD specifications in the development of a set of scenarios covering a wide array of potential configurations that can occur over time in the repository. The configurations developed within this analysis are representative of the degradation sequences that have been identified in *Disposal Criticality Analysis Methodology Topical Report* (YMP 2003 [DIRS 165505], Section 3.3). In the development of the loading curves, configurations that result in the highest $k_{eff}$ are used to set an upper bounding limit that encompasses all other configurations. Therefore, the selection of a bounding configuration is based on sensitivity studies. Potential configurations that could occur in the repository over the 10,000-year regulatory period are evaluated to determine which results in the highest $k_{eff}$ values. The configurations demonstrate the effects on system reactivity as the waste package internal components degrade and the geometry changes. The loading curve is established such that the reactivity of a waste package fully loaded with assemblies selected from the curve will be less than a certain critical limit under postulated postclosure conditions. The critical limit includes margins representing code bias and uncertainty.

The intended use of these results will be in establishing CSNF TAD loading specifications (loading curves), and to assess the impacts on the loading curves for varying the different parameters that effect CSNF reactivity.

The scope of this analysis is limited to in-package criticality evaluations for the CSNF waste forms – PWR and BWR fuel assemblies.

The development of this report is consistent with Work Package S31018 specified in *Technical Work Plan for: Postclosure Criticality* (SNL 2007 [DIRS 178869], Table 1).

INTENTIONALLY LEFT BLANK

# 2. QUALITY ASSURANCE

Development of this report has been determined to be subject to the Yucca Mountain Project quality assurance requirements as described in *Technical Work Plan for: Postclosure Criticality* (SNL 2007 [DIRS 178869], Section 8.1). Approved quality assurance procedures identified in the technical work plan (SNL 2007 [DIRS 178869], Section 4.1) have been used to conduct and document the activities described in this report. The technical work plan also identifies the methods used to control the electronic management of data (SNL 2007 [DIRS 178869], Section 8.4) during the calculation and documentation activities.

This report is prepared in accordance with SCI-PRO-005, *Scientific Analyses and Calculations*.

INTENTIONALLY LEFT BLANK

# 3. USE OF SOFTWARE

## 3.1 MONTE CARLO N-PARTICLE TRANSPORT CODE

The baselined Monte Carlo N-Particle (MCNP) transport code (MCNP5 V. 1.40. STN: 11199-1.40-00 [DIRS 180515]) is used to calculate the neutron multiplication factor for the various evaluations. The software specifications are as follows:

- Software Title: MCNP5
- Version/Revision Number: version 1.40
- Status/Operating System: Qualified/Windows XP
- Software Tracking Number: 11199-1.40-00
- Computer Type: Dell Precision 690 Personal Computer; Barcode: S885588, S887083, S885597.

The input and output files for the MCNP calculations are located in Output DTN: MO0711LOADCURV.000 and described in Section 6, Appendix A, and Appendix B, so that an independent repetition of the software use may be performed. The MCNP software used is (1) appropriate for the application of multiplication factor calculations, (2) used only within the range of validation as documented throughout *Software Validation Report for: MCNP5 v1.40* (DOE 2007 [DIRS 180516]), and (3) obtained from Software Configuration Management in accordance with appropriate procedures.

*Rationale for Selection*: The MCNP5 V. 1.40 program employs the Monte Carlo method to perform radiation transport calculations. The Monte Carlo method stochastically simulates and records the behavior of individual particles within a system. This approach applies random selections of particle transport characteristics and interactions based on probabilities, cross sections, and system geometry. The behavior of the simulated particles is extrapolated to describe the average behavior of all the particles within the system. The primary reasons for using this code are the following: (1) it is accepted by the U.S. Nuclear Regulatory Commission (NRC) for criticality safety applications; (2) it allows explicit geometrical modeling of material configurations; and (3) it uses continuous-energy cross sections.

## 3.2 EXCEL

- Software Title: Excel
- Version/Revision number: Microsoft® Excel 2003 Service Pack 2
- Computer Environment: Software is installed on a personal computer, Sandia Property tag number S885588, running Microsoft Windows XP Professional Version 2002 Service Pack 2.

Microsoft Office Excel 2003 Service Pack 2 is used in calculations and analyses to manipulate the inputs using standard mathematical expressions and operations. It is also used to generate input files and tabulate and chart results. The input file generation process is automated using Excel macros documented in Appendix A. The user-defined macros, formulas, inputs, and results are documented in sufficient detail to allow an independent repetition of the computations. Microsoft Office Excel 2003 Service Pack 2 is an exempt software product in accordance with IM-PRO-003, *Software Management*, Section 2.0.

The spreadsheet files for the Excel calculations are documented in Output DTN: MO0711LOADCURV.000.

# 4. INPUTS

## 4.1 DIRECT INPUTS

The following data are used as direct inputs to the analyses described in Section 6. Table 4-1 lists qualified data by DTN used as direct inputs, and Table 4-2 lists other direct inputs obtained from other sources with justification for use as direct inputs.

Table 4-1. Data Used as Input

| Parameter | Value | Source |
|---|---|---|
| Molal volume for metaschoepite<br><br>Stoichiometry | 66.080 $cm^3$/mol<br><br>$UO_3 \cdot 2H_2O$ | DTN: SN0612T0502404.014 [DIRS 178850], file: *sn0612T0502404_014.zip*, "data0.ymp.r5" |
| J13 Well Water Composition | See Table 4-13 | DTN: MO006J13WTRCM.000 [DIRS 151029] |
| Lower bound tolerance limits for PWR and BWR Waste Packages | See Table 4-15 | DTN: MO0711RABDPCSF.000 [DIRS 184166], file: *ORNL_TM_2007_127_RoABias_Final_10_16_07.pdf*, Table 20 |
| CSNF alteration phase-porosity estimates | 5% to 30% porosity | DTN: LL010902212241.026 [DIRS 163089] |

Table 4-2. Other Direct Input

| Parameter | Value | Source | Justification |
|---|---|---|---|
| Waste package and TAD canister specifications | See Table 4-3. | SNL 2007 [DIRS 179394], Section 4 and Appendix A | Approved technical product developed in accordance with QARD requirements |
| TAD internal basket specifications | See Table 4-4 | Holtec International 2002 [DIRS 168494], Figures 6.3.2 and 6.3.3 | Approved NRC design for spent nuclear fuel storage |
| BWR fuel assembly specifications | See Table 4-6 | Larsen et al. 1976 [DIRS 146576], pp. A-1 to A-3, Figure 10 | Considered established fact data because they are obtained from a report from the Electric Power Research Institute that is accepted by the scientific and engineering community |
| PWR fuel assembly specifications | See Table 4-5 and Figure 4-1 | BSC 2006 [DIRS 177193], Figure 1, Table 28, and Table 71 | Approved technical product developed in accordance with *Quality Assurance Requirements and Description* (QARD) |
| Tuff composition and density | See Table 4-7; dry density 2.241 g/cm$^3$ wet density 2.359 g/cm$^3$ | BSC 2006 [DIRS 177193], Table 1 | Approved technical product developed in accordance with QARD requirements |
| SB-575 N06022 composition and density | See Table 4-8; density 8.69 g/cm$^3$ | BSC 2006 [DIRS 177193], Table 4 | Approved technical product developed in accordance with QARD requirements |
| SA–240 S31603 composition and density | See Table 4-9; density 7.98 g/cm$^3$ | BSC 2006 [DIRS 177193], Table 6 | Approved technical product developed in accordance with QARD requirements |
| Zircaloy-4 composition and density | See Table 4-10; density 6.56 g/cm$^3$ | BSC 2006 [DIRS 177193], Table 10 | Approved technical product developed in accordance with QARD requirements |
| Zircaloy-2 composition and density | See Table 4-11; density 6.55 g/cm$^3$ | BSC 2006 [DIRS 177193], Table 11 | Approved technical product developed in accordance with QARD requirements |
| SA-240 S30464 composition | See Table 4-12 | ASTM A 887-89 [DIRS 178058], Table 1 | Considered established fact data because this is a consensus standard from ASTM |
| SA-240 S30464 density | 7.8 g/cm$^3$ (0.282 lb/in$^3$) | SNL 2007 [DIRS 179394], Appendix A | Approved technical product developed in accordance with QARD requirements |
| PWR spent fuel isotopic compositions | See Output DTN: MO0711LOADCURV.000 file: *LoadingCurve.xls*, worksheet: "FuelIsotopics" density 10.741 g/cm$^3$ | BSC 2003 [DIRS 166142], p. 19 and Section 6 | Approved technical product developed in accordance with QARD requirements |
| BWR spent fuel isotopic compositions | See Output DTN: MO0711LOADCURV.000 file: *LoadingCurve.xls*, worksheet: "FuelIsotopics" density 10.741 g/cm$^3$ | Wimmer 2004 [DIRS 169319], Section 6, p. 18 Massie 2004 [DIRS 173618] | Qualified supplier approved technical product developed in accordance with QARD requirements |

Table 4-2. Other Direct Input (Continued)

| Parameter | Value | Source | Justification |
|---|---|---|---|
| PWR Axial Profile Data | See Table 4-14 | BSC 2003 [DIRS 166138], Table 32 | Approved technical product developed in accordance with QARD requirements |
| CSNF element degradation minerals | $NpO_2$, $PuO_2(OH)_2{:}H_2O$, $UO_3(H_2O)_2$, $RuO_2$, $AmO_2$, $Gd_2(CO_3)_3$, $Sm_2(CO_3)_3$, $Eu_2(CO_3)_3$, $Nd_2(CO_3)_3$ | SNL 2007 [DIRS 181165], Section 6.3.16 | Approved technical product developed in accordance with QARD requirements |
| Lanthanide fraction in degraded CSNF waste form | 85% | SNL 2007 [DIRS 181165], Section 8.1.1. | Approved technical product developed in accordance with QARD requirements |
| Principal Isotopes for CSNF Burnup Credit | See Table 4-16 | YMP 2003 [DIRS 165505], Table 3-1 | Approved technical product developed in accordance with QARD requirements |
| Isotopic Bias and Uncertainty | $-0.0249\ \Delta k$ | BSC 2004 [DIRS 168554], Table 10 | Approved technical product developed in accordance with QARD requirements |
| PWR Waste Stream Arrival Forecast | See Output DTN: MO0711LOADCURV.000 file: *LoadingCurve.xls*, worksheet: "Inventory" | CRWMS M&O 2000 [DIRS 138239], Attachment III | Approved technical product developed in accordance with QARD requirements |
| MCNP Nuclide Identifiers and Atomic Mass Values | See Table 4-17 and Output DTN: MO0711LOADCURV.000 file: *LoadingCurve.xls*, worksheet: "Materials" | MCNP5 V. 1.40. STN: 11199 1.40-00 [DIRS 180515], file: "xsdir" | Considered established fact data because these identifiers are a component of the approved baseline software. |
| Natural abundance of $^{10}B$ in boron | Natural variation of 19.1% to 20.3%. | Parrington, et al. 1996 [DIRS 103896], p. 7 | Considered established fact data because this is regarded as a handbook that is the primary source for the nuclear industry nuclide information |
| SA-240 S30464 corrosion rate | 0.0678 µm/yr | SNL 2007 [DIRS 181165], Table 6.3-6 | Approved technical product developed in accordance with QARD requirements |
| Theoretical density of $UO_2$ | 10.96 $g/cm^3$ | Todreas and Kazimi 1990 [DIRS 107735], p. 296 | Considered established fact data because this is regarded as a handbook that is the primary source for the nuclear industry nuclide information |
| Bounding uncertainty in assembly burnup values | 4.2% | Massie 2004 [DIRS 170651], Tables 10A, Table 10B, Table 10C | Approved technical product developed in accordance with QARD requirements |
| Recommended minimum absorber plate thickness | 6 mm | BSC 2006 [DIRS 180664], p. 1 | Approved technical product developed in accordance with QARD requirements |

NOTE: BSC 2006 [DIRS 177193] is the recommended source for waste form dimensions and materials as identified in SNL 2007 [DIRS 179394], Table 4-1, Parameter 04-07.

Table 4-3. Waste Package and TAD Canister Specifications

| Component | Material | Parameter | Dimension (mm) |
|---|---|---|---|
| Waste Package Outer Corrosion Barrier | SB-575 N06022 (Alloy 22) | Outer diameter | 1,881.6 (74.08 in.) |
| | | Thickness | 25.40 (1.00 in.) |
| | | Inner diameter | 1,830.8 (calculated) |
| | | Total length | 5,691.38 (224.07 in.)[b] |
| | | Thickness of top | 25.40 (1.00 in.) |
| | | Thickness of bottom | 25.40 (1.00 in.) |
| | | Top gap above IV | 44.50 (1.75 in.) |
| | | Bottom gap below IV | 68.30 (2.69 in.) |
| Waste Package Inner Vessel | SA-240 S31600[a] (Stainless Steel Type 316) | Outer diameter | 1,821.20 (71.70 in.) |
| | | Thickness | 50.80 |
| | | Inner diameter | 1,719.6 (calculated) |
| | | Total length | 5,499.10 (216.50 in)[c] |
| | | Thickness of top | 50.8 (2 in.) |
| | | Thickness of bottom | 50.8 (2 in.) |
| TAD Canister | SA-240 S31603 (Stainless Steel Type 316L) | Outer diameter | 1,689.1 (66.5 in.) |
| | | Thickness | 25.4 (1.00 in.) |
| | | Inner diameter | 1,638.3 (calculated) |
| | | Total length | 5,384.8 (212.0 in.) |
| | | Thickness of bottom | 88.9 (3.5 in.) |
| TAD Canister Shield Plug | SA-240 S31603 (Stainless Steel Type 316L) | Thickness | 381 (15.0 in.) |

Source: SNL 2007 [DIRS 179394], Section 4 and Appendix A, Tables A-5 and A-6.

[a] Represented as SA-240 S31603 in MCNP representations. This is considered to have a negligible impact on the results since the TAD canister acts as the primary reflector.

[b,c] Actual values used (5675.38 mm for outer corrosion barrier and 5511.8 mm for inner vessel) as shown in Figure 6-5 are slightly less than the reference values and only affect the location of the lids external to the TAD. These lids are too many neutron mean free paths away from the fuel to have an impact on system reactivity, and the reflective properties would also be negligible since they are external to the TAD. Therefore, this discrepancy in the inner vessel and outer corrosion barrier lengths has a negligible impact on the results.

Table 4-4. Internal Basket Specifications

| Type | Component | Material | Parameter | Dimension (mm) |
|---|---|---|---|---|
| PWR | Fuel Basket Tube | SA-240 S31603 (Stainless Steel 316L) | Internal distance across flats | 220.726 (8.69 in.)[a] |
| | | | Thickness | 7.9375 (5/16 in.) |
| | | | Length | 4889.5 (192.5 in.)[b] |
| | Neutron Absorber Plate | SA-240 S30464 (Borated Stainless Steel) | Thickness | 11.1125 (nominal) |
| | | | Width | 190.5 (7.50 in.)[a] |
| | | | Length | 4889.5[c] |
| BWR | Fuel Basket Tube | SA-240 S31603 (Stainless Steel 316L) | Internal distance across flats | 152.2222 (5.993 in.)[a] |
| | | | Thickness | 6.3500 (1/4 in.) |
| | | | Length | 4889.5 (192.5 in.)[b] |
| | Neutron Absorber Plate | SA-240 S30464 (Borated Stainless Steel) | Thickness | 11.1125 (nominal) |
| | | | Width | 120.65 (4.75 in.)[a] |
| | | | Length | 4889.5[c] |

[a] Holtec International 2002 [DIRS 168494], Figures 6.3.2 and 6.3.3.

[b] Derived based on total TAD canister length and having 1” clearance between top of basket and lid to allow for thermal expansion.

[c] Same length as FBT.

Table 4-5. Pressurized Water Reactor Fuel Assembly Specifications

| Assembly Component | Specification |
|---|---|
| Lattice | 15 × 15 |
| Fuel pellet (outer radius) | 0.46990 cm |
| Fuel rod cladding (inner radius) | 0.47879 cm |
| Fuel rod cladding (outer radius) | 0.54610 cm |
| Pin pitch | 1.44272 cm |
| Guide tube (outer radius) | 0.67310 cm |
| Guide tube (wall thickness) | 0.04064 cm |
| Instrument tube (outer radius) | 0.69097 cm |
| Instrument tube (wall thickness) | 0.13090 cm |
| Active fuel length | 360.172 cm |
| Upper fitting length | 37.49700 cm[a] |
| Lower fitting length | 16.72300 cm |
| Clad material | Zircaloy 4 |

[a] Value includes total plenum length from BSC 2006 [DIRS 177193], Table 71. This parameter has no effect on system reactivity because the end fitting regions are represented using the same material as present in the cavity region of the canister.

Source: BSC 2006 [DIRS 177193], Table 28 and Table 71.

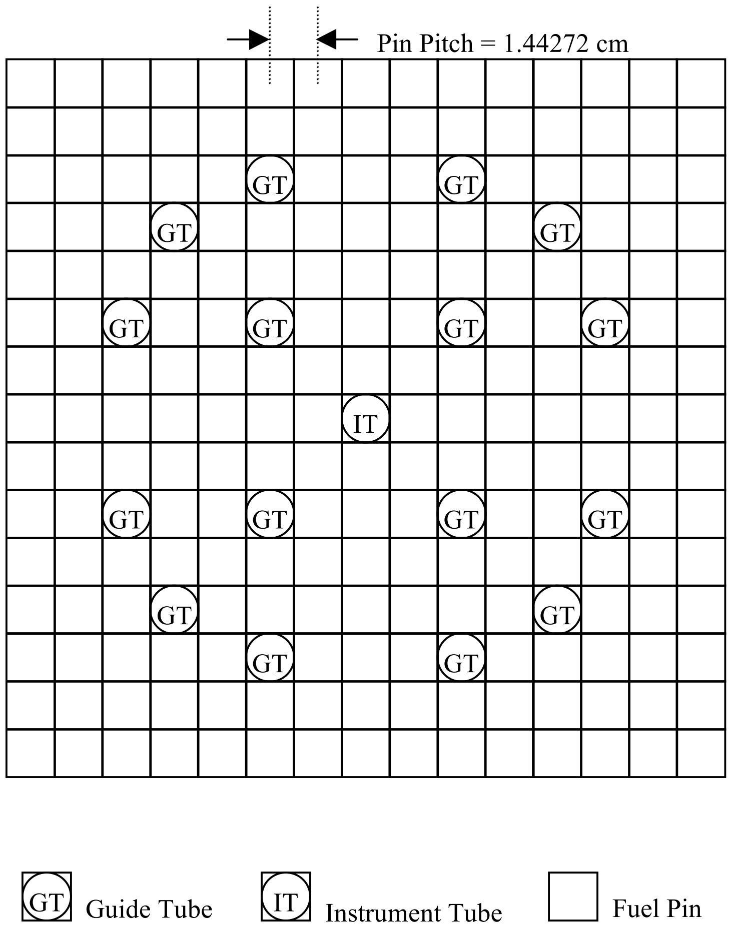


This sketch is not to scale.

Source: BSC 2006 [DIRS 177193], Figure 1.

Figure 4-1. Fuel Pin, Guide Tube, and Instrument Tube Locations in Fuel Assembly

Table 4-6. Boiling Water Reactor Fuel Assembly Specifications

| Assembly Component | Specification |
|---|---|
| Lattice | 7 × 7 |
| Fuel pellet (outer radius) | 0.61976 cm (0.244 in.) |
| Fuel rod cladding (thickness) | 0.08128 cm (0.032 in.) |
| Fuel rod cladding (outer radius) | 0.71501 cm (0.2815 in) |
| Active fuel length | 365.76 cm (144 in.) |
| Clad material | Zircaloy-2 |
| Channel material | Zircaloy-4 |
| Pin pitch | 1.87452 cm (0.738 in.) |
| Channel (outer width) | 13.81252 cm (5.438 in) |
| Channel (thickness) | 0.2032 cm (0.08 in) |
| Lower fitting length | 18.8341 cm (7.415 in) |
| Assembly length | 435.0258 cm (171.27 in) |

Source: Larsen et al. 1976 [DIRS 146576], pp. A-1 to A-3, Figure 10.

The following provides an overview of typical materials that are represented in the MCNP inputs describing the waste forms and waste package configurations. It should be noted that the CSNF will be placed into a transportation, aging, and disposal (TAD) canister, which will then be emplaced into a waste package. Therefore, any reference to the term "waste package" throughout the remainder of this report is referring to the complete system of a TAD canister filled with CSNF inside a waste package.

Table 4-7. Material Specifications for Tuff

| Isotope | Dry Tuff Atom Density [a/b-cm] | Wet Tuff Atom Density [a/b-cm] |
|---|---|---|
| si | 1.7281E-02 | 1.7281E-02 |
| al-27 | 3.3505E-03 | 3.3505E-03 |
| fe-54 | 1.1224E-05 | 1.1224E-05 |
| fe-56 | 1.7604E-04 | 1.7604E-04 |
| fe-57 | 4.0676E-06 | 4.0676E-06 |
| fe-58 | 5.3724E-07 | 5.3724E-07 |
| mg | 4.3900E-05 | 4.3900E-05 |
| ca | 1.2135E-04 | 1.2135E-04 |
| na-23 | 1.5460E-03 | 1.5460E-03 |
| k | 1.3958E-03 | 1.3958E-03 |
| ti | 1.8746E-05 | 1.8746E-05 |
| p-31 | 9.5885E-06 | 9.5885E-06 |
| mn-55 | 1.3431E-05 | 1.3431E-05 |
| o-16 | 4.1574E-02 | 4.5507E-02 |
| h-1 | – | 7.8665E-03 |

Source: BSC 2006 [DIRS 177193], Table 1.

Table 4-8. Material Specifications for SB-575 N06022

| Isotope | Wt. % |
|---|---|
| c | 0.0150 |
| si | 0.0800 |
| p-31 | 0.0200 |
| s-32 | 0.0200 |
| v | 0.3500 |
| cr-50 | 0.8879 |
| cr-52 | 17.7863 |
| cr-53 | 2.0554 |
| cr-54 | 0.5202 |
| mn-55 | 0.5000 |
| fe-54 | 0.2260 |
| fe-56 | 3.6759 |
| fe-57 | 0.0865 |
| fe-58 | 0.0116 |
| co-59 | 2.5000 |
| ni-58 | 36.8024 |
| ni-60 | 14.6621 |
| ni-61 | 0.6481 |
| ni-62 | 2.0975 |
| ni-64 | 0.5547 |
| mo | 13.5000 |
| w-182 | 0.7877 |
| w-183 | 0.4278 |
| w-184 | 0.9209 |
| w-186 | 0.8636 |

Source: BSC 2006 [DIRS 177193], Table 4.

Table 4-9. Material Specifications for SA-240 S31603

| Isotope | Wt. % |
|---|---|
| c | 0.0300 |
| n-14 | 0.1000 |
| si | 0.7500 |
| p-31 | 0.0450 |
| s-32 | 0.0300 |
| cr-50 | 0.7103 |
| cr-52 | 14.2291 |
| cr-53 | 1.6443 |
| cr-54 | 0.4162 |
| mn-55 | 2.0000 |
| fe-54 | 3.7036 |
| fe-56 | 60.2343 |
| fe-57 | 1.4167 |
| fe-58 | 0.1904 |
| ni-58 | 8.0641 |
| ni-60 | 3.2127 |
| ni-61 | 0.1420 |
| ni-62 | 0.4596 |
| ni-64 | 0.1216 |
| mo | 2.5000 |

Source: BSC 2006 [DIRS 177193], Table 6.

Table 4-10. Material Specifications for Zircaloy-4

| Isotope | Wt. % |
|---|---|
| cr-50 | 0.0042 |
| cr-52 | 0.0837 |
| cr-53 | 0.0097 |
| cr-54 | 0.0024 |
| fe-54 | 0.0119 |
| fe-56 | 0.1930 |
| fe-57 | 0.0045 |
| fe-58 | 0.0006 |
| o-16 | 0.1250 |
| zr | 98.1150 |
| sn | 1.4500 |

Source: BSC 2006 [DIRS 177193], Table 10.

Table 4-11. Material Specifications for Zircaloy-2

| Isotope | Wt. % |
|---|---|
| cr-50 | 0.0042 |
| cr-52 | 0.0837 |
| cr-53 | 0.0097 |
| cr-54 | 0.0024 |
| fe-54 | 0.0076 |
| fe-56 | 0.1241 |
| fe-57 | 0.0029 |
| fe-58 | 0.0004 |
| ni-58 | 0.0370 |
| ni-60 | 0.0147 |
| ni-61 | 0.0007 |
| ni-62 | 0.0021 |
| ni-64 | 0.0006 |
| o-16 | 0.1250 |
| zr | 98.1350 |
| sn | 1.4500 |

Source: BSC 2006 [DIRS 177193], Table 11.

Table 4-12. Material Specifications for SA-240 S30464

| Isotope | Wt. % |
|---|---|
| c | 0.0800 |
| n-14 | 0.1000 |
| b-10[a] | 0.1540 |
| b-11 | 0.6860 |
| si | 0.7500 |
| p-31 | 0.0450 |
| s-32 | 0.0300 |
| cr-50 | 0.7939 |
| cr-52 | 15.9031 |
| cr-53 | 1.8378 |
| cr-54 | 0.4652 |
| mn-55 | 2.0000 |
| fe-54 | 3.5855 |
| fe-56 | 58.3137 |
| fe-57 | 1.3715 |
| fe-58 | 0.1843 |
| ni-58 | 9.0721 |
| co-59 | 0.2000 |
| ni-60 | 3.6143 |
| ni-61 | 0.1598 |
| ni-62 | 0.5171 |
| ni-64 | 0.1367 |

[a] Natural variation of $^{10}B$ in boron ranges from 19.1% (atom percent) to 20.3% (Parrington et. al. 1996 [DIRS 103896], p. 7). A value of 19.8% is used in this analysis.

Source: ASTM A 887-89 [DIRS 178058], Table 1.

Table 4-13. J-13 Well Water Composition

| Isotope | Atom Density [a/b-cm] | Mass Density [g/cm$^3$] |
|---|---|---|
| h-1[a] | 6.6873E-02 | 1.1191E-01 |
| o-16[b] | 3.3437E-02 | 8.8810E-01 |
| ca | 1.9534E-07 | 1.3000E-05 |
| mg | 4.9802E-08 | 2.0100E-06 |
| na-23 | 1.1997E-06 | 4.5800E-05 |
| k | 7.7629E-08 | 5.0400E-06 |
| cl | 1.2128E-07 | 7.1400E-06 |
| s-32 | 1.1548E-07 | 6.1311E-06 |
| n-14 | 8.5298E-08 | 1.9834E-06 |
| f-19 | 6.9102E-08 | 2.1800E-06 |
| si | 6.1110E-07 | 2.8500E-05 |
| Density | 1.0031E-01 | 1.0001 |

[a] Hydrogen atom density based on pure water at 1.0 g/cm$^3$.

[b] Oxygen atom density based on pure water at 1.0 g/cm$^3$ plus contributions from sulfate ($SO_4$) and nitrate ($NO_3$).

Source: DTN: MO0006J13WTRCM.000 [DIRS 151029].

Table 4-14. PWR Axial Profile Burnup Weight Factors

| Axial Zone | Zone Height[b] | Group 1 10≤x<15[a] | Group 2 15≤x<20 | Group 3 20≤x<25 | Group 4 25≤x<30 | Group 5 30≤x<35 | Group 6 35≤x<40 | Group 7 40≤x<45 | Group 8 45≤x |
|---|---|---|---|---|---|---|---|---|---|
| 1 | 0.0556 | 0.497 | 0.554 | 0.525 | 0.587 | 0.599 | 0.619 | 0.635 | 0.640 |
| 2 | 0.1111 | 0.837 | 0.882 | 0.882 | 0.903 | 0.907 | 0.914 | 0.923 | 0.926 |
| 3 | 0.1667 | 1.009 | 1.021 | 0.986 | 1.016 | 1.028 | 1.027 | 1.024 | 1.023 |
| 4 | 0.8333 | 1.150 | 1.126 | 1.122 | 1.113 | 1.104 | 1.094 | 1.094 | 1.086 |
| 5 | 0.8889 | 0.859 | 0.920 | 0.934 | 0.950 | 0.971 | 0.988 | 0.991 | 0.998 |
| 6 | 0.9444 | 0.664 | 0.694 | 0.766 | 0.738 | 0.778 | 0.822 | 0.800 | 0.841 |
| 7 | 1.0000 | 0.333 | 0.416 | 0.440 | 0.454 | 0.471 | 0.506 | 0.502 | 0.541 |

[a] Parameter x is the assembly average burnup in GWd/MTU.

[b] Fraction of active fuel height at top of zone measured from bottom of active fuel region. Zone height values are based on the seven zone axial profile developed in BSC 2003 [DIRS 166138] in which zones 1 through 3 and 5 through 7 are each 1/18th of the active fuel height and zone 4 is the balance.

Source: BSC 2003 [DIRS 166138], Table 32.

Table 4-15. Lower Bound Tolerance Limits for PWR and BWR Packages

| **Application Systems** | **LBTL** | **Range of Applicability EALF in eV[1]** |
|---|---|---|
| 21-PWR waste packages containing fresh fuel | 0.9905 | 0.0977 ≤ EALF ≤ 0.3882 |
| 21-PWR waste packages containing burned fuel | 0.9778 | 0.0684 ≤ EALF ≤ 1.0410 |
| 44-BWR waste packages containing fresh fuel | 0.9905 | 0.0977 ≤ EALF ≤ 0.3882 |
| 44-PWR waste packages containing burned fuel | 0.9778 | 0.0421 ≤ EALF ≤ 0.9679 |

[1] Parameter EALF is the energy corresponding to the average neutron lethargy causing fission.

Source: DTN: MO0711RABDPCSF.000 [DIRS 184166], file: *ORNL_TM_2007_127_RoABias_Final_10_16_07.pdf*, Table 20.

Table 4-16. Principal Isotopes for CSNF Burnup Credit

| | | | | |
|---|---|---|---|---|
| mo-95 | nd-145 | eu-151 | u-236 | pu-241 |
| tc-99 | sm-147 | eu-153 | u-238 | pu-242 |
| ru-101 | sm-149 | gd-155 | np-237 | am-241 |
| rh-103 | sm-150 | u-233 | pu-238 | am-242m |
| ag-109 | sm-151 | u-234 | pu-239 | am-243 |
| nd-143 | sm-152 | u-235 | pu-240 | |

Source: YMP 2003 [DIRS 165505], Table 3-1.

Table 4-17. MCNP Nuclide Identifier (ZAID) and Atomic Mass Values

| Isotope | ZAID | Mass [amu] | Isotope | ZAID | Mass [amu] |
|---|---|---|---|---|---|
| h-1 | 1001.62c | 1.00783 | sn | 50000.42c | 118.71091 |
| c | 6000.66c | 12.01104 | w-182 | 74182.62c | 181.94821 |
| b-10 | 5010.66c | 10.01294 | w-183 | 74183.62c | 182.95022 |
| b-11 | 5011.66c | 11.00931 | w-184 | 74184.62c | 183.95093 |
| n-14 | 7014.62c | 14.00307 | w-186 | 74186.62c | 185.95436 |
| o-16 | 8016.62c | 15.99491 | mo-95 | 42095.50c | 94.90584 |
| f-19 | 9019.62c | 18.99840 | tc-99 | 43099.66c | 98.90625 |
| na-23 | 11023.62c | 22.98977 | ru-101 | 44101.50c | 100.90558 |
| mg | 12000.62c | 24.30505 | rh-103 | 45103.66c | 102.90550 |
| al-27 | 13027.62c | 26.98154 | ag-109 | 47109.66c | 108.90476 |
| si | 14000.60c | 28.08551 | nd-143 | 60143.50c | 142.90981 |
| p-31 | 15031.66c | 30.97376 | nd-145 | 60145.50c | 144.91257 |
| s-32 | 16032.62c | 31.97207 | sm-147 | 62147.66c | 146.91489 |
| cl | 17000.66c | 35.45274 | sm-149 | 62149.66c | 148.91718 |
| k | 19000.62c | 39.09830 | sm-150 | 62150.49c | 149.91727 |
| ca | 20000.62c | 40.07802 | sm-151 | 62151.50c | 150.91993 |
| ti | 22000.62c | 47.87843 | sm-152 | 62152.49c | 151.91973 |
| v | 23000.62c | 50.94147 | eu-151 | 63151.66c | 150.91985 |
| cr-50 | 24050.62c | 49.94605 | eu-153 | 63153.66c | 152.92123 |
| cr-52 | 24052.62c | 51.94051 | gd-155 | 64155.66c | 154.92262 |
| cr-53 | 24053.62c | 52.94065 | u-233 | 92233.66c | 233.03963 |
| cr-54 | 24054.62c | 53.93888 | u-234 | 92234.66c | 234.04094 |
| mn-55 | 25055.62c | 54.93805 | u-235 | 92235.66c | 235.04392 |
| fe-54 | 26054.62c | 53.93961 | u-236 | 92236.66c | 236.04556 |
| fe-56 | 26056.62c | 55.93494 | u-238 | 92238.66c | 238.05078 |
| fe-57 | 26057.62c | 56.93540 | np-237 | 93237.66c | 237.04817 |
| fe-58 | 26058.62c | 57.93328 | pu-238 | 94238.66c | 238.04955 |
| co-59 | 27059.66c | 58.93320 | pu-239 | 94239.66c | 239.05216 |
| ni-58 | 28058.62c | 57.93535 | pu-240 | 94240.66c | 240.05381 |
| ni-60 | 28060.62c | 59.93079 | pu-241 | 94241.66c | 241.05684 |
| ni-61 | 28061.62c | 60.93106 | pu-242 | 94242.66c | 242.05874 |
| ni-62 | 28062.62c | 61.92835 | am-241 | 95241.66c | 241.05682 |
| ni-64 | 28064.62c | 63.92797 | am-242m | 95242.66c | 242.05954 |
| zr | 40000.66c | 91.22365 | am-243 | 95243.66c | 243.06137 |
| mo | 42000.66c | 95.93129 | | | |

Source: MCNP5 V. 1.40. STN: 11199N 1.40-00 [DIRS 180515], file: “xsdir.”

## 4.2 CRITERIA

The safety criteria for postclosure criticality are described in *Criticality Input to Canister-Based System Performance Specification for Disposal* (SNL 2007 [DIRS 178236], Section 1) as follows:

> There are no specific design criteria for postclosure criticality control in 10 CFR Part 63 [DIRS 180319] but requirements are consistent with a risk-informed, performance-based regulation, which treats criticality in 10 CFR Part 63 [DIRS 180319] as one of the FEPs that must be considered for the overall system performance assessment, i.e.:
>
> > …The features, events, and processes considered in the performance assessment should represent a wide range of both beneficial and potentially adverse effects on performance (e.g., beneficial effects of radionuclide sorption; potentially adverse effects of fracture flow or a criticality event)…. [§ 63.102(j)]
>
> Various measures are implemented to satisfy the 10 CFR Part 63 [DIRS 180319] acceptance criteria applicable to the postclosure performance assessment for the Yucca Mountain site; these include examining the significant factors contributing to the probability of criticality in the repository and possibly implementing additional analyses or design enhancements to reduce the overall probability of criticality if the respective criteria are exceeded. Such measures are addressed in 10 CFR Part 63 [DIRS 180319], which, in discussing "concepts" of the performance assessment regulations, states in part:
>
> > …Those features, events, and processes expected to materially affect compliance with § 63.113(b) or be potentially adverse to performance are included, while events (event classes or scenario classes) that are very unlikely (less than one chance in 10,000 over 10,000 years) can be excluded from the analysis… [§ 63.102(j)]
>
> The allowance to screen out events on the basis of low probability of occurrence is included in 10 CFR Part 63 [DIRS 180319].

## 4.3 CODES, STANDARDS, AND REGULATIONS

This report has been prepared to comply with the NRC acceptance criteria (SNL 2007 [DIRS 178869], Section 3.2), as well as NRC high-level waste rule 10 CFR Part 63 [DIRS 180319].

INTENTIONALLY LEFT BLANK

# 5. ASSUMPTIONS

None.

INTENTIONALLY LEFT BLANK

# 6. SCIENTIFIC ANALYSIS DISCUSSION

This report evaluates the minimum required burnup of an assembly, for a specific initial enrichment, at which the calculated $k_{eff}$ is equal to the critical limit (CL). The CL is the value of $k_{eff}$ at which the configuration is potentially critical, and accounts for the criticality analysis methodology bias and uncertainty. In equation notation the CL is represented as shown in Equation 1.

$$CL(x) = f(x) - \Delta k_{EROA} - \Delta k_{ISO} - \Delta k_m \quad \text{(Eq. 1)}$$

where

| | | |
|---|---|---|
| x | = | neutronic parameter used for trending |
| f(x) | = | the lower bound tolerance limit function accounting for biases and uncertainties that cause the calculation results to deviate from the true value of $k_{eff}$ for a critical experiment, as reflected over an appropriate set of critical experiments |
| $\Delta k_{EROA}$ | = | penalty for extending the range of applicability |
| $\Delta k_{ISO}$ | = | penalty for isotopic composition bias and uncertainty |
| $\Delta k_m$ | = | an administrative margin to ensure subcriticality for preclosure that turns the CL function into an upper subcritical limit function. This value is set to zero consistent with the methodology described in *Disposal Criticality Analysis Methodology Topical Report* (YMP 2003 [DIRS 165505], Section 3.5.3). |

A more detailed discussion of the CL calculation is provided in *Disposal Criticality Analysis Methodology Topical Report* (YMP 2003 [DIRS 165505], Section 3.5.3). A series of computer calculations was performed in order to develop a set of curves which show $k_{eff}$ versus burnup for different initial enrichments, and the minimum burnup required to reach the CL.

A loading curve depicts the relationship between the initial enrichment of a fuel assembly and the required minimum burnup needed to suppress the reactivity of that fuel assembly sufficiently to allow it to be safely loaded into the waste package. Any assembly whose burnup exceeds the required minimum burnup, given the initial enrichment of the fuel assembly, may be loaded into the waste package.

During the postclosure time period a variety of conditions may affect the waste package internal configurations. A process to identify configuration classes that have the potential for criticality is provided in *Disposal Criticality Analysis Methodology Topical Report* (YMP 2003 [DIRS 165505], Section 3.6). This analysis is based only on configurations which may occur within the repository during the postclosure period; preclosure event sequences and configurations are evaluated separately following *Preclosure Criticality Analysis Process Report* (BSC 2007 [DIRS 182214]).

## 6.1 MCNP INPUT DEVELOPMENT

When developing a loading curve, configurations that result in conservatively high $k_{eff}$ values should be used in order to conservatively bound all other configurations. Therefore, the selection of a bounding configuration follows a linear progression based upon the results of other cases (sensitivity studies). Several potential configurations that could occur in the repository over a 10,000-year regulatory period are evaluated to determine which result in the highest $k_{eff}$ values. The configurations are intended to investigate the effects on system reactivity as the waste package internal components degrade and the geometry changes. A series of configurations is evaluated with the descriptions and results provided in the following sections. Based on the results, a combination of parameters is selected to produce the most reactive representation for the generation of the loading curve.

### 6.1.1 Base Case Analysis

The base case analysis is a conservative representation of the waste package, TAD canister, basket, and fuel payload. The representation considers only the fuel assemblies, fuel basket tubes (FBT), and absorber plates in the representation of the canister contents. Dimensions of basket components are based on conservative representations, and sensitivities to these parameters are considered in Section 6.2.

#### 6.1.1.1 Materials

##### 6.1.1.1.1 Non-Fuel Materials

Structural material models are based on the material inputs described in Section 4. MCNP material composition cross section libraries are taken from the latest ENDF/B data available in the MCNP5 V. 1.40 (STN: 11199-1.40-00 [DIRS 180515], file: "xsdir") distribution, generally corresponding to ENDF/B-VI data.

##### 6.1.1.1.2 Fuel Materials

Fuel material isotopic concentrations are taken from *Isotopic Generation and Confirmation of the PWR Application Model* (BSC 2003 [DIRS 166142]) for PWR fuel and *Isotopic Generation and Confirmation of the BWR Appl. Model* (Wimmer 2004 [DIRS 169319]) and *Isotopic Generation and Confirmation of the BWR Application Model* (Massie 2004 [DIRS 173618]) for BWR fuel. The five-year decay time isotopics are used because they bound fuel that is cooled longer with respect to reactivity. The isotopic data are provided in Output DTN: MO0711LOADCURV.000, workbook: *LoadingCurve.xls*, worksheet: "FuelIsotopics."

The data are provided at one-half percent enrichment steps between 1.5 and 5.0 wt% $^{235}U$ and at the discrete burnup values shown in the tables in Output DTN: MO0711LOADCURV.000, workbook: *LoadingCurve.xls*, worksheet: "FuelIsotopics." Isotopic concentrations at intermediate burnup values are obtained by linear interpolation.

The fresh fuel uranium isotopic vector credits only $^{235}U$ and $^{238}U$ isotopes. Trace quantities of $^{234}U$ and $^{236}U$ in fresh fuel are not represented in order to maximize reactivity.

Fresh $UO_2$ fuel densities are expected to approach 98% of theoretical density (10.96 g/cm$^3$ (Todreas and Kazimi 1990 [DIRS 107735], p. 296)) in next generation fuel, therefore a value of 10.741 g/cm$^3$ is used for all intact fuel configurations in order to maximize fissile loading in all cases, including depleted fuel.

#### 6.1.1.1.3 Axial Burnup Profile

As fuel is burned in a reactor, the burnup of the fuel becomes distributed axially. The profile of this axial burnup distribution attains a flattened cosine curve shape with time, although the exact profile will vary significantly with operating history and other effects unique to the individual reactor. An axial profile database has been composed for various PWR fuel assembly designs, which included variations in enrichment, burnup, and burnable absorbers (Cacciapouti and Van Volkinburg 1997 [DIRS 137617]). To develop a loading curve, which would encompass the isotopic axial variations caused by different assembly irradiation histories, requires the development of a limiting axial profile that takes credit for fuel burnup.

The PWR axial profiles used in this analysis were developed from an axial profile database (Cacciapouti and Van Volkinburg 1997 [DIRS 137617]). Limiting axial profiles were developed for a set of 8 burnup groups in *PWR Axial Burnup Profile Analysis* (BSC 2003 [DIRS 166138], Table 32) as listed in Table 4-14.

BWR axial burnup profiles are not evaluated or used in this analysis because the methodology used for generating the bounding isotopic compositions in *Isotopic Generation and Confirmation of the BWR Appl. Model* (Wimmer 2004 [DIRS 169319]) and *Isotopic Generation and Confirmation of the BWR Application Model* (Massie 2004 [DIRS 173618]) is considered to sufficiently bound any increase in reactivity resulting from the lower burned fuel ends. Several reasons contribute to this conclusion:

1) BWR fuel assemblies with initial enrichments for which burnup credit is taken (greater than 4.5 wt. % as shown in Section 6.3.3) typically have burnups far in excess of the required minimum burnup. This is because the projected waste stream inventory shows that the BWR fuel assemblies at higher initial enrichments are also at the highest average burnups, and a significant portion of the BWR fuel inventory can already be loaded without burnup credit. In addition, the effects on reactivity of an axial burnup profile at low burnups is small, and shown to actually be less conservative for PWR assembly evaluations, as seen in Figure 6-9.

2) Axial burnup profiles are typically used as an indicator of the residual reactivity left in the ends of the assemblies. BWR fuel assemblies typically use natural uranium $UO_2$ axial blanket fuel at the ends, and vary the $^{235}U$ fuel loading axially. This loading scheme reduces the extreme end-effects and provides a flatter axial power distribution.

3) Since bulk boiling occurs within BWRs the axial burnup profile distribution must be coupled with the spectral hardening effects caused by the change in moderator density axially in order to account for the residual reactivity built in through $^{239}$Pu generation. This effect was considered in *Isotopic Generation and Confirmation of the BWR Appl. Model* (Wimmer 2004 [DIRS 169319] Section 5.1.1) and *Isotopic Generation and Confirmation of the BWR Application Model* (Massie 2004 [DIRS 173618]) and an alternative method to ensure that the spectrum hardening effects were maximized in order to have the highest $^{239}$Pu production rate was used (control blades inserted for final 15 GWd/MTU of the simulated irradiation) to generate conservative isotopic compositions with respect to criticality.

These conservative isotopic compositions are applied over the entire axial length of the fuel assembly, including the axial blanket zones which typically have low enrichment. This approach results in a conservative representation which is expected to bound the end-effect reactivity increase that may be observed at higher burnups.

#### 6.1.1.1.4 CSNF Isotopes

Sensitivity evaluations are performed in order to evaluate the impact of modifications to the total number of fission product principal isotopes listed in Table 4-16. Table 6-1 lists the principal isotopes and the variations of this isotope set used in this analysis. Each isotope set provides a multiplicative weight factor which is used to fully credit, partially credit, or exclude a given principal isotope from the fuel material description. A value of one fully credits the principal isotope in the fuel material description, and a value of zero removes the isotope completely. Values between zero and one represent partial credit taken for certain isotopes and are employed in the degraded fuel isotope set discussed below.

The "Principal Actinide" set includes full credit only for actinide isotopes in the principal isotope list. The "Principal Actinide" and "Actinide Only" sets correspond to the more limited set of actinides used in *Criticality Model* (BSC 2004 [DIRS 168553], Table 4). The "Degraded Fuel" isotope set is used in the degraded fuel analysis. This set credits lanthanide isotopes at 85% within the degraded fuel matrix based on results of CSNF waste form degradation analyses in *Geochemistry Model Validation Report: Material Degradation and Release Model* (SNL 2007 [DIRS 181165], Section 8.1.1.1).

Three additional isotope sets are defined by including or excluding two defined subsets of isotopes. The "Metal" isotope subset is comprised of $^{95}$Mo, $^{99}$Tc, $^{101}$Ru, $^{103}$Rh, and $^{109}$Ag. By excluding this subset from the Principal Isotope set, the "PI – Metal" subset is defined.

Similarly, a subset of isotopes for which certain specific experimental data may be acquired is referred to as the "French" subset, and is comprised of $^{103}$Rh, $^{143}$Nd, $^{149}$Sm, $^{152}$Sm, and $^{155}$Gd. This subset combined with the Principal Actinide set defines the "PA + French" isotope set. By further excluding the "Metal" subset from this set, the "PA + French – Metal" isotope set is defined.

Table 6-1. Burnup Credit Isotope Selection

| Isotope | Principal Isotope | Principal Actinide | Actinide Only | Degraded Fuel | PI – Metal | PA + French | PA + French – Metal |
|---|---|---|---|---|---|---|---|
| o-16 | 1.0 | 1.0 | 1.0 | 1.0 | 1.0 | 1.0 | 1.0 |
| mo-95 | 1.0 | 0.0 | 0.0 | 0.0 | 0.0 | 0.0 | 0.0 |
| tc-99 | 1.0 | 0.0 | 0.0 | 0.0 | 0.0 | 0.0 | 0.0 |
| ru-101 | 1.0 | 0.0 | 0.0 | 0.0 | 0.0 | 0.0 | 0.0 |
| rh-103 | 1.0 | 0.0 | 0.0 | 0.0 | 0.0 | 1.0 | 0.0 |
| ag-109 | 1.0 | 0.0 | 0.0 | 0.0 | 0.0 | 0.0 | 0.0 |
| nd-143 | 1.0 | 0.0 | 0.0 | 0.85 | 1.0 | 1.0 | 1.0 |
| nd-145 | 1.0 | 0.0 | 0.0 | 0.85 | 1.0 | 0.0 | 0.0 |
| sm-147 | 1.0 | 0.0 | 0.0 | 0.85 | 1.0 | 0.0 | 0.0 |
| sm-149 | 1.0 | 0.0 | 0.0 | 0.85 | 1.0 | 1.0 | 1.0 |
| sm-150 | 1.0 | 0.0 | 0.0 | 0.85 | 1.0 | 0.0 | 0.0 |
| sm-151 | 1.0 | 0.0 | 0.0 | 0.85 | 1.0 | 0.0 | 0.0 |
| sm-152 | 1.0 | 0.0 | 0.0 | 0.85 | 1.0 | 1.0 | 1.0 |
| eu-151 | 1.0 | 0.0 | 0.0 | 0.85 | 1.0 | 0.0 | 0.0 |
| eu-153 | 1.0 | 0.0 | 0.0 | 0.85 | 1.0 | 0.0 | 0.0 |
| gd-155 | 1.0 | 0.0 | 0.0 | 0.85 | 1.0 | 1.0 | 1.0 |
| u-233 | 1.0 | 1.0 | 0.0 | 1.0 | 1.0 | 1.0 | 1.0 |
| u-234 | 1.0 | 1.0 | 1.0 | 1.0 | 1.0 | 1.0 | 1.0 |
| u-235 | 1.0 | 1.0 | 1.0 | 1.0 | 1.0 | 1.0 | 1.0 |
| u-236 | 1.0 | 1.0 | 1.0 | 1.0 | 1.0 | 1.0 | 1.0 |
| u-238 | 1.0 | 1.0 | 1.0 | 1.0 | 1.0 | 1.0 | 1.0 |
| np-237 | 1.0 | 1.0 | 0.0 | 1.0 | 1.0 | 1.0 | 1.0 |
| pu-238 | 1.0 | 1.0 | 1.0 | 1.0 | 1.0 | 1.0 | 1.0 |
| pu-239 | 1.0 | 1.0 | 1.0 | 1.0 | 1.0 | 1.0 | 1.0 |
| pu-240 | 1.0 | 1.0 | 1.0 | 1.0 | 1.0 | 1.0 | 1.0 |
| pu-241 | 1.0 | 1.0 | 1.0 | 1.0 | 1.0 | 1.0 | 1.0 |
| pu-242 | 1.0 | 1.0 | 1.0 | 1.0 | 1.0 | 1.0 | 1.0 |
| am-241 | 1.0 | 1.0 | 1.0 | 1.0 | 1.0 | 1.0 | 1.0 |
| am-242m | 1.0 | 1.0 | 0.0 | 1.0 | 1.0 | 1.0 | 1.0 |
| am-243 | 1.0 | 1.0 | 0.0 | 1.0 | 1.0 | 1.0 | 1.0 |

Source: Output DTN: MO0711LOADCURV.000, file: *LoadingCurve.xls,* worksheet: "FuelIsotopics."

#### 6.1.1.2 Geometry

The MCNP representation of the waste package is derived from the geometric input data provided in Section 4. The representation is developed from descriptions of the fuel assembly, basket structure, TAD canister and waste package, and surrounding tuff material.

MCNP coordinates are specified such that the z dimension is the axial extent of the waste package. The y dimension corresponds to the vertical dimension for the horizontally emplaced waste package. The remaining x dimension is defined such that the coordinate system is right handed.

Each MCNP model universe may be specified with respect to its own local origin. However, the global origin of the model is placed at the bottom center of the canister cavity.

#### 6.1.1.2.1 Fuel Assembly

The fuel assembly is represented as a stacked array of regions representing the lower assembly, fuel pin array, and upper assembly. The lower and upper assemblies are represented as water regions since this places additional moderator near the fuel region. The pin array includes both fuel and non-fuel cells. Non-fuel cell types represent guide tubes, instrument tubes, and water rods (if any are present).

In order to facilitate studies which offset the assembly within the fuel basket tube (FBT), the assembly is represented with an exterior region tightly fitting the outer pin array in the x and y dimensions.

Variations in fuel assembly lattice design were evaluated in *Evaluation of Neutron Absorber Materials Used for Criticality Control in Waste Packages* (BSC 2006 [DIRS 180664]). This evaluation was performed in order to assess which fuel assembly lattice design would result in the highest $k_{eff}$ values when loaded in a waste package configuration. Fuel assembly lattices were varied using Babcock & Wilcox (B&W), Westinghouse (W), and Combustion Engineering (CE) geometric arrangements in pure water. The results of this evaluation indicate that the B&W 15 × 15 fuel assembly design is the most reactive design (BSC 2006 [DIRS 180664], Section 7); therefore, it is selected as the bounding PWR assembly design.

The GE 7 × 7 assembly is selected as the bounding BWR fuel assembly based on the analysis in *Isotopic Generation and Confirmation of the BWR Appl. Model* (Wimmer 2004 [DIRS 169319]) and *Isotopic Generation and Confirmation of the BWR Application Model* (Massie 2004 [DIRS 173618]) which showed the highest reactivity for the GE 7 × 7 assembly.

#### 6.1.1.2.2 Basket Position

Although the actual basket design will likely include numerous structural and thermal components which would tend to reduce system reactivity, the basket representation credits only the FBTs and the absorber plates. FBT dimensions are based on a previously licensed cask design (Holtec International 2002 [DIRS 168494], Figures 6.3.2 and 6.3.3). The absorber plate thickness is based on the specification in *Total System Performance Assessment Data Input Package for Requirements Analysis for Transportation Aging and Disposal Canister and Related Waste Package Physical Attributes Basis for Performance Assessment* (SNL 2007 [DIRS 179394]) with a conservative allowance made for corrosion.

The nominal thickness of the absorber plate material is 11 mm. For postclosure criticality analysis, a conservative thickness of 6 mm is used based on the recommendation in *Evaluation of Neutron Absorber Materials Used for Criticality Control in Waste Packages* (BSC 2006 [DIRS 180664]) and consistent with *Transportation, Aging and Disposal Canister System Performance Specification* (DOE 2007 [DIRS 181403]) specification 3.1.5(2)(a)(2) (page 15). The results in *Geochemistry Model Validation Report: Material Degradation and Release Model* (SNL 2007 [DIRS 181165], Table 6.3-6) show that expected corrosion rates of the SS304B4 material would leave more than 9 mm after 10,000 years of exposure in a corrosive environment based on the base case SS304B4 corrosion rate of 0.0678 μm/yr. In addition, consistent with guidance in NUREG-1536 (NRC 1997 [DIRS 101903]), for fixed-neutron absorbers used for criticality control in the packages, no more than 75% credit for the neutron absorber content is modeled (i.e., the design-specified absorber content is reduced by 25% in the analyses).

The absorber plate width (extent in the x or y directions along the sides of the FBT) is based on a previous NRC-approved transportation cask design (Holtec International 2002 [DIRS 168494], Figures 6.3.2 and 6.3.3) as shown in Table 4-4. The absorber width is less than the full width of the FBT, permitting corner-to-corner communication between neighboring assemblies.

Geometrical features of the representation which maximize waste package reactivity include: the compact FBT representation, omission of structural components, and narrow and thin absorber plates.

The MCNP representation of the PWR and BWR basket positions are shown in Figure 6-1 and Figure 6-2, respectively. The basket unit cell includes absorber plates on the +x and +y faces. Arrays of these unit cells are used to form the basket structure, as shown for the 21-PWR and 44-BWR baskets in Figure 6-3 and Figure 6-4, respectively.

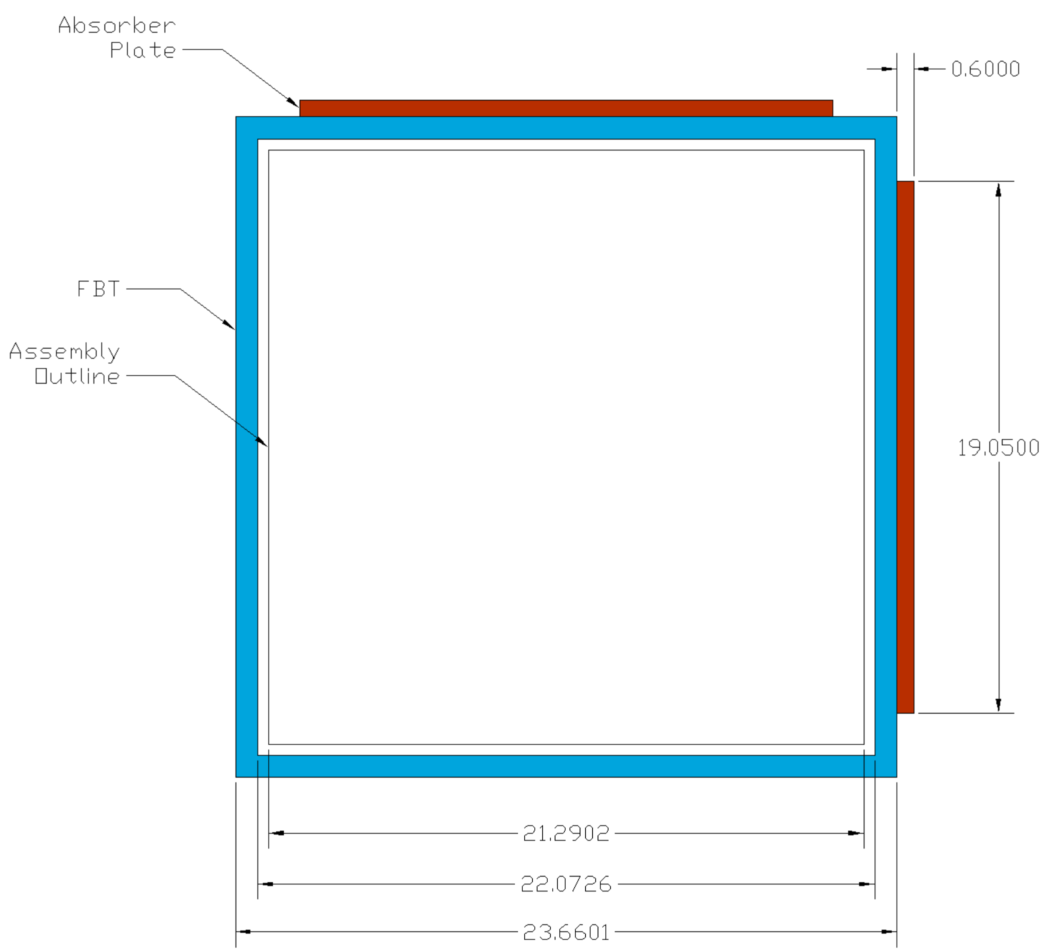


Source: For illustrative purposes.

Figure 6-1. Representation of 21-PWR Basket Unit Cell (dimensions in cm)

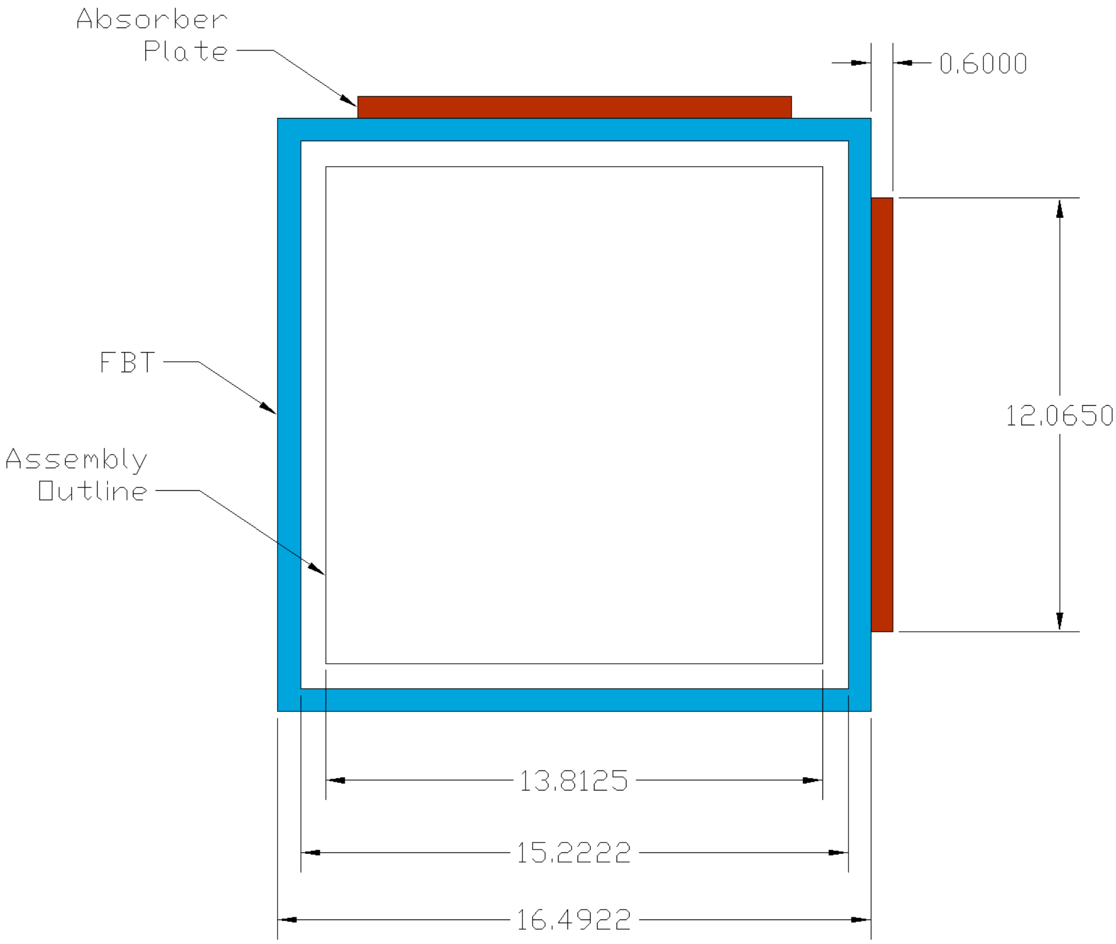


Source: For illustrative purposes.

Figure 6-2. Representation of 44-BWR Basket Unit Cell (dimensions in cm)

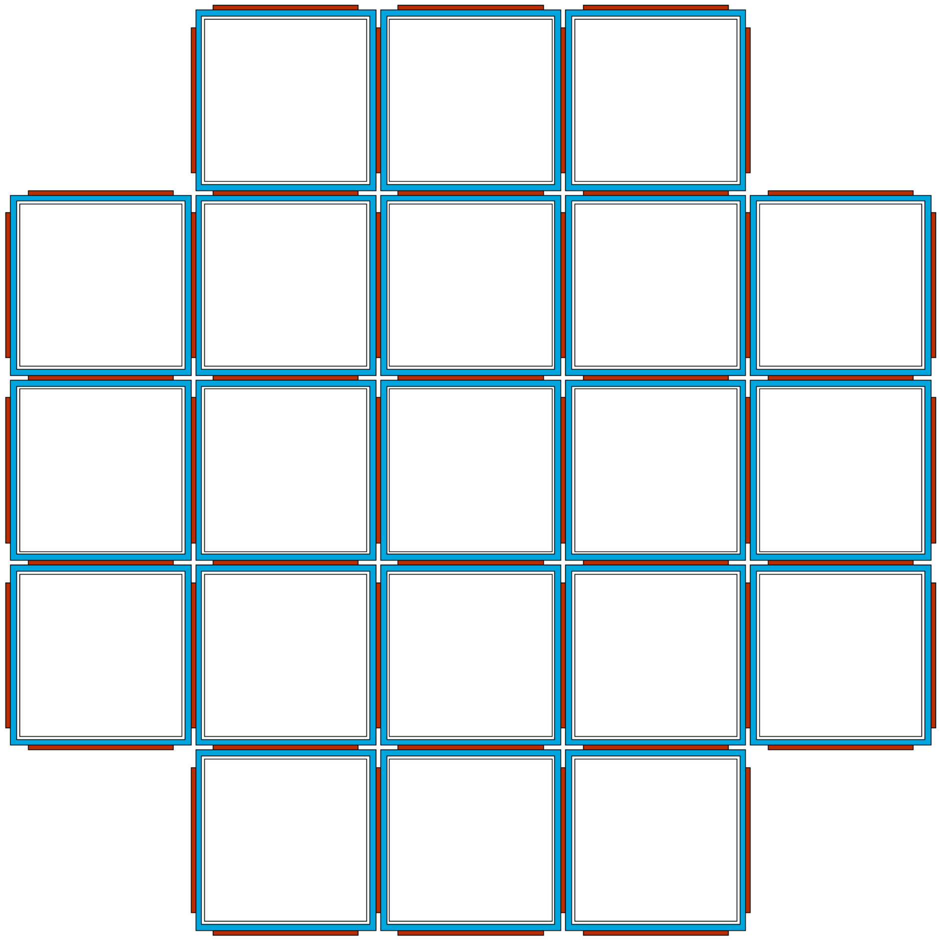

Source: For illustrative purposes.

Figure 6-3. Representation of 21-PWR Basket

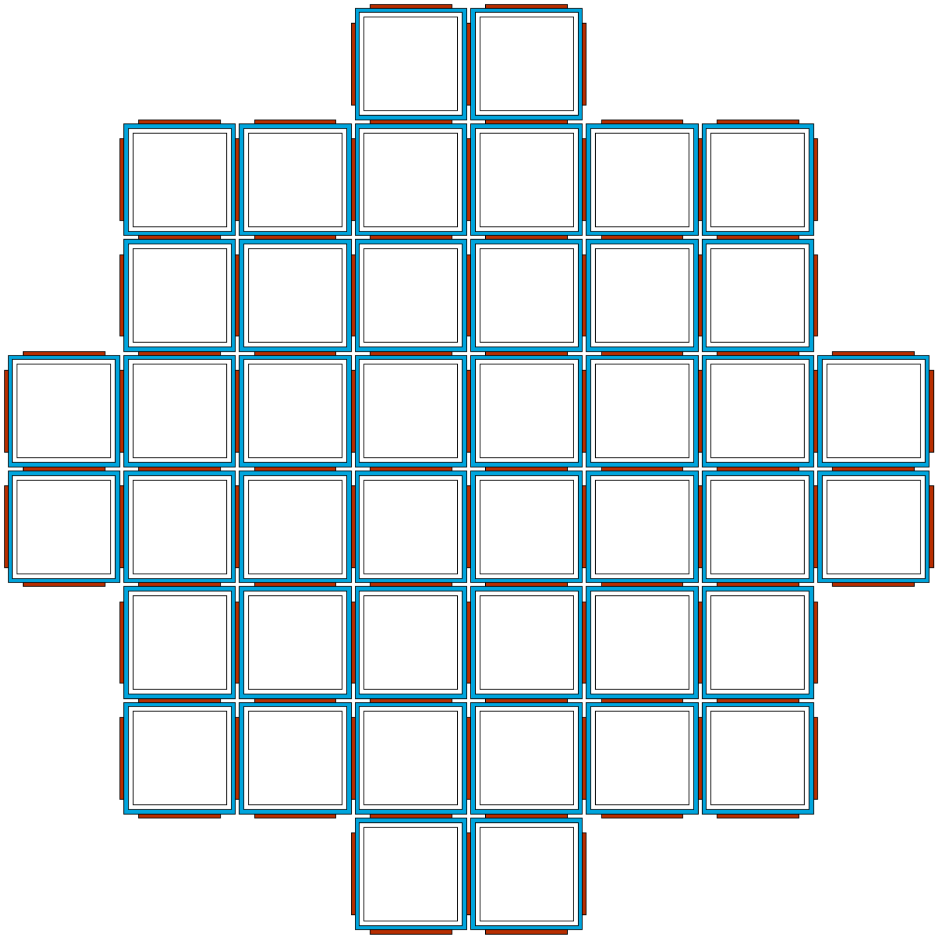

Source: For illustrative purposes.

Figure 6-4. Representation of 44-BWR Basket

#### 6.1.1.2.3 Waste Package

The TAD canister, inner vessel (IV), and outer corrosion barrier (OCB) are represented based on the materials and dimensions provided in Table 4-3. The MCNP representation is shown in Figure 6-5. In both the PWR and BWR representations, the fuel assemblies are positioned axially with the fuel axial midplane coincident with the basket midplane. For clarity, Figure 6-5 shows the representation with a single PWR fuel assembly in order to illustrate the axial position of the fuel within the waste package.

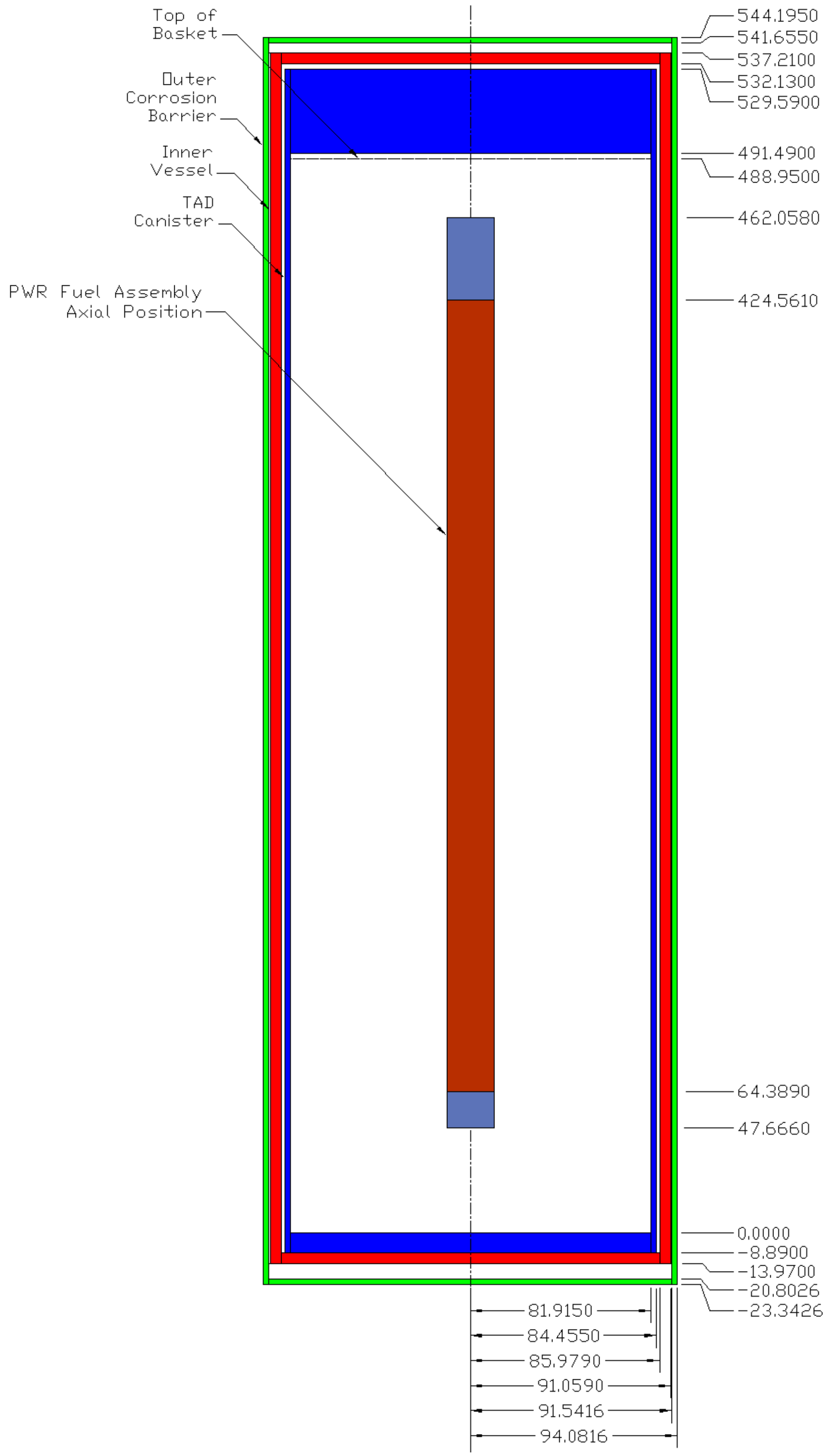


Source: For illustrative purposes. A single assembly is shown to indicate axial position.

Figure 6-5. Representation of Waste Package with PWR Assembly (dimensions in cm)

#### 6.1.1.3 Code Execution

Generally, the MCNP cases are executed with sufficient histories to reduce the Monte Carlo uncertainty to 0.0005 or less.

As a result of certain code MCNP limitations associated with surfaces that meet at a point, particles are occasionally "lost" when moving across a surface at a point of tangency. This problem occurs rarely (approximately once every two billion histories), and the code permits up to ten lost particles in a single case before stopping. In no cases are more than ten particles lost during execution of any case.

Output files are scanned for important warning or error messages, and any issues are considered and resolved.

### 6.1.2 Radial Burnup Profile

Radial variations in the neutron flux, which are mainly due to leakage at the core periphery and near reactivity control components, result in a non-uniform horizontal burnup distribution over the radial extent of the reactor core. As the reactor operates, the radial flux shape flattens due to fuel depletion and fission product poisoning near the core center. However, because of the high leakage, burnup drops off rapidly near the core periphery. At the end of a cycle, the individual assemblies located near the center of the core will have a relatively uniform horizontal burnup distribution, while the assemblies near the core periphery may have a significant horizontal variation in burnup (DOE 1997 [DIRS 181316], Section 1.2, p. 1). Thus, it is possible for fuel rods on one side of an assembly to have experienced less burnup than fuel rods on the opposite side of the same assembly.

The radial burnup (RBU) representation was developed in order to accommodate radial variation of burnup within an assembly. Each fuel assembly is represented with a "high-side" and a "low-side" burnup, with the burnup variation specified as a weight factor relative to the assembly average burnup (or the average burnup within an axial zone, in the case of an axial burnup profile case).

#### 6.1.2.1 Materials

With a specified radial burnup weight factor, the fuel material isotopics for each side of the assembly are determined in the same manner as is done in the axial zone case. The isotopic data are interpolated on burnup to determine the high-and low side fuel descriptions. Note that the radial burnup profile can be applied in conjunction with the axial profile. In this case, the axial burnup profile weight factors are first applied to determine an average burnup within each axial zone. Then the radial burnup weight factor is applied to this value resulting in a "high-side" and "low-side" burnup for each axial zone. These burnup values are then interpolated in the isotopic data tables to determine fuel material descriptions for each side of each axial zone.

### 6.1.2.2 Geometry

In order to accommodate the various radial burnup distributions, nine fuel pin array configurations were developed as shown in Figure 6-6. In each configuration, half of the pin cells are represented with the high-burnup isotopics and the other half with the low-burnup isotopics. In the case of an odd number of fuel pin cells, the remaining fuel pin is assigned the low-burnup isotopics, in order to be conservative with respect to reactivity.

Additionally, a mechanism for specifying the basket layout is provided. An example layout is shown in Figure 6-7. Although the RBU representation is provided in Output DTN: MO0711LOADCURV.000, workbook: *LoadingCurve.xls*, it is not used in this analysis because *PWR Radial Burnup Gradient Reactivity Evaluation* (SNL 2007 [DIRS 182953], Section 7) concludes that the change in $k_{eff}$ due to the radial burnup gradient on actual loaded waste packages is expected to be inconsequential to system reactivity.

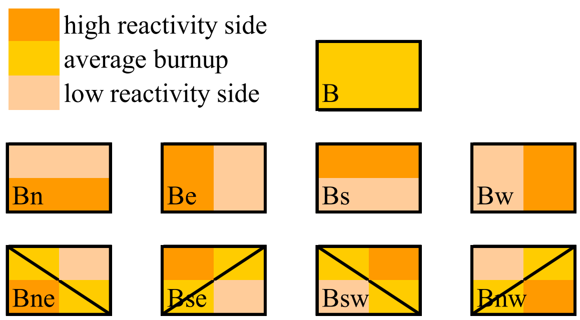


Source: For illustrative purposes.

Figure 6-6. Radial Burnup Model Pin Array Configurations

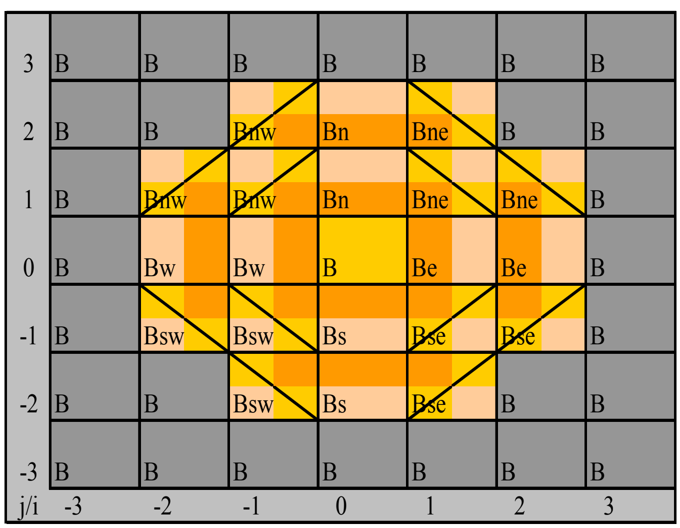


Source: For illustrative purposes.

Figure 6-7. Example Basket Layout for the Radial Burnup Model

### 6.1.3 Degraded Waste Form Representation

For the in-package degraded configuration scenarios the internals are degraded and the cladding is considered breached within a failed waste package and the interior of the fuel rods are exposed to the repository environment. As the temperature of the repository decreases after the initial thermal spike, the relative humidity to which the CSNF matrix will be exposed will increase and is expected to approach 100% when the temperature decreases to 100°C and lower (SNL 2008 [DIRS 184433], Figure 7.5-6). The plausible mechanisms for waste form degradation are discussed in detail in *CSNF Waste Form Degradation: Summary Abstraction* (BSC 2004 [DIRS 169987], Section 6.2.2), but these discussions indicate that the overall oxidative dissolution process involves a coupled series of redox, surface complexation and dissolution, and precipitation reactions depending on the fluid environment (water film on the fuel surfaces). Upon contact with air-saturated condensate (i.e., water), $UO_2$ (and CSNF) is expected to undergo reactions of the following type to form dehydrated schoepite and metaschoepite:

$$UO_2\text{ (s)} + \tfrac{1}{2}\,O_2\text{ (aq)} + 0.8\,H_2O\text{ (l)} = UO_3{\cdot}0.8H_2O\text{ (s)} \qquad \text{Dehydrated schoepite}$$

$$UO_2\text{ (s)} + \tfrac{1}{2}\,O_2\text{ (aq)} + 2\,H_2O\text{ (l)} = UO_3{\cdot}2H_2O\text{ (s)} \qquad \text{Metaschoepite}$$

Not all of the uranium atoms are expected to form into fully hydrated schoepite. This is because as schoepite forms, it starts at the exposed surface of the fuel pellets/fragments and moves inwards towards the center of the pellet/fragment depending on the availability of oxygen and hydrogen. As the process works inwards, the less-soluble elements will resist the tendency to oxidize to a higher state and are expected to effectively block the inner uranium atoms from oxidizing, eventually arresting schoepite formation.

As the fuel degradation products expand into the free space of the assembly pin array, and ultimately into the FBT or assembly channel (in the BWR case), the degradation process is expected to be arrested as the occupied volume would obstruct vapor diffusion through the FBT and inhibit exposure to potentially chemically reactive fuel.

The prospective degradation of the fuel while remaining in a package is considered with this representation. Since the metaschoepite form contains more hydrogen than the dehydrated schoepite form, only the metaschoepite form is considered in this analysis. In the following, *metaschoepite* will be referred to as *schoepite* for convenience. This material has a lower density than $UO_2$, and will occupy more volume as $UO_2$ is converted into schoepite. The reactivity of the system as a function of the fuel degradation is investigated.

The volumetric expansion that the $UO_2$ undergoes as it converts to schoepite is governed by the density ratio between the materials. The represented density of the schoepite material is based on both its theoretical density and the porosity of the material. From Table 4-1, the molar volume of schoepite is 66.08 $cm^3$/mol. Neglecting the minor effect of the specific uranium isotopic vector and taking the molecular weight of uranium as that of natural uranium (238.02891 g/mol), the theoretical density of schoepite is then $\rho_{s,TD}$ = 4.8737 g/$cm^3$. For a represented porosity of $x$, the schoepite density is $(1-x)\rho_{s,TD}$.

However, in order to conserve $UO_2$ molecules between the original fuel form and the schoepite material, the quantity of interest in determining the volumetric expansion factor is the density of $UO_2$ in the schoepite. For notational convenience this quantity will be labeled simply $\rho_s$. Hence, the factor by which a given volume of fuel with density $\rho_f$ expands upon degradation to schoepite is simply $\rho_f / \rho_s$. It is important to note that the quantity $\rho_s$ is *not* the density of porous schoepite; it is the density of $UO_2$ in porous schoepite. The weight fraction of $UO_2$ in schoepite is found from molecular weight ratios to be 0.83845. Hence:

$$\rho_s = (0.83845)(1 - x)\rho_{s,TD}$$

And the quantity $\rho_f / \rho_s$ represents the volume factor by which the $UO_2$ in the fuel expands upon degradation to schoepite at a porosity of $x$.

In addition to being *porous*, the schoepite may also have a *saturation* value between 0 and 100%. The saturation represents the volume fraction of the porous space within the schoepite that is occupied by water. Note that the saturation value has no effect on the volumetric expansion factor $\rho_f / \rho_s$. The schoepite material at the specified saturation value is referred to as *wet schoepite*.

Results for the degraded waste form representation are provided in Section 6.2.5.

#### 6.1.3.1 Degraded Waste Form Material Composition

The actinide and fission product isotopes in the fuel material also undergo reactions. The stoichiometry of the resulting products is shown in Table 6-2 based on the input data provided in Table 4-2. The schoepite material description is developed in three steps.

In the first step, the fuel isotopics for the $UO_2$ fuel at the desired burnup and enrichment is normalized to the represented fuel density (10.741 g/cm$^3$). Also, any isotopic weight factors associated with the selected burnup credit isotope model are applied. In the second step, the normalization factor for each fuel zone is applied to the isotopic atom densities. In addition, the additional fuel degradation product constituents are included according to their stoichiometric ratios from Table 6-2. Also, any contribution from saturation water in the porous void space in the schoepite is added. In the final step the data for duplicated isotopes is summed in order to represent schoepite, other degradation products, and any saturation water present as a homogeneous material. The schoepite material description is developed in Output DTN: MO0711LOADCURV.000, workbook: *LoadingCurve.xls*, worksheet: “Schoepite.”

Table 6-2. Stoichiometry of Fuel Degradation Products

| Isotope | Compound | Stoichiometry | | |
|---|---|---|---|---|
| | | h-1 | c | o-16 |
| mo-95 | – | – | – | – |
| tc-99 | – | – | – | – |
| ru-101 | $^{101}RuO_2$ | – | – | 2 |
| rh-103 | – | – | – | – |
| ag-109 | – | – | – | – |
| nd-143 | $^{143}Nd_2(CO_3)_3$ | – | 1.5 | 4.5 |
| nd-145 | $^{145}Nd_2(CO_3)_3$ | – | 1.5 | 4.5 |
| sm-147 | $^{147}Sm_2(CO_3)_3$ | – | 1.5 | 4.5 |
| sm-149 | $^{149}Sm_2(CO_3)_3$ | – | 1.5 | 4.5 |
| sm-150 | $^{150}Sm_2(CO_3)_3$ | – | 1.5 | 4.5 |
| sm-151 | $^{151}Sm_2(CO_3)_3$ | – | 1.5 | 4.5 |
| sm-152 | $^{152}Sm_2(CO_3)_3$ | – | 1.5 | 4.5 |
| eu-151 | $^{151}Eu_2(CO_3)_3$ | – | 1.5 | 4.5 |
| eu-153 | $^{153}Eu_2(CO_3)_3$ | – | 1.5 | 4.5 |
| gd-155 | $^{155}Gd_2(CO_3)_3$ | – | 1.5 | 4.5 |
| u-233 | $^{233}UO_3(H_2O)_2$ | 4 | – | 5 |
| u-234 | $^{234}UO_3(H_2O)_2$ | 4 | – | 5 |
| u-235 | $^{235}UO_3(H_2O)_2$ | 4 | – | 5 |
| u-236 | $^{236}UO_3(H_2O)_2$ | 4 | – | 5 |
| u-238 | $^{238}UO_3(H_2O)_2$ | 4 | – | 5 |
| np-237 | $^{237}NpO_2$ | – | – | 2 |
| pu-238 | $^{238}PuO_2(OH)_2{:}H_2O$ | 4 | – | 5 |
| pu-239 | $^{239}PuO_2(OH)_2{:}H_2O$ | 4 | – | 5 |
| pu-240 | $^{240}PuO_2(OH)_2{:}H_2O$ | 4 | – | 5 |
| pu-241 | $^{241}PuO_2(OH)_2{:}H_2O$ | 4 | – | 5 |
| pu-242 | $^{242}PuO_2(OH)_2{:}H_2O$ | 4 | – | 5 |
| am-241 | $^{241}AmO_2$ | – | – | 2 |
| am-242m | $^{242m}AmO_2$ | – | – | 2 |
| am-243 | $^{243}AmO_2$ | – | – | 2 |

Source: SNL 2007 [DIRS 181165], Section 6.3.16.

#### 6.1.3.2 Geometry

The representations are parameterized with respect to a quantity $\alpha$ which is the volume fraction of $UO_2$ converted into schoepite. The quantity $\alpha$ can theoretically vary from 0 to 1; however, depending on the represented porosity of the schoepite, there may be insufficient free volume within the FBT (or fuel assembly channel, in the BWR case) to permit full degradation of the fuel. The degradation process is stopped once the free volume within a FBT or channel is occupied by schoepite. The schoepite is only permitted to form within the axial extent of the fuel region.

Although the model is characterized in terms of $\alpha$, its use as a free parameter is difficult because the expression for the schoepite radius, $r_s$, as a function of $\alpha$ is transcendental when $r_s > r_e = \frac{p}{2}$, where $p$ is the fuel pin pitch and $r_e$ is the radius to the "edge" of a pin cell. That is, when the schoepite volume begins to fill the corners of a pin cell as shown in Figure 6-8 Instead, if $r_c$ represents the half-diagonal across a pin cell, $r_c = \frac{\sqrt{2}}{2}p$ (the radius to a pin cell corner), then as $r_s$ varies between $r_e$ and $r_c$ the void space within non-fuel pin cells is uniformly (in $r_s^2$) filled with schoepite. When $\alpha = \alpha(r_c)$, the free space within the fuel assembly is completely filled with schoepite. As $\alpha$ increases from $\alpha(r_c)$, the region within the FBT (or channel) but outside the now filled fuel assembly is progressively filled with bands of schoepite until either the FBT (or channel) is completely filled or the fuel material is completely degraded. The band thickness is determined based on conserved volume for the amount of schoepite corresponding to the difference $\alpha - \alpha(r_c)$.

The schoepite representations are developed in five stages with possibly multiple parametric steps per stage. The completion of each stage is associated with a certain critical value of $\alpha$.

The initial stage is simply the base case in which no schoepite has formed. It is retained in the analysis in order to provide a check against the base case results.

In the second stage, the schoepite expands to fill the gap between the fuel pellet and clad. Although the clad has necessarily ruptured in order for schoepite to have formed. The clad is retained in its original geometry since the material will necessarily be present within the degraded assembly. If $r$ is the radius of the fuel remaining once some fraction $\alpha$ has converted to schoepite, then:

$$\alpha(r) = 1 - \frac{r^2}{r_f^2} \qquad \text{(Eq. 2)}$$

or

$$r(\alpha) = r_f\sqrt{1-\alpha} \qquad \text{(Eq. 3)}$$

where $r_f$ is the original fuel radius. The corresponding volume of schoepite formed is:

$$V_s(\alpha) = \pi(r_s^2 - r^2) = \frac{\rho_f}{\rho_s}\alpha\pi r_f^2$$

Note that what is referred to as volume in this development is actually "volume per unit length" or cross sectional area.

Since the gap is small, this stage is completed by taking a single step out to the clad inner radius, $r_g$. At this point, the corresponding critical value of $\alpha$ is:

$$\alpha_{crit,g} = \frac{\left(1 - \frac{r_g^2}{r_f^2}\right)}{\left(1 - \frac{\rho_f}{\rho_s}\right)} \qquad \text{(Eq. 4)}$$

and the corresponding value of the fuel radius $r(\alpha)$ is found from Equation 3.

In the third stage, the schoepite grows from the clad outer radius $r_o$ to the edge of the pin cell, $r_e = \frac{p}{2}$. The clad volume is:

$$V_c = \pi(r_o^2 - r_g^2)$$

and for a given schoepite radius $r_s$, equating the volume of schoepite with the expanded volume of converted fuel:

$$V_s(\alpha) = \pi r_s^2 - \pi r(\alpha)^2 - V_c = \frac{\rho_f}{\rho_s}\alpha\pi r_f^2$$

from which:

$$\alpha = \frac{r_s^2 - r_f^2 - \frac{V_c}{\pi}}{r_f^2\left(\frac{\rho_f}{\rho_s} - 1\right)} \qquad \text{(Eq. 5)}$$

and $r(\alpha)$ is again determined from Equation 3. For this stage, five values of $r_s$ are selected uniformly in $r_s^2$ between $r_o$ and $r_e$. At the limiting value $r_e$, $\alpha$ reaches a critical value:

$$\alpha_{crit,e} = \alpha(r_e)$$

In the fourth stage, the schoepite radius varies from $r_e$ to the half-diagonal value $r_c = \frac{\sqrt{2}}{2}p$. However, the schoepite is truncated at the pin cell edge so that the area of the segment $A_{seg}$ in Figure 6-8 must be accounted for in determining the schoepite volume.

Furthermore, during this stage, as the schoepite radius parameter $r_s$ increases from $r_e$ to $r_c$, the available free space in non-fuel pin cells (guide tube cells, etc.) is filled with schoepite. The schoepite material in these non-fuel cells is determined simply by varying the volume fraction of material represented outside the non-fuel cell constituent rod (i.e., guide, instrument, or water rod). That is, within the non-fuel pin cell, no specific schoepite geometric feature is represented. Instead, the material properties of the region outside the rod are simply varied uniformly from water (at $r_s = r_e$) to wet schoepite (at $r_s = r_c$) by varying the schoepite volume fraction $f$ between 0 and 1 while representing the water at a volume fraction of $(1-f)$. The rod present in each non-fuel pin cell remains intact, and no schoepite forms inside the rod.

In order to determine the fuel radius $r(\alpha)$, we need an expression for $\alpha$ as a function of $r_s$. Generalizing Equation 5 for any excluded volume $V_x$,

$$\alpha = \frac{r_s^2 - r_f^2 - \dfrac{V_x}{\pi}}{r_f^2\left(\dfrac{\rho_f}{\rho_s} - 1\right)} \qquad \text{(Eq. 6)}$$

In this case:

$$V_x = V_c + 4A_{seg} - fV_{NF} \qquad \text{(Eq. 7)}$$

where $V_{NF}$ is the ratio of the total available free volume in non-fuel cells to the number of fuel pin cells. Hence, $V_{NF}$ is the total non-fuel cell available volume per fuel pin cell.

For this stage, five steps are taken uniformly in $r_s^2$, and the value of $f$ at each step is uniformly selected between 0 and 1. The quantity $A_{seg}$ is given by:

$$A_{seg} = \theta r_s^2 - \frac{p}{2} r_s \sin\theta$$

where

$$\cos\theta = \frac{p/2}{r_s}$$

as shown in Figure 6-8.

At the limiting value $r_s = r_c$, the critical value of $\alpha$ is obtained from Equation 6 as:

$$\alpha_{crit,c} = \alpha(r_c)$$

In the final stage, any remaining fuel left available to convert to schoepite is placed in a series of rectangular bands outside the fuel assembly. The overall width $w(\alpha)$ of a band as a function of $\alpha$ is determined by:

$$w(\alpha)^2 = N_F\left[\left(\frac{\rho_f}{\rho_s} - 1\right)\pi r_f^2\alpha + \pi r_f^2 + x\right] \quad \text{(Eq. 8)}$$

where $N_F$ is the number of fuel pin cells and $x$ is the total non-fuel volume per fuel pin cell from which schoepite is precluded. This volume is comprised of the fuel cladding and any non-fuel rods and their interiors. The maximum value of the overall width $w(\alpha)$ is limited to the FBT or channel (in the BWR case) inner dimension. This stage is completed by taking five steps uniformly in $\alpha$ between $\alpha_{crit,c}$ and either 1, if the remaining fuel upon degradation to schoepite is insufficient to fill the remaining space, or the limiting value of $\alpha$ at which the remaining space is filled.

Representative parameters are shown in Table 6-3 and Table 6-4 for BW 15 × 15 and GE 7 × 7 assemblies for a schoepite porosity of 20%. Experimental evaluations of schoepite have indicated that the porosity varies from 5% to 30% depending on the fluid environment (DTN: LL010902212241.026 [DIRS 163089]). The complete parametric representation over this range of porosities is provided in Output DTN: MO0711LOADCURV.000, workbook: *LoadingCurve.xls*, worksheet: “Schoepite.”

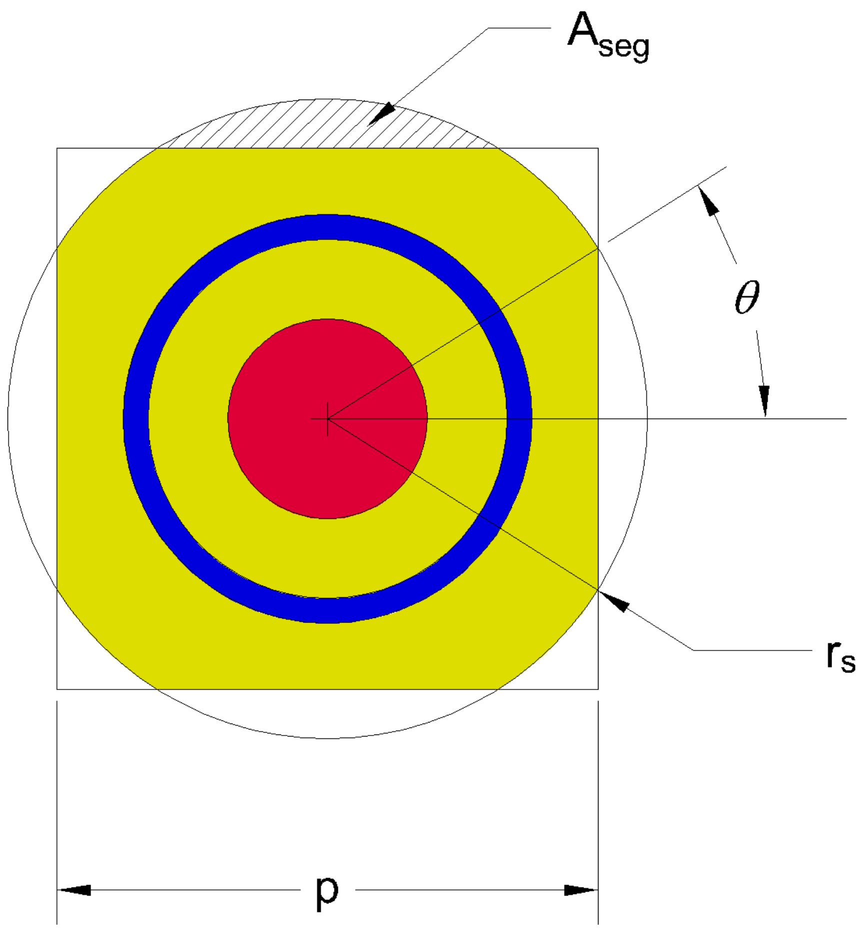


Source: For illustrative purposes.

NOTE: Red region is remaining non-degraded fuel, blue region is fuel cladding, and yellow region is degraded fuel.

Figure 6-8. Geometric Parameters for $r_e < r_s < r_c$ , Where $r_e$ is the Radial Distance to the Cell Edge and $r_c$ is the Distance to the Cell Corner

Table 6-3. Schoepite Model Parameters at 20% Porosity for BW 15 × 15 Assembly

| Condition | $r_s$ [cm] | Alpha | r [cm] | w [cm] | theta [rad] | $A_{seg}$ [$cm^2$] | f | Excluded vol [$cm^3$/cm] | $V_s$ [$cm^3$/cm] | Alpha $V_f$ [$cm^3$/cm] |
|---|---|---|---|---|---|---|---|---|---|---|
| Initial | 0.46990 | 0.00000 | 0.46990 | 21.29028 | – | – | 0.00000 | 0.00000 | 0.00000 | 0.00000 |
| Fill gap | 0.47879 | 0.01671 | 0.46596 | 21.29028 | – | – | 0.00000 | 0.00000 | 0.03809 | 0.01159 |
| Fill to edge (1 of 5) | 0.58537 | 0.10474 | 0.44461 | 21.36881 | – | – | 0.00000 | 0.21672 | 0.23872 | 0.07266 |
| Fill to edge (2 of 5) | 0.62216 | 0.19277 | 0.42219 | 21.44239 | – | – | 0.00000 | 0.21672 | 0.43936 | 0.13372 |
| Fill to edge (3 of 5) | 0.65689 | 0.28079 | 0.39850 | 21.51186 | – | – | 0.00000 | 0.21672 | 0.63999 | 0.19478 |
| Fill to edge (4 of 5) | 0.68988 | 0.36882 | 0.37332 | 21.57784 | – | – | 0.00000 | 0.21672 | 0.84063 | 0.25584 |
| Filled to edge | 0.72136 | 0.45685 | 0.34631 | 21.64080 | – | – | 0.00000 | 0.21672 | 1.04126 | 0.31691 |
| Fill corners (1 of 5) | 0.79021 | 0.59441 | 0.29926 | 21.64080 | 0.42053 | 0.02988 | 0.20000 | 0.32557 | 1.35479 | 0.41233 |
| Fill corners (2 of 5) | 0.85352 | 0.67655 | 0.26724 | 21.64080 | 0.56394 | 0.08173 | 0.40000 | 0.52228 | 1.54202 | 0.46931 |
| Fill corners (3 of 5) | 0.91246 | 0.72825 | 0.24496 | 21.64080 | 0.65906 | 0.14565 | 0.60000 | 0.76726 | 1.65985 | 0.50517 |
| Fill corners (4 of 5) | 0.96781 | 0.75848 | 0.23093 | 21.64080 | 0.72973 | 0.21807 | 0.80000 | 1.04628 | 1.72874 | 0.52614 |
| Filled corners | 1.02016 | 0.77226 | 0.22425 | 21.64080 | 0.78540 | 0.29702 | 1.00000 | 1.35138 | 1.76016 | 0.53570 |
| Fill boundary (1 of 5) | n/a | 0.78371 | 0.21854 | 21.72785 | – | – | 1.00000 | 0.33342 | 1.78625 | 0.54364 |
| Fill boundary (2 of 5) | n/a | 0.79515 | 0.21268 | 21.81455 | – | – | 1.00000 | 0.33342 | 1.81234 | 0.55158 |
| Fill boundary (3 of 5) | n/a | 0.80660 | 0.20665 | 21.90090 | – | – | 1.00000 | 0.33342 | 1.83843 | 0.55953 |
| Fill boundary (4 of 5) | n/a | 0.81805 | 0.20044 | 21.98692 | – | – | 1.00000 | 0.33342 | 1.86452 | 0.56747 |
| Final | n/a | 0.82949 | 0.19403 | 22.07260 | – | – | 1.00000 | 0.33342 | 1.89061 | 0.57541 |

Source: Output DTN: MO0711LOADCURV.000, file: *LoadingCurve.xls*, worksheet: “Schoepite.”

Table 6-4. Schoepite Model Parameters at 20% Porosity for GE 7 × 7 Assembly

| Condition | $r_s$ [cm] | Alpha | r [cm] | w [cm] | theta [rad] | $A_{seg}$ [$cm^2$] | f | Excluded vol [$cm^3$/cm] | $V_s$ [$cm^3$/cm] | Alpha $V_f$ [$cm^3$/cm] |
|---|---|---|---|---|---|---|---|---|---|---|
| Initial | 0.61976 | 0.00000 | 0.61976 | 12.67714 | – | – | 0.00000 | 0.00000 | 0.00000 | 0.00000 |
| Fill gap | 0.63373 | 0.01995 | 0.61355 | 12.67714 | – | – | 0.00000 | 0.00000 | 0.07908 | 0.02407 |
| Fill to edge (1 of 5) | 0.76465 | 0.10360 | 0.58678 | 12.77641 | – | – | 0.00000 | 0.34440 | 0.41076 | 0.12501 |
| Fill to edge (2 of 5) | 0.81125 | 0.18725 | 0.55873 | 12.86962 | – | – | 0.00000 | 0.34440 | 0.74243 | 0.22596 |
| Fill to edge (3 of 5) | 0.85532 | 0.27091 | 0.52919 | 12.95776 | – | – | 0.00000 | 0.34440 | 1.07410 | 0.32690 |
| Fill to edge (4 of 5) | 0.89723 | 0.35456 | 0.49791 | 13.04157 | – | – | 0.00000 | 0.34440 | 1.40578 | 0.42785 |
| Filled to edge | 0.93726 | 0.43822 | 0.46452 | 13.12164 | – | – | 0.00000 | 0.34440 | 1.73745 | 0.52879 |
| Fill corners (1 of 5) | 1.02672 | 0.56517 | 0.40868 | 13.12164 | 0.42053 | 0.05045 | 0.20000 | 0.54619 | 2.24081 | 0.68199 |
| Fill corners (2 of 5) | 1.10898 | 0.63835 | 0.37270 | 13.12164 | 0.56394 | 0.13797 | 0.40000 | 0.89629 | 2.53096 | 0.77030 |
| Fill corners (3 of 5) | 1.18555 | 0.68199 | 0.34950 | 13.12164 | 0.65906 | 0.24588 | 0.60000 | 1.32791 | 2.70395 | 0.82295 |
| Fill corners (4 of 5) | 1.25747 | 0.70478 | 0.33674 | 13.12164 | 0.72973 | 0.36815 | 0.80000 | 1.81698 | 2.79433 | 0.85046 |
| Filled corners | 1.32549 | 0.71162 | 0.33282 | 13.12164 | 0.78540 | 0.50142 | 1.00000 | 2.35008 | 2.82144 | 0.85870 |
| Fill boundary (1 of 5) | n/a | 0.72279 | 0.32631 | 13.17903 | – | – | 1.00000 | 0.34440 | 2.86572 | 0.87218 |
| Fill boundary (2 of 5) | n/a | 0.73395 | 0.31967 | 13.23617 | – | – | 1.00000 | 0.34440 | 2.90999 | 0.88566 |
| Fill boundary (3 of 5) | n/a | 0.74512 | 0.31289 | 13.29306 | – | – | 1.00000 | 0.34440 | 2.95427 | 0.89913 |
| Fill boundary (4 of 5) | n/a | 0.75629 | 0.30596 | 13.34971 | – | – | 1.00000 | 0.34440 | 2.99855 | 0.91261 |
| Final | n/a | 0.76746 | 0.29887 | 13.40612 | – | – | 1.00000 | 0.34440 | 3.04283 | 0.92609 |

Source: Output DTN: MO0711LOADCURV.000, file: *LoadingCurve.xls*, worksheet: “Schoepite.”

## 6.2 SENSITIVITY ANALYSIS

### 6.2.1 Base Case Results

Results for the PWR base case representation are shown in Table 6-6 and Table 6-8 for the axial zone and the average burnup representations, respectively. BWR results for the average burnup case are shown in Table 6-10. The data are evaluated at enrichment values varying from 1.5 to 5.0 wt% $^{235}$U, and burnup steps in increments of 5 GWd/MTU up to 50 GWd/MTU. The base case results are based on the "Principal Isotope" burnup credit isotopes shown in Table 6-1. These base case results are used to determine the loading curves, as shown in Section 6.3. Case names refer to corresponding MCNP input and output files available in Output DTN: MO0711LOADCURV.000.

Results at selected enrichment values are shown graphically in Figure 6-9 for the PWR base case with one-zone and seven-zone axial representations. At enrichments above 2.0 wt%, the one-zone representation is limiting at burnups lower than 25 GWd/MTU. BWR base case results are shown in Figure 6-10 for the enrichment values for which burnup credit is required.

Note that the BWR waste package has significantly lower reactivity than the PWR package. Hence, in the sensitivity analysis discussed below, the PWR representation is used as the basis for parameter variation.

In order to ensure that sensitivity results are applicable across the range of assembly enrichments, results for parameter variation cases are obtained at the enrichment and burnup combinations shown in Table 6-5. These values correspond to the PWR loading curve required minimum burnup values developed in Section 6.3., with fresh fuel used at the 2.0 wt. % $^{235}$U enrichment value.

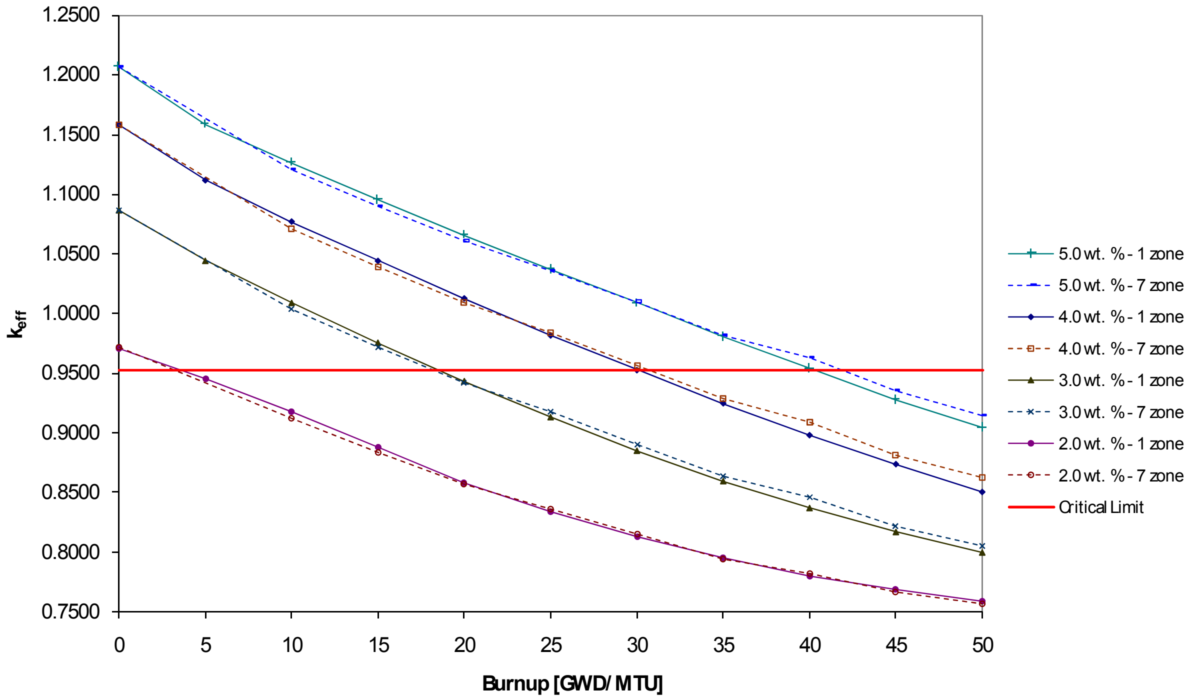


Source: Output DTN: MO0711LOADCURV.000, file: *LoadingCurve.xls*, worksheet: "Results."

Figure 6-9. Comparison of PWR Base Case Results for One Axial Zone and Seven Axial Zone Representations

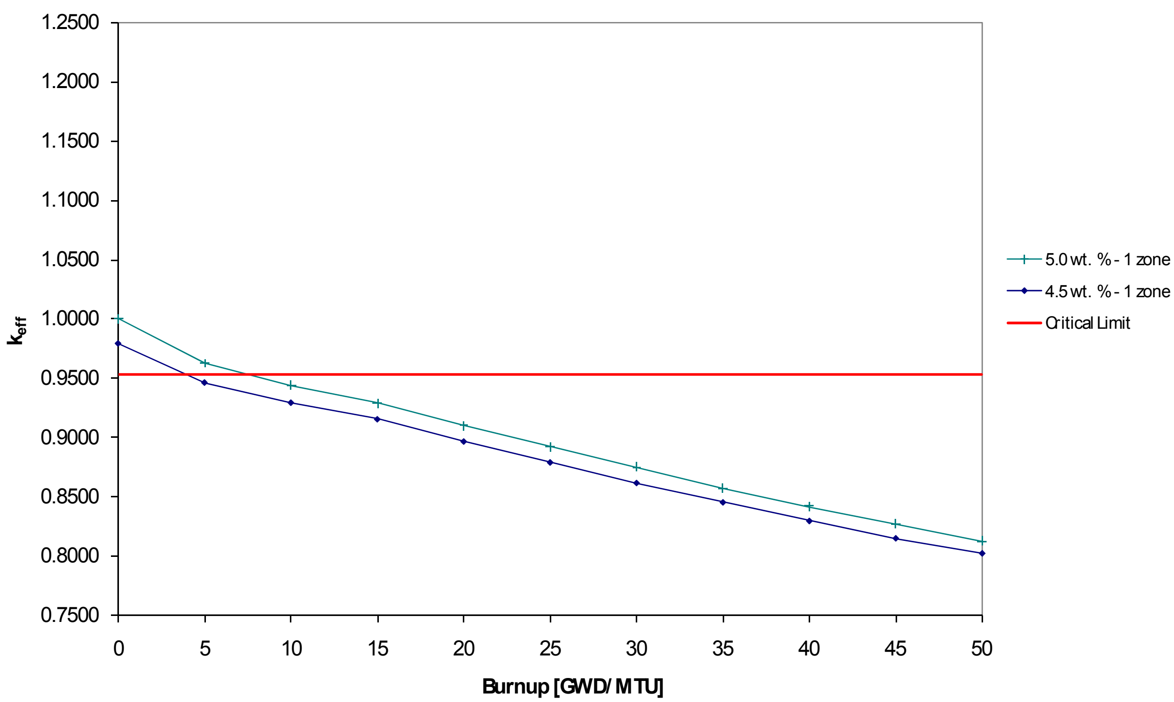


Source: Output DTN: MO0711LOADCURV.000, file: *LoadingCurve.xls*, worksheet: "Results."

Figure 6-10. BWR Base Case Results for One Axial Zone Representation

Table 6-5. Enrichment and Burnup Combinations for PWR Sensitivity Analysis

| Enrichment [wt. %] | Burnup [GWd/MTU] |
|---|---|
| 1.5 | 0.0 |
| 2.0 | 0.0 |
| 2.5 | 12.8 |
| 3.0 | 19.5 |
| 3.5 | 26.2 |
| 4.0 | 32.2 |
| 4.5 | 37.9 |
| 5.0 | 44.1 |

Source: Output DTN: MO0711LOADCURV.000, file: *LoadingCurve.xls*, worksheet: "LoadingCurve."

### 6.2.2 Moderation Cases

Figure 6-11 shows the variation of PWR waste package reactivity as a function of water density for selected enrichment and burnup combinations. The enrichment and burnup combinations correspond to the PWR loading curve established in Section 6.3. Results are tabulated in.

The results show that the waste package is undermoderated, since the reactivity falls rapidly as water density decreases and continues to rise as water density increases in a hypothetical case with density greater than the physical limit of 1.0 g/cm$^3$. Hence, neglecting waste package structural material and other material occupying cavity space in the actual package design is conservative with respect to criticality.

The effect of water composition variation is shown in Figure 6-12. In this figure, the $k_{eff}$ at various enrichment and burnup combinations (see Table 6-13) for J13 well water is compared with the base case (pure water at 1.0 g/cm$^3$). There is no statistically significant difference in the computed reactivity; hence, pure water is represented.

The presence of saturated tuff outside the waste package is shown to result in no significant change over the base case representation of dry tuff.

Table 6-13 also shows results for the dry waste package. For burnup and enrichment combinations shown in Table 6-5, the maximum dry case reactivity is 0.33427 ± 0.00014.

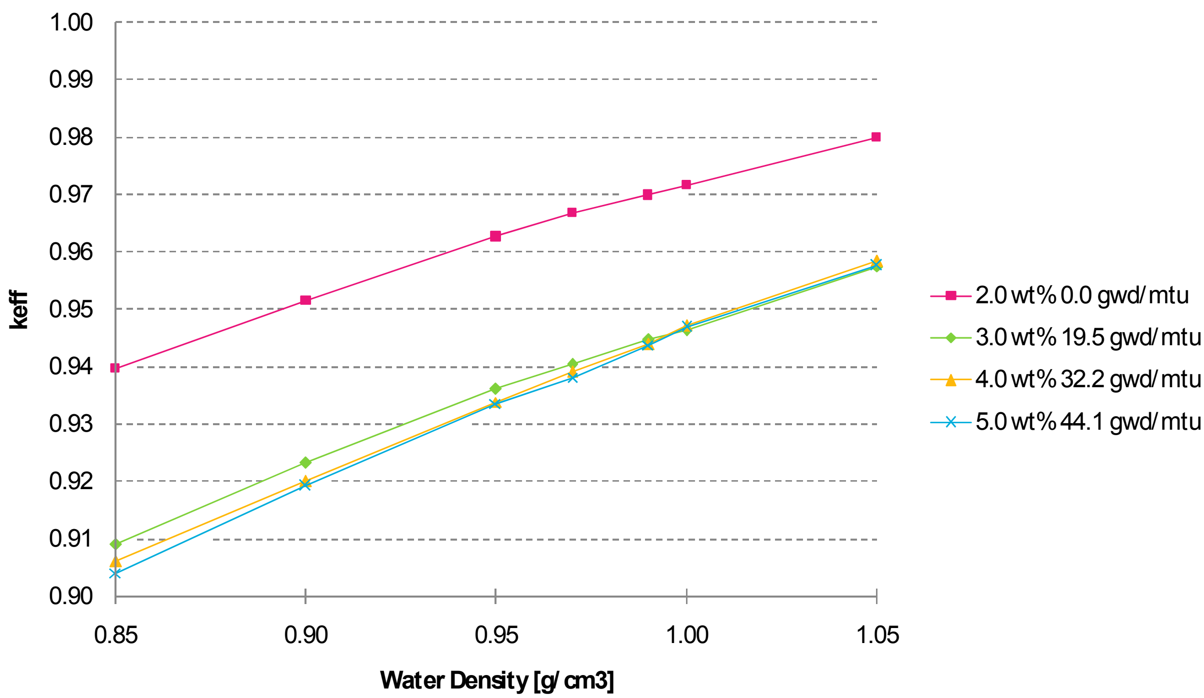


Source: Output DTN: MO0711LOADCURV.000, file: *LoadingCurve.xls*, worksheet: "Results."

Figure 6-11. Variation of Water Density for Various PWR Base Case Conditions

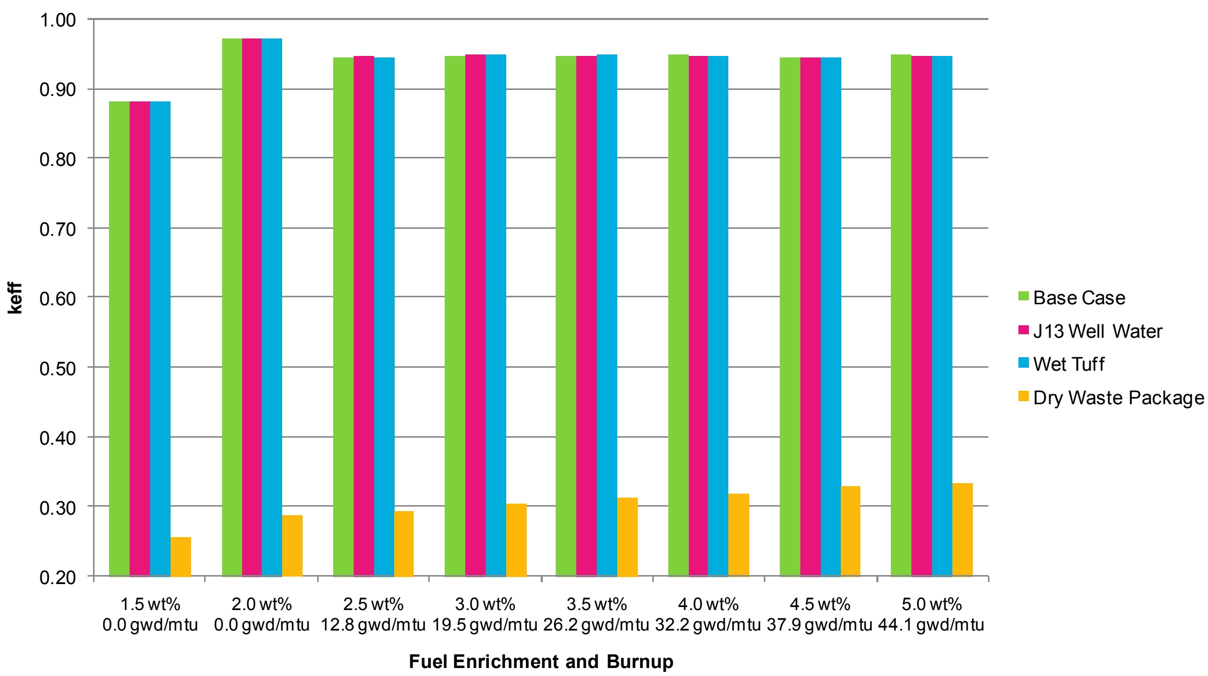


Source: Output DTN: MO0711LOADCURV.000, file: *LoadingCurve.xls*, worksheet: "Results."

Figure 6-12. Variation of Water Composition for Various PWR Base Case Conditions

### 6.2.3 Materials Cases

#### 6.2.3.1 Boron Credit

Boron in the absorber plates is credited in the analysis at only 75% of the specified loading. The effect of this lower credit is illustrated in Figure 6-13 for various PWR enrichment and burnup combinations. Reactivity decreases somewhat slowly with increasing boron credit, suggesting that the results are not sensitive to the boron loading, once the amount of boron present has effectively absorbed all available thermal neutrons passing through the absorber plate. Data for various fuel conditions are tabulated in Table 6-14.

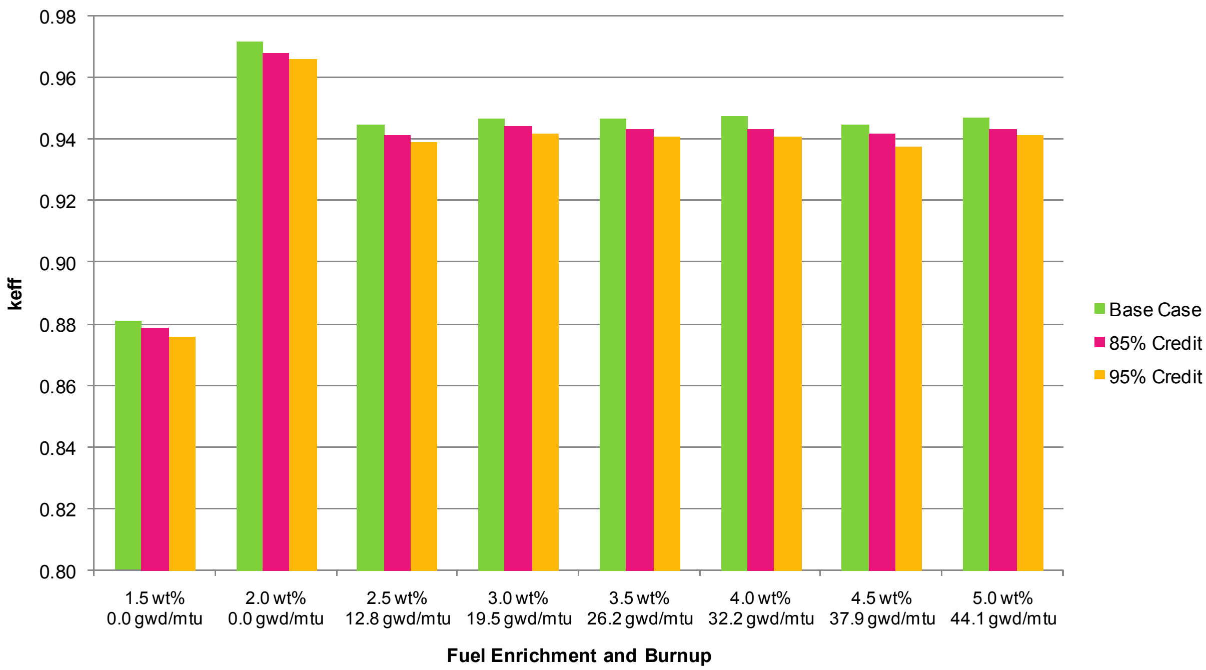


Source: Output DTN: MO0711LOADCURV.000, file: *LoadingCurve.xls*, worksheet: "Results."

Figure 6-13. Variation of Boron Credit for Various PWR Base Case Conditions

### 6.2.3.2 Fuel Density

The sensitivity of reactivity to fuel density variation is shown in Figure 6-14 for various combinations of PWR enrichment and burnup. The reactivity decreases with densities less than the base case value of 10.741 g/cm$^3$. Results at fuel densities higher than the base case are included to show that the reactivity is not sensitively dependent on the limiting value. Detailed results are presented in Table 6-15.

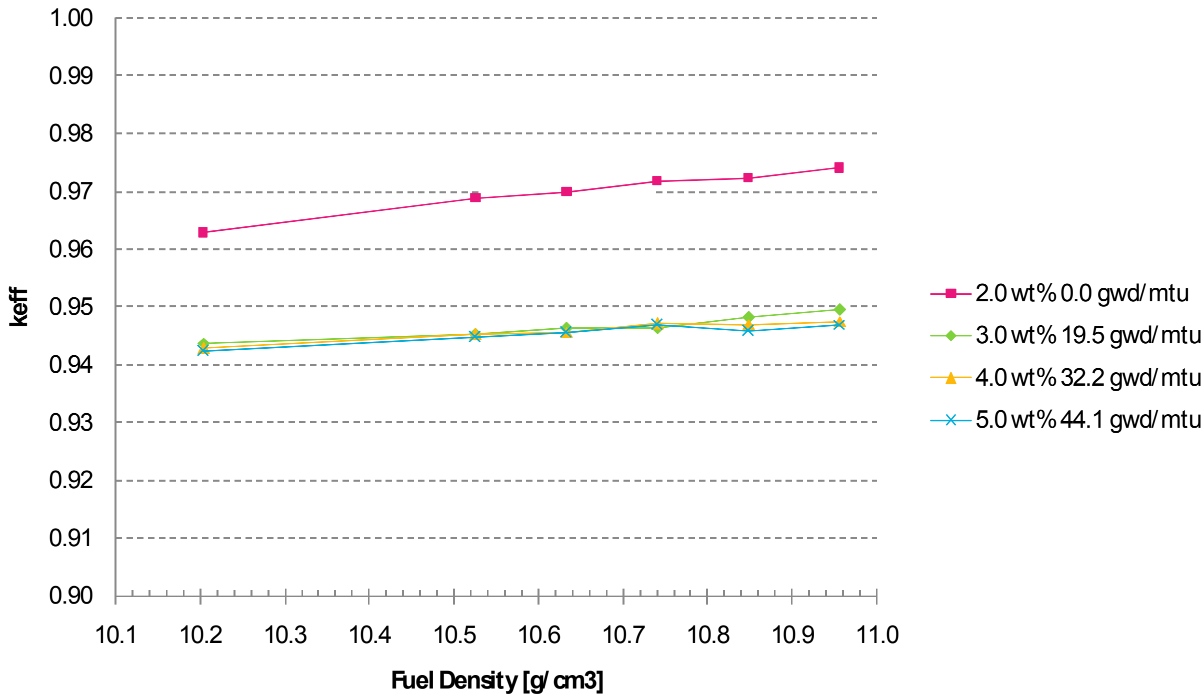


Source: Output DTN: MO0711LOADCURV.000, file: *LoadingCurve.xls*, worksheet: "Results."

Figure 6-14. Variation of Fuel Density for Various PWR Base Case Conditions

### 6.2.3.3 Burnup Credit Isotope Set Variation

The sensitivity of reactivity to burnup credit isotope set variation is shown in Figure 6-15 for various combinations of PWR enrichment and burnup. Detailed results are presented in Table 6-16. The "Delta-k" results shown in Figure 6-15 give the change in reactivity for each indicated isotope set relative to the base case "Principal Isotope" set. For example, for the case with 5.0 wt% and 44.1 GWd/MTU burnup, changing from the "Principal Isotope" set to the "Actinide Only" isotope set causes $k_{eff}$ to increase by 0.0781.

An analysis showing the impact of the various burnup credit isotope sets on the non-loadable fraction of the PWR fuel inventory is presented in Section 6.3.4.

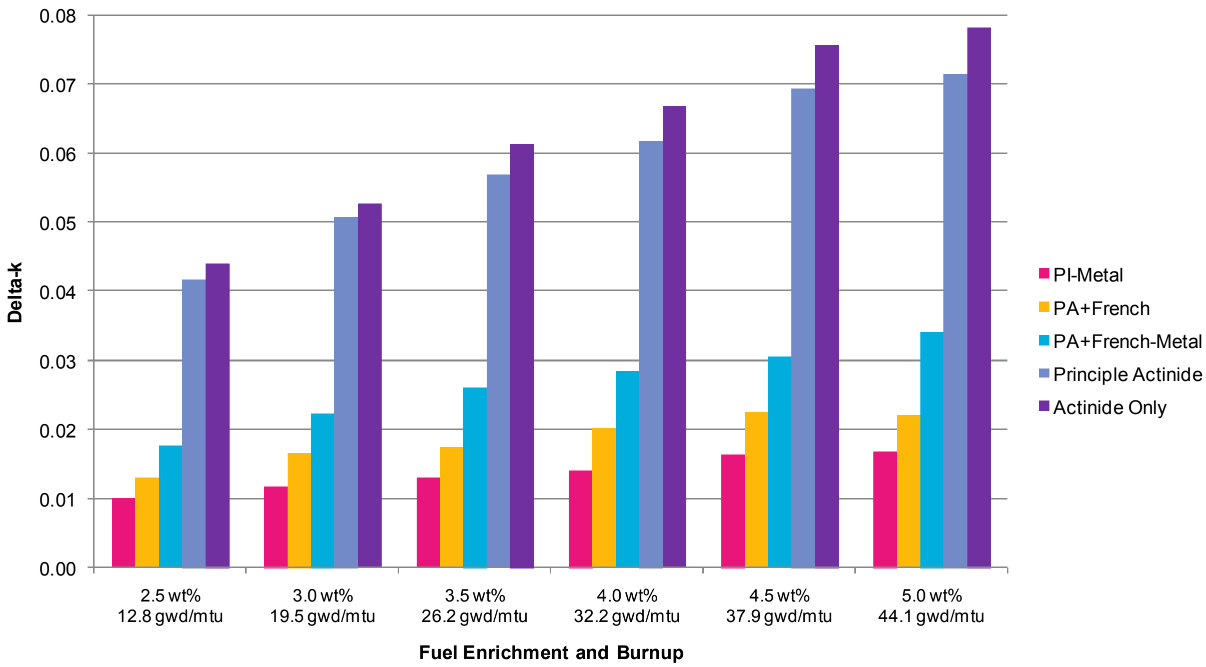


Source: Output DTN: MO0711LOADCURV.000, file: *LoadingCurve.xls*, worksheet: "Results."

Figure 6-15. Variation of Burnup Credit Isotope Set for Various PWR Base Case Conditions

### 6.2.4 Geometry Cases

#### 6.2.4.1 Assembly Position in Fuel Basket Tube

With the waste package stored in a horizontal position, fuel assemblies within the basket will rest in contact with the bottom surface of their enclosing FBT. The base case represents the assembly centered in the basket position because this provides a higher reactivity. The effect of assembly offset within the FBT is shown in Table 6-17. The bottom centered position corresponds to an offset in the –y direction of the base case representation, as shown in Figure 6-16 where the region between the assembly and the FBT is highlighted in order to emphasize the assembly offset. A similar case with offsets in both –x and –y directions, placing the assembly in a corner of the FBT is also considered. Results are shown graphically in Figure 6-17 for various combinations of PWR assembly enrichment and burnup. The base case with centered assembly is bounding.

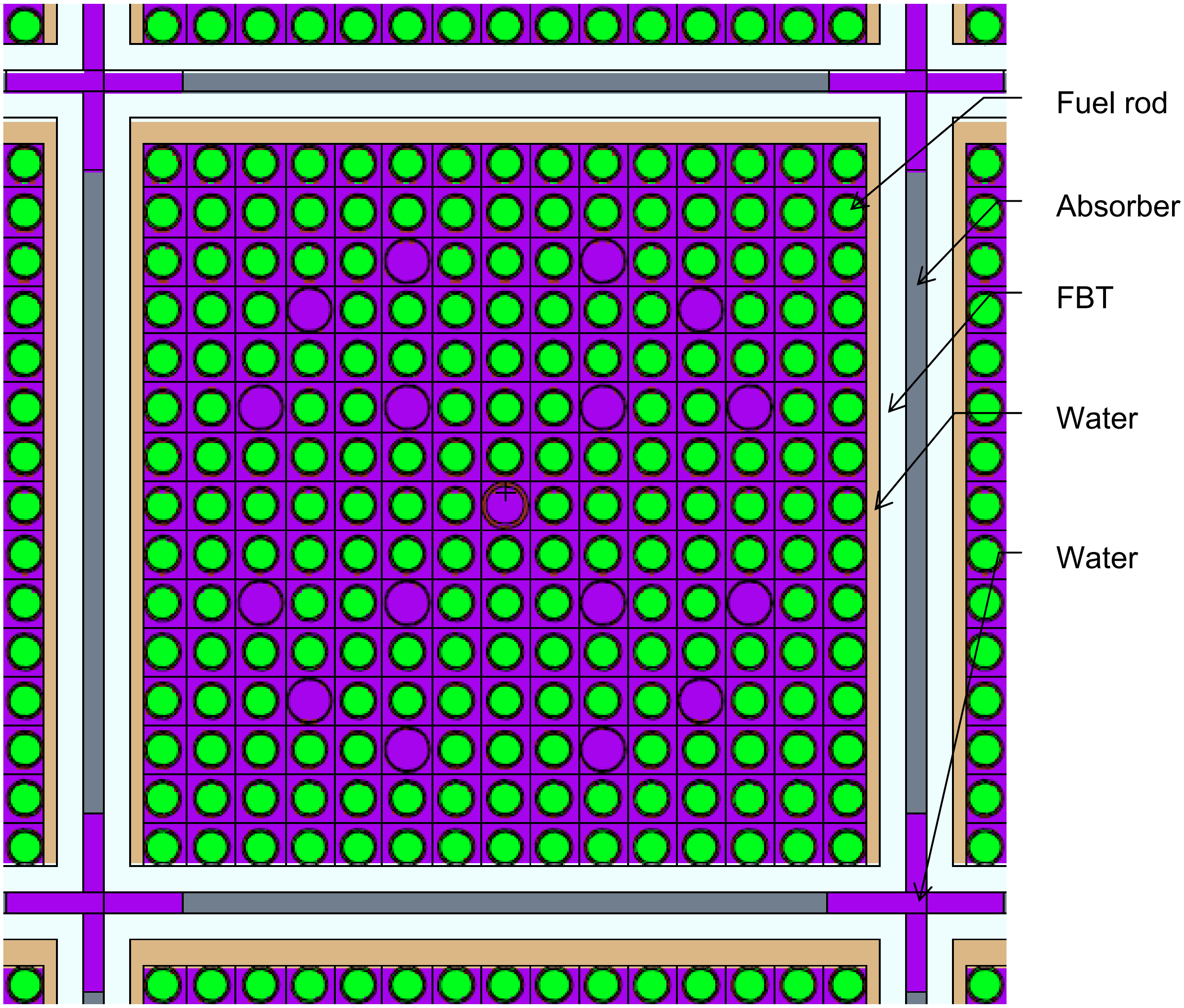


Source: For illustrative purposes.

Figure 6-16. PWR Assembly Offset in –y Direction

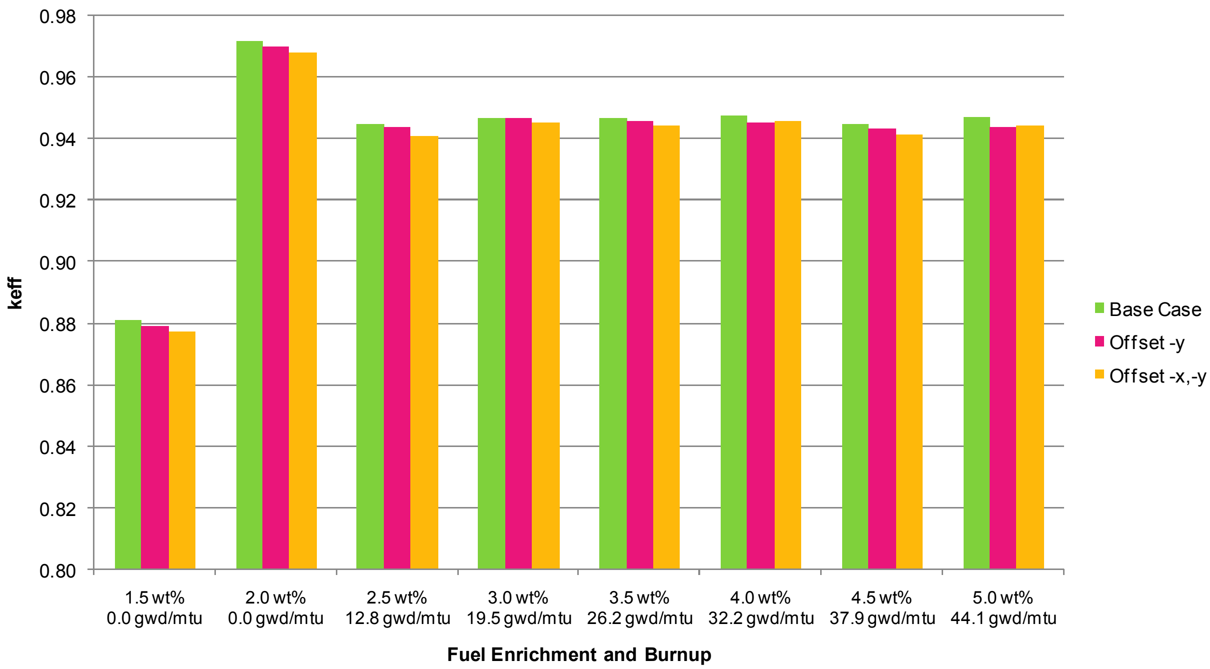


Source: Output DTN: MO0711LOADCURV.000, file: *LoadingCurve.xls*, worksheet: "Results."

Figure 6-17. Effect of PWR Assembly Offset within FBT

### 6.2.4.2 Fuel Basket Tube Thickness

The effect of varying the FBT thickness is shown in Figure 6-18 based on the results presented in Table 6-18. Two cases are considered. In the first, the FBT wall thickness is decreased 10% by increasing the inside dimension of the FBT, preserving the assembly spacing in the package. This variation shows an insignificant effect on reactivity. In the second case, the outside dimension of the FBT is adjusted to reduce the wall thickness by 10%. This variation has the effect of making the entire basket more compact, with assembly to assembly spacing reduced. As expected, the reactivity of the package increases slightly. However, the FBT and absorber plate dimensions, which determine the effective assembly spacing in the package, have minimum expected values in the base case representation. Furthermore, as the material corrodes it will expand in volume due to oxidation, effectively increasing the assembly spacing.

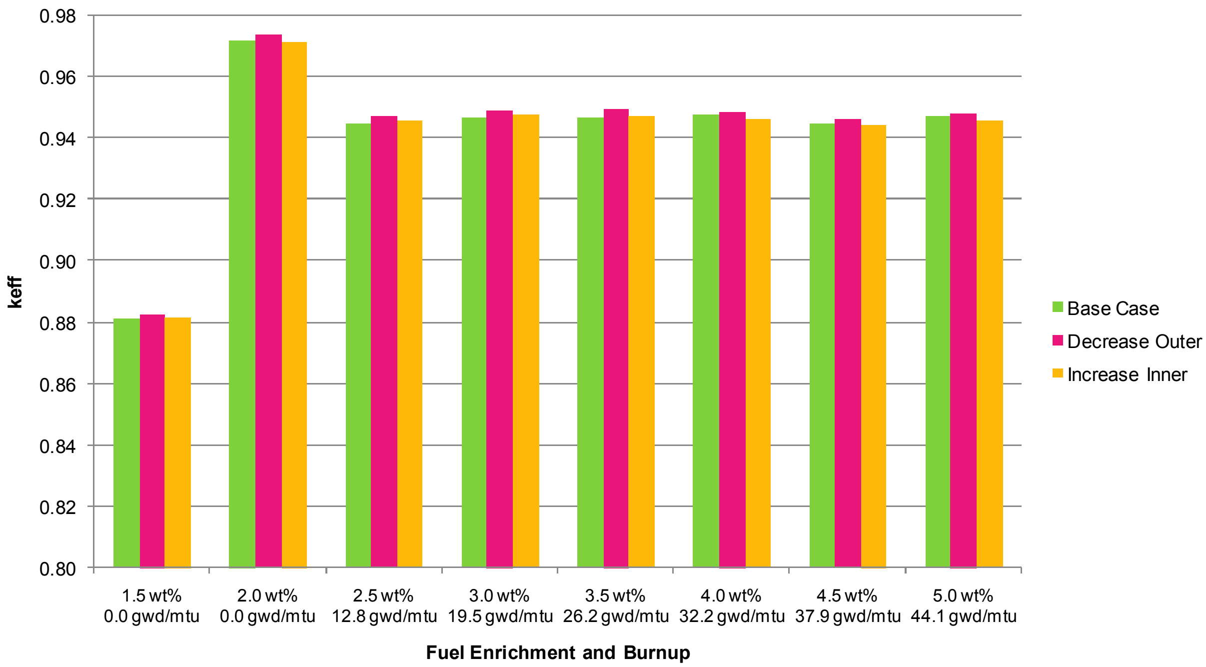


Source: Output DTN: MO0711LOADCURV.000, file: *LoadingCurve.xls*, worksheet: "Results."

Figure 6-18. Effect of Decreasing FBT Thickness 10%

#### 6.2.4.3 Absorber Plate Thickness

The effect of varying the absorber plate thickness is shown in Figure 6-19 based on the results presented in Table 6-19. As expected, a 1 mm decrease in the limiting represented thickness of 6 mm results in slightly higher reactivities for various combinations of PWR enrichment and burnup. The effect of representing the absorber at a more realistic value of 9 mm (see Section 6.1.1.2.2) results in almost a 2% reduction in $k_{eff}$. Hence, the represented absorber plate thickness of 6 mm is a significant source of conservatism in the representation.

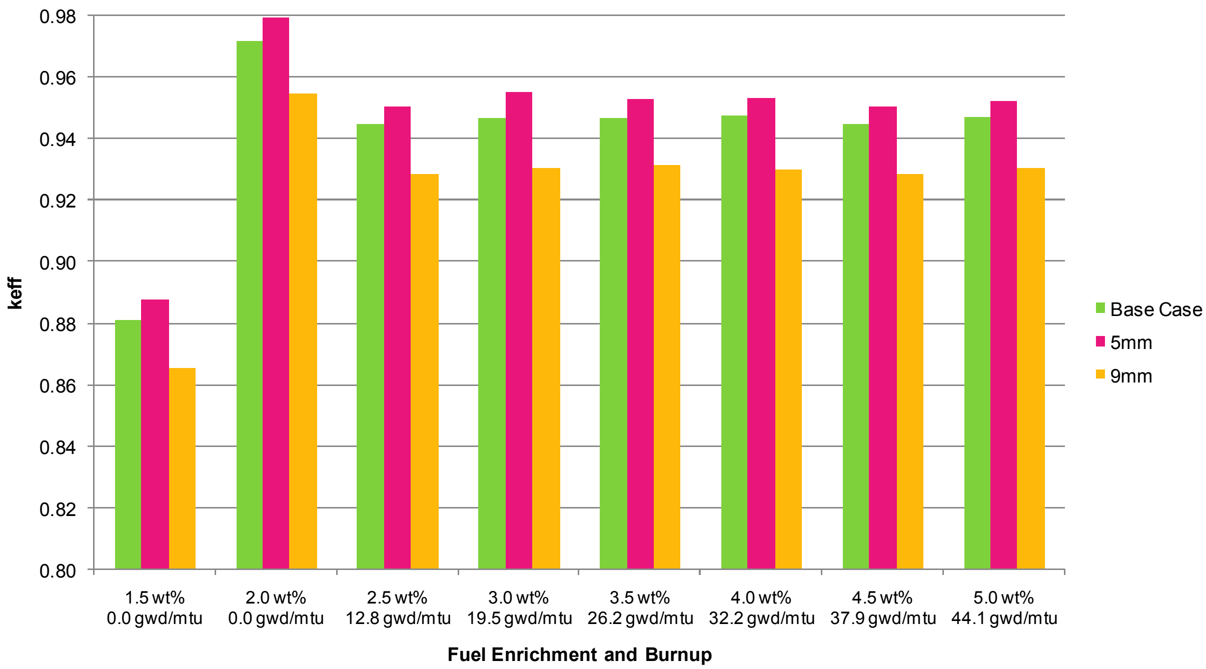


Source: Output DTN: MO0711LOADCURV.000, file: *LoadingCurve.xls*, worksheet: "Results."

Figure 6-19. Effect of Varying Absorber Thickness

### 6.2.5 Degraded Waste Form

The degraded waste form results show that all degraded conditions are less reactive than the base case representation. Figure 6-20 through Figure 6-22 show reactivity as a function of the fraction of fuel converted to schoepite (parameter $\alpha$) for PWR fuel cases at three combinations of enrichment and burnup, respectively: (3.0 wt%, 19.5 GWd/MTU), (4.0 wt%, 32.2 GWd/MTU), and (5.0 wt%, 44.1 GWd/MTU) at full saturation conditions. The fuel degradation products are represented using the "Degraded Fuel" isotopic model of Table 6-1. As the fuel degrades, the $k_{eff}$ of the waste package decreases. Also, as porosity increases, the reactivity decreases. Data are shown in Table 6-20 through Table 6-22.

The effect of saturation is shown in Figure 6-23 for the (4.0 wt%, 32.2 GWd/MTU) fuel condition with a fixed porosity of 20%. As expected, the most reactive condition is the full saturation case, and again in all cases the reactivity is less than the base case result. Data are shown in Table 6-23.

As schoepite begins to grow outside the fuel assembly, an increase in reactivity is observed as shown in Figure 6-20 through Figure 6-22. This effect is due to fissile material expanding outside of the width of the absorber plates. This effect results in line-of-sight communication between neighboring fuel assemblies and accounts for the increase in reactivity. Note that in no case is the reactivity effect significant enough to exceed the base case (no fuel degradation) reactivity.

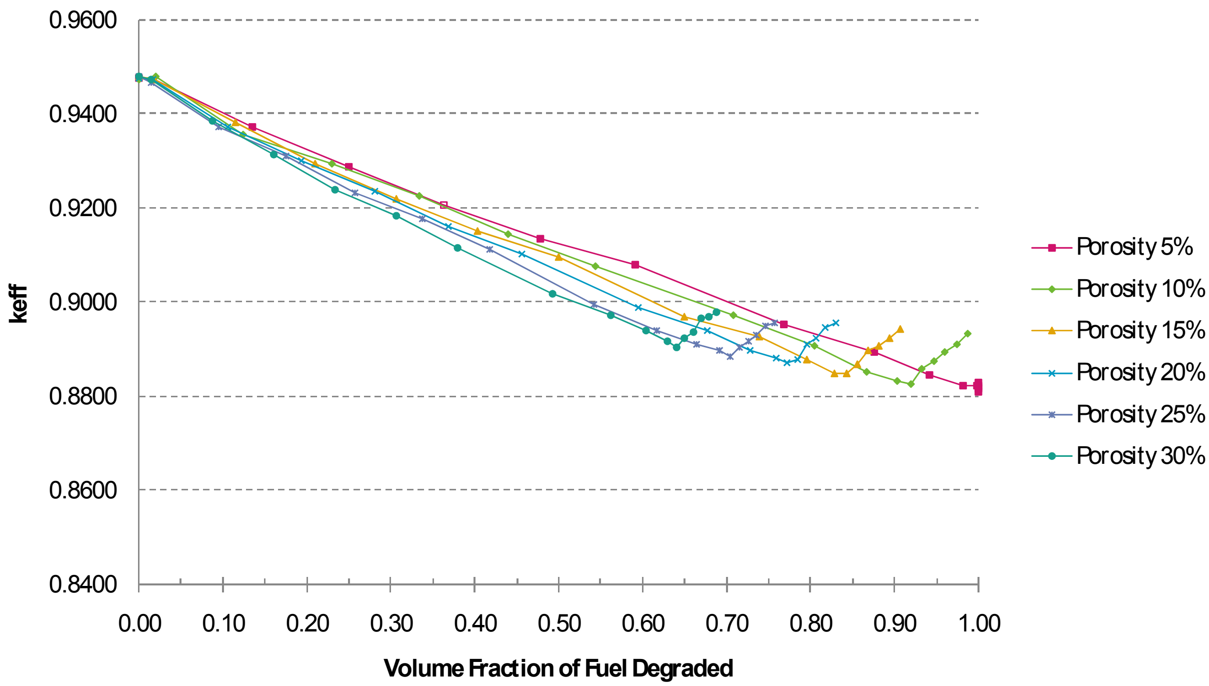


Source: Output DTN: MO0711LOADCURV.000, file: *LoadingCurve.xls*, worksheet: "Results."

Figure 6-20. Degraded Waste Form Results at Full Saturation for PWR Fuel at 3.0 wt% and 19.5 GWd/MTU

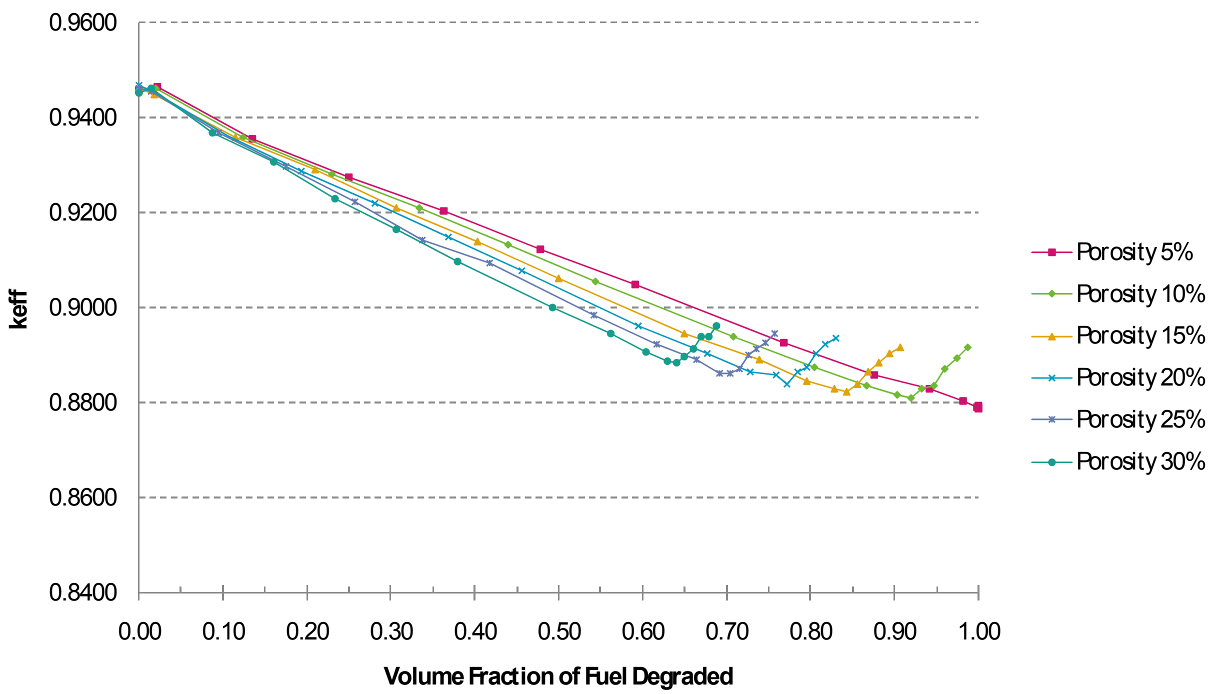


Source: Output DTN: MO0711LOADCURV.000, file: *LoadingCurve.xls*, worksheet: "Results."

Figure 6-21. Degraded Waste Form Results at Full Saturation for PWR Fuel at 4.0 wt% and 32.2 GWd/MTU

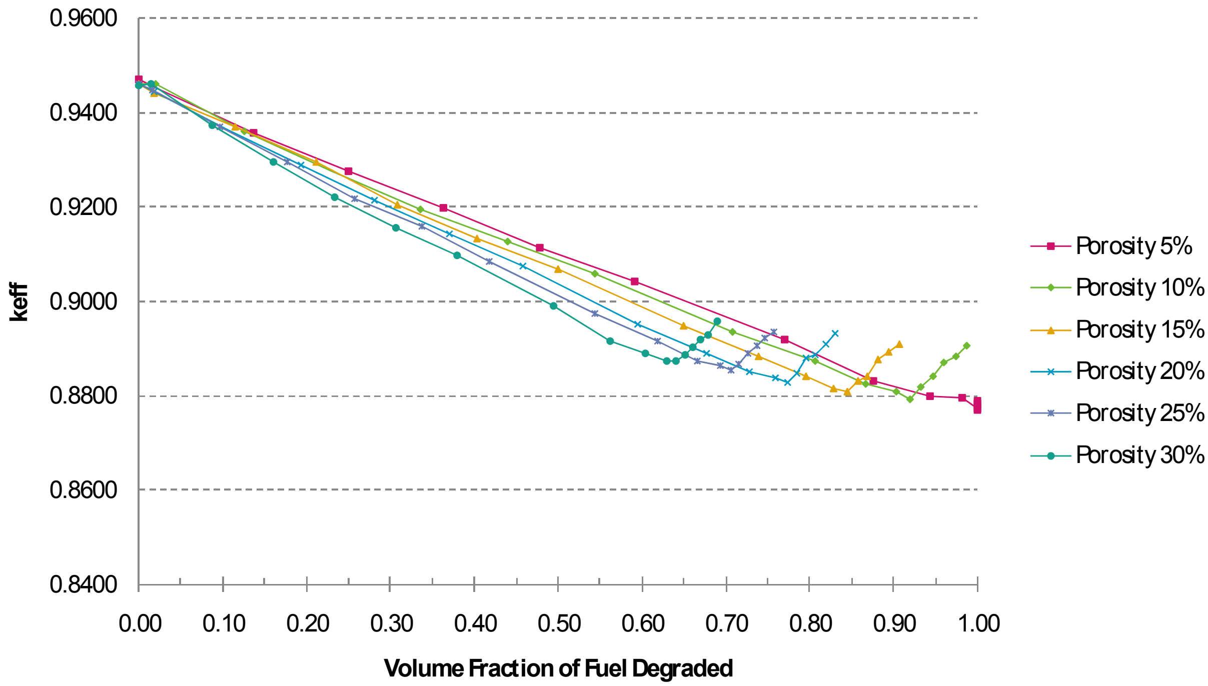


Source: Output DTN: MO0711LOADCURV.000, file: *LoadingCurve.xls*, worksheet: "Results."

Figure 6-22. Degraded Waste Form Results at Full Saturation for PWR Fuel at 5.0 wt% and 44.1 GWd/MTU

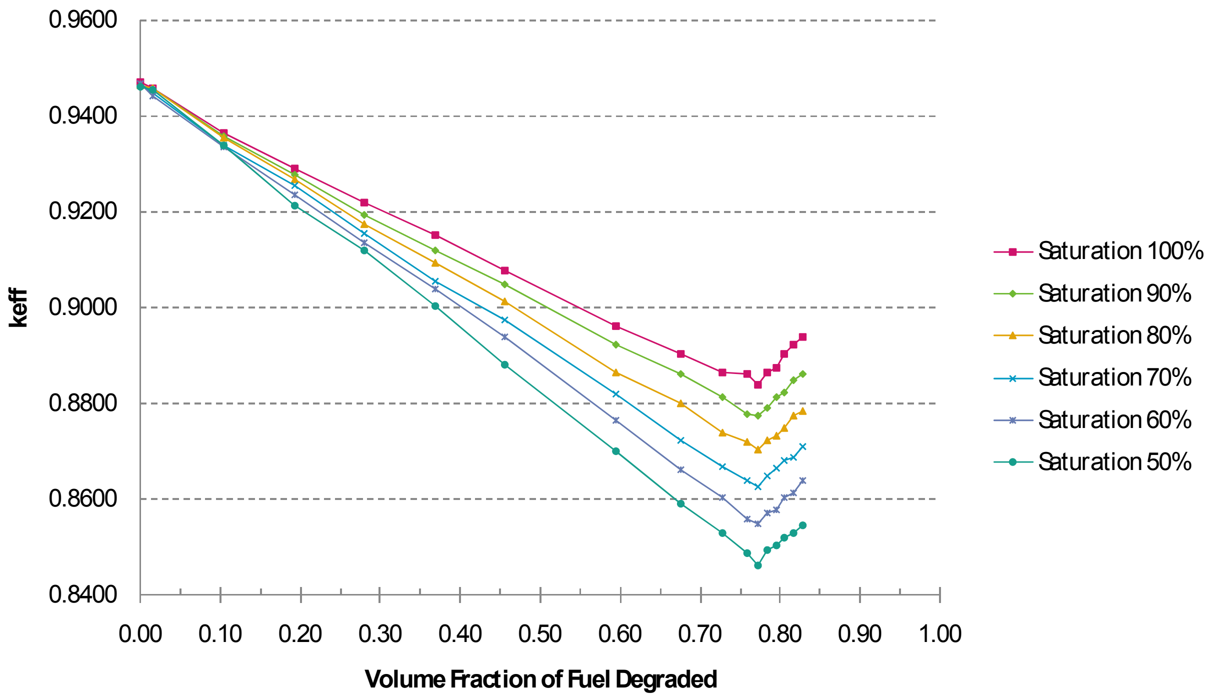


Source: Output DTN: MO0711LOADCURV.000, file: *LoadingCurve.xls*, worksheet: "Results."

Figure 6-23. Degraded Waste Form Results at 20% Porosity for PWR Fuel at 4.0 wt% and 32.2 GWd/MTU at Various Saturation Values

INTENTIONALLY LEFT BLANK

Table 6-6. Base Case Results for BW 15 × 15 with Seven Axial Zones

| Burnup | Enrichment [wt. %] | | | | | | | | | | | | | | | | | | | | | | | |
|---|---|---|---|---|---|---|---|---|---|---|---|---|---|---|---|---|---|---|---|---|---|---|---|---|
| | 1.5 | | | 2.0 | | | 2.5 | | | 3.0 | | | 3.5 | | | 4.0 | | | 4.5 | | | 5.0 | | |
| [GWd/MTU] | Case | $k_{eff}$ | σ | Case | $k_{eff}$ | σ | Case | $k_{eff}$ | σ | Case | $k_{eff}$ | σ | Case | $k_{eff}$ | σ | Case | $k_{eff}$ | σ | Case | $k_{eff}$ | σ | Case | $k_{eff}$ | σ |
| 0 | da00 | 0.88179 | 0.00019 | db00 | 0.97138 | 0.00019 | dc00 | 1.03656 | 0.00022 | dd00 | 1.08629 | 0.00022 | de00 | 1.12503 | 0.00022 | df00 | 1.15770 | 0.00022 | dg00 | 1.18447 | 0.00023 | dh00 | 1.20679 | 0.00023 |
| 10 | da10 | 0.85470 | 0.00020 | db10 | 0.91165 | 0.00020 | dc10 | 0.96081 | 0.00021 | dd10 | 1.00347 | 0.00021 | de10 | 1.03956 | 0.00022 | df10 | 1.07060 | 0.00022 | dg10 | 1.09671 | 0.00023 | dh10 | 1.12090 | 0.00023 |
| 15 | da15 | 0.83159 | 0.00019 | db15 | 0.88341 | 0.00020 | dc15 | 0.93091 | 0.00021 | dd15 | 0.97168 | 0.00022 | de15 | 1.00791 | 0.00021 | df15 | 1.03875 | 0.00022 | dg15 | 1.06629 | 0.00022 | dh15 | 1.08991 | 0.00023 |
| 20 | da20 | 0.81003 | 0.00019 | db20 | 0.85695 | 0.00020 | dc20 | 0.90074 | 0.00021 | dd20 | 0.94188 | 0.00021 | de20 | 0.97650 | 0.00022 | df20 | 1.00919 | 0.00022 | dg20 | 1.03635 | 0.00022 | dh20 | 1.06101 | 0.00022 |
| 25 | da25 | 0.79443 | 0.00018 | db25 | 0.83604 | 0.00020 | dc25 | 0.87804 | 0.00021 | dd25 | 0.91756 | 0.00021 | de25 | 0.95207 | 0.00021 | df25 | 0.98381 | 0.00022 | dg25 | 1.01190 | 0.00022 | dh25 | 1.03624 | 0.00023 |
| 30 | da30 | 0.77940 | 0.00019 | db30 | 0.81451 | 0.00019 | dc30 | 0.85336 | 0.00020 | dd30 | 0.89077 | 0.00021 | de30 | 0.92521 | 0.00021 | df30 | 0.95641 | 0.00021 | dg30 | 0.98468 | 0.00022 | dh30 | 1.01015 | 0.00023 |
| 35 | da35 | 0.76663 | 0.00019 | db35 | 0.79455 | 0.00019 | dc35 | 0.82854 | 0.00020 | dd35 | 0.86371 | 0.00021 | de35 | 0.89755 | 0.00022 | df35 | 0.92860 | 0.00021 | dg35 | 0.95675 | 0.00022 | dh35 | 0.98204 | 0.00022 |
| 40 | da40 | 0.75770 | 0.00018 | db40 | 0.78164 | 0.00019 | dc40 | 0.81341 | 0.00020 | dd40 | 0.84616 | 0.00020 | de40 | 0.87876 | 0.00021 | df40 | 0.90868 | 0.00022 | dg40 | 0.93703 | 0.00022 | dh40 | 0.96333 | 0.00022 |
| 45 | da45 | 0.74904 | 0.00019 | db45 | 0.76662 | 0.00019 | dc45 | 0.79255 | 0.00020 | dd45 | 0.82231 | 0.00020 | de45 | 0.85199 | 0.00021 | df45 | 0.88184 | 0.00021 | dg45 | 0.90994 | 0.00022 | dh45 | 0.93566 | 0.00022 |
| 50 | da50 | 0.74353 | 0.00019 | db50 | 0.75662 | 0.00019 | dc50 | 0.77880 | 0.00020 | dd50 | 0.80578 | 0.00020 | de50 | 0.83412 | 0.00021 | df50 | 0.86266 | 0.00021 | dg50 | 0.89063 | 0.00022 | dh50 | 0.91508 | 0.00022 |

Source: Output DTN: MO0711LOADCURV.000, file: *LoadingCurve.xls*, worksheet: "Results."

Table 6-7. Base Case Results for BW 15 × 15 with Seven Axial Zones – $k_{eff}$ + 2σ and EALF Values

| Burnup | Enrichment [wt. %] | | | | | | | | | | | | | | | | | | | | | | | |
|---|---|---|---|---|---|---|---|---|---|---|---|---|---|---|---|---|---|---|---|---|---|---|---|---|
| | 1.5 | | | 2.0 | | | 2.5 | | | 3.0 | | | 3.5 | | | 4.0 | | | 4.5 | | | 5.0 | | |
| [GWd/MTU] | Case | $k_{eff}$ +2σ | EALF | Case | $k_{eff}$ +2σ | EALF | Case | $k_{eff}$ +2σ | EALF | Case | $k_{eff}$ +2σ | EALF | Case | $k_{eff}$ +2σ | EALF | Case | $k_{eff}$ +2σ | EALF | Case | $k_{eff}$ +2σ | EALF | Case | $k_{eff}$ +2σ | EALF |
| 0 | da00 | 0.88217 | 0.19 | db00 | 0.97176 | 0.20 | dc00 | 1.03700 | 0.21 | dd00 | 1.08673 | 0.23 | de00 | 1.12547 | 0.25 | df00 | 1.15814 | 0.27 | dg00 | 1.18493 | 0.30 | dh00 | 1.20725 | 0.33 |
| 10 | da10 | 0.85510 | 0.30 | db10 | 0.91205 | 0.29 | dc10 | 0.96123 | 0.29 | dd10 | 1.00389 | 0.30 | de10 | 1.04000 | 0.31 | df10 | 1.07104 | 0.33 | dg10 | 1.09717 | 0.36 | dh10 | 1.12136 | 0.38 |
| 15 | da15 | 0.83197 | 0.33 | db15 | 0.88381 | 0.31 | dc15 | 0.93133 | 0.31 | dd15 | 0.97212 | 0.32 | de15 | 1.00833 | 0.33 | df15 | 1.03919 | 0.35 | dg15 | 1.06673 | 0.37 | dh15 | 1.09037 | 0.39 |
| 20 | da20 | 0.81041 | 0.36 | db20 | 0.85735 | 0.33 | dc20 | 0.90116 | 0.33 | dd20 | 0.94230 | 0.33 | de20 | 0.97694 | 0.35 | df20 | 1.00963 | 0.36 | dg20 | 1.03679 | 0.38 | dh20 | 1.06145 | 0.40 |
| 25 | da25 | 0.79479 | 0.38 | db25 | 0.83644 | 0.35 | dc25 | 0.87846 | 0.35 | dd25 | 0.91798 | 0.35 | de25 | 0.95249 | 0.36 | df25 | 0.98425 | 0.37 | dg25 | 1.01234 | 0.39 | dh25 | 1.03670 | 0.41 |
| 30 | da30 | 0.77978 | 0.41 | db30 | 0.81489 | 0.38 | dc30 | 0.85376 | 0.37 | dd30 | 0.89119 | 0.36 | de30 | 0.92563 | 0.37 | df30 | 0.95683 | 0.38 | dg30 | 0.98512 | 0.40 | dh30 | 1.01061 | 0.42 |
| 35 | da35 | 0.76701 | 0.44 | db35 | 0.79493 | 0.41 | dc35 | 0.82894 | 0.39 | dd35 | 0.86413 | 0.39 | de35 | 0.89799 | 0.39 | df35 | 0.92902 | 0.40 | dg35 | 0.95719 | 0.41 | dh35 | 0.98248 | 0.43 |
| 40 | da40 | 0.75806 | 0.46 | db40 | 0.78202 | 0.43 | dc40 | 0.81381 | 0.41 | dd40 | 0.84656 | 0.40 | de40 | 0.87918 | 0.40 | df40 | 0.90912 | 0.41 | dg40 | 0.93747 | 0.42 | dh40 | 0.96377 | 0.43 |
| 45 | da45 | 0.74942 | 0.49 | db45 | 0.76700 | 0.46 | dc45 | 0.79295 | 0.44 | dd45 | 0.82271 | 0.42 | de45 | 0.85241 | 0.42 | df45 | 0.88226 | 0.42 | dg45 | 0.91038 | 0.43 | dh45 | 0.93610 | 0.45 |
| 50 | da50 | 0.74391 | 0.51 | db50 | 0.75700 | 0.49 | dc50 | 0.77920 | 0.46 | dd50 | 0.80618 | 0.44 | de50 | 0.83454 | 0.44 | df50 | 0.86308 | 0.44 | dg50 | 0.89107 | 0.44 | dh50 | 0.91552 | 0.46 |

EALF is the energy corresponding to the average neutron lethargy causing fission, in eV.

Source: Output DTN: MO0711LOADCURV.000, file: *LoadingCurve.xls*, worksheet: "Results."

INTENTIONALLY LEFT BLANK

Table 6-8. Base Case Results for BW 15 × 15 with One Axial Zone

| Burnup | Enrichment [wt. %] | | | | | | | | | | | | | | | | | | | | | | | |
|---|---|---|---|---|---|---|---|---|---|---|---|---|---|---|---|---|---|---|---|---|---|---|---|---|
| | 1.5 | | | 2.0 | | | 2.5 | | | 3.0 | | | 3.5 | | | 4.0 | | | 4.5 | | | 5.0 | | |
| [GWd/MTU] | Case | $k_{eff}$ | σ | Case | $k_{eff}$ | σ | Case | $k_{eff}$ | σ | Case | $k_{eff}$ | σ | Case | $k_{eff}$ | σ | Case | $k_{eff}$ | σ | Case | $k_{eff}$ | σ | Case | $k_{eff}$ | σ |
| 0 | d0a00 | 0.88172 | 0.00019 | d0b00 | 0.97105 | 0.00020 | d0c00 | 1.03629 | 0.00020 | d0d00 | 1.08662 | 0.00021 | d0e00 | 1.12532 | 0.00022 | d0f00 | 1.15761 | 0.00023 | d0g00 | 1.18412 | 0.00023 | d0h00 | 1.20678 | 0.00023 |
| 5 | d0a05 | 0.88112 | 0.00019 | d0b05 | 0.94533 | 0.00021 | d0c05 | 1.00049 | 0.00021 | d0d05 | 1.04424 | 0.00021 | d0e05 | 1.08039 | 0.00022 | d0f05 | 1.11126 | 0.00023 | d0g05 | 1.13750 | 0.00022 | d0h05 | 1.15871 | 0.00022 |
| 10 | d0a10 | 0.86083 | 0.00019 | d0b10 | 0.91835 | 0.00020 | d0c10 | 0.96744 | 0.00021 | d0d10 | 1.00900 | 0.00022 | d0e10 | 1.04542 | 0.00022 | d0f10 | 1.07672 | 0.00022 | d0g10 | 1.10356 | 0.00022 | d0h10 | 1.12672 | 0.00023 |
| 15 | d0a15 | 0.83609 | 0.00019 | d0b15 | 0.88801 | 0.00020 | d0c15 | 0.93377 | 0.00020 | d0d15 | 0.97563 | 0.00021 | d0e15 | 1.01182 | 0.00022 | d0f15 | 1.04384 | 0.00022 | d0g15 | 1.07075 | 0.00022 | d0h15 | 1.09547 | 0.00022 |
| 20 | d0a20 | 0.81470 | 0.00019 | d0b20 | 0.85904 | 0.00020 | d0c20 | 0.90285 | 0.00021 | d0d20 | 0.94339 | 0.00021 | d0e20 | 0.98014 | 0.00022 | d0f20 | 1.01251 | 0.00021 | d0g20 | 1.04078 | 0.00023 | d0h20 | 1.06607 | 0.00023 |
| 25 | d0a25 | 0.79671 | 0.00018 | d0b25 | 0.83457 | 0.00019 | d0c25 | 0.87443 | 0.00020 | d0d25 | 0.91318 | 0.00021 | d0e25 | 0.94918 | 0.00021 | d0f25 | 0.98157 | 0.00022 | d0g25 | 1.01106 | 0.00022 | d0h25 | 1.03731 | 0.00022 |
| 30 | d0a30 | 0.78161 | 0.00019 | d0b30 | 0.81413 | 0.00019 | d0c30 | 0.84823 | 0.00020 | d0d30 | 0.88505 | 0.00020 | d0e30 | 0.92035 | 0.00021 | d0f30 | 0.95253 | 0.00021 | d0g30 | 0.98175 | 0.00022 | d0h30 | 1.00896 | 0.00021 |
| 35 | d0a35 | 0.77013 | 0.00019 | d0b35 | 0.79600 | 0.00019 | d0c35 | 0.82688 | 0.00019 | d0d35 | 0.85961 | 0.00020 | d0e35 | 0.89295 | 0.00021 | d0f35 | 0.92485 | 0.00022 | d0g35 | 0.95445 | 0.00022 | d0h35 | 0.98115 | 0.00022 |
| 40 | d0a40 | 0.76089 | 0.00019 | d0b40 | 0.78086 | 0.00019 | d0c40 | 0.80832 | 0.00020 | d0d40 | 0.83697 | 0.00020 | d0e40 | 0.86738 | 0.00020 | d0f40 | 0.89816 | 0.00021 | d0g40 | 0.92809 | 0.00021 | d0h40 | 0.95406 | 0.00021 |
| 45 | d0a45 | 0.75311 | 0.00019 | d0b45 | 0.76902 | 0.00019 | d0c45 | 0.79176 | 0.00019 | d0d45 | 0.81690 | 0.00020 | d0e45 | 0.84465 | 0.00020 | d0f45 | 0.87396 | 0.00020 | d0g45 | 0.90138 | 0.00021 | d0h45 | 0.92820 | 0.00022 |
| 50 | d0a50 | 0.74654 | 0.00018 | d0b50 | 0.75966 | 0.00019 | d0c50 | 0.77741 | 0.00019 | d0d50 | 0.79973 | 0.00019 | d0e50 | 0.82413 | 0.00019 | d0f50 | 0.85069 | 0.00020 | d0g50 | 0.87808 | 0.00020 | d0h50 | 0.90462 | 0.00021 |

Source: Output DTN: MO0711LOADCURV.000, file: *LoadingCurve.xls*, worksheet: "Results."

Table 6-9. Base Case Results for BW 15 × 15 with One Axial Zone – $k_{eff}$ + 2σ and EALF Values

| Burnup | Enrichment [wt. %] | | | | | | | | | | | | | | | | | | | | | | | |
|---|---|---|---|---|---|---|---|---|---|---|---|---|---|---|---|---|---|---|---|---|---|---|---|---|
| | 1.5 | | | 2.0 | | | 2.5 | | | 3.0 | | | 3.5 | | | 4.0 | | | 4.5 | | | 5.0 | | |
| [GWd/MTU] | Case | $k_{eff}$ +2σ | EALF[1] | Case | $k_{eff}$ +2σ | EALF | Case | $k_{eff}$ +2σ | EALF | Case | $k_{eff}$ +2σ | EALF | Case | $k_{eff}$ +2σ | EALF | Case | $k_{eff}$ +2σ | EALF | Case | $k_{eff}$ +2σ | EALF | Case | $k_{eff}$ +2σ | EALF |
| 0 | d0a00 | 0.88210 | 0.19 | d0b00 | 0.97145 | 0.20 | d0c00 | 1.03669 | 0.21 | d0d00 | 1.08704 | 0.23 | d0e00 | 1.12576 | 0.25 | d0f00 | 1.15807 | 0.27 | d0g00 | 1.18458 | 0.30 | d0h00 | 1.20724 | 0.33 |
| 5 | d0a05 | 0.88150 | 0.25 | d0b05 | 0.94575 | 0.25 | d0c05 | 1.00091 | 0.26 | d0d05 | 1.04466 | 0.27 | d0e05 | 1.08083 | 0.29 | d0f05 | 1.11172 | 0.31 | d0g05 | 1.13794 | 0.34 | d0h05 | 1.15915 | 0.36 |
| 10 | d0a10 | 0.86121 | 0.29 | d0b10 | 0.91875 | 0.29 | d0c10 | 0.96786 | 0.29 | d0d10 | 1.00944 | 0.30 | d0e10 | 1.04586 | 0.31 | d0f10 | 1.07716 | 0.33 | d0g10 | 1.10400 | 0.36 | d0h10 | 1.12718 | 0.38 |
| 15 | d0a15 | 0.83647 | 0.33 | d0b15 | 0.88841 | 0.32 | d0c15 | 0.93417 | 0.32 | d0d15 | 0.97605 | 0.32 | d0e15 | 1.01226 | 0.34 | d0f15 | 1.04428 | 0.35 | d0g15 | 1.07119 | 0.37 | d0h15 | 1.09591 | 0.40 |
| 20 | d0a20 | 0.81508 | 0.36 | d0b20 | 0.85944 | 0.35 | d0c20 | 0.90327 | 0.34 | d0d20 | 0.94381 | 0.34 | d0e20 | 0.98058 | 0.35 | d0f20 | 1.01293 | 0.37 | d0g20 | 1.04124 | 0.39 | d0h20 | 1.06653 | 0.41 |
| 25 | d0a25 | 0.79707 | 0.39 | d0b25 | 0.83495 | 0.37 | d0c25 | 0.87483 | 0.37 | d0d25 | 0.91360 | 0.36 | d0e25 | 0.94960 | 0.37 | d0f25 | 0.98201 | 0.38 | d0g25 | 1.01150 | 0.40 | d0h25 | 1.03775 | 0.42 |
| 30 | d0a30 | 0.78199 | 0.42 | d0b30 | 0.81451 | 0.40 | d0c30 | 0.84863 | 0.39 | d0d30 | 0.88545 | 0.39 | d0e30 | 0.92077 | 0.39 | d0f30 | 0.95295 | 0.40 | d0g30 | 0.98219 | 0.41 | d0h30 | 1.00938 | 0.43 |
| 35 | d0a35 | 0.77051 | 0.44 | d0b35 | 0.79638 | 0.43 | d0c35 | 0.82726 | 0.41 | d0d35 | 0.86001 | 0.41 | d0e35 | 0.89337 | 0.41 | d0f35 | 0.92529 | 0.41 | d0g35 | 0.95489 | 0.42 | d0h35 | 0.98159 | 0.44 |
| 40 | d0a40 | 0.76127 | 0.46 | d0b40 | 0.78124 | 0.45 | d0c40 | 0.80872 | 0.44 | d0d40 | 0.83737 | 0.43 | d0e40 | 0.86778 | 0.43 | d0f40 | 0.89858 | 0.43 | d0g40 | 0.92851 | 0.44 | d0h40 | 0.95448 | 0.45 |
| 45 | d0a45 | 0.75349 | 0.48 | d0b45 | 0.76940 | 0.47 | d0c45 | 0.79214 | 0.46 | d0d45 | 0.81730 | 0.45 | d0e45 | 0.84505 | 0.45 | d0f45 | 0.87436 | 0.45 | d0g45 | 0.90180 | 0.45 | d0h45 | 0.92864 | 0.46 |
| 50 | d0a50 | 0.74690 | 0.50 | d0b50 | 0.76004 | 0.49 | d0c50 | 0.77779 | 0.48 | d0d50 | 0.80011 | 0.48 | d0e50 | 0.82451 | 0.47 | d0f50 | 0.85109 | 0.47 | d0g50 | 0.87848 | 0.47 | d0h50 | 0.90504 | 0.48 |

[1] EALF is the energy corresponding to the average neutron lethargy causing fission, in eV.

Source: Output DTN: MO0711LOADCURV.000, file: *LoadingCurve.xls*, worksheet: "Results."

INTENTIONALLY LEFT BLANK

Table 6-10. Base Case Results for GE 7 × 7 with One Axial Zone

| Burnup | Enrichment [wt. %] | | | | | | | | | | | | | | | | | | | | | | | |
|---|---|---|---|---|---|---|---|---|---|---|---|---|---|---|---|---|---|---|---|---|---|---|---|---|
| | 1.5 | | | 2.0 | | | 2.5 | | | 3.0 | | | 3.5 | | | 4.0 | | | 4.5 | | | 5.0 | | |
| [GWd/MTU] | Case | $k_{eff}$ | σ | Case | $k_{eff}$ | σ | Case | $k_{eff}$ | σ | Case | $k_{eff}$ | σ | Case | $k_{eff}$ | σ | Case | $k_{eff}$ | σ | Case | $k_{eff}$ | σ | Case | $k_{eff}$ | σ |
| 0 | e0a00 | 0.71378 | 0.00020 | e0b00 | 0.79055 | 0.00021 | e0c00 | 0.84772 | 0.00022 | e0d00 | 0.89098 | 0.00023 | e0e00 | 0.92602 | 0.00023 | e0f00 | 0.95601 | 0.00024 | e0g00 | 0.97970 | 0.00024 | e0h00 | 1.00071 | 0.00025 |
| 5 | e0a05 | 0.79312 | 0.00021 | e0b05 | 0.82597 | 0.00022 | e0c05 | 0.85602 | 0.00023 | e0d05 | 0.88271 | 0.00023 | e0e05 | 0.90642 | 0.00024 | e0f05 | 0.92753 | 0.00023 | e0g05 | 0.94668 | 0.00025 | e0h05 | 0.96306 | 0.00024 |
| 10 | e0a10 | 0.81493 | 0.00021 | e0b10 | 0.83602 | 0.00022 | e0c10 | 0.85660 | 0.00023 | e0d10 | 0.87657 | 0.00023 | e0e10 | 0.89557 | 0.00023 | e0f10 | 0.91350 | 0.00024 | e0g10 | 0.92966 | 0.00024 | e0h10 | 0.94435 | 0.00024 |
| 15 | e0a15 | 0.82347 | 0.00022 | e0b15 | 0.83879 | 0.00023 | e0c15 | 0.85414 | 0.00023 | e0d15 | 0.87054 | 0.00022 | e0e15 | 0.88656 | 0.00023 | e0f15 | 0.90125 | 0.00023 | e0g15 | 0.91566 | 0.00023 | e0h15 | 0.92910 | 0.00024 |
| 20 | e0a20 | 0.81126 | 0.00022 | e0b20 | 0.82468 | 0.00023 | e0c20 | 0.83914 | 0.00023 | e0d20 | 0.85365 | 0.00022 | e0e20 | 0.86813 | 0.00023 | e0f20 | 0.88217 | 0.00024 | e0g20 | 0.89689 | 0.00023 | e0h20 | 0.91017 | 0.00023 |
| 25 | e0a25 | 0.80040 | 0.00022 | e0b25 | 0.81156 | 0.00022 | e0c25 | 0.82411 | 0.00022 | e0d25 | 0.83777 | 0.00022 | e0e25 | 0.85105 | 0.00023 | e0f25 | 0.86530 | 0.00023 | e0g25 | 0.87919 | 0.00023 | e0h25 | 0.89234 | 0.00023 |
| 30 | e0a30 | 0.78953 | 0.00022 | e0b30 | 0.79898 | 0.00022 | e0c30 | 0.81090 | 0.00022 | e0d30 | 0.82288 | 0.00022 | e0e30 | 0.83577 | 0.00022 | e0f30 | 0.84847 | 0.00023 | e0g30 | 0.86188 | 0.00023 | e0h30 | 0.87511 | 0.00023 |
| 35 | e0a35 | 0.78090 | 0.00022 | e0b35 | 0.78877 | 0.00022 | e0c35 | 0.79831 | 0.00022 | e0d35 | 0.80937 | 0.00022 | e0e35 | 0.82008 | 0.00023 | e0f35 | 0.83292 | 0.00023 | e0g35 | 0.84551 | 0.00023 | e0h35 | 0.85721 | 0.00023 |
| 40 | e0a40 | 0.77264 | 0.00021 | e0b40 | 0.77940 | 0.00022 | e0c40 | 0.78705 | 0.00022 | e0d40 | 0.79634 | 0.00022 | e0e40 | 0.80710 | 0.00022 | e0f40 | 0.81857 | 0.00023 | e0g40 | 0.82978 | 0.00022 | e0h40 | 0.84188 | 0.00023 |
| 45 | e0a45 | 0.76560 | 0.00021 | e0b45 | 0.77039 | 0.00021 | e0c45 | 0.77827 | 0.00022 | e0d45 | 0.78482 | 0.00022 | e0e45 | 0.79471 | 0.00022 | e0f45 | 0.80509 | 0.00022 | e0g45 | 0.81516 | 0.00022 | e0h45 | 0.82720 | 0.00022 |
| 50 | e0a50 | 0.75977 | 0.00022 | e0b50 | 0.76303 | 0.00022 | e0c50 | 0.76878 | 0.00022 | e0d50 | 0.77442 | 0.00021 | e0e50 | 0.78344 | 0.00021 | e0f50 | 0.79306 | 0.00021 | e0g50 | 0.80246 | 0.00022 | e0h50 | 0.81249 | 0.00023 |

Source: Output DTN: MO0711LOADCURV.000, file: *LoadingCurve.xls*, worksheet: "Results."

Table 6-11. Base Case Results for GE 7 × 7 with One Axial Zone – $k_{eff}$ + 2σ and EALF Values

| Burnup | Enrichment [wt. %] | | | | | | | | | | | | | | | | | | | | | | | |
|---|---|---|---|---|---|---|---|---|---|---|---|---|---|---|---|---|---|---|---|---|---|---|---|---|
| | 1.5 | | | 2.0 | | | 2.5 | | | 3.0 | | | 3.5 | | | 4.0 | | | 4.5 | | | 5.0 | | |
| [GWd/MTU] | Case | $k_{eff}$ +2σ | EALF[1] | Case | $k_{eff}$ +2σ | EALF | Case | $k_{eff}$ +2σ | EALF | Case | $k_{eff}$ +2σ | EALF | Case | $k_{eff}$ +2σ | EALF | Case | $k_{eff}$ +2σ | EALF | Case | $k_{eff}$ +2σ | EALF | Case | $k_{eff}$ +2σ | EALF |
| 0 | e0a00 | 0.71418 | 0.24 | e0b00 | 0.79097 | 0.24 | e0c00 | 0.84816 | 0.26 | e0d00 | 0.89144 | 0.28 | e0e00 | 0.92648 | 0.30 | e0f00 | 0.95649 | 0.32 | e0g00 | 0.98018 | 0.35 | e0h00 | 1.00121 | 0.38 |
| 5 | e0a05 | 0.79354 | 0.36 | e0b05 | 0.82641 | 0.36 | e0c05 | 0.85648 | 0.37 | e0d05 | 0.88317 | 0.38 | e0e05 | 0.90690 | 0.40 | e0f05 | 0.92799 | 0.42 | e0g05 | 0.94718 | 0.45 | e0h05 | 0.96354 | 0.48 |
| 10 | e0a10 | 0.81535 | 0.44 | e0b10 | 0.83646 | 0.44 | e0c10 | 0.85706 | 0.45 | e0d10 | 0.87703 | 0.46 | e0e10 | 0.89603 | 0.48 | e0f10 | 0.91398 | 0.50 | e0g10 | 0.93014 | 0.52 | e0h10 | 0.94483 | 0.55 |
| 15 | e0a15 | 0.82391 | 0.51 | e0b15 | 0.83925 | 0.51 | e0c15 | 0.85460 | 0.52 | e0d15 | 0.87098 | 0.53 | e0e15 | 0.88702 | 0.54 | e0f15 | 0.90171 | 0.56 | e0g15 | 0.91612 | 0.58 | e0h15 | 0.92958 | 0.61 |
| 20 | e0a20 | 0.81170 | 0.55 | e0b20 | 0.82514 | 0.55 | e0c20 | 0.83960 | 0.55 | e0d20 | 0.85409 | 0.56 | e0e20 | 0.86859 | 0.57 | e0f20 | 0.88265 | 0.59 | e0g20 | 0.89735 | 0.61 | e0h20 | 0.91063 | 0.63 |
| 25 | e0a25 | 0.80084 | 0.58 | e0b25 | 0.81200 | 0.58 | e0c25 | 0.82455 | 0.58 | e0d25 | 0.83821 | 0.59 | e0e25 | 0.85151 | 0.60 | e0f25 | 0.86576 | 0.61 | e0g25 | 0.87965 | 0.63 | e0h25 | 0.89280 | 0.65 |
| 30 | e0a30 | 0.78997 | 0.61 | e0b30 | 0.79942 | 0.61 | e0c30 | 0.81134 | 0.61 | e0d30 | 0.82332 | 0.62 | e0e30 | 0.83621 | 0.63 | e0f30 | 0.84893 | 0.64 | e0g30 | 0.86234 | 0.65 | e0h30 | 0.87557 | 0.67 |
| 35 | e0a35 | 0.78134 | 0.64 | e0b35 | 0.78921 | 0.64 | e0c35 | 0.79875 | 0.64 | e0d35 | 0.80981 | 0.65 | e0e35 | 0.82054 | 0.66 | e0f35 | 0.83338 | 0.66 | e0g35 | 0.84597 | 0.68 | e0h35 | 0.85767 | 0.70 |
| 40 | e0a40 | 0.77306 | 0.67 | e0b40 | 0.77984 | 0.67 | e0c40 | 0.78749 | 0.67 | e0d40 | 0.79678 | 0.68 | e0e40 | 0.80754 | 0.68 | e0f40 | 0.81903 | 0.69 | e0g40 | 0.83022 | 0.70 | e0h40 | 0.84234 | 0.72 |
| 45 | e0a45 | 0.76602 | 0.70 | e0b45 | 0.77081 | 0.70 | e0c45 | 0.77871 | 0.70 | e0d45 | 0.78526 | 0.71 | e0e45 | 0.79515 | 0.71 | e0f45 | 0.80553 | 0.72 | e0g45 | 0.81560 | 0.73 | e0h45 | 0.82764 | 0.74 |
| 50 | e0a50 | 0.76021 | 0.72 | e0b50 | 0.76347 | 0.72 | e0c50 | 0.76922 | 0.73 | e0d50 | 0.77484 | 0.73 | e0e50 | 0.78386 | 0.74 | e0f50 | 0.79348 | 0.75 | e0g50 | 0.80290 | 0.75 | e0h50 | 0.81295 | 0.77 |

[1] EALF is the energy corresponding to the average neutron lethargy causing fission, in eV.

Source: Output DTN: MO0711LOADCURV.000, file: *LoadingCurve.xls*, worksheet: "Results."

INTENTIONALLY LEFT BLANK

Table 6-12. Water Density Variation for PWR Base Case – Seven Zones

| Enrichment | Burnup | Water Density Variation | | | | | | | | | | | | | | | | | | | | |
|---|---|---|---|---|---|---|---|---|---|---|---|---|---|---|---|---|---|---|---|---|---|---|
| | | –15% | | | –10% | | | –5% | | | –3% | | | –1% | | | Base Case | | | +5% | | |
| [wt. %] | [GWd/MTU] | Case | $k_{eff}$ | σ | Case | $k_{eff}$ | σ | Case | $k_{eff}$ | σ | Case | $k_{eff}$ | σ | Case | $k_{eff}$ | σ | Case | $k_{eff}$ | σ | Case | $k_{eff}$ | σ |
| 1.5 | 0.0 | jha01 | 0.85340 | 0.00036 | jha02 | 0.86443 | 0.00035 | jha03 | 0.87275 | 0.00034 | jha06 | 0.87713 | 0.00034 | jha04 | 0.87963 | 0.00034 | j0a00 | 0.88101 | 0.00034 | jha05 | 0.88788 | 0.00035 |
| 2.0 | 0.0 | jhb01 | 0.93971 | 0.00036 | jhb02 | 0.95159 | 0.00037 | jhb03 | 0.96273 | 0.00037 | jhb06 | 0.96681 | 0.00037 | jhb04 | 0.96991 | 0.00037 | j0b00 | 0.97176 | 0.00037 | jhb05 | 0.97993 | 0.00036 |
| 2.5 | 12.8 | jhc01 | 0.90836 | 0.00038 | jhc02 | 0.92226 | 0.00039 | jhc03 | 0.93320 | 0.00039 | jhc06 | 0.93870 | 0.00040 | jhc04 | 0.94233 | 0.00038 | j0c00 | 0.94427 | 0.00038 | jhc05 | 0.95488 | 0.00038 |
| 3.0 | 19.5 | jhd01 | 0.90902 | 0.00039 | jhd02 | 0.92325 | 0.00041 | jhd03 | 0.93623 | 0.00038 | jhd06 | 0.94041 | 0.00039 | jhd04 | 0.94479 | 0.00040 | j0d00 | 0.94639 | 0.00040 | jhd05 | 0.95748 | 0.00038 |
| 3.5 | 26.2 | jhe01 | 0.90818 | 0.00039 | jhe02 | 0.92239 | 0.00040 | jhe03 | 0.93453 | 0.00039 | jhe06 | 0.93945 | 0.00040 | jhe04 | 0.94419 | 0.00039 | j0e00 | 0.94628 | 0.00038 | jhe05 | 0.95744 | 0.00039 |
| 4.0 | 32.2 | jhf01 | 0.90618 | 0.00040 | jhf02 | 0.91998 | 0.00040 | jhf03 | 0.93386 | 0.00041 | jhf06 | 0.93910 | 0.00040 | jhf04 | 0.94403 | 0.00041 | j0f00 | 0.94722 | 0.00040 | jhf05 | 0.95839 | 0.00040 |
| 4.5 | 37.9 | jhg01 | 0.90349 | 0.00039 | jhg02 | 0.91893 | 0.00039 | jhg03 | 0.93113 | 0.00039 | jhg06 | 0.93678 | 0.00041 | jhg04 | 0.94157 | 0.00041 | j0g00 | 0.94441 | 0.00040 | jhg05 | 0.95623 | 0.00040 |
| 5.0 | 44.1 | jhh01 | 0.90409 | 0.00039 | jhh02 | 0.91929 | 0.00040 | jhh03 | 0.93366 | 0.00039 | jhh06 | 0.93822 | 0.00039 | jhh04 | 0.94385 | 0.00040 | j0h00 | 0.94685 | 0.00040 | jhh05 | 0.95762 | 0.00041 |

Source: Output DTN: MO0711LOADCURV.000, file: *LoadingCurve.xls*, worksheet: "Results."

Table 6-13. Moderator Type Variation

| Enrichment | Burnup | Moderator Variation | | | | | | | | | | | |
|---|---|---|---|---|---|---|---|---|---|---|---|---|---|
| | | Base Case | | | Dry Waste Package | | | J13 Well Water | | | Wet Tuff | | |
| [wt. %] | [GWd/MTU] | Case | $k_{eff}$ | σ | Case | $k_{eff}$ | σ | Case | $k_{eff}$ | σ | Case | $k_{eff}$ | σ |
| 1.5 | 0.0 | j0a00 | 0.88101 | 0.00034 | jia00 | 0.25578 | 0.00012 | jja00 | 0.88157 | 0.00035 | jva00 | 0.88162 | 0.00034 |
| 2.0 | 0.0 | j0b00 | 0.97176 | 0.00037 | jib00 | 0.28795 | 0.00013 | jjb00 | 0.97160 | 0.00037 | jvb00 | 0.97114 | 0.00037 |
| 2.5 | 12.8 | j0c00 | 0.94427 | 0.00038 | jic00 | 0.29383 | 0.00014 | jjc00 | 0.94574 | 0.00038 | jvc00 | 0.94427 | 0.00038 |
| 3.0 | 19.5 | j0d00 | 0.94639 | 0.00040 | jid00 | 0.30362 | 0.00014 | jjd00 | 0.94693 | 0.00039 | jvd00 | 0.94735 | 0.00040 |
| 3.5 | 26.2 | j0e00 | 0.94628 | 0.00038 | jie00 | 0.31212 | 0.00013 | jje00 | 0.94580 | 0.00039 | jve00 | 0.94734 | 0.00038 |
| 4.0 | 32.2 | j0f00 | 0.94722 | 0.00040 | jif00 | 0.32004 | 0.00014 | jjf00 | 0.94606 | 0.00039 | jvf00 | 0.94640 | 0.00039 |
| 4.5 | 37.9 | j0g00 | 0.94441 | 0.00040 | jig00 | 0.32893 | 0.00014 | jjg00 | 0.94398 | 0.00039 | jvg00 | 0.94422 | 0.00039 |
| 5.0 | 44.1 | j0h00 | 0.94685 | 0.00040 | jih00 | 0.33427 | 0.00014 | jjh00 | 0.94665 | 0.00041 | jvh00 | 0.94644 | 0.00040 |

Source: Output DTN: MO0711LOADCURV.000, file: *LoadingCurve.xls*, worksheet: "Results."

Table 6-14. Variation of Boron Credit

| Enrichment | Burnup | Boron Credit | | | | | | | | | | | | | | |
|---|---|---|---|---|---|---|---|---|---|---|---|---|---|---|---|---|
| | | Base Case (75%) | | | 85% Credit | | | | | | 95% Credit | | | | | |
| [wt. %] | [GWd/MTU] | Case | $k_{eff}$ | σ | Case | $k_{eff}$ | σ | Δk | Δk/σ | % Diff | Case | $k_{eff}$ | σ | Δk | Δk/σ | % Diff |
| 1.5 | 0.0 | j0a00 | 0.88101 | 0.00034 | jga17 | 0.87864 | 0.00035 | -0.00237 | -7.0 | -0.27% | jga19 | 0.87598 | 0.00035 | -0.00503 | -14.8 | -0.57% |
| 2.0 | 0.0 | j0b00 | 0.97176 | 0.00037 | jgb17 | 0.96780 | 0.00038 | -0.00396 | -10.7 | -0.41% | jgb19 | 0.96568 | 0.00037 | -0.00608 | -16.4 | -0.63% |
| 2.5 | 12.8 | j0c00 | 0.94427 | 0.00038 | jgc17 | 0.94114 | 0.00038 | -0.00313 | -8.2 | -0.33% | jgc19 | 0.93894 | 0.00038 | -0.00533 | -14.0 | -0.56% |
| 3.0 | 19.5 | j0d00 | 0.94639 | 0.00040 | jgd17 | 0.94416 | 0.00039 | -0.00223 | -5.6 | -0.24% | jgd19 | 0.94184 | 0.00039 | -0.00455 | -11.4 | -0.48% |
| 3.5 | 26.2 | j0e00 | 0.94628 | 0.00038 | jge17 | 0.94301 | 0.00039 | -0.00327 | -8.6 | -0.35% | jge19 | 0.94075 | 0.00039 | -0.00553 | -14.6 | -0.58% |
| 4.0 | 32.2 | j0f00 | 0.94722 | 0.00040 | jgf17 | 0.94316 | 0.00040 | -0.00406 | -10.1 | -0.43% | jgf19 | 0.94079 | 0.00042 | -0.00643 | -16.1 | -0.68% |
| 4.5 | 37.9 | j0g00 | 0.94441 | 0.00040 | jgg17 | 0.94166 | 0.00041 | -0.00275 | -6.9 | -0.29% | jgg19 | 0.93738 | 0.00041 | -0.00703 | -17.6 | -0.74% |
| 5.0 | 44.1 | j0h00 | 0.94685 | 0.00040 | jgh17 | 0.94319 | 0.00041 | -0.00366 | -9.1 | -0.39% | jgh19 | 0.94097 | 0.00040 | -0.00588 | -14.7 | -0.62% |

Source: Output DTN: MO0711LOADCURV.000, file: *LoadingCurve.xls*, worksheet: "Results."

INTENTIONALLY LEFT BLANK

Table 6-15. Fuel Density Variation

| Enrichment | Burnup | Fuel Density Variation | | | | | | | | | | | | | | | | | |
|---|---|---|---|---|---|---|---|---|---|---|---|---|---|---|---|---|---|---|---|
| | | –5% | | | –2% | | | –1% | | | Base Case | | | +1% | | | +2% | | |
| [wt. %] | [GWd/MTU] | Case | $k_{eff}$ | σ | Case | $k_{eff}$ | σ | Case | $k_{eff}$ | σ | Case | $k_{eff}$ | σ | Case | $k_{eff}$ | σ | Case | $k_{eff}$ | σ |
| 1.5 | 0.0 | jka00 | 0.87282 | 0.00033 | jla00 | 0.87873 | 0.00035 | jma00 | 0.87938 | 0.00035 | j0a00 | 0.88101 | 0.00034 | jna00 | 0.88324 | 0.00034 | joa00 | 0.88394 | 0.00034 |
| 2.0 | 0.0 | jkb00 | 0.96292 | 0.00037 | jlb00 | 0.96896 | 0.00037 | jmb00 | 0.96994 | 0.00037 | j0b00 | 0.97176 | 0.00037 | jnb00 | 0.97242 | 0.00037 | job00 | 0.97408 | 0.00037 |
| 2.5 | 12.8 | jkc00 | 0.93860 | 0.00038 | jlc00 | 0.94276 | 0.00038 | jmc00 | 0.94278 | 0.00039 | j0c00 | 0.94427 | 0.00038 | jnc00 | 0.94554 | 0.00038 | joc00 | 0.94669 | 0.00038 |
| 3.0 | 19.5 | jkd00 | 0.94389 | 0.00039 | jld00 | 0.94526 | 0.00038 | jmd00 | 0.94634 | 0.00037 | j0d00 | 0.94639 | 0.00040 | jnd00 | 0.94825 | 0.00039 | jod00 | 0.94951 | 0.00038 |
| 3.5 | 26.2 | jke00 | 0.94321 | 0.00039 | jle00 | 0.94525 | 0.00039 | jme00 | 0.94550 | 0.00040 | j0e00 | 0.94628 | 0.00038 | jne00 | 0.94780 | 0.00040 | joe00 | 0.94854 | 0.00038 |
| 4.0 | 32.2 | jkf00 | 0.94297 | 0.00040 | jlf00 | 0.94537 | 0.00040 | jmf00 | 0.94575 | 0.00040 | j0f00 | 0.94722 | 0.00040 | jnf00 | 0.94710 | 0.00040 | jof00 | 0.94761 | 0.00040 |
| 4.5 | 37.9 | jkg00 | 0.94121 | 0.00041 | jlg00 | 0.94342 | 0.00038 | jmg00 | 0.94286 | 0.00040 | j0g00 | 0.94441 | 0.00040 | jng00 | 0.94449 | 0.00041 | jog00 | 0.94536 | 0.00039 |
| 5.0 | 44.1 | jkh00 | 0.94246 | 0.00040 | jlh00 | 0.94482 | 0.00041 | jmh00 | 0.94552 | 0.00040 | j0h00 | 0.94685 | 0.00040 | jnh00 | 0.94581 | 0.00040 | joh00 | 0.94710 | 0.00041 |

Source: Output DTN: MO0711LOADCURV.000, file: *LoadingCurve.xls*, worksheet: "Results."

Table 6-16. Isotope Set Variation

| Enrichment | Burnup | Principal Isotope | | | PI-Metal | | | | PA+French | | | | PA+French-Metal | | | | Principal Actinide | | | | Actinide Only | | | |
|---|---|---|---|---|---|---|---|---|---|---|---|---|---|---|---|---|---|---|---|---|---|---|---|---|
| [wt. %] | [GWd/MTU] | Case | $k_{eff}$ | σ | Case | $k_{eff}$ | σ | Δk | Case | $k_{eff}$ | σ | Δk | Case | $k_{eff}$ | σ | Δk | Case | $k_{eff}$ | σ | Δk | Case | $k_{eff}$ | σ | Δk |
| 2.5 | 12.8 | j0c00 | 0.94427 | 0.00038 | jpc00 | 0.95432 | 0.00039 | 0.01005 | jqc00 | 0.95722 | 0.00038 | 0.01295 | jrc00 | 0.96183 | 0.00038 | 0.01756 | jtc00 | 0.98599 | 0.00038 | 0.04172 | jsc00 | 0.98831 | 0.00039 | 0.04404 |
| 3.0 | 19.5 | j0d00 | 0.94639 | 0.00040 | jpd00 | 0.95820 | 0.00039 | 0.01181 | jqd00 | 0.96290 | 0.00039 | 0.01651 | jrd00 | 0.96864 | 0.00039 | 0.02225 | jtd00 | 0.99709 | 0.00038 | 0.05070 | jsd00 | 0.99912 | 0.00040 | 0.05273 |
| 3.5 | 26.2 | j0e00 | 0.94628 | 0.00038 | jpe00 | 0.95939 | 0.00039 | 0.01311 | jqe00 | 0.96369 | 0.00039 | 0.01741 | jre00 | 0.97229 | 0.00039 | 0.02601 | jte00 | 1.00323 | 0.00041 | 0.05695 | jse00 | 1.00750 | 0.00040 | 0.06122 |
| 4.0 | 32.2 | j0f00 | 0.94722 | 0.00040 | jpf00 | 0.96138 | 0.00040 | 0.01416 | jqf00 | 0.96738 | 0.00040 | 0.02016 | jrf00 | 0.97554 | 0.00039 | 0.02832 | jtf00 | 1.00883 | 0.00042 | 0.06161 | jsf00 | 1.01401 | 0.00039 | 0.06679 |
| 4.5 | 37.9 | j0g00 | 0.94441 | 0.00040 | jpg00 | 0.96078 | 0.00039 | 0.01637 | jqg00 | 0.96700 | 0.00040 | 0.02259 | jrg00 | 0.97484 | 0.00042 | 0.03043 | jtg00 | 1.01377 | 0.00042 | 0.06936 | jsg00 | 1.01998 | 0.00040 | 0.07557 |
| 5.0 | 44.1 | j0h00 | 0.94685 | 0.00040 | jph00 | 0.96356 | 0.00040 | 0.01671 | jqh00 | 0.96903 | 0.00040 | 0.02218 | jrh00 | 0.98098 | 0.00040 | 0.03413 | jth00 | 1.01824 | 0.00041 | 0.07139 | jsh00 | 1.02492 | 0.00042 | 0.07807 |

Source: Output DTN: MO0711LOADCURV.000, file: *LoadingCurve.xls*, worksheet: "Results."

Table 6-17. Assembly Position within FBT

| Enrichment | Burnup | Assembly Offset | | | | | | | | |
|---|---|---|---|---|---|---|---|---|---|---|
| | | Base Case | | | Offset –y | | | Offset –x,–y | | |
| [wt. %] | [GWd/MTU] | Case | $k_{eff}$ | σ | Case | $k_{eff}$ | σ | Case | $k_{eff}$ | σ |
| 1.5 | 0.0 | j0a00 | 0.88101 | 0.00034 | jaa00 | 0.87892 | 0.00035 | jba00 | 0.87702 | 0.00034 |
| 2.0 | 0.0 | j0b00 | 0.97176 | 0.00037 | jab00 | 0.96944 | 0.00036 | jbb00 | 0.96784 | 0.00036 |
| 2.5 | 12.8 | j0c00 | 0.94427 | 0.00038 | jac00 | 0.94356 | 0.00038 | jbc00 | 0.94060 | 0.00038 |
| 3.0 | 19.5 | j0d00 | 0.94639 | 0.00040 | jad00 | 0.94661 | 0.00039 | jbd00 | 0.94500 | 0.00039 |
| 3.5 | 26.2 | j0e00 | 0.94628 | 0.00038 | jae00 | 0.94536 | 0.00038 | jbe00 | 0.94419 | 0.00039 |
| 4.0 | 32.2 | j0f00 | 0.94722 | 0.00040 | jaf00 | 0.94481 | 0.00041 | jbf00 | 0.94536 | 0.00039 |
| 4.5 | 37.9 | j0g00 | 0.94441 | 0.00040 | jag00 | 0.94310 | 0.00039 | jbg00 | 0.94109 | 0.00041 |
| 5.0 | 44.1 | j0h00 | 0.94685 | 0.00040 | jah00 | 0.94342 | 0.00042 | jbh00 | 0.94424 | 0.00041 |

Source: Output DTN: MO0711LOADCURV.000, file: *LoadingCurve.xls*, worksheet: "Results."

INTENTIONALLY LEFT BLANK

Table 6-18. Variation of Fuel Basket Tube Thickness

| Enrichment | Burnup | FBT Thickness | | | | | | | | |
|---|---|---|---|---|---|---|---|---|---|---|
| | | Base Case | | | –10%, Adjust Outer | | | –10%, Adjust Inner | | |
| [wt. %] | [GWd/MTU] | Case | $k_{eff}$ | σ | Case | $k_{eff}$ | σ | Case | $k_{eff}$ | σ |
| 1.5 | 0.0 | j0a00 | 0.88101 | 0.00034 | jca00 | 0.88237 | 0.00034 | jda00 | 0.88161 | 0.00033 |
| 2.0 | 0.0 | j0b00 | 0.97176 | 0.00037 | jcb00 | 0.97330 | 0.00037 | jdb00 | 0.97116 | 0.00037 |
| 2.5 | 12.8 | j0c00 | 0.94427 | 0.00038 | jcc00 | 0.94690 | 0.00040 | jdc00 | 0.94532 | 0.00038 |
| 3.0 | 19.5 | j0d00 | 0.94639 | 0.00040 | jcd00 | 0.94867 | 0.00040 | jdd00 | 0.94729 | 0.00040 |
| 3.5 | 26.2 | j0e00 | 0.94628 | 0.00038 | jce00 | 0.94933 | 0.00039 | jde00 | 0.94684 | 0.00040 |
| 4.0 | 32.2 | j0f00 | 0.94722 | 0.00040 | jcf00 | 0.94816 | 0.00039 | jdf00 | 0.94614 | 0.00040 |
| 4.5 | 37.9 | j0g00 | 0.94441 | 0.00040 | jcg00 | 0.94589 | 0.00040 | jdg00 | 0.94390 | 0.00041 |
| 5.0 | 44.1 | j0h00 | 0.94685 | 0.00040 | jch00 | 0.94765 | 0.00039 | jdh00 | 0.94540 | 0.00041 |

Source: Output DTN: MO0711LOADCURV.000, file: *LoadingCurve.xls*, worksheet: "Results."

Table 6-19. Absorber Plate Thickness Variation

| Enrichment | Burnup | Absorber Plate Thickness | | | | | | | | |
|---|---|---|---|---|---|---|---|---|---|---|
| | | 5mm | | | Base Case | | | 9mm | | |
| [wt. %] | [GWd/MTU] | Case | $k_{eff}$ | σ | Case | $k_{eff}$ | σ | Case | $k_{eff}$ | σ |
| 1.5 | 0.0 | jfa00 | 0.88749 | 0.00035 | j0a00 | 0.88101 | 0.00034 | jea00 | 0.86535 | 0.00034 |
| 2.0 | 0.0 | jfb00 | 0.97892 | 0.00036 | j0b00 | 0.97176 | 0.00037 | jeb00 | 0.95441 | 0.00038 |
| 2.5 | 12.8 | jfc00 | 0.95042 | 0.00038 | j0c00 | 0.94427 | 0.00038 | jec00 | 0.92815 | 0.00038 |
| 3.0 | 19.5 | jfd00 | 0.95481 | 0.00039 | j0d00 | 0.94639 | 0.00040 | jed00 | 0.93051 | 0.00039 |
| 3.5 | 26.2 | jfe00 | 0.95279 | 0.00040 | j0e00 | 0.94628 | 0.00038 | jee00 | 0.93116 | 0.00040 |
| 4.0 | 32.2 | jff00 | 0.95296 | 0.00041 | j0f00 | 0.94722 | 0.00040 | jef00 | 0.92973 | 0.00039 |
| 4.5 | 37.9 | jfg00 | 0.95016 | 0.00039 | j0g00 | 0.94441 | 0.00040 | jeg00 | 0.92820 | 0.00040 |
| 5.0 | 44.1 | jfh00 | 0.95189 | 0.00041 | j0h00 | 0.94685 | 0.00040 | jeh00 | 0.93017 | 0.00040 |

Source: Output DTN: MO0711LOADCURV.000, file: *LoadingCurve.xls*, worksheet: "Results."

INTENTIONALLY LEFT BLANK

Table 6-20. Degraded Waste Form Results for PWR Fuel at 3.0 wt% and 19.5 GWd/MTU at 100% Saturation for Various Porosities

| | Porosity 5% | | | | Porosity 10% | | | | Porosity 15% | | | | Porosity 20% | | | | Porosity 25% | | | | Porosity 30% | | | |
|---|---|---|---|---|---|---|---|---|---|---|---|---|---|---|---|---|---|---|---|---|---|---|---|---|
| Condition | alpha | Case | $k_{eff}$ | σ | alpha | Case | $k_{eff}$ | σ | alpha | Case | $k_{eff}$ | σ | alpha | Case | $k_{eff}$ | σ | alpha | Case | $k_{eff}$ | σ | alpha | Case | $k_{eff}$ | σ |
| Initial | 0.0000 | ur01 | 0.94773 | 0.00035 | 0.0000 | us01 | 0.94748 | 0.00035 | 0.0000 | ut01 | 0.94805 | 0.00035 | 0.0000 | uu01 | 0.94775 | 0.00035 | 0.0000 | uv01 | 0.94821 | 0.00035 | 0.0000 | uw01 | 0.94804 | 0.00034 |
| Fill gap | 0.0216 | ur02 | 0.94726 | 0.00036 | 0.0199 | us02 | 0.94800 | 0.00036 | 0.0183 | ut02 | 0.94728 | 0.00035 | 0.0167 | uu02 | 0.94736 | 0.00035 | 0.0152 | uv02 | 0.94668 | 0.00034 | 0.0139 | uw02 | 0.94744 | 0.00034 |
| Fill to edge (1 of 5) | 0.1355 | ur03 | 0.93721 | 0.00035 | 0.1246 | us03 | 0.93569 | 0.00036 | 0.1144 | ut03 | 0.93822 | 0.00036 | 0.1047 | uu03 | 0.93731 | 0.00035 | 0.0956 | uv03 | 0.93748 | 0.00035 | 0.0869 | uw03 | 0.93858 | 0.00036 |
| Fill to edge (2 of 5) | 0.2494 | ur04 | 0.92879 | 0.00037 | 0.2294 | us04 | 0.92946 | 0.00035 | 0.2106 | ut04 | 0.92951 | 0.00035 | 0.1928 | uu04 | 0.93022 | 0.00036 | 0.1759 | uv04 | 0.93132 | 0.00035 | 0.1599 | uw04 | 0.93148 | 0.00035 |
| Fill to edge (3 of 5) | 0.3632 | ur05 | 0.92092 | 0.00036 | 0.3342 | us05 | 0.92270 | 0.00036 | 0.3067 | ut05 | 0.92194 | 0.00036 | 0.2808 | uu05 | 0.92361 | 0.00035 | 0.2562 | uv05 | 0.92333 | 0.00035 | 0.2330 | uw05 | 0.92411 | 0.00036 |
| Fill to edge (4 of 5) | 0.4771 | ur06 | 0.91356 | 0.00035 | 0.4389 | us06 | 0.91449 | 0.00036 | 0.4029 | ut06 | 0.91511 | 0.00036 | 0.3688 | uu06 | 0.91605 | 0.00035 | 0.3366 | uv06 | 0.91786 | 0.00035 | 0.3060 | uw06 | 0.91845 | 0.00036 |
| Filled to edge | 0.5910 | ur07 | 0.90792 | 0.00036 | 0.5437 | us07 | 0.90785 | 0.00037 | 0.4990 | ut07 | 0.90967 | 0.00035 | 0.4568 | uu07 | 0.91044 | 0.00036 | 0.4169 | uv07 | 0.91119 | 0.00036 | 0.3790 | uw07 | 0.91168 | 0.00036 |
| Fill corners (1 of 5) | 0.7689 | ur08 | 0.89529 | 0.00037 | 0.7074 | us08 | 0.89726 | 0.00036 | 0.6493 | ut08 | 0.89686 | 0.00036 | 0.5944 | uu08 | 0.89891 | 0.00036 | 0.5424 | uv08 | 0.89959 | 0.00036 | 0.4931 | uw08 | 0.90183 | 0.00036 |
| Fill corners (2 of 5) | 0.8752 | ur09 | 0.88939 | 0.00036 | 0.8052 | us09 | 0.89093 | 0.00036 | 0.7390 | ut09 | 0.89265 | 0.00035 | 0.6766 | uu09 | 0.89397 | 0.00037 | 0.6174 | uv09 | 0.89412 | 0.00036 | 0.5613 | uw09 | 0.89736 | 0.00037 |
| Fill corners (3 of 5) | 0.9421 | ur10 | 0.88474 | 0.00035 | 0.8667 | us10 | 0.88524 | 0.00037 | 0.7955 | ut10 | 0.88794 | 0.00036 | 0.7283 | uu10 | 0.89000 | 0.00037 | 0.6646 | uv10 | 0.89113 | 0.00036 | 0.6042 | uw10 | 0.89397 | 0.00037 |
| Fill corners (4 of 5) | 0.9812 | ur11 | 0.88224 | 0.00038 | 0.9027 | us11 | 0.88331 | 0.00037 | 0.8285 | ut11 | 0.88508 | 0.00037 | 0.7585 | uu11 | 0.88826 | 0.00036 | 0.6921 | uv11 | 0.88974 | 0.00037 | 0.6293 | uw11 | 0.89168 | 0.00036 |
| Filled corners | 0.9990 | ur12 | 0.88245 | 0.00037 | 0.9191 | us12 | 0.88281 | 0.00036 | 0.8436 | ut12 | 0.88499 | 0.00036 | 0.7723 | uu12 | 0.88714 | 0.00036 | 0.7047 | uv12 | 0.88862 | 0.00036 | 0.6407 | uw12 | 0.89049 | 0.00035 |
| Fill boundary (1 of 5) | 0.9992 | ur13 | 0.88236 | 0.00038 | 0.9327 | us13 | 0.88606 | 0.00037 | 0.8561 | ut13 | 0.88677 | 0.00038 | 0.7837 | uu13 | 0.88799 | 0.00035 | 0.7152 | uv13 | 0.89066 | 0.00036 | 0.6502 | uw13 | 0.89232 | 0.00036 |
| Fill boundary (2 of 5) | 0.9994 | ur14 | 0.88166 | 0.00036 | 0.9463 | us14 | 0.88773 | 0.00036 | 0.8686 | ut14 | 0.88972 | 0.00037 | 0.7952 | uu14 | 0.89124 | 0.00036 | 0.7256 | uv14 | 0.89192 | 0.00036 | 0.6597 | uw14 | 0.89386 | 0.00036 |
| Fill boundary (3 of 5) | 0.9996 | ur15 | 0.88218 | 0.00037 | 0.9599 | us15 | 0.88953 | 0.00037 | 0.8811 | ut15 | 0.89074 | 0.00037 | 0.8066 | uu15 | 0.89246 | 0.00037 | 0.7361 | uv15 | 0.89310 | 0.00036 | 0.6692 | uw15 | 0.89681 | 0.00036 |
| Fill boundary (4 of 5) | 0.9998 | ur16 | 0.88299 | 0.00037 | 0.9735 | us16 | 0.89101 | 0.00037 | 0.8936 | ut16 | 0.89244 | 0.00037 | 0.8180 | uu16 | 0.89462 | 0.00036 | 0.7465 | uv16 | 0.89518 | 0.00037 | 0.6787 | uw16 | 0.89704 | 0.00036 |
| Final | 1.0000 | ur17 | 0.88123 | 0.00037 | 0.9872 | us17 | 0.89334 | 0.00036 | 0.9061 | ut17 | 0.89430 | 0.00036 | 0.8295 | uu17 | 0.89567 | 0.00035 | 0.7570 | uv17 | 0.89587 | 0.00037 | 0.6882 | uw17 | 0.89784 | 0.00036 |

Source: Output DTN: MO0711LOADCURV.000, file: *LoadingCurve.xls*, worksheet: "Results."

Table 6-21. Degraded Waste Form Results for PWR Fuel at 4.0 wt% and 32.2 GWd/MTU at 100% Saturation for Various Porosities

| | Porosity 5% | | | | Porosity 10% | | | | Porosity 15% | | | | Porosity 20% | | | | Porosity 25% | | | | Porosity 30% | | | |
|---|---|---|---|---|---|---|---|---|---|---|---|---|---|---|---|---|---|---|---|---|---|---|---|---|
| Condition | alpha | Case | $k_{eff}$ | σ | alpha | Case | $k_{eff}$ | σ | alpha | Case | $k_{eff}$ | σ | alpha | Case | $k_{eff}$ | σ | alpha | Case | $k_{eff}$ | σ | alpha | Case | $k_{eff}$ | σ |
| Initial | 0.0000 | ua01 | 0.94597 | 0.00036 | 0.0000 | ub01 | 0.94586 | 0.00036 | 0.0000 | uc01 | 0.94635 | 0.00035 | 0.0000 | ud01 | 0.94689 | 0.00035 | 0.0000 | ue01 | 0.94609 | 0.00035 | 0.0000 | uf01 | 0.94536 | 0.00037 |
| Fill gap | 0.0216 | ua02 | 0.94645 | 0.00035 | 0.0199 | ub02 | 0.94614 | 0.00034 | 0.0183 | uc02 | 0.94492 | 0.00036 | 0.0167 | ud02 | 0.94566 | 0.00035 | 0.0152 | ue02 | 0.94562 | 0.00036 | 0.0139 | uf02 | 0.94625 | 0.00036 |
| Fill to edge (1 of 5) | 0.1355 | ua03 | 0.93574 | 0.00037 | 0.1246 | ub03 | 0.93596 | 0.00036 | 0.1144 | uc03 | 0.93604 | 0.00035 | 0.1047 | ud03 | 0.93630 | 0.00037 | 0.0956 | ue03 | 0.93703 | 0.00036 | 0.0869 | uf03 | 0.93704 | 0.00036 |
| Fill to edge (2 of 5) | 0.2494 | ua04 | 0.92767 | 0.00037 | 0.2294 | ub04 | 0.92829 | 0.00036 | 0.2106 | uc04 | 0.92914 | 0.00036 | 0.1928 | ud04 | 0.92895 | 0.00036 | 0.1759 | ue04 | 0.92984 | 0.00036 | 0.1599 | uf04 | 0.93072 | 0.00036 |
| Fill to edge (3 of 5) | 0.3632 | ua05 | 0.92058 | 0.00036 | 0.3342 | ub05 | 0.92108 | 0.00037 | 0.3067 | uc05 | 0.92095 | 0.00037 | 0.2808 | ud05 | 0.92195 | 0.00037 | 0.2562 | ue05 | 0.92226 | 0.00037 | 0.2330 | uf05 | 0.92289 | 0.00035 |
| Fill to edge (4 of 5) | 0.4771 | ua06 | 0.91239 | 0.00036 | 0.4389 | ub06 | 0.91318 | 0.00037 | 0.4029 | uc06 | 0.91407 | 0.00036 | 0.3688 | ud06 | 0.91503 | 0.00037 | 0.3366 | ue06 | 0.91416 | 0.00037 | 0.3060 | uf06 | 0.91661 | 0.00037 |
| Filled to edge | 0.5910 | ua07 | 0.90493 | 0.00038 | 0.5437 | ub07 | 0.90563 | 0.00037 | 0.4990 | uc07 | 0.90638 | 0.00037 | 0.4568 | ud07 | 0.90784 | 0.00037 | 0.4169 | ue07 | 0.90944 | 0.00036 | 0.3790 | uf07 | 0.90983 | 0.00037 |
| Fill corners (1 of 5) | 0.7689 | ua08 | 0.89260 | 0.00038 | 0.7074 | ub08 | 0.89384 | 0.00038 | 0.6493 | uc08 | 0.89464 | 0.00037 | 0.5944 | ud08 | 0.89614 | 0.00037 | 0.5424 | ue08 | 0.89838 | 0.00036 | 0.4931 | uf08 | 0.90011 | 0.00037 |
| Fill corners (2 of 5) | 0.8752 | ua09 | 0.88587 | 0.00036 | 0.8052 | ub09 | 0.88739 | 0.00039 | 0.7390 | uc09 | 0.88908 | 0.00037 | 0.6766 | ud09 | 0.89027 | 0.00036 | 0.6174 | ue09 | 0.89242 | 0.00036 | 0.5613 | uf09 | 0.89451 | 0.00037 |
| Fill corners (3 of 5) | 0.9421 | ua10 | 0.88308 | 0.00037 | 0.8667 | ub10 | 0.88363 | 0.00037 | 0.7955 | uc10 | 0.88460 | 0.00039 | 0.7283 | ud10 | 0.88657 | 0.00037 | 0.6646 | ue10 | 0.88918 | 0.00037 | 0.6042 | uf10 | 0.89089 | 0.00038 |
| Fill corners (4 of 5) | 0.9812 | ua11 | 0.88039 | 0.00038 | 0.9027 | ub11 | 0.88186 | 0.00037 | 0.8285 | uc11 | 0.88291 | 0.00037 | 0.7585 | ud11 | 0.88605 | 0.00035 | 0.6921 | ue11 | 0.88621 | 0.00038 | 0.6293 | uf11 | 0.88894 | 0.00036 |
| Filled corners | 0.9990 | ua12 | 0.87912 | 0.00037 | 0.9191 | ub12 | 0.88113 | 0.00037 | 0.8436 | uc12 | 0.88250 | 0.00038 | 0.7723 | ud12 | 0.88403 | 0.00039 | 0.7047 | ue12 | 0.88633 | 0.00037 | 0.6407 | uf12 | 0.88858 | 0.00037 |
| Fill boundary (1 of 5) | 0.9992 | ua13 | 0.87888 | 0.00038 | 0.9327 | ub13 | 0.88288 | 0.00037 | 0.8561 | uc13 | 0.88399 | 0.00038 | 0.7837 | ud13 | 0.88650 | 0.00037 | 0.7152 | ue13 | 0.88721 | 0.00038 | 0.6502 | uf13 | 0.88964 | 0.00037 |
| Fill boundary (2 of 5) | 0.9994 | ua14 | 0.87943 | 0.00038 | 0.9463 | ub14 | 0.88379 | 0.00037 | 0.8686 | uc14 | 0.88643 | 0.00037 | 0.7952 | ud14 | 0.88748 | 0.00037 | 0.7256 | ue14 | 0.88999 | 0.00039 | 0.6597 | uf14 | 0.89145 | 0.00037 |
| Fill boundary (3 of 5) | 0.9996 | ua15 | 0.87896 | 0.00037 | 0.9599 | ub15 | 0.88732 | 0.00037 | 0.8811 | uc15 | 0.88838 | 0.00037 | 0.8066 | ud15 | 0.89038 | 0.00037 | 0.7361 | ue15 | 0.89147 | 0.00036 | 0.6692 | uf15 | 0.89388 | 0.00038 |
| Fill boundary (4 of 5) | 0.9998 | ua16 | 0.87901 | 0.00036 | 0.9735 | ub16 | 0.88946 | 0.00037 | 0.8936 | uc16 | 0.89053 | 0.00037 | 0.8180 | ud16 | 0.89221 | 0.00037 | 0.7465 | ue16 | 0.89254 | 0.00036 | 0.6787 | uf16 | 0.89413 | 0.00036 |
| Final | 1.0000 | ua17 | 0.87867 | 0.00039 | 0.9872 | ub17 | 0.89183 | 0.00038 | 0.9061 | uc17 | 0.89158 | 0.00039 | 0.8295 | ud17 | 0.89378 | 0.00037 | 0.7570 | ue17 | 0.89451 | 0.00037 | 0.6882 | uf17 | 0.89634 | 0.00035 |

Source: Output DTN: MO0711LOADCURV.000, file: *LoadingCurve.xls*, worksheet: "Results."

INTENTIONALLY LEFT BLANK

Table 6-22. Degraded Waste Form Results for PWR Fuel at 5.0 wt% and 44.1 GWd/MTU at 100% Saturation for Various Porosities

| | Porosity 5% | | | | Porosity 10% | | | | Porosity 15% | | | | Porosity 20% | | | | Porosity 25% | | | | Porosity 30% | | | |
|---|---|---|---|---|---|---|---|---|---|---|---|---|---|---|---|---|---|---|---|---|---|---|---|---|
| Condition | alpha | Case | $k_{eff}$ | σ | alpha | Case | $k_{eff}$ | σ | alpha | Case | $k_{eff}$ | σ | alpha | Case | $k_{eff}$ | σ | alpha | Case | $k_{eff}$ | σ | alpha | Case | $k_{eff}$ | σ |
| Initial | 0.0000 | ul01 | 0.94701 | 0.00035 | 0.0000 | um01 | 0.94601 | 0.00037 | 0.0000 | un01 | 0.94601 | 0.00036 | 0.0000 | uo01 | 0.94602 | 0.00035 | 0.0000 | up01 | 0.94627 | 0.00037 | 0.0000 | uq01 | 0.94589 | 0.00036 |
| Fill gap | 0.0216 | ul02 | 0.94504 | 0.00036 | 0.0199 | um02 | 0.94624 | 0.00036 | 0.0183 | un02 | 0.94422 | 0.00037 | 0.0167 | uo02 | 0.94459 | 0.00037 | 0.0152 | up02 | 0.94500 | 0.00036 | 0.0139 | uq02 | 0.94612 | 0.00037 |
| Fill to edge (1 of 5) | 0.1355 | ul03 | 0.93567 | 0.00036 | 0.1246 | um03 | 0.93618 | 0.00037 | 0.1144 | un03 | 0.93708 | 0.00036 | 0.1047 | uo03 | 0.93636 | 0.00036 | 0.0956 | up03 | 0.93697 | 0.00037 | 0.0869 | uq03 | 0.93727 | 0.00036 |
| Fill to edge (2 of 5) | 0.2494 | ul04 | 0.92773 | 0.00037 | 0.2294 | um04 | 0.92758 | 0.00037 | 0.2106 | un04 | 0.92948 | 0.00036 | 0.1928 | uo04 | 0.92907 | 0.00036 | 0.1759 | up04 | 0.92960 | 0.00036 | 0.1599 | uq04 | 0.92967 | 0.00037 |
| Fill to edge (3 of 5) | 0.3632 | ul05 | 0.92004 | 0.00037 | 0.3342 | um05 | 0.91952 | 0.00036 | 0.3067 | un05 | 0.92039 | 0.00036 | 0.2808 | uo05 | 0.92137 | 0.00038 | 0.2562 | up05 | 0.92185 | 0.00035 | 0.2330 | uq05 | 0.92210 | 0.00037 |
| Fill to edge (4 of 5) | 0.4771 | ul06 | 0.91154 | 0.00037 | 0.4389 | um06 | 0.91288 | 0.00037 | 0.4029 | un06 | 0.91356 | 0.00036 | 0.3688 | uo06 | 0.91426 | 0.00037 | 0.3366 | up06 | 0.91614 | 0.00037 | 0.3060 | uq06 | 0.91568 | 0.00037 |
| Filled to edge | 0.5910 | ul07 | 0.90443 | 0.00038 | 0.5437 | um07 | 0.90596 | 0.00037 | 0.4990 | un07 | 0.90694 | 0.00037 | 0.4568 | uo07 | 0.90759 | 0.00037 | 0.4169 | up07 | 0.90862 | 0.00035 | 0.3790 | uq07 | 0.90986 | 0.00038 |
| Fill corners (1 of 5) | 0.7689 | ul08 | 0.89198 | 0.00038 | 0.7074 | um08 | 0.89370 | 0.00037 | 0.6493 | un08 | 0.89482 | 0.00038 | 0.5944 | uo08 | 0.89521 | 0.00037 | 0.5424 | up08 | 0.89742 | 0.00036 | 0.4931 | uq08 | 0.89911 | 0.00038 |
| Fill corners (2 of 5) | 0.8752 | ul09 | 0.88338 | 0.00037 | 0.8052 | um09 | 0.88738 | 0.00038 | 0.7390 | un09 | 0.88841 | 0.00039 | 0.6766 | uo09 | 0.88907 | 0.00038 | 0.6174 | up09 | 0.89160 | 0.00038 | 0.5613 | uq09 | 0.89176 | 0.00037 |
| Fill corners (3 of 5) | 0.9421 | ul10 | 0.87983 | 0.00039 | 0.8667 | um10 | 0.88242 | 0.00037 | 0.7955 | un10 | 0.88432 | 0.00037 | 0.7283 | uo10 | 0.88528 | 0.00038 | 0.6646 | up10 | 0.88760 | 0.00038 | 0.6042 | uq10 | 0.88913 | 0.00038 |
| Fill corners (4 of 5) | 0.9812 | ul11 | 0.87951 | 0.00037 | 0.9027 | um11 | 0.88112 | 0.00038 | 0.8285 | un11 | 0.88168 | 0.00038 | 0.7585 | uo11 | 0.88388 | 0.00036 | 0.6921 | up11 | 0.88638 | 0.00038 | 0.6293 | uq11 | 0.88733 | 0.00037 |
| Filled corners | 0.9990 | ul12 | 0.87733 | 0.00038 | 0.9191 | um12 | 0.87928 | 0.00039 | 0.8436 | un12 | 0.88097 | 0.00038 | 0.7723 | uo12 | 0.88295 | 0.00036 | 0.7047 | up12 | 0.88536 | 0.00037 | 0.6407 | uq12 | 0.88757 | 0.00037 |
| Fill boundary (1 of 5) | 0.9992 | ul13 | 0.87764 | 0.00038 | 0.9327 | um13 | 0.88178 | 0.00038 | 0.8561 | un13 | 0.88312 | 0.00038 | 0.7837 | uo13 | 0.88501 | 0.00038 | 0.7152 | up13 | 0.88664 | 0.00037 | 0.6502 | uq13 | 0.88876 | 0.00037 |
| Fill boundary (2 of 5) | 0.9994 | ul14 | 0.87711 | 0.00038 | 0.9463 | um14 | 0.88427 | 0.00037 | 0.8686 | un14 | 0.88408 | 0.00039 | 0.7952 | uo14 | 0.88811 | 0.00038 | 0.7256 | up14 | 0.88895 | 0.00038 | 0.6597 | uq14 | 0.89030 | 0.00036 |
| Fill boundary (3 of 5) | 0.9996 | ul15 | 0.87889 | 0.00037 | 0.9599 | um15 | 0.88716 | 0.00039 | 0.8811 | un15 | 0.88790 | 0.00038 | 0.8066 | uo15 | 0.88862 | 0.00038 | 0.7361 | up15 | 0.89070 | 0.00038 | 0.6692 | uq15 | 0.89203 | 0.00038 |
| Fill boundary (4 of 5) | 0.9998 | ul16 | 0.87830 | 0.00038 | 0.9735 | um16 | 0.88835 | 0.00039 | 0.8936 | un16 | 0.88926 | 0.00038 | 0.8180 | uo16 | 0.89110 | 0.00037 | 0.7465 | up16 | 0.89237 | 0.00038 | 0.6787 | uq16 | 0.89285 | 0.00037 |
| Final | 1.0000 | ul17 | 0.87841 | 0.00039 | 0.9872 | um17 | 0.89081 | 0.00038 | 0.9061 | un17 | 0.89106 | 0.00039 | 0.8295 | uo17 | 0.89316 | 0.00037 | 0.7570 | up17 | 0.89362 | 0.00039 | 0.6882 | uq17 | 0.89603 | 0.00039 |

Source: Output DTN: MO0711LOADCURV.000, file: *LoadingCurve.xls*, worksheet: "Results."

Table 6-23. Degraded Waste Form Results for PWR Fuel at 4.0 wt% and 32.2 GWd/MTU at 20% Porosity for Various Saturations

| | Saturation 100% | | | | Saturation 90% | | | | Saturation 80% | | | | Saturation 70% | | | | Saturation 60% | | | | Saturation 50% | | | |
|---|---|---|---|---|---|---|---|---|---|---|---|---|---|---|---|---|---|---|---|---|---|---|---|---|
| Condition | alpha | Case | $k_{eff}$ | σ | alpha | Case | $k_{eff}$ | σ | alpha | Case | $k_{eff}$ | σ | alpha | Case | $k_{eff}$ | σ | alpha | Case | $k_{eff}$ | σ | alpha | Case | $k_{eff}$ | σ |
| Initial | 0.0000 | ud01 | 0.94689 | 0.00035 | 0.0000 | ug01 | 0.94609 | 0.00035 | 0.0000 | uh01 | 0.94638 | 0.00036 | 0.0000 | ui01 | 0.94655 | 0.00037 | 0.0000 | uj01 | 0.94664 | 0.00037 | 0.0000 | uk01 | 0.94613 | 0.00036 |
| Fill gap | 0.0167 | ud02 | 0.94566 | 0.00035 | 0.0167 | ug02 | 0.94557 | 0.00035 | 0.0167 | uh02 | 0.94558 | 0.00035 | 0.0167 | ui02 | 0.94492 | 0.00036 | 0.0167 | uj02 | 0.94422 | 0.00034 | 0.0167 | uk02 | 0.94544 | 0.00035 |
| Fill to edge (1 of 5) | 0.1047 | ud03 | 0.93630 | 0.00037 | 0.1047 | ug03 | 0.93584 | 0.00037 | 0.1047 | uh03 | 0.93541 | 0.00036 | 0.1047 | ui03 | 0.93381 | 0.00037 | 0.1047 | uj03 | 0.93353 | 0.00035 | 0.1047 | uk03 | 0.93370 | 0.00036 |
| Fill to edge (2 of 5) | 0.1928 | ud04 | 0.92895 | 0.00036 | 0.1928 | ug04 | 0.92758 | 0.00036 | 0.1928 | uh04 | 0.92669 | 0.00035 | 0.1928 | ui04 | 0.92551 | 0.00037 | 0.1928 | uj04 | 0.92343 | 0.00037 | 0.1928 | uk04 | 0.92116 | 0.00036 |
| Fill to edge (3 of 5) | 0.2808 | ud05 | 0.92195 | 0.00037 | 0.2808 | ug05 | 0.91941 | 0.00037 | 0.2808 | uh05 | 0.91752 | 0.00036 | 0.2808 | ui05 | 0.91532 | 0.00038 | 0.2808 | uj05 | 0.91345 | 0.00037 | 0.2808 | uk05 | 0.91184 | 0.00036 |
| Fill to edge (4 of 5) | 0.3688 | ud06 | 0.91503 | 0.00037 | 0.3688 | ug06 | 0.91178 | 0.00037 | 0.3688 | uh06 | 0.90928 | 0.00037 | 0.3688 | ui06 | 0.90551 | 0.00036 | 0.3688 | uj06 | 0.90397 | 0.00037 | 0.3688 | uk06 | 0.90042 | 0.00037 |
| Filled to edge | 0.4568 | ud07 | 0.90784 | 0.00037 | 0.4568 | ug07 | 0.90469 | 0.00038 | 0.4568 | uh07 | 0.90123 | 0.00038 | 0.4568 | ui07 | 0.89756 | 0.00036 | 0.4568 | uj07 | 0.89387 | 0.00037 | 0.4568 | uk07 | 0.88805 | 0.00036 |
| Fill corners (1 of 5) | 0.5944 | ud08 | 0.89614 | 0.00037 | 0.5944 | ug08 | 0.89225 | 0.00038 | 0.5944 | uh08 | 0.88641 | 0.00036 | 0.5944 | ui08 | 0.88210 | 0.00037 | 0.5944 | uj08 | 0.87658 | 0.00036 | 0.5944 | uk08 | 0.87004 | 0.00036 |
| Fill corners (2 of 5) | 0.6766 | ud09 | 0.89027 | 0.00036 | 0.6766 | ug09 | 0.88604 | 0.00037 | 0.6766 | uh09 | 0.88007 | 0.00037 | 0.6766 | ui09 | 0.87234 | 0.00036 | 0.6766 | uj09 | 0.86613 | 0.00036 | 0.6766 | uk09 | 0.85908 | 0.00035 |
| Fill corners (3 of 5) | 0.7283 | ud10 | 0.88657 | 0.00037 | 0.7283 | ug10 | 0.88131 | 0.00037 | 0.7283 | uh10 | 0.87381 | 0.00038 | 0.7283 | ui10 | 0.86668 | 0.00038 | 0.7283 | uj10 | 0.86029 | 0.00037 | 0.7283 | uk10 | 0.85310 | 0.00037 |
| Fill corners (4 of 5) | 0.7585 | ud11 | 0.88605 | 0.00035 | 0.7585 | ug11 | 0.87786 | 0.00038 | 0.7585 | uh11 | 0.87197 | 0.00037 | 0.7585 | ui11 | 0.86401 | 0.00038 | 0.7585 | uj11 | 0.85583 | 0.00037 | 0.7585 | uk11 | 0.84862 | 0.00037 |
| Filled corners | 0.7723 | ud12 | 0.88403 | 0.00039 | 0.7723 | ug12 | 0.87729 | 0.00037 | 0.7723 | uh12 | 0.87026 | 0.00037 | 0.7723 | ui12 | 0.86278 | 0.00036 | 0.7723 | uj12 | 0.85503 | 0.00037 | 0.7723 | uk12 | 0.84627 | 0.00036 |
| Fill boundary (1 of 5) | 0.7837 | ud13 | 0.88650 | 0.00037 | 0.7837 | ug13 | 0.87895 | 0.00037 | 0.7837 | uh13 | 0.87237 | 0.00037 | 0.7837 | ui13 | 0.86478 | 0.00038 | 0.7837 | uj13 | 0.85711 | 0.00036 | 0.7837 | uk13 | 0.84935 | 0.00037 |
| Fill boundary (2 of 5) | 0.7952 | ud14 | 0.88748 | 0.00037 | 0.7952 | ug14 | 0.88137 | 0.00038 | 0.7952 | uh14 | 0.87328 | 0.00037 | 0.7952 | ui14 | 0.86638 | 0.00038 | 0.7952 | uj14 | 0.85782 | 0.00037 | 0.7952 | uk14 | 0.85039 | 0.00037 |
| Fill boundary (3 of 5) | 0.8066 | ud15 | 0.89038 | 0.00037 | 0.8066 | ug15 | 0.88232 | 0.00036 | 0.8066 | uh15 | 0.87474 | 0.00036 | 0.8066 | ui15 | 0.86823 | 0.00038 | 0.8066 | uj15 | 0.86040 | 0.00037 | 0.8066 | uk15 | 0.85191 | 0.00038 |
| Fill boundary (4 of 5) | 0.8180 | ud16 | 0.89221 | 0.00037 | 0.8180 | ug16 | 0.88495 | 0.00037 | 0.8180 | uh16 | 0.87743 | 0.00038 | 0.8180 | ui16 | 0.86881 | 0.00037 | 0.8180 | uj16 | 0.86125 | 0.00036 | 0.8180 | uk16 | 0.85295 | 0.00038 |
| Final | 0.8295 | ud17 | 0.89378 | 0.00037 | 0.8295 | ug17 | 0.88603 | 0.00036 | 0.8295 | uh17 | 0.87833 | 0.00037 | 0.8295 | ui17 | 0.87110 | 0.00037 | 0.8295 | uj17 | 0.86378 | 0.00038 | 0.8295 | uk17 | 0.85456 | 0.00038 |

Source: Output DTN: MO0711LOADCURV.000, file: *LoadingCurve.xls*, worksheet: "Results."

INTENTIONALLY LEFT BLANK

## 6.3 LOADING CURVE ANALYSIS

The base case reactivities obtained as a function of enrichment and burnup in Section 6.2.1 are used to develop loading curves for PWR and BWR fuel types. The loading curve specifies the minimum required burnup a fuel assembly must have to permit loading in a waste package, as a function of assembly initial enrichment. The curves are obtained by determining the burnup value at which waste package reactivity is equal to a certain critical limit as given by Equation 1 on p. 6-1.

### 6.3.1 Critical Limits

The critical limit for PWR and BWR assemblies with burnup is 0.9529. This value accounts for the lower bound tolerance limit f(x) shown in Table 4-15 of 0.9778 and an isotopic composition bias, $\Delta k_{ISO}$, of 0.0249 from Table 4-2. All calculations fall within the required energy corresponding to the average neutron lethargy causing fission (EALF) parameter range; hence no extension of the range of applicability is required and the term $\Delta k_{EROA}$ in Equation 1 is zero.

The combined critical limit for burned fuel is therefore set at 0.9778 – 0.0249 = 0.9529 for both PWR and BWR analyses.

For fresh fuel assemblies, the lower bound tolerance limit from Table 4-15 is 0.9905. All calculations fall within the required EALF parameter range; hence no adjustment for range of applicability bias is necessary for the cases presented here. Also, since the fresh fuel isotopics are known, no isotopic uncertainty bias is required. Hence, the critical limit for fresh fuel assemblies is 0.9905.

### 6.3.2 PWR Loading Curve

The PWR loading curve analysis is summarized in Table 6-24 and Table 6-25 for the seven-zone and one-zone results, respectively. In each case, the applicable fresh fuel and burned fuel critical limits are evaluated. The maximum analyzed enrichment value which meets the fresh fuel critical limit is determined, and the required minimum burnup is zero for enrichments less than this value. For enrichments equal to or greater than this maximum fresh fuel enrichment, the required minimum burnup is determined by linearly interpolating to find the burnup at which package reactivity is equal to the critical limit in the $k_{eff} + 2\sigma$ reactivity results of Table 6-7 and Table 6-9. This procedure introduces a step in the loading curve at the maximum allowable fresh fuel enrichment.

The analysis also checks whether the EALF values for each case fall within the applicable range of applicability for the fresh fuel and burned fuel critical limits. In all cases, the EALF values fall within the range of applicability.

The loading curve exhibits a step at the transition between the fresh fuel critical limit and the burnup credit critical limit.

The maximum of the seven- and one-zone required minimum burnup values is used. The resulting minimum burnup value is increased by 5% to provide margin against uncertainty in measured assembly burnup values. This margin conservatively bounds the 4.2% maximum burnup uncertainty determined in *Reactor Record Uncertainty Determination* (Massie 2004 [DIRS 170651], Tables 10A, 10B, and 10C). The resulting loading curve is shown in Figure 6-24 and Table 6-26.

By fitting the loading curve data in Table 6-26 above the step at 2.0 wt. %, the PWR loading curve is accurately represented using the following formula which gives the minimum required burnup $b$ in GWd/MTU as a function of enrichment, $e$, in wt. %. Note carefully that the quantity $e$ employed in the formula has units of weight *percent*, not weight *fraction*.

$$b = \begin{cases} 0 \text{ for } e < 2.0\,\text{wt.\%} \\ 0.4854\text{e}^5 - 8.6621e^4 + 60.9498e^3 - 211.9900e^2 + 378.3106e - 269.4040 \\ \text{for } 2.0\,\text{wt.\%} \le e \le 5.0\,\text{wt.\%} \end{cases}$$

Source: Output DTN: MO0711LOADCURV.000, file: *LoadingCurve.xls,* worksheet: "LoadingCurve."

Table 6-24. PWR Loading Curve Analysis for Seven Zone Axial Results

| | Fresh Fuel | | | | Burned Fuel | | | | Burnup at |
|---|---|---|---|---|---|---|---|---|---|
| Enrichment [wt %] | Critical Limit | EALF Range [eV] | EALF In Range? | Limit Met? | Critical Limit | EALF Range [eV] | EALF In Range? | Burnup [GWd/MTU] | Critical Limit [GWd/MTU] |
| 1.5 | 0.9905 | 0.0977 ≤ EALF ≤ 0.3882 | TRUE | TRUE | 0.9529 | 0.0684 ≤ EALF ≤ 1.041 | TRUE | 0.0 | 0.0 |
| 2.0 | 0.9905 | 0.0977 ≤ EALF ≤ 0.3882 | TRUE | TRUE | 0.9529 | 0.0684 ≤ EALF ≤ 1.041 | TRUE | 3.2 | 0.0 |
| 2.5 | 0.9905 | 0.0977 ≤ EALF ≤ 0.3882 | TRUE | FALSE | 0.9529 | 0.0684 ≤ EALF ≤ 1.041 | TRUE | 11.4 | 11.4 |
| 3.0 | 0.9905 | 0.0977 ≤ EALF ≤ 0.3882 | TRUE | FALSE | 0.9529 | 0.0684 ≤ EALF ≤ 1.041 | TRUE | 18.2 | 18.2 |
| 3.5 | 0.9905 | 0.0977 ≤ EALF ≤ 0.3882 | TRUE | FALSE | 0.9529 | 0.0684 ≤ EALF ≤ 1.041 | TRUE | 24.9 | 24.9 |
| 4.0 | 0.9905 | 0.0977 ≤ EALF ≤ 0.3882 | TRUE | FALSE | 0.9529 | 0.0684 ≤ EALF ≤ 1.041 | TRUE | 30.7 | 30.7 |
| 4.5 | 0.9905 | 0.0977 ≤ EALF ≤ 0.3882 | TRUE | FALSE | 0.9529 | 0.0684 ≤ EALF ≤ 1.041 | TRUE | 36.1 | 36.1 |
| 5.0 | 0.9905 | 0.0977 ≤ EALF ≤ 0.3882 | TRUE | FALSE | 0.9529 | 0.0684 ≤ EALF ≤ 1.041 | TRUE | 42.0 | 42.0 |

Source: Output DTN: MO0711LOADCURV.000, file: *LoadingCurve.xls*, worksheet: “Results.”

Table 6-25. PWR Loading Curve Analysis for One Zone Axial Results

| | Fresh Fuel | | | | Burned Fuel | | | | Burnup at |
|---|---|---|---|---|---|---|---|---|---|
| Enrichment [wt %] | Critical Limit | EALF Range [eV] | EALF In Range? | Limit Met? | Critical Limit | EALF Range [eV] | EALF In Range? | Burnup [GWd/MTU] | Critical Limit [GWd/MTU] |
| 1.5 | 0.9905 | 0.0977 ≤ EALF ≤ 0.3882 | TRUE | TRUE | 0.9529 | 0.0684 ≤ EALF ≤ 1.041 | TRUE | 0.0 | 0.0 |
| 2.0 | 0.9905 | 0.0977 ≤ EALF ≤ 0.3882 | TRUE | TRUE | 0.9529 | 0.0684 ≤ EALF ≤ 1.041 | TRUE | 3.6 | 0.0 |
| 2.5 | 0.9905 | 0.0977 ≤ EALF ≤ 0.3882 | TRUE | FALSE | 0.9529 | 0.0684 ≤ EALF ≤ 1.041 | TRUE | 12.2 | 12.2 |
| 3.0 | 0.9905 | 0.0977 ≤ EALF ≤ 0.3882 | TRUE | FALSE | 0.9529 | 0.0684 ≤ EALF ≤ 1.041 | TRUE | 18.6 | 18.6 |
| 3.5 | 0.9905 | 0.0977 ≤ EALF ≤ 0.3882 | TRUE | FALSE | 0.9529 | 0.0684 ≤ EALF ≤ 1.041 | TRUE | 24.5 | 24.5 |
| 4.0 | 0.9905 | 0.0977 ≤ EALF ≤ 0.3882 | TRUE | FALSE | 0.9529 | 0.0684 ≤ EALF ≤ 1.041 | TRUE | 30.0 | 30.0 |
| 4.5 | 0.9905 | 0.0977 ≤ EALF ≤ 0.3882 | TRUE | FALSE | 0.9529 | 0.0684 ≤ EALF ≤ 1.041 | TRUE | 35.4 | 35.4 |
| 5.0 | 0.9905 | 0.0977 ≤ EALF ≤ 0.3882 | TRUE | FALSE | 0.9529 | 0.0684 ≤ EALF ≤ 1.041 | TRUE | 40.3 | 40.3 |

Source: Output DTN: MO0711LOADCURV.000, file: *LoadingCurve.xls*, worksheet: “Results.”

Table 6-26. PWR Loading Curve

| Enrichment [wt %] | Burnup Limit [GWd/MTU] | With 5% Margin [GWd/MTU] |
|---|---|---|
| 1.5 | 0.0 | 0.0 |
| < 2.0 | 0.0 | 0.0 |
| ≥ 2.0 | 3.6 | 3.8 |
| 2.5 | 12.2 | 12.8 |
| 3.0 | 18.6 | 19.5 |
| 3.5 | 24.9 | 26.2 |
| 4.0 | 30.7 | 32.2 |
| 4.5 | 36.1 | 37.9 |
| 5.0 | 42.0 | 44.1 |

Source: Output DTN: MO0711LOADCURV.000, file: *LoadingCurve.xls*, worksheet: "Results."

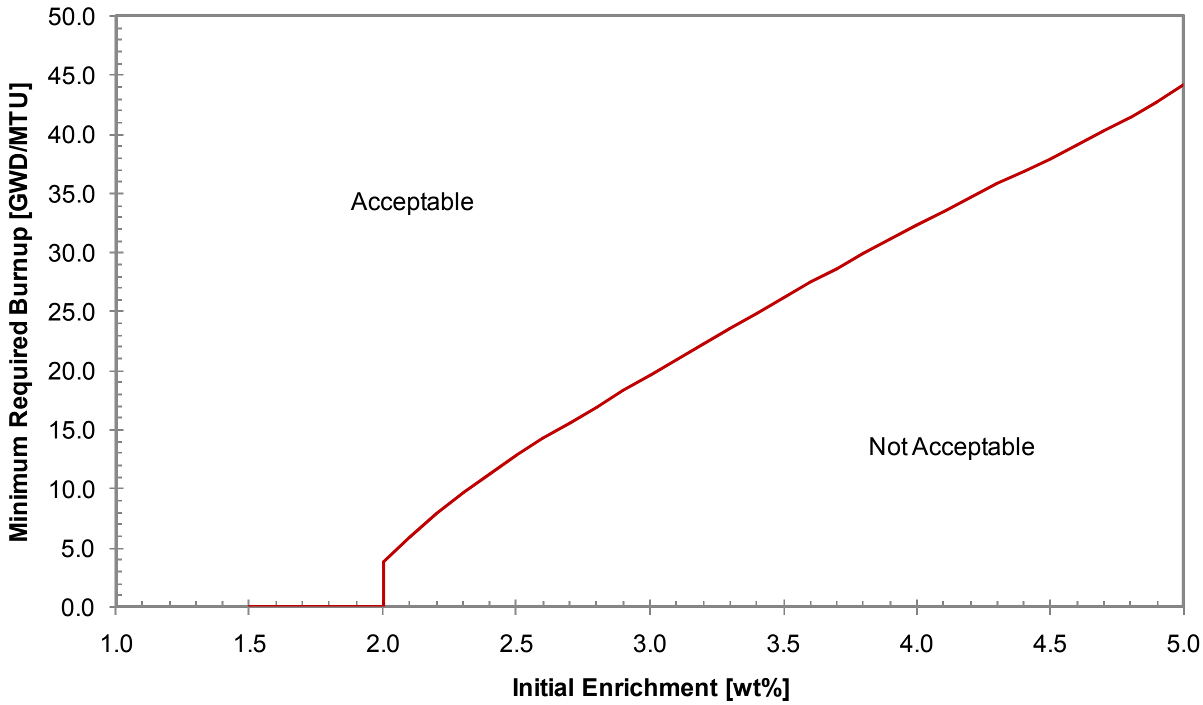


Source: Output DTN: MO0711LOADCURV.000, file: *LoadingCurve.xls*, worksheet: "Results."

Figure 6-24. PWR Loading Curve

### 6.3.3 BWR Loading Curve

The BWR loading curve analysis is summarized in Table 6-27. In the BWR case, all enrichments meet the fresh fuel critical limit except at the highest enrichment. Again, a 5% margin is added to the computed minimum burnup result to account for uncertainty in measured assembly burnup. This margin conservatively bounds the 4.2% maximum burnup uncertainty determined in *Reactor Record Uncertainty Determination* (Massie 2004 [DIRS 170651], Tables 10A, 10B, and 10C). Results are shown in Figure 6-25 and Table 6-28. The loading curve exhibits a step at the transition between the fresh fuel critical limit and the burnup credit critical limit.

By fitting the loading curve data shown in Table 6-28 above the step at 4.5 wt. %, the BWR loading curve is accurately represented using the following formula which gives the minimum required burnup $b$ in GWd/MTU as a function of enrichment, $e$, in wt. %. Note carefully that the quantity $e$ employed in the formula has units of weight *percent*, not weight *fraction*.

$$b = \begin{cases} 0 \text{ for } e < 4.5\,\text{wt.\%} \\ 7.7911\text{e} - 30.7201 \text{ for } 4.5\,\text{wt.\%} \le e \le 5.0\,\text{wt.\%} \end{cases}$$

Source: Output DTN: MO0711LOADCURV.000, file: *LoadingCurve.xls*, worksheet: “LoadingCurve.”

Table 6-27. BWR Loading Curve Analysis for One Zone Axial Results

| | Fresh Fuel | | | | Burned Fuel | | | | Burnup at |
|---|---|---|---|---|---|---|---|---|---|
| **Enrichment [wt %]** | **Critical Limit** | **EALF Range [eV]** | **EALF In Range?** | **Limit Met?** | **Critical Limit** | **EALF Range [eV]** | **EALF In Range?** | **Burnup [GWd/MTU]** | **Critical Limit [GWd/MTU]** |
| 1.5 | 0.9905 | 0.0977 ≤ EALF ≤ 0.3882 | TRUE | TRUE | 0.9529 | 0.0421 ≤ EALF ≤ 0.9679 | TRUE | 0.0 | 0.0 |
| 2.0 | 0.9905 | 0.0977 ≤ EALF ≤ 0.3882 | TRUE | TRUE | 0.9529 | 0.0421 ≤ EALF ≤ 0.9679 | TRUE | 0.0 | 0.0 |
| 2.5 | 0.9905 | 0.0977 ≤ EALF ≤ 0.3882 | TRUE | TRUE | 0.9529 | 0.0421 ≤ EALF ≤ 0.9679 | TRUE | 0.0 | 0.0 |
| 3.0 | 0.9905 | 0.0977 ≤ EALF ≤ 0.3882 | TRUE | TRUE | 0.9529 | 0.0421 ≤ EALF ≤ 0.9679 | TRUE | 0.0 | 0.0 |
| 3.5 | 0.9905 | 0.0977 ≤ EALF ≤ 0.3882 | TRUE | TRUE | 0.9529 | 0.0421 ≤ EALF ≤ 0.9679 | TRUE | 0.0 | 0.0 |
| 4.0 | 0.9905 | 0.0977 ≤ EALF ≤ 0.3882 | TRUE | TRUE | 0.9529 | 0.0421 ≤ EALF ≤ 0.9679 | TRUE | 0.6 | 0.0 |
| 4.5 | 0.9905 | 0.0977 ≤ EALF ≤ 0.3882 | TRUE | TRUE | 0.9529 | 0.0421 ≤ EALF ≤ 0.9679 | TRUE | 4.1 | 0.0 |
| 5.0 | 0.9905 | 0.0977 ≤ EALF ≤ 0.3882 | TRUE | FALSE | 0.9529 | 0.0421 ≤ EALF ≤ 0.9679 | TRUE | 7.8 | 7.8 |

Source: Output DTN: MO0711LOADCURV.000, file: *LoadingCurve.xls*, worksheet: “Results.”

Table 6-28. BWR Loading Curve

| Enrichment [wt %] | Burnup Limit [GWd/MTU] | With 5% Margin [GWd/MTU] |
|---|---|---|
| 1.5 | 0.0 | 0.0 |
| 2.0 | 0.0 | 0.0 |
| 2.5 | 0.0 | 0.0 |
| 3.0 | 0.0 | 0.0 |
| 3.5 | 0.0 | 0.0 |
| 4.0 | 0.0 | 0.0 |
| < 4.5 | 0.0 | 0.0 |
| ≥ 4.5 | 4.1 | 4.3 |
| 5.0 | 7.8 | 8.2 |

Source: Output DTN: MO0711LOADCURV.000, file: *LoadingCurve.xls*, worksheet: "Results."

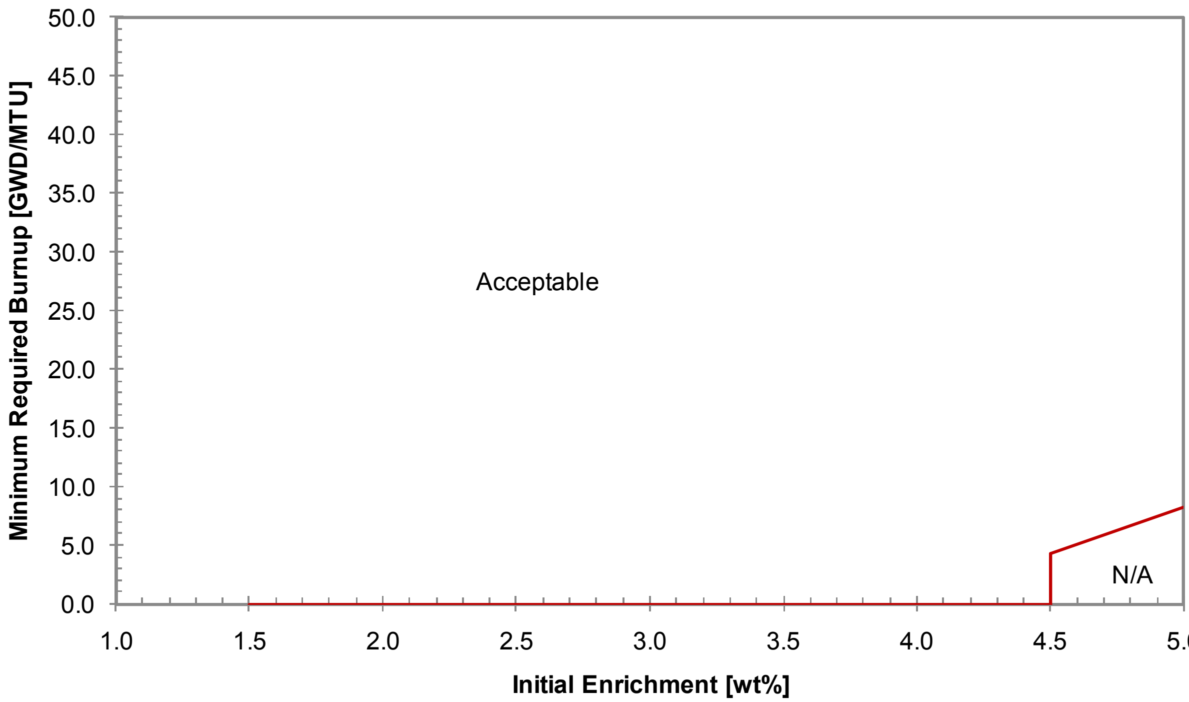


Source: Output DTN: MO0711LOADCURV.000, file: *LoadingCurve.xls*, worksheet: "Results."

Figure 6-25. BWR Loading Curve

### 6.3.4 Variation of Non-Loadable Inventory Fraction with Isotope Set Selection

The base case results presented above are based on the "Principal Isotope" burnup credit isotope set following the methodology described in *Disposal Criticality Analysis Methodology Topical Report* (YMP 2003 [DIRS 165505]). The development of loading curves corresponding to other isotope sets (see Table 6-1) would require the determination of separate critical limits for each isotope set and is beyond the scope of this analysis.

An initial comparison of the various burnup credit isotope sets in terms of waste package reactivity is presented in Section 6.2.3.3. However, an alternative comparison of the various burnup credit isotope sets may be performed by developing loading curves as a *function* of critical limit. A convenient means of comparing the resulting curves is available by determining the fraction of the PWR fuel inventory that would not be loadable for each isotope set as a function of critical limit.

For this analysis, the PWR fuel inventory is based on the characterization of the projected PWR fuel assembly waste stream presented in (CRWMS M&O 2000 [DIRS 138239], Attachment III) using the "Case A" arrival forecast. This arrival forecast is selected based on Licensing Position LP-009, Waste Stream Parameters (Williams 2003 [DIRS 166132], Section 3.4). A graphical representation of the PWR fuel inventory is shown in Figure 6-32 in Section 6.4.

For each isotope set, $k_{eff}$ results are generated at the same enrichment and burnup values used for the base case representation (as shown in Table 6-7 and Table 6-9). Following the same procedure used to develop the base case loading curves, the resulting $k_{eff} + 2\sigma$ values are linearly interpolated to determine burnup values at which the reactivity is equal to the critical limit. Consistent with the base case analysis, a 5% margin is added to the determined minimum burnup values to bound uncertainty in actual assembly burnup. The resulting loading curve data are then compared with the PWR fuel inventory to determine the fraction of assemblies which are not loadable (i.e., with enrichment and burnup values which fall below the loading curve). Results of the analysis are shown in Table 6-29 and Figure 6-26.

Reactivity results for the various additional burnup credit isotope sets are shown in Table 6-30 through Table 6-39. Results for selected enrichment values are plotted in Figure 6-27 through Figure 6-31 for illustration. In order to determine loading curves for each isotope set at a given critical limit value, the burnup required to meet the critical limit is linearly interpolated at each enrichment value. In some cases, linear extrapolation outside the available data is necessary in order to determine the required minimum burnup, and this extrapolation procedure is justified below. The resulting loading curve data are shown in Table 6-40.

### 6.3.4.1 Justification for Linear Extrapolation of Reactivity Data

In order to present trends in the computed non-loadable fraction as a function of critical limit, loading curves are generated for a range of critical limit values. Certain alternative isotope sets require greater than 50 GWd/MTU minimum burnup in order to meet the critical limit. In these cases, linear interpolation within the reactivity data tables is impossible since reactivity results have been obtained only up to a maximum of 50 GWd/MTU. However, for the purposes of this comparative analysis, a linear extrapolation of reactivity data is justified for several reasons.

First, considering the variation of reactivity with burnup for the various isotope sets shown in Figure 6-27 through Figure 6-31, reactivity behaves in an approximately linear fashion with increasing burnup. Hence, a linear extrapolation would not be expected to be inaccurate.

Second, to the extent that the curves are not linear, the figures show that the rate of decrease in reactivity tends to decrease with increasing burnup. Hence, the linear extrapolation procedure will tend to underestimate the required minimum burnup, and the resulting non-loadable fraction will be lower than a more detailed analysis may determine. For the purposes of this comparative analysis, this underestimation has the salutary effect of showing the alternative isotope sets in a more favorable light.

Third, the actual critical limit values determined for the alternative isotope sets are expected to be higher than that for the base case since fewer isotopes are credited. Biases and uncertainties associated with the omitted isotopes, included in the terms f(x) and $\Delta k_{ISO}$ of Equation 1 (see p. 6-1), will not be present, and the critical limit would be expected to increase. In this analysis, only the Actinide Only and Principle Actinide burnup credit isotope sets require extrapolation at critical limit values higher than the base case value of 0.9529 and only at enrichments of 4.5 wt. % and 5.0 wt. %. Minimum required burnup values shown in Table 6-40 that exceed 52.5 GWd/MTU (recall that the tabulated values include a 5% margin) are values determined using a linear extrapolation of the data. For critical limits greater than 0.9529, the maximum extrapolation at the 4.5 wt. % enrichment value is 6 GWd/MTU, and at the 5.0 wt. % value is 14 GWd/MTU.

Finally, in order to quantify the potential worst case impact of inaccuracies in the linear extrapolation process, consider that 1) extrapolation less than 5 GWd/MTU is expected to be accurate based on the linearity of the reactivity data with burnup and 2) in the entire PWR inventory, 6643 assemblies have enrichment values that exceed 4.5 wt. % and burnup in excess of 55 GWd/MTU. This figure represents 7% of the entire inventory. Hence, with the worst case assumption that *every* assembly above 4.5 wt% and 55 GWd/MTU is mischaracterized as loadable as a result of inaccuracy in the linear extrapolation, the non-loadable inventory fraction results for the Actinide Only and Principle Actinide isotope sets, at critical limits above 0.9529, may be too *low* by at most seven percentage points. Since the results for these two actinide-only isotope sets are the outlying curves in the final results shown in Figure 6-26, one sees that potential inaccuracies in the linear extrapolation process can hardly affect conclusions about the potential applicability of these isotope sets.

#### 6.3.4.2 Computation of Non-Loadable Fraction

Given the loading curve data for each isotope set at each critical limit value, the non-loadable inventory fraction is computed by representing the loading curve data as a piecewise linear function of enrichment. For each assembly record in the PWR fuel inventory database, the minimum required burnup is determined by linearly interpolating the assembly record enrichment on the loading curve data.

The resulting minimum required burnup is compared to the assembly record burnup. If the assembly record burnup is less than the minimum required burnup, the number of assemblies in that record is tallied. The final tally gives the total number $N_{NL}$ of assemblies that are not loadable out of the total $N_{TOT} = 93770$ assemblies. The non-loadable fraction is then computed as:

$$f_{NL} = \frac{N_{NL}}{N_{TOT}}$$

As a simplification, no step is accounted for in the loading curve at the transition between the fresh fuel critical limit and the burnup credit critical limit. This introduces a slight mischaracterization of assemblies with low burnup between 2.0 wt. % and 2.5 wt. % in which assemblies are characterized as loadable when a step-wise treatment would characterize them as non-loadable. In order to quantify the potential impact of this simplification consider the largest fresh-fuel to burnup-credit step (amongst the realistic critical limit values exceeding the base case) which occurs for the Actinide Only isotope set at a burnup credit critical limit of 0.96 (see Table 6-40). The omission of the step in the analysis results in the mischaracterization of 148 assemblies as loadable when the step-wise treatment would show them as non-loadable. These assemblies represent 148/93770 = 0.16% of the fuel inventory. Hence, even the worst case error associated with the simplified treatment amounts to an insignificantly small underestimate of the non-loadable inventory fraction.

#### 6.3.4.3 Non-Loadable Inventory Fraction Results

The resulting non-loadable inventory fractions are tabulated in Table 6-29 and shown graphically in Figure 6-26 based on the reactivity data shown in Table 6-30 through Table 6-39. Note that an appropriate comparison of the various isotope sets should take into consideration the likely increase in critical limit values for the alternative isotope sets. Hence, it may not be appropriate to draw conclusions by comparing non-loadable fractions of two isotope sets at the *same* critical limit value.

The results show that the Principal Actinide and Actinide Only isotope sets introduce a significant penalty on the loadable fraction of the inventory.

Table 6-29. Non-Loadable Fraction of PWR Fuel Inventory for Various Burnup Credit Isotope Sets

| Burned Fuel | Isotope Set | | | | | | | | | | | |
|---|---|---|---|---|---|---|---|---|---|---|---|---|
| | Principal Isotope | | Principal Actinide | | Actinide Only | | PI-Metal | | PA+French | | PA+French-Metal | |
| Critical Limit | Num Assy | % Inv | Num Assy | % Inv | Num Assy | % Inv | Num Assy | % Inv | Num Assy | % Inv | Num Assy | % Inv |
| 0.9300 | 4860 | 5.2% | 85354 | 91.0% | 86282 | 92.0% | 15639 | 16.7% | 22744 | 24.3% | 38067 | 40.6% |
| 0.9400 | 3289 | 3.5% | 81537 | 87.0% | 85025 | 90.7% | 7798 | 8.3% | 11523 | 12.3% | 23016 | 24.5% |
| 0.9500 | 2165 | 2.3% | 72129 | 76.9% | 80777 | 86.1% | 3805 | 4.1% | 5658 | 6.0% | 11332 | 12.1% |
| 0.9529 | 1990 | 2.1% | 68217 | 72.7% | 78304 | 83.5% | 3488 | 3.7% | 4465 | 4.8% | 9575 | 10.2% |
| 0.9600 | 1534 | 1.6% | 56986 | 60.8% | 70950 | 75.7% | 2504 | 2.7% | 3323 | 3.5% | 5487 | 5.9% |
| 0.9700 | 1083 | 1.2% | 38269 | 40.8% | 55465 | 59.2% | 1692 | 1.8% | 2133 | 2.3% | 3208 | 3.4% |
| 0.9800 | 857 | 0.9% | 22108 | 23.6% | 36643 | 39.1% | 1187 | 1.3% | 1520 | 1.6% | 2001 | 2.1% |
| 0.9900 | 792 | 0.8% | 10656 | 11.4% | 20124 | 21.5% | 919 | 1.0% | 989 | 1.1% | 1435 | 1.5% |
| 1.0000 | 698 | 0.7% | 5387 | 5.7% | 9239 | 9.9% | 795 | 0.8% | 850 | 0.9% | 970 | 1.0% |

Source: Output DTN: MO0711LOADCURV.000, file: *LoadingCurve.xls*, worksheet: "LoadingCurve."

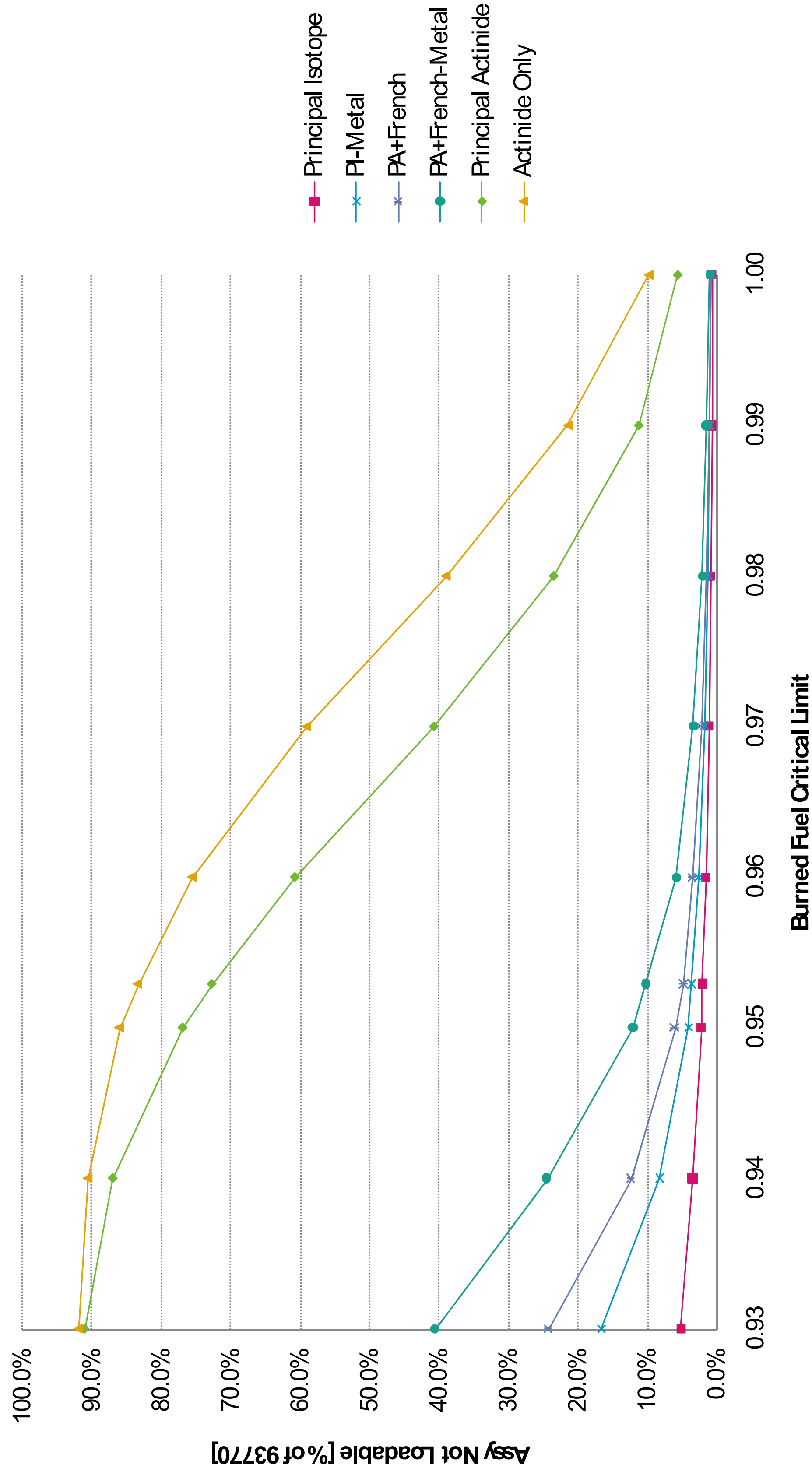


Source: Output DTN: MO0711LOADCURV.000, file: *LoadingCurve.xls*, worksheet: "LoadingCurve."

Figure 6-26. Fraction of PWR Fuel Inventory Not Loadable for Various Burnup Credit Isotope Sets

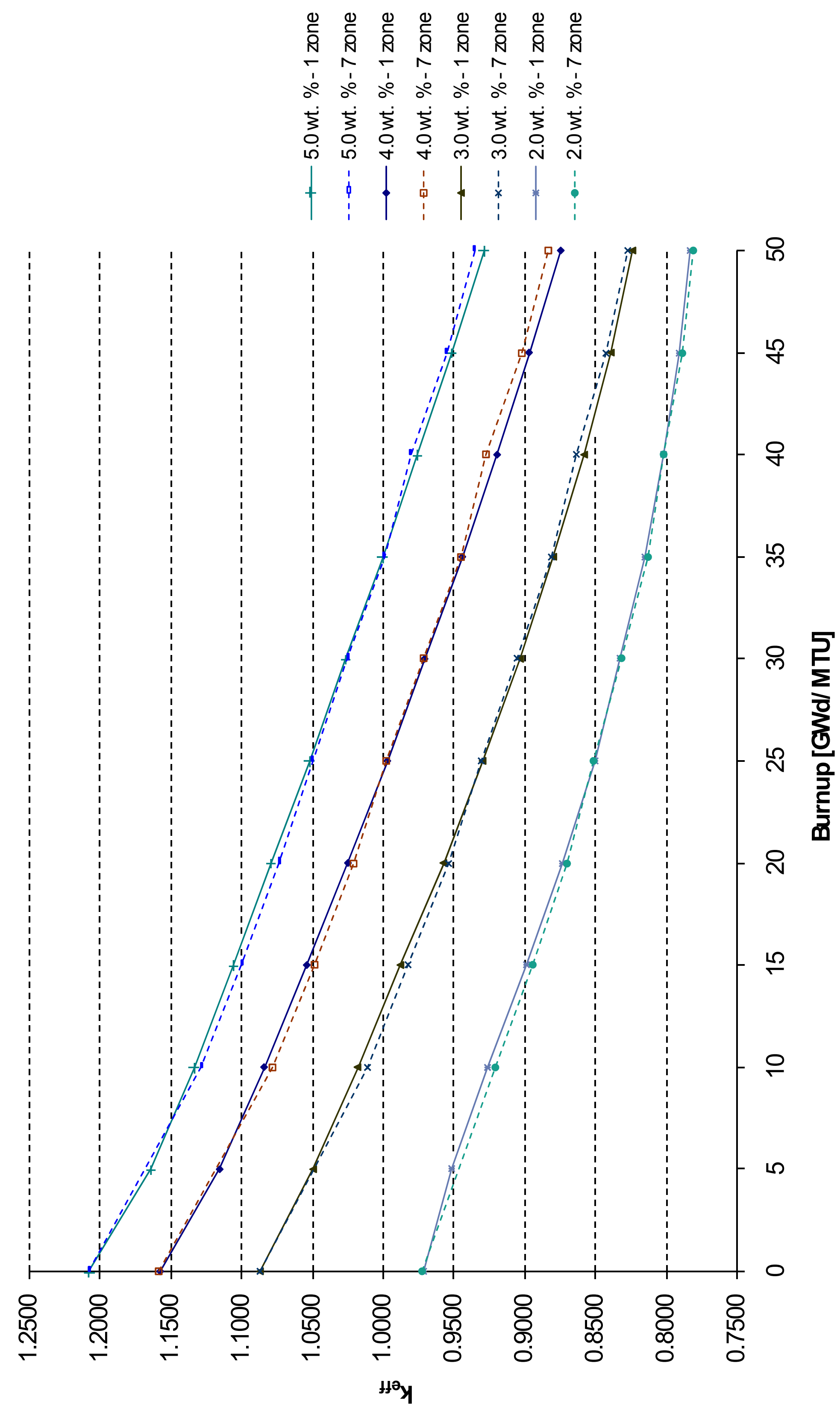


Source: Output DTN: MO0711LOADCURV.000, file: *LoadingCurve.xls*, worksheet: "Results."

Figure 6-27. Variation of Reactivity with Burnup for Isotope Set PI–Metal

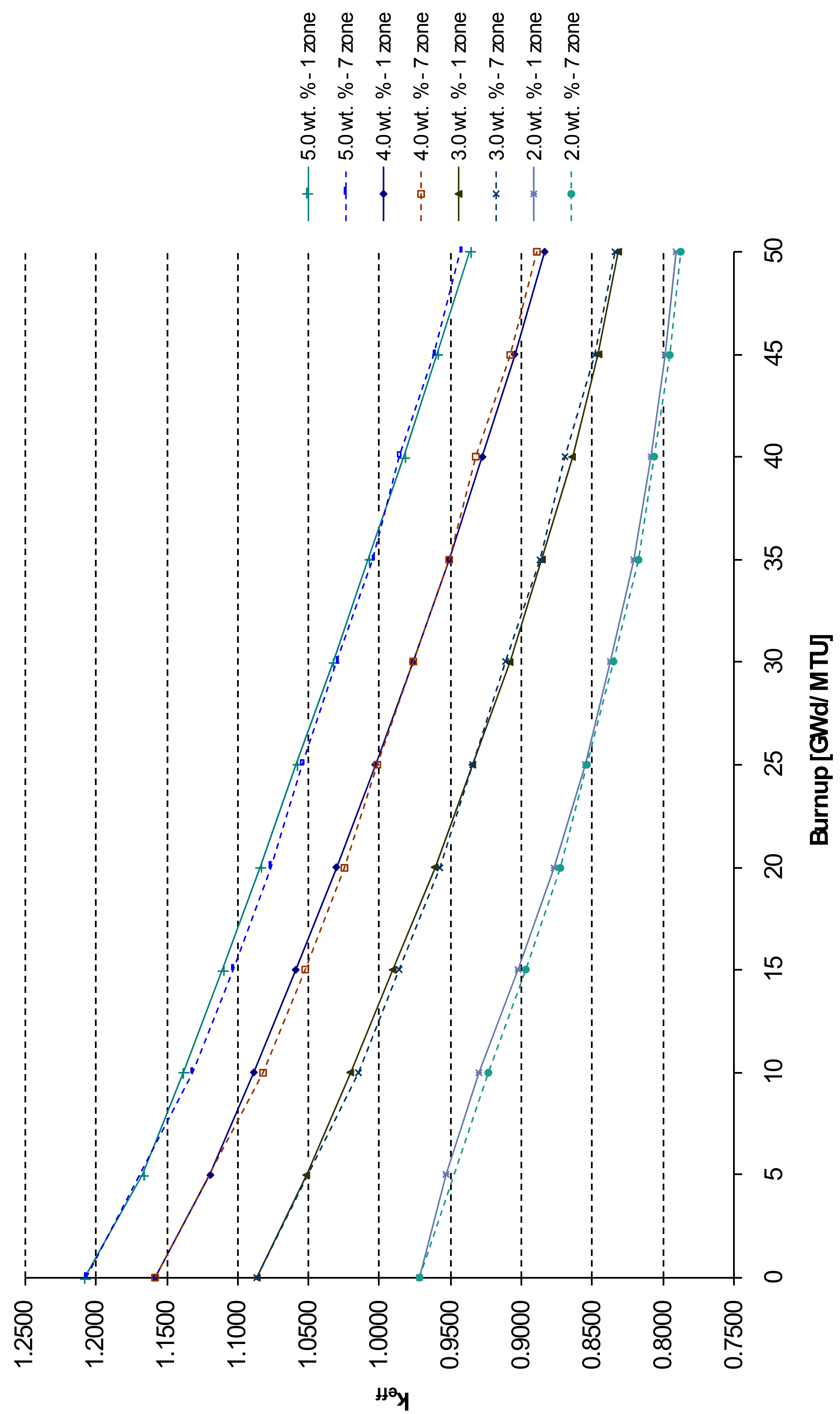


Source: Output DTN: MO0711LOADCURV.000, file: *LoadingCurve.xls*, worksheet: “Results.”

Figure 6-28. Variation of Reactivity with Burnup for Isotope Set PA+French

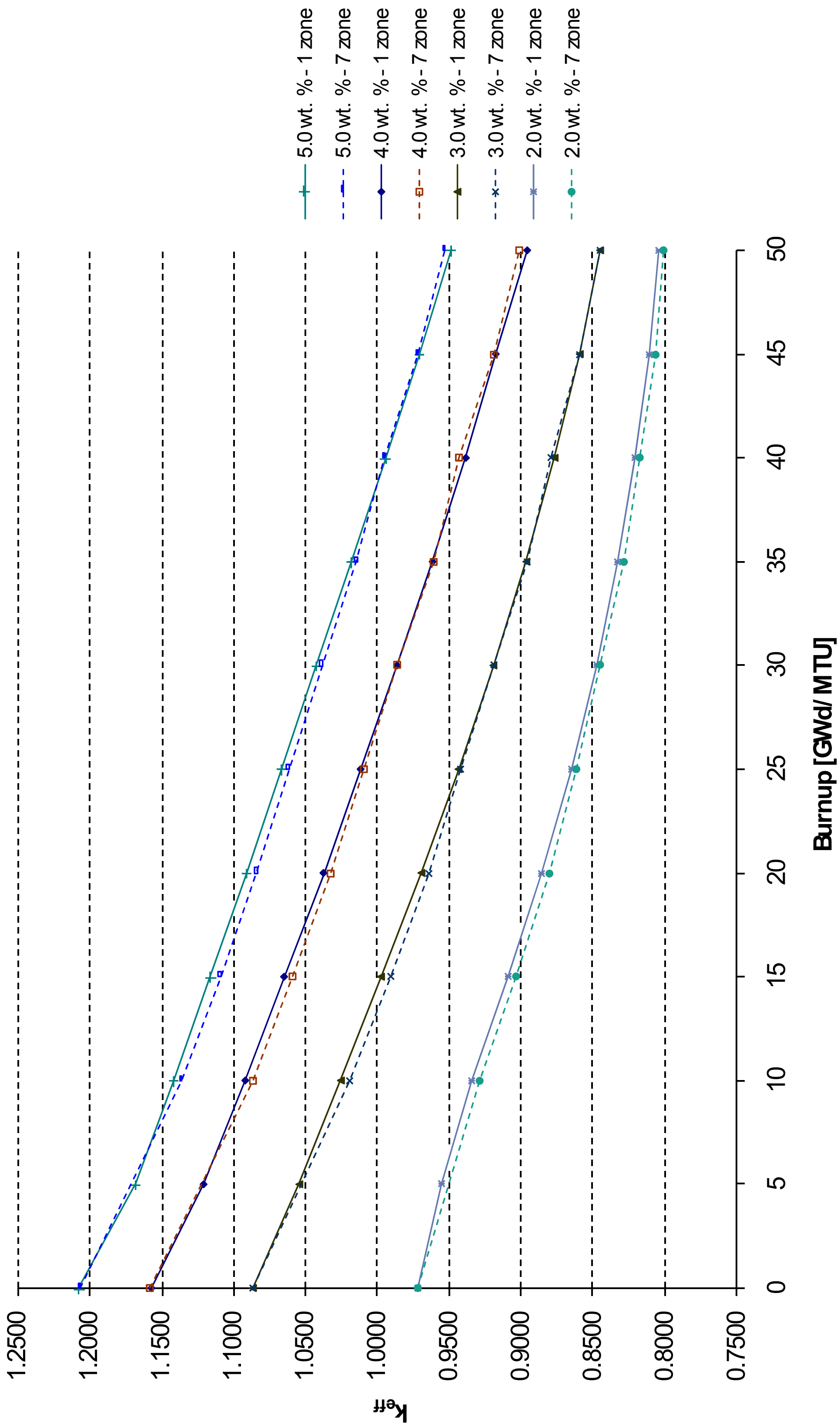


Source: Output DTN: MO0711LOADCURV.000, file: *LoadingCurve.xls*, worksheet: "Results."

Figure 6-29. Variation of Reactivity with Burnup for Isotope Set PA+French–Metal

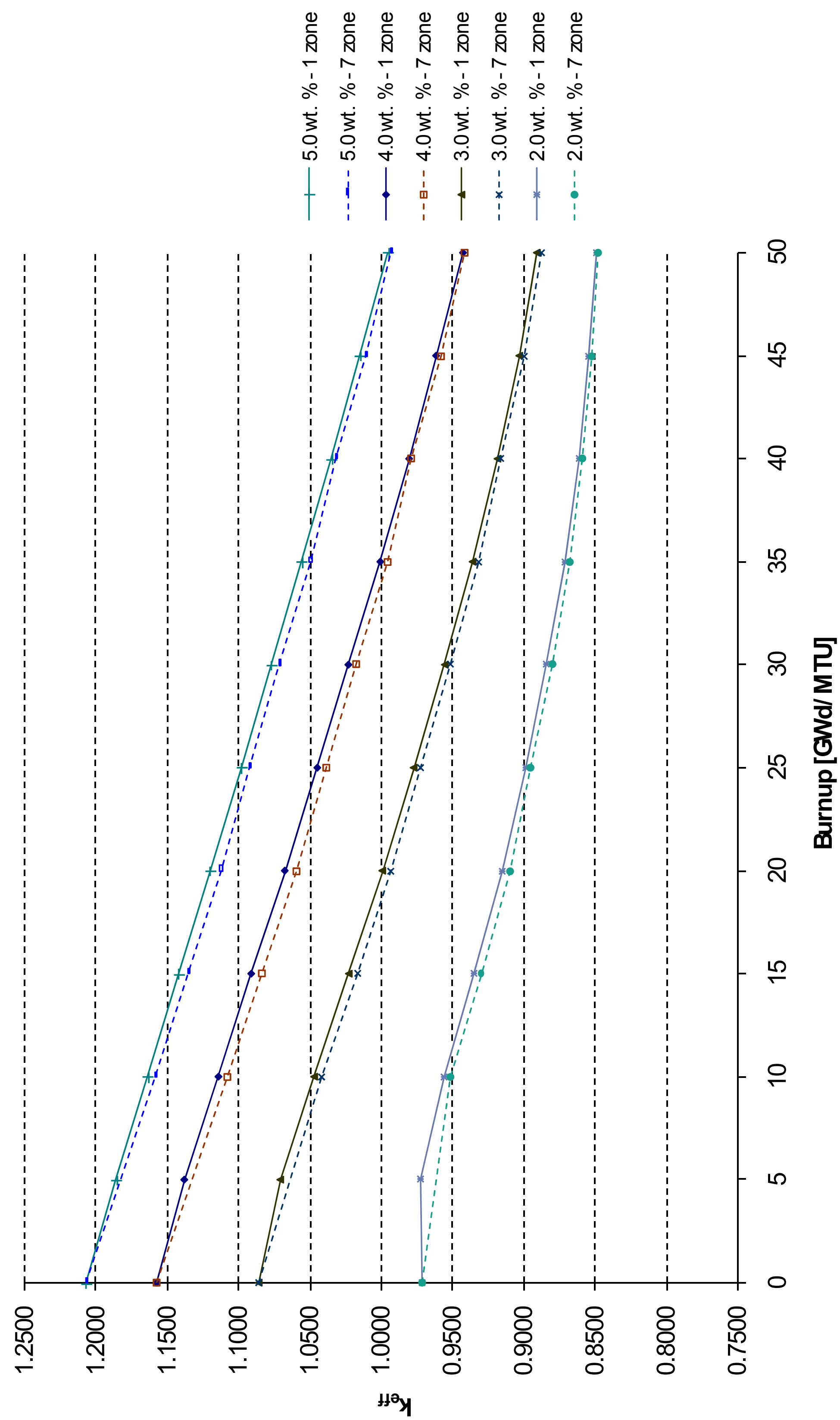


Source: Output DTN: MO0711LOADCURV.000, file: *LoadingCurve.xls*, worksheet: "Results."

Figure 6-30. Variation of Reactivity with Burnup for Isotope Set Principal Actinide

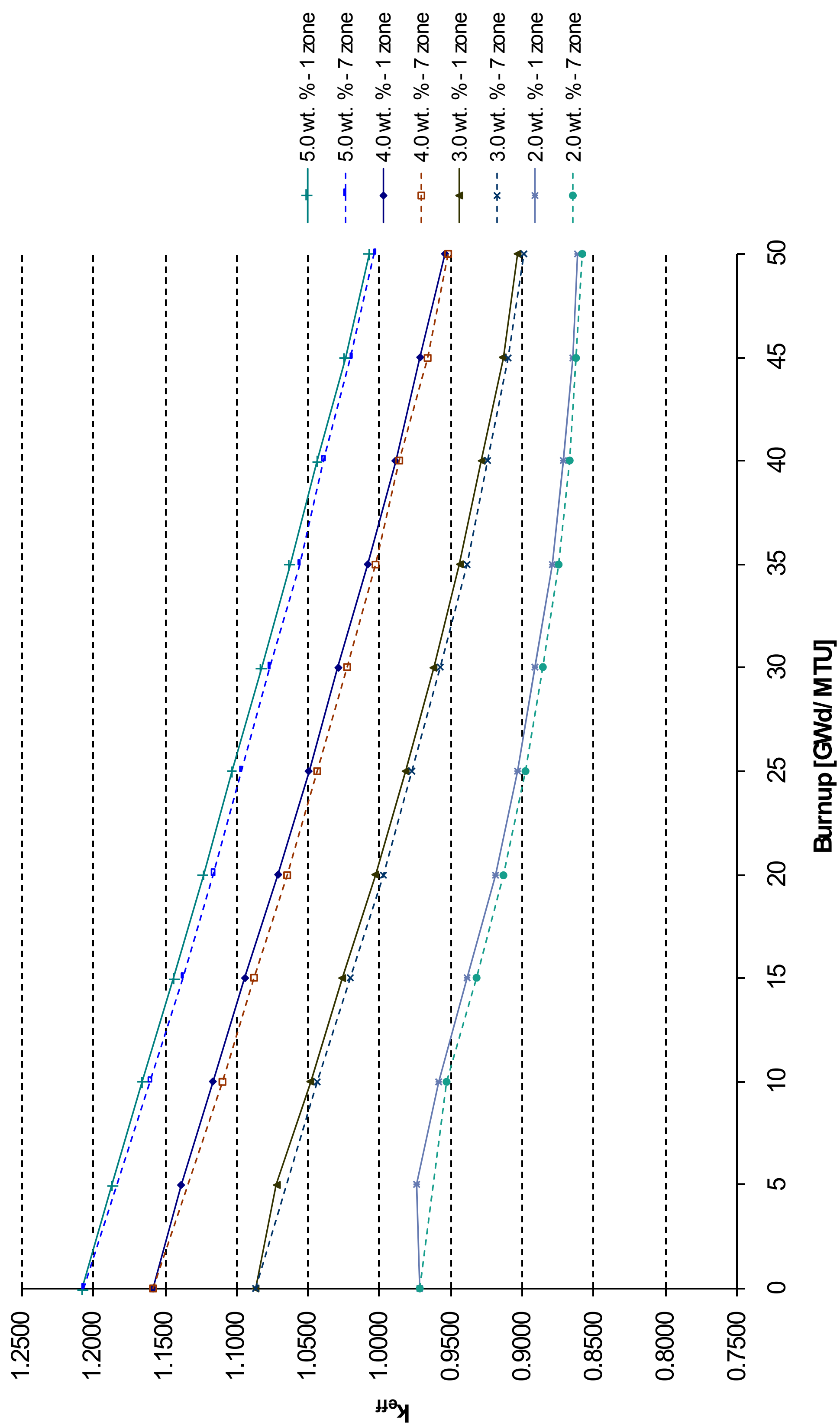


Source: Output DTN: MO0711LOADCURV.000, file: *LoadingCurve.xls*, worksheet: "Results."

Figure 6-31. Variation of Reactivity with Burnup for Isotope Set Actinide Only

INTENTIONALLY LEFT BLANK

Table 6-30. Results for BW 15 × 15 with Seven Axial Zones – $k_{eff}$ + 2σ and EALF Values – Isotope Set PI-Metal

| Burnup | Enrichment [wt. %] | | | | | | | | | | | | | | | | | | | | | | | |
|---|---|---|---|---|---|---|---|---|---|---|---|---|---|---|---|---|---|---|---|---|---|---|---|---|
| | 1.5 | | | 2.0 | | | 2.5 | | | 3.0 | | | 3.5 | | | 4.0 | | | 4.5 | | | 5.0 | | |
| [GWd/MTU] | Case | $k_{eff}$ +2σ | EALF[1] | Case | $k_{eff}$ +2σ | EALF | Case | $k_{eff}$ +2σ | EALF | Case | $k_{eff}$ +2σ | EALF | Case | $k_{eff}$ +2σ | EALF | Case | $k_{eff}$ +2σ | EALF | Case | $k_{eff}$ +2σ | EALF | Case | $k_{eff}$ +2σ | EALF |
| 0 | mca00 | 0.88199 | 0.19 | mcb00 | 0.97171 | 0.20 | mcc00 | 1.03677 | 0.21 | mcd00 | 1.08628 | 0.23 | mce00 | 1.12589 | 0.25 | mcf00 | 1.15840 | 0.27 | mcg00 | 1.18462 | 0.30 | mch00 | 1.20727 | 0.33 |
| 10 | mca10 | 0.86393 | 0.29 | mcb10 | 0.92029 | 0.28 | mcc10 | 0.96929 | 0.28 | mcd10 | 1.01087 | 0.30 | mce10 | 1.04709 | 0.31 | mcf10 | 1.07793 | 0.33 | mcg10 | 1.10468 | 0.35 | mch10 | 1.12787 | 0.38 |
| 15 | mca15 | 0.84380 | 0.32 | mcb15 | 0.89360 | 0.31 | mcc15 | 0.94044 | 0.31 | mcd15 | 0.98176 | 0.31 | mce15 | 1.01788 | 0.33 | mcf15 | 1.04837 | 0.34 | mcg15 | 1.07552 | 0.37 | mch15 | 1.09958 | 0.39 |
| 20 | mca20 | 0.82428 | 0.35 | mcb20 | 0.86908 | 0.33 | mcc20 | 0.91319 | 0.32 | mcd20 | 0.95354 | 0.33 | mce20 | 0.98897 | 0.34 | mcf20 | 1.02017 | 0.36 | mcg20 | 1.04850 | 0.38 | mch20 | 1.07297 | 0.40 |
| 25 | mca25 | 0.80933 | 0.37 | mcb25 | 0.85022 | 0.35 | mcc25 | 0.89141 | 0.34 | mcd25 | 0.92974 | 0.34 | mce25 | 0.96575 | 0.35 | mcf25 | 0.99691 | 0.36 | mcg25 | 1.02498 | 0.38 | mch25 | 1.04926 | 0.40 |
| 30 | mca30 | 0.79631 | 0.40 | mcb30 | 0.83068 | 0.37 | mcc30 | 0.86795 | 0.36 | mcd30 | 0.90502 | 0.36 | mce30 | 0.94008 | 0.36 | mcf30 | 0.97094 | 0.38 | mcg30 | 0.99947 | 0.39 | mch30 | 1.02456 | 0.41 |
| 35 | mca35 | 0.78681 | 0.42 | mcb35 | 0.81260 | 0.40 | mcc35 | 0.84627 | 0.38 | mcd35 | 0.88091 | 0.38 | mce35 | 0.91411 | 0.38 | mcf35 | 0.94483 | 0.39 | mcg35 | 0.97353 | 0.40 | mch35 | 0.99889 | 0.42 |
| 40 | mca40 | 0.77884 | 0.44 | mcb40 | 0.80122 | 0.42 | mcc40 | 0.83141 | 0.40 | mcd40 | 0.86279 | 0.39 | mce40 | 0.89608 | 0.39 | mcf40 | 0.92685 | 0.40 | mcg40 | 0.95443 | 0.41 | mch40 | 0.97988 | 0.42 |
| 45 | mca45 | 0.77222 | 0.46 | mcb45 | 0.78859 | 0.45 | mcc45 | 0.81335 | 0.42 | mcd45 | 0.84169 | 0.41 | mce45 | 0.87181 | 0.41 | mcf45 | 0.90098 | 0.41 | mcg45 | 0.92908 | 0.42 | mch45 | 0.95450 | 0.43 |
| 50 | mca50 | 0.76771 | 0.48 | mcb50 | 0.78038 | 0.47 | mcc50 | 0.79984 | 0.44 | mcd50 | 0.82649 | 0.43 | mce50 | 0.85414 | 0.42 | mcf50 | 0.88277 | 0.42 | mcg50 | 0.90993 | 0.43 | mch50 | 0.93502 | 0.44 |

[1] EALF is the energy of the average neutron lethargy causing fission, in eV.

Source: Output DTN: MO0711LOADCURV.000, file: *LoadingCurve.xls*, worksheet: "Results."

Table 6-31. Results for BW 15 × 15 with One Axial Zone – $k_{eff}$ + 2σ and EALF Values – Isotope Set PI-Metal

| Burnup | Enrichment [wt. %] | | | | | | | | | | | | | | | | | | | | | | | |
|---|---|---|---|---|---|---|---|---|---|---|---|---|---|---|---|---|---|---|---|---|---|---|---|---|
| | 1.5 | | | 2.0 | | | 2.5 | | | 3.0 | | | 3.5 | | | 4.0 | | | 4.5 | | | 5.0 | | |
| [GWd/MTU] | Case | $k_{eff}$ +2σ | EALF[1] | Case | $k_{eff}$ +2σ | EALF | Case | $k_{eff}$ +2σ | EALF | Case | $k_{eff}$ +2σ | EALF | Case | $k_{eff}$ +2σ | EALF | Case | $k_{eff}$ +2σ | EALF | Case | $k_{eff}$ +2σ | EALF | Case | $k_{eff}$ +2σ | EALF |
| 0 | mda00 | 0.88188 | 0.19 | mdb00 | 0.97145 | 0.20 | mdc00 | 1.03629 | 0.21 | mdd00 | 1.08611 | 0.23 | mde00 | 1.12550 | 0.25 | mdf00 | 1.15751 | 0.27 | mdg00 | 1.18401 | 0.30 | mdh00 | 1.20759 | 0.33 |
| 5 | mda05 | 0.88532 | 0.25 | mdb05 | 0.95146 | 0.25 | mdc05 | 1.00462 | 0.26 | mdd05 | 1.04867 | 0.27 | mde05 | 1.08522 | 0.29 | mdf05 | 1.11554 | 0.31 | mdg05 | 1.14131 | 0.33 | mdh05 | 1.16381 | 0.36 |
| 10 | mda10 | 0.86932 | 0.29 | mdb10 | 0.92625 | 0.28 | mdc10 | 0.97547 | 0.29 | mdd10 | 1.01738 | 0.30 | mde10 | 1.05276 | 0.31 | mdf10 | 1.08417 | 0.33 | mdg10 | 1.11141 | 0.35 | mdh10 | 1.13326 | 0.38 |
| 15 | mda15 | 0.84727 | 0.32 | mdb15 | 0.89877 | 0.31 | mdc15 | 0.94552 | 0.31 | mdd15 | 0.98718 | 0.32 | mde15 | 1.02303 | 0.33 | mdf15 | 1.05402 | 0.35 | mdg15 | 1.08233 | 0.37 | mdh15 | 1.10539 | 0.39 |
| 20 | mda20 | 0.82823 | 0.35 | mdb20 | 0.87322 | 0.34 | mdc20 | 0.91675 | 0.33 | mdd20 | 0.95687 | 0.34 | mde20 | 0.99325 | 0.35 | mdf20 | 1.02487 | 0.36 | mdg20 | 1.05340 | 0.38 | mdh20 | 1.07898 | 0.40 |
| 25 | mda25 | 0.81328 | 0.38 | mdb25 | 0.85089 | 0.36 | mdc25 | 0.89068 | 0.35 | mdd25 | 0.92926 | 0.35 | mde25 | 0.96526 | 0.36 | mdf25 | 0.99712 | 0.37 | mdg25 | 1.02721 | 0.39 | mdh25 | 1.05193 | 0.41 |
| 30 | mda30 | 0.79992 | 0.40 | mdb30 | 0.83228 | 0.39 | mdc30 | 0.86681 | 0.38 | mdd30 | 0.90275 | 0.37 | mde30 | 0.93770 | 0.38 | mdf30 | 0.97078 | 0.39 | mdg30 | 0.99972 | 0.40 | mdh30 | 1.02591 | 0.42 |
| 35 | mda35 | 0.79004 | 0.42 | mdb35 | 0.81557 | 0.41 | mdc35 | 0.84648 | 0.40 | mdd35 | 0.87942 | 0.39 | mde35 | 0.91220 | 0.39 | mdf35 | 0.94414 | 0.40 | mdg35 | 0.97314 | 0.41 | mdh35 | 1.00002 | 0.43 |
| 40 | mda40 | 0.78296 | 0.44 | mdb40 | 0.80195 | 0.43 | mdc40 | 0.82959 | 0.42 | mdd40 | 0.85760 | 0.41 | mde40 | 0.88908 | 0.41 | mdf40 | 0.91952 | 0.41 | mdg40 | 0.94845 | 0.42 | mdh40 | 0.97528 | 0.43 |
| 45 | mda45 | 0.77563 | 0.46 | mdb45 | 0.79099 | 0.45 | mdc45 | 0.81424 | 0.44 | mdd45 | 0.83884 | 0.43 | mde45 | 0.86683 | 0.43 | mdf45 | 0.89698 | 0.43 | mdg45 | 0.92418 | 0.44 | mdh45 | 0.95112 | 0.45 |
| 50 | mda50 | 0.76992 | 0.47 | mdb50 | 0.78332 | 0.47 | mdc50 | 0.80131 | 0.46 | mdd50 | 0.82358 | 0.45 | mde50 | 0.84840 | 0.45 | mdf50 | 0.87455 | 0.45 | mdg50 | 0.90228 | 0.45 | mdh50 | 0.92826 | 0.46 |

[1] EALF is the energy of the average neutron lethargy causing fission, in eV.

Source: Output DTN: MO0711LOADCURV.000, file: *LoadingCurve.xls*, worksheet: "Results."

INTENTIONALLY LEFT BLANK

Table 6-32. Results for BW 15 ×1 5 with Seven Axial Zones – $k_{eff}$ + 2σ and EALF Values – Isotope Set PA+French

| Burnup | Enrichment [wt. %] | | | | | | | | | | | | | | | | | | | | | | | |
|---|---|---|---|---|---|---|---|---|---|---|---|---|---|---|---|---|---|---|---|---|---|---|---|---|
| | 1.5 | | | 2.0 | | | 2.5 | | | 3.0 | | | 3.5 | | | 4.0 | | | 4.5 | | | 5.0 | | |
| [GWd/MTU] | Case | $k_{eff}$ +2σ | EALF[1] | Case | $k_{eff}$ +2σ | EALF | Case | $k_{eff}$ +2σ | EALF | Case | $k_{eff}$ +2σ | EALF | Case | $k_{eff}$ +2σ | EALF | Case | $k_{eff}$ +2σ | EALF | Case | $k_{eff}$ +2σ | EALF | Case | $k_{eff}$ +2σ | EALF |
| 0 | ka00 | 0.88231 | 0.19 | kb00 | 0.97169 | 0.20 | kc00 | 1.03706 | 0.21 | kd00 | 1.08619 | 0.23 | ke00 | 1.12602 | 0.25 | kf00 | 1.15798 | 0.27 | kg00 | 1.18448 | 0.30 | kh00 | 1.20662 | 0.33 |
| 10 | ka10 | 0.86678 | 0.29 | kb10 | 0.92308 | 0.28 | kc10 | 0.97266 | 0.28 | kd10 | 1.01484 | 0.29 | ke10 | 1.05141 | 0.31 | kf10 | 1.08189 | 0.33 | kg10 | 1.10888 | 0.35 | kh10 | 1.13207 | 0.38 |
| 15 | ka15 | 0.84663 | 0.32 | kb15 | 0.89719 | 0.30 | kc15 | 0.94465 | 0.30 | kd15 | 0.98558 | 0.31 | ke15 | 1.02114 | 0.32 | kf15 | 1.05272 | 0.34 | kg15 | 1.08037 | 0.36 | kh15 | 1.10337 | 0.39 |
| 20 | ka20 | 0.82788 | 0.35 | kb20 | 0.87335 | 0.33 | kc20 | 0.91726 | 0.32 | kd20 | 0.95726 | 0.33 | ke20 | 0.99382 | 0.34 | kf20 | 1.02478 | 0.35 | kg20 | 1.05325 | 0.37 | kh20 | 1.07700 | 0.39 |
| 25 | ka25 | 0.81353 | 0.37 | kb25 | 0.85431 | 0.34 | kc25 | 0.89625 | 0.33 | kd25 | 0.93445 | 0.34 | ke25 | 0.97038 | 0.35 | kf25 | 1.00156 | 0.36 | kg25 | 1.02961 | 0.38 | kh25 | 1.05444 | 0.40 |
| 30 | ka30 | 0.80154 | 0.39 | kb30 | 0.83538 | 0.37 | kc30 | 0.87318 | 0.35 | kd30 | 0.91066 | 0.35 | ke30 | 0.94506 | 0.36 | kf30 | 0.97670 | 0.37 | kg30 | 1.00513 | 0.39 | kh30 | 1.02999 | 0.41 |
| 35 | ka35 | 0.79268 | 0.42 | kb35 | 0.81830 | 0.39 | kc35 | 0.85163 | 0.38 | kd35 | 0.88614 | 0.37 | ke35 | 0.91992 | 0.37 | kf35 | 0.95104 | 0.38 | kg35 | 0.97987 | 0.39 | kh35 | 1.00480 | 0.41 |
| 40 | ka40 | 0.78516 | 0.43 | kb40 | 0.80693 | 0.41 | kc40 | 0.83760 | 0.39 | kd40 | 0.86884 | 0.38 | ke40 | 0.90197 | 0.38 | kf40 | 0.93240 | 0.39 | kg40 | 0.96092 | 0.40 | kh40 | 0.98616 | 0.42 |
| 45 | ka45 | 0.77962 | 0.45 | kb45 | 0.79593 | 0.44 | kc45 | 0.81977 | 0.42 | kd45 | 0.84846 | 0.40 | ke45 | 0.87855 | 0.40 | kf45 | 0.90781 | 0.40 | kg45 | 0.93532 | 0.41 | kh45 | 0.96172 | 0.43 |
| 50 | ka50 | 0.77554 | 0.47 | kb50 | 0.78821 | 0.45 | kc50 | 0.80754 | 0.43 | kd50 | 0.83360 | 0.42 | ke50 | 0.86160 | 0.41 | kf50 | 0.88924 | 0.42 | kg50 | 0.91723 | 0.42 | kh50 | 0.94303 | 0.43 |

[1] EALF is the energy of the average neutron lethargy causing fission, in eV.

Source: Output DTN: MO0711LOADCURV.000, file: *LoadingCurve.xls*, worksheet: “Results.”

Table 6-33. Results for BW 15 × 15 with One Axial Zone – $k_{eff}$ + 2σ and EALF Values – Isotope Set PA+French

| Burnup | Enrichment [wt. %] | | | | | | | | | | | | | | | | | | | | | | | |
|---|---|---|---|---|---|---|---|---|---|---|---|---|---|---|---|---|---|---|---|---|---|---|---|---|
| | 1.5 | | | 2.0 | | | 2.5 | | | 3.0 | | | 3.5 | | | 4.0 | | | 4.5 | | | 5.0 | | |
| [GWd/MTU] | Case | $k_{eff}$ +2σ | EALF[1] | Case | $k_{eff}$ +2σ | EALF | Case | $k_{eff}$ +2σ | EALF | Case | $k_{eff}$ +2σ | EALF | Case | $k_{eff}$ +2σ | EALF | Case | $k_{eff}$ +2σ | EALF | Case | $k_{eff}$ +2σ | EALF | Case | $k_{eff}$ +2σ | EALF |
| 0 | k1a00 | 0.88131 | 0.19 | k1b00 | 0.97172 | 0.20 | k1c00 | 1.03668 | 0.21 | k1d00 | 1.08639 | 0.23 | k1e00 | 1.12620 | 0.25 | k1f00 | 1.15794 | 0.27 | k1g00 | 1.18526 | 0.30 | k1h00 | 1.20750 | 0.33 |
| 5 | k1a05 | 0.88826 | 0.25 | k1b05 | 0.95326 | 0.25 | k1c05 | 1.00788 | 0.25 | k1d05 | 1.05169 | 0.27 | k1e05 | 1.08863 | 0.29 | k1f05 | 1.11891 | 0.31 | k1g05 | 1.14457 | 0.33 | k1h05 | 1.16649 | 0.36 |
| 10 | k1a10 | 0.87220 | 0.29 | k1b10 | 0.92943 | 0.28 | k1c10 | 0.97875 | 0.28 | k1d10 | 1.02076 | 0.29 | k1e10 | 1.05693 | 0.31 | k1f10 | 1.08830 | 0.33 | k1g10 | 1.11515 | 0.35 | k1h10 | 1.13802 | 0.37 |
| 15 | k1a15 | 0.85030 | 0.32 | k1b15 | 0.90296 | 0.31 | k1c15 | 0.94914 | 0.31 | k1d15 | 0.99089 | 0.31 | k1e15 | 1.02699 | 0.33 | k1f15 | 1.05877 | 0.34 | k1g15 | 1.08696 | 0.36 | k1h15 | 1.11016 | 0.39 |
| 20 | k1a20 | 0.83197 | 0.35 | k1b20 | 0.87750 | 0.33 | k1c20 | 0.92128 | 0.33 | k1d20 | 0.96150 | 0.33 | k1e20 | 0.99794 | 0.34 | k1f20 | 1.03014 | 0.36 | k1g20 | 1.05863 | 0.37 | k1h20 | 1.08390 | 0.40 |
| 25 | k1a25 | 0.81726 | 0.37 | k1b25 | 0.85517 | 0.36 | k1c25 | 0.89535 | 0.35 | k1d25 | 0.93500 | 0.35 | k1e25 | 0.97036 | 0.36 | k1f25 | 1.00272 | 0.37 | k1g25 | 1.03274 | 0.38 | k1h25 | 1.05820 | 0.40 |
| 30 | k1a30 | 0.80493 | 0.39 | k1b30 | 0.83742 | 0.38 | k1c30 | 0.87164 | 0.37 | k1d30 | 0.90873 | 0.37 | k1e30 | 0.94445 | 0.37 | k1f30 | 0.97623 | 0.38 | k1g30 | 1.00592 | 0.39 | k1h30 | 1.03230 | 0.41 |
| 35 | k1a35 | 0.79556 | 0.41 | k1b35 | 0.82162 | 0.40 | k1c35 | 0.85264 | 0.39 | k1d35 | 0.88602 | 0.39 | k1e35 | 0.91914 | 0.39 | k1f35 | 0.95062 | 0.39 | k1g35 | 0.98056 | 0.40 | k1h35 | 1.00732 | 0.42 |
| 40 | k1a40 | 0.78896 | 0.43 | k1b40 | 0.80889 | 0.42 | k1c40 | 0.83658 | 0.41 | k1d40 | 0.86487 | 0.40 | k1e40 | 0.89595 | 0.40 | k1f40 | 0.92709 | 0.41 | k1g40 | 0.95590 | 0.42 | k1h40 | 0.98232 | 0.43 |
| 45 | k1a45 | 0.78264 | 0.45 | k1b45 | 0.79880 | 0.44 | k1c45 | 0.82160 | 0.43 | k1d45 | 0.84625 | 0.42 | k1e45 | 0.87454 | 0.42 | k1f45 | 0.90446 | 0.42 | k1g45 | 0.93254 | 0.43 | k1h45 | 0.95940 | 0.44 |
| 50 | k1a50 | 0.77768 | 0.46 | k1b50 | 0.79146 | 0.45 | k1c50 | 0.80914 | 0.45 | k1d50 | 0.83246 | 0.44 | k1e50 | 0.85657 | 0.44 | k1f50 | 0.88325 | 0.44 | k1g50 | 0.91058 | 0.44 | k1h50 | 0.93617 | 0.45 |

[1] EALF is the energy of the average neutron lethargy causing fission, in eV.

Source: Output DTN: MO0711LOADCURV.000, file: *LoadingCurve.xls*, worksheet: “Results.”

INTENTIONALLY LEFT BLANK

Table 6-34. Results for BW 15 × 15 with Seven Axial Zones – $k_{eff}$ + 2σ and EALF Values – Isotope Set PA+French-Metal

| Burnup | Enrichment [wt. %] | | | | | | | | | | | | | | | | | | | | | | | |
|---|---|---|---|---|---|---|---|---|---|---|---|---|---|---|---|---|---|---|---|---|---|---|---|
| | 1.5 | | | 2.0 | | | 2.5 | | | 3.0 | | | 3.5 | | | 4.0 | | | 4.5 | | | 5.0 | | |
| [GWd/MTU] | Case | $k_{eff}$ +2σ | EALF[1] | Case | $k_{eff}$ +2σ | EALF | Case | $k_{eff}$ +2σ | EALF | Case | $k_{eff}$ +2σ | EALF | Case | $k_{eff}$ +2σ | EALF | Case | $k_{eff}$ +2σ | EALF | Case | $k_{eff}$ +2σ | EALF | Case | $k_{eff}$ +2σ | EALF |
| 0 | maa00 | 0.88180 | 0.19 | mab00 | 0.97142 | 0.20 | mac00 | 1.03716 | 0.21 | mad00 | 1.08655 | 0.23 | mae00 | 1.12527 | 0.25 | maf00 | 1.15771 | 0.27 | mag00 | 1.18479 | 0.30 | mah00 | 1.20675 | 0.33 |
| 10 | maa10 | 0.87196 | 0.29 | mab10 | 0.92829 | 0.28 | mac10 | 0.97740 | 0.28 | mad10 | 1.01913 | 0.29 | mae10 | 1.05536 | 0.31 | maf10 | 1.08630 | 0.33 | mag10 | 1.11341 | 0.35 | mah10 | 1.13607 | 0.37 |
| 15 | maa15 | 0.85336 | 0.32 | mab15 | 0.90313 | 0.30 | mac15 | 0.94985 | 0.30 | mad15 | 0.99104 | 0.31 | mae15 | 1.02726 | 0.32 | maf15 | 1.05809 | 0.34 | mag15 | 1.08511 | 0.36 | mah15 | 1.10922 | 0.38 |
| 20 | maa20 | 0.83600 | 0.34 | mab20 | 0.88054 | 0.32 | mac20 | 0.92377 | 0.32 | mad20 | 0.96454 | 0.32 | mae20 | 0.99976 | 0.33 | maf20 | 1.03159 | 0.35 | mag20 | 1.06028 | 0.37 | mah20 | 1.08407 | 0.39 |
| 25 | maa25 | 0.82309 | 0.36 | mab25 | 0.86192 | 0.34 | mac25 | 0.90313 | 0.33 | mad25 | 0.94215 | 0.33 | mae25 | 0.97766 | 0.34 | maf25 | 1.00927 | 0.36 | mag25 | 1.03749 | 0.37 | mah25 | 1.06173 | 0.39 |
| 30 | maa30 | 0.81170 | 0.38 | mab30 | 0.84475 | 0.36 | mac30 | 0.88152 | 0.35 | mad30 | 0.91889 | 0.35 | mae30 | 0.95384 | 0.35 | maf30 | 0.98531 | 0.36 | mag30 | 1.01304 | 0.38 | mah30 | 1.03848 | 0.40 |
| 35 | maa35 | 0.80375 | 0.40 | mab35 | 0.82868 | 0.39 | mac35 | 0.86196 | 0.37 | mad35 | 0.89582 | 0.36 | mae35 | 0.92937 | 0.37 | maf35 | 0.96054 | 0.38 | mag35 | 0.98863 | 0.39 | mah35 | 1.01450 | 0.41 |
| 40 | maa40 | 0.79716 | 0.42 | mab40 | 0.81757 | 0.40 | mac40 | 0.84800 | 0.38 | mad40 | 0.87934 | 0.38 | mae40 | 0.91106 | 0.38 | maf40 | 0.94253 | 0.38 | mag40 | 0.97006 | 0.40 | mah40 | 0.99500 | 0.41 |
| 45 | maa45 | 0.79179 | 0.44 | mab45 | 0.80729 | 0.42 | mac45 | 0.83100 | 0.41 | mad45 | 0.85919 | 0.40 | mae45 | 0.88851 | 0.39 | maf45 | 0.91899 | 0.40 | mag45 | 0.94668 | 0.41 | mah45 | 0.97179 | 0.42 |
| 50 | maa50 | 0.78833 | 0.45 | mab50 | 0.80142 | 0.44 | mac50 | 0.81929 | 0.42 | mad50 | 0.84490 | 0.41 | mae50 | 0.87243 | 0.41 | maf50 | 0.90083 | 0.41 | mag50 | 0.92853 | 0.41 | mah50 | 0.95333 | 0.42 |

[1] EALF is the energy of the average neutron lethargy causing fission, in eV.

Source: Output DTN: MO0711LOADCURV.000, file: *LoadingCurve.xls*, worksheet: "Results."

Table 6-35. Results for BW 15 × 15 with One Axial Zone – $k_{eff}$ + 2σ and EALF Values – Isotope Set PA+French-Metal

| Burnup | Enrichment [wt. %] | | | | | | | | | | | | | | | | | | | | | | | |
|---|---|---|---|---|---|---|---|---|---|---|---|---|---|---|---|---|---|---|---|---|---|---|---|
| | 1.5 | | | 2.0 | | | 2.5 | | | 3.0 | | | 3.5 | | | 4.0 | | | 4.5 | | | 5.0 | | |
| [GWd/MTU] | Case | $k_{eff}$ +2σ | EALF[1] | Case | $k_{eff}$ +2σ | EALF | Case | $k_{eff}$ +2σ | EALF | Case | $k_{eff}$ +2σ | EALF | Case | $k_{eff}$ +2σ | EALF | Case | $k_{eff}$ +2σ | EALF | Case | $k_{eff}$ +2σ | EALF | Case | $k_{eff}$ +2σ | EALF |
| 0 | mba00 | 0.88213 | 0.19 | mbb00 | 0.97192 | 0.20 | mbc00 | 1.03692 | 0.21 | mbd00 | 1.08597 | 0.23 | mbe00 | 1.12581 | 0.25 | mbf00 | 1.15746 | 0.27 | mbg00 | 1.18505 | 0.30 | mbh00 | 1.20741 | 0.33 |
| 5 | mba05 | 0.89148 | 0.25 | mbb05 | 0.95572 | 0.25 | mbc05 | 1.01027 | 0.25 | mbd05 | 1.05373 | 0.27 | mbe05 | 1.09051 | 0.29 | mbf05 | 1.12112 | 0.31 | mbg05 | 1.14695 | 0.33 | mbh05 | 1.16823 | 0.36 |
| 10 | mba10 | 0.87732 | 0.28 | mbb10 | 0.93444 | 0.28 | mbc10 | 0.98281 | 0.28 | mbd10 | 1.02493 | 0.29 | mbe10 | 1.06067 | 0.31 | mbf10 | 1.09202 | 0.33 | mbg10 | 1.11877 | 0.35 | mbh10 | 1.14172 | 0.37 |
| 15 | mba15 | 0.85749 | 0.31 | mbb15 | 0.90934 | 0.30 | mbc15 | 0.95554 | 0.30 | mbd15 | 0.99711 | 0.31 | mbe15 | 1.03268 | 0.32 | mbf15 | 1.06498 | 0.34 | mbg15 | 1.09222 | 0.36 | mbh15 | 1.11575 | 0.38 |
| 20 | mba20 | 0.83990 | 0.34 | mbb20 | 0.88528 | 0.33 | mbc20 | 0.92898 | 0.32 | mbd20 | 0.96904 | 0.33 | mbe20 | 1.00605 | 0.34 | mbf20 | 1.03751 | 0.35 | mbg20 | 1.06607 | 0.37 | mbh20 | 1.09075 | 0.39 |
| 25 | mba25 | 0.82626 | 0.36 | mbb25 | 0.86459 | 0.35 | mbc25 | 0.90454 | 0.34 | mbd25 | 0.94331 | 0.34 | mbe25 | 0.97913 | 0.35 | mbf25 | 1.01162 | 0.36 | mbg25 | 1.04108 | 0.38 | mbh25 | 1.06673 | 0.40 |
| 30 | mba30 | 0.81542 | 0.38 | mbb30 | 0.84760 | 0.37 | mbc30 | 0.88233 | 0.36 | mbd30 | 0.91907 | 0.36 | mbe30 | 0.95427 | 0.36 | mbf30 | 0.98618 | 0.37 | mbg30 | 1.01536 | 0.39 | mbh30 | 1.04206 | 0.40 |
| 35 | mba35 | 0.80641 | 0.40 | mbb35 | 0.83243 | 0.39 | mbc35 | 0.86382 | 0.38 | mbd35 | 0.89619 | 0.38 | mbe35 | 0.93002 | 0.38 | mbf35 | 0.96139 | 0.38 | mbg35 | 0.99074 | 0.40 | mbh35 | 1.01786 | 0.41 |
| 40 | mba40 | 0.80114 | 0.42 | mbb40 | 0.82038 | 0.41 | mbc40 | 0.84816 | 0.40 | mbd40 | 0.87658 | 0.39 | mbe40 | 0.90750 | 0.39 | mbf40 | 0.93821 | 0.40 | mbg40 | 0.96747 | 0.41 | mbh40 | 0.99420 | 0.42 |
| 45 | mba45 | 0.79448 | 0.43 | mbb45 | 0.81101 | 0.42 | mbc45 | 0.83407 | 0.42 | mbd45 | 0.85911 | 0.41 | mbe45 | 0.88703 | 0.41 | mbf45 | 0.91740 | 0.41 | mbg45 | 0.94520 | 0.42 | mbh45 | 0.97078 | 0.43 |
| 50 | mba50 | 0.79025 | 0.45 | mbb50 | 0.80395 | 0.44 | mbc50 | 0.82186 | 0.43 | mbd50 | 0.84503 | 0.43 | mbe50 | 0.86896 | 0.42 | mbf50 | 0.89548 | 0.42 | mbg50 | 0.92334 | 0.43 | mbh50 | 0.94910 | 0.44 |

[1] EALF is the energy of the average neutron lethargy causing fission, in eV.

Source: Output DTN: MO0711LOADCURV.000, file: *LoadingCurve.xls*, worksheet: "Results."

INTENTIONALLY LEFT BLANK

Table 6-36. Results for BW 15 × 15 with Seven Axial Zones – $k_{eff}$ + 2σ and EALF Values – Isotope Set Principal Actinide

| Burnup | Enrichment [wt. %] | | | | | | | | | | | | | | | | | | | | | | | |
|---|---|---|---|---|---|---|---|---|---|---|---|---|---|---|---|---|---|---|---|---|---|---|---|---|
| | 1.5 | | | 2.0 | | | 2.5 | | | 3.0 | | | 3.5 | | | 4.0 | | | 4.5 | | | 5.0 | | |
| [GWd/MTU] | Case | $k_{eff}$ +2σ | EALF[1] | Case | $k_{eff}$ +2σ | EALF | Case | $k_{eff}$ +2σ | EALF | Case | $k_{eff}$ +2σ | EALF | Case | $k_{eff}$ +2σ | EALF | Case | $k_{eff}$ +2σ | EALF | Case | $k_{eff}$ +2σ | EALF | Case | $k_{eff}$ +2σ | EALF |
| 0 | mga00 | 0.88130 | 0.19 | mgb00 | 0.97181 | 0.20 | mgc00 | 1.03735 | 0.21 | mgd00 | 1.08663 | 0.23 | mge00 | 1.12598 | 0.25 | mgf00 | 1.15791 | 0.27 | mgg00 | 1.18450 | 0.30 | mgh00 | 1.20703 | 0.33 |
| 10 | mga10 | 0.89508 | 0.27 | mgb10 | 0.95136 | 0.27 | mgc10 | 1.00003 | 0.27 | mgd10 | 1.04215 | 0.28 | mge10 | 1.07792 | 0.29 | mgf10 | 1.10882 | 0.31 | mgg10 | 1.13562 | 0.33 | mgh10 | 1.15878 | 0.36 |
| 15 | mga15 | 0.88016 | 0.30 | mgb15 | 0.93033 | 0.29 | mgc15 | 0.97659 | 0.29 | mgd15 | 1.01719 | 0.29 | mge15 | 1.05341 | 0.31 | mgf15 | 1.08427 | 0.32 | mgg15 | 1.11148 | 0.34 | mgh15 | 1.13551 | 0.36 |
| 20 | mga20 | 0.86703 | 0.32 | mgb20 | 0.91034 | 0.30 | mgc20 | 0.95386 | 0.30 | mgd20 | 0.99402 | 0.30 | mge20 | 1.02927 | 0.31 | mgf20 | 1.06031 | 0.33 | mgg20 | 1.08859 | 0.35 | mgh20 | 1.11292 | 0.37 |
| 25 | mga25 | 0.85668 | 0.33 | mgb25 | 0.89499 | 0.32 | mgc25 | 0.93448 | 0.31 | mgd25 | 0.97261 | 0.31 | mge25 | 1.00879 | 0.32 | mgf25 | 1.03957 | 0.33 | mgg25 | 1.06757 | 0.35 | mgh25 | 1.09258 | 0.37 |
| 30 | mga30 | 0.84891 | 0.35 | mgb30 | 0.88029 | 0.33 | mgc30 | 0.91581 | 0.33 | mgd30 | 0.95244 | 0.32 | mge30 | 0.98688 | 0.33 | mgf30 | 1.01821 | 0.34 | mgg30 | 1.04643 | 0.36 | mgh30 | 1.07164 | 0.37 |
| 35 | mga35 | 0.84400 | 0.36 | mgb35 | 0.86807 | 0.35 | mgc35 | 0.89938 | 0.34 | mgd35 | 0.93209 | 0.34 | mge35 | 0.96576 | 0.34 | mgf35 | 0.99611 | 0.35 | mgg35 | 1.02454 | 0.36 | mgh35 | 1.05021 | 0.38 |
| 40 | mga40 | 0.84017 | 0.37 | mgb40 | 0.85919 | 0.36 | mgc40 | 0.88678 | 0.35 | mgd40 | 0.91721 | 0.35 | mge40 | 0.94954 | 0.35 | mgf40 | 0.97943 | 0.35 | mgg40 | 1.00669 | 0.36 | mgh40 | 1.03211 | 0.38 |
| 45 | mga45 | 0.83703 | 0.38 | mgb45 | 0.85203 | 0.38 | mgc45 | 0.87409 | 0.37 | mgd45 | 0.90055 | 0.36 | mge45 | 0.92967 | 0.36 | mgf45 | 0.95891 | 0.36 | mgg45 | 0.98611 | 0.37 | mgh45 | 1.01150 | 0.38 |
| 50 | mga50 | 0.83560 | 0.39 | mgb50 | 0.84793 | 0.39 | mgc50 | 0.86402 | 0.38 | mgd50 | 0.88832 | 0.37 | mge50 | 0.91486 | 0.37 | mgf50 | 0.94226 | 0.37 | mgg50 | 0.96953 | 0.38 | mgh50 | 0.99385 | 0.39 |

[1] EALF is the energy of the average neutron lethargy causing fission, in eV.

Source: Output DTN: MO0711LOADCURV.000, file: *LoadingCurve.xls*, worksheet: "Results."

Table 6-37. Results for BW 15 × 15 with One Axial Zone – $k_{eff}$ + 2σ and EALF Values – Isotope Set Principal Actinide

| Burnup | Enrichment [wt. %] | | | | | | | | | | | | | | | | | | | | | | | |
|---|---|---|---|---|---|---|---|---|---|---|---|---|---|---|---|---|---|---|---|---|---|---|---|---|
| | 1.5 | | | 2.0 | | | 2.5 | | | 3.0 | | | 3.5 | | | 4.0 | | | 4.5 | | | 5.0 | | |
| [GWd/MTU] | Case | $k_{eff}$ +2σ | EALF[1] | Case | $k_{eff}$ +2σ | EALF | Case | $k_{eff}$ +2σ | EALF | Case | $k_{eff}$ +2σ | EALF | Case | $k_{eff}$ +2σ | EALF | Case | $k_{eff}$ +2σ | EALF | Case | $k_{eff}$ +2σ | EALF | Case | $k_{eff}$ +2σ | EALF |
| 0 | mha00 | 0.88187 | 0.19 | mhb00 | 0.97168 | 0.20 | mhc00 | 1.03713 | 0.21 | mhd00 | 1.08676 | 0.23 | mhe00 | 1.12606 | 0.25 | mhf00 | 1.15763 | 0.27 | mhg00 | 1.18382 | 0.30 | mhh00 | 1.20701 | 0.33 |
| 5 | mha05 | 0.90755 | 0.24 | mhb05 | 0.97297 | 0.24 | mhc05 | 1.02758 | 0.24 | mhd05 | 1.07163 | 0.26 | mhe05 | 1.10704 | 0.28 | mhf05 | 1.13829 | 0.30 | mhg05 | 1.16419 | 0.32 | mhh05 | 1.18561 | 0.35 |
| 10 | mha10 | 0.89937 | 0.27 | mhb10 | 0.95701 | 0.26 | mhc10 | 1.00593 | 0.27 | mhd10 | 1.04782 | 0.28 | mhe10 | 1.08392 | 0.29 | mhf10 | 1.11424 | 0.31 | mhg10 | 1.14156 | 0.33 | mhh10 | 1.16384 | 0.36 |
| 15 | mha15 | 0.88364 | 0.29 | mhb15 | 0.93615 | 0.29 | mhc15 | 0.98197 | 0.29 | mhd15 | 1.02344 | 0.29 | mhe15 | 1.05973 | 0.31 | mhf15 | 1.09128 | 0.32 | mhg15 | 1.11798 | 0.34 | mhh15 | 1.14212 | 0.36 |
| 20 | mha20 | 0.87021 | 0.31 | mhb20 | 0.91575 | 0.30 | mhc20 | 0.95987 | 0.30 | mhd20 | 0.99991 | 0.31 | mhe20 | 1.03616 | 0.32 | mhf20 | 1.06777 | 0.33 | mhg20 | 1.09551 | 0.35 | mhh20 | 1.12016 | 0.37 |
| 25 | mha25 | 0.86018 | 0.33 | mhb25 | 0.89886 | 0.32 | mhc25 | 0.93862 | 0.32 | mhd25 | 0.97787 | 0.32 | mhe25 | 1.01286 | 0.32 | mhf25 | 1.04493 | 0.34 | mhg25 | 1.07357 | 0.35 | mhh25 | 1.09820 | 0.37 |
| 30 | mha30 | 0.85148 | 0.35 | mhb30 | 0.88479 | 0.34 | mhc30 | 0.91925 | 0.33 | mhd30 | 0.95591 | 0.33 | mhe30 | 0.99141 | 0.33 | mhf30 | 1.02314 | 0.35 | mhg30 | 1.05146 | 0.36 | mhh30 | 1.07738 | 0.38 |
| 35 | mha35 | 0.84556 | 0.36 | mhb35 | 0.87224 | 0.35 | mhc35 | 0.90303 | 0.34 | mhd35 | 0.93642 | 0.34 | mhe35 | 0.97015 | 0.34 | mhf35 | 1.00072 | 0.35 | mhg35 | 1.02998 | 0.36 | mhh35 | 1.05592 | 0.38 |
| 40 | mha40 | 0.84234 | 0.37 | mhb40 | 0.86208 | 0.36 | mhc40 | 0.89041 | 0.36 | mhd40 | 0.91888 | 0.35 | mhe40 | 0.94964 | 0.35 | mhf40 | 0.98050 | 0.36 | mhg40 | 1.00959 | 0.37 | mhh40 | 1.03527 | 0.38 |
| 45 | mha45 | 0.83883 | 0.38 | mhb45 | 0.85487 | 0.37 | mhc45 | 0.87846 | 0.37 | mhd45 | 0.90356 | 0.36 | mhe45 | 0.93167 | 0.36 | mhf45 | 0.96159 | 0.37 | mhg45 | 0.98927 | 0.37 | mhh45 | 1.01518 | 0.39 |
| 50 | mha50 | 0.83552 | 0.39 | mhb50 | 0.84990 | 0.38 | mhc50 | 0.86811 | 0.38 | mhd50 | 0.89123 | 0.38 | mhe50 | 0.91619 | 0.37 | mhf50 | 0.94274 | 0.38 | mhg50 | 0.97025 | 0.38 | mhh50 | 0.99556 | 0.39 |

[1] EALF is the energy of the average neutron lethargy causing fission, in eV.

Source: Output DTN: MO0711LOADCURV.000, file: *LoadingCurve.xls*, worksheet: "Results."

INTENTIONALLY LEFT BLANK

Table 6-38. Results for BW 15 × 15 with Seven Axial Zones – $k_{eff}$ + 2σ and EALF Values – Isotope Set Actinide Only

| Burnup | Enrichment [wt. %] | | | | | | | | | | | | | | | | | | | | | | | |
|---|---|---|---|---|---|---|---|---|---|---|---|---|---|---|---|---|---|---|---|---|---|---|---|---|
| | 1.5 | | | 2.0 | | | 2.5 | | | 3.0 | | | 3.5 | | | 4.0 | | | 4.5 | | | 5.0 | | |
| [GWd/MTU] | Case | $k_{eff}$ +2σ | EALF[1] | Case | $k_{eff}$ +2σ | EALF | Case | $k_{eff}$ +2σ | EALF | Case | $k_{eff}$ +2σ | EALF | Case | $k_{eff}$ +2σ | EALF | Case | $k_{eff}$ +2σ | EALF | Case | $k_{eff}$ +2σ | EALF | Case | $k_{eff}$ +2σ | EALF |
| 0 | mea00 | 0.88198 | 0.19 | meb00 | 0.97175 | 0.20 | mec00 | 1.03700 | 0.21 | med00 | 1.08642 | 0.23 | mee00 | 1.12590 | 0.25 | mef00 | 1.15774 | 0.27 | meg00 | 1.18495 | 0.30 | meh00 | 1.20689 | 0.33 |
| 10 | mea10 | 0.89654 | 0.27 | meb10 | 0.95286 | 0.27 | mec10 | 1.00140 | 0.27 | med10 | 1.04328 | 0.28 | mee10 | 1.07986 | 0.29 | mef10 | 1.10971 | 0.31 | meg10 | 1.13715 | 0.33 | meh10 | 1.16029 | 0.36 |
| 15 | mea15 | 0.88309 | 0.29 | meb15 | 0.93231 | 0.28 | mec15 | 0.97829 | 0.29 | med15 | 1.02005 | 0.29 | mee15 | 1.05592 | 0.30 | mef15 | 1.08715 | 0.32 | meg15 | 1.11408 | 0.34 | meh15 | 1.13736 | 0.36 |
| 20 | mea20 | 0.87061 | 0.31 | meb20 | 0.91360 | 0.30 | mec20 | 0.95727 | 0.30 | med20 | 0.99686 | 0.30 | mee20 | 1.03293 | 0.31 | mef20 | 1.06388 | 0.33 | meg20 | 1.09174 | 0.35 | meh20 | 1.11613 | 0.37 |
| 25 | mea25 | 0.86168 | 0.33 | meb25 | 0.89886 | 0.32 | mec25 | 0.93843 | 0.31 | med25 | 0.97753 | 0.31 | mee25 | 1.01210 | 0.32 | mef25 | 1.04334 | 0.33 | meg25 | 1.07200 | 0.35 | meh25 | 1.09674 | 0.37 |
| 30 | mea30 | 0.85509 | 0.34 | meb30 | 0.88599 | 0.33 | mec30 | 0.92132 | 0.32 | med30 | 0.95755 | 0.32 | mee30 | 0.99189 | 0.33 | mef30 | 1.02308 | 0.34 | meg30 | 1.05151 | 0.35 | meh30 | 1.07693 | 0.37 |
| 35 | mea35 | 0.85147 | 0.35 | meb35 | 0.87556 | 0.34 | mec35 | 0.90613 | 0.34 | med35 | 0.93902 | 0.33 | mee35 | 0.97174 | 0.34 | mef35 | 1.00275 | 0.34 | meg35 | 1.03077 | 0.36 | meh35 | 1.05588 | 0.37 |
| 40 | mea40 | 0.84866 | 0.36 | meb40 | 0.86772 | 0.36 | mec40 | 0.89462 | 0.35 | med40 | 0.92460 | 0.34 | mee40 | 0.95626 | 0.34 | mef40 | 0.98658 | 0.35 | meg40 | 1.01421 | 0.36 | meh40 | 1.03900 | 0.37 |
| 45 | mea45 | 0.84673 | 0.37 | meb45 | 0.86285 | 0.37 | mec45 | 0.88332 | 0.36 | med45 | 0.90994 | 0.35 | mee45 | 0.93839 | 0.35 | mef45 | 0.96704 | 0.35 | meg45 | 0.99505 | 0.36 | meh45 | 1.01947 | 0.38 |
| 50 | mea50 | 0.84653 | 0.38 | meb50 | 0.85889 | 0.38 | mec50 | 0.87537 | 0.37 | med50 | 0.89916 | 0.36 | mee50 | 0.92446 | 0.36 | mef50 | 0.95238 | 0.36 | meg50 | 0.97844 | 0.37 | meh50 | 1.00341 | 0.38 |

[1] EALF is the energy of the average neutron lethargy causing fission, in eV.

Source: Output DTN: MO0711LOADCURV.000, file: *LoadingCurve.xls*, worksheet: “Results.”

Table 6-39. Results for BW 15 × 15 with One Axial Zone – $k_{eff}$ + 2σ and EALF Values – Isotope Set Actinide Only

| Burnup | Enrichment [wt. %] | | | | | | | | | | | | | | | | | | | | | | | |
|---|---|---|---|---|---|---|---|---|---|---|---|---|---|---|---|---|---|---|---|---|---|---|---|---|
| | 1.5 | | | 2.0 | | | 2.5 | | | 3.0 | | | 3.5 | | | 4.0 | | | 4.5 | | | 5.0 | | |
| [GWd/MTU] | Case | $k_{eff}$ +2σ | EALF[1] | Case | $k_{eff}$ +2σ | EALF | Case | $k_{eff}$ +2σ | EALF | Case | $k_{eff}$ +2σ | EALF | Case | $k_{eff}$ +2σ | EALF | Case | $k_{eff}$ +2σ | EALF | Case | $k_{eff}$ +2σ | EALF | Case | $k_{eff}$ +2σ | EALF |
| 0 | mfa00 | 0.88180 | 0.19 | mfb00 | 0.97142 | 0.20 | mfc00 | 1.03671 | 0.21 | mfd00 | 1.08668 | 0.23 | mfe00 | 1.12598 | 0.25 | mff00 | 1.15763 | 0.27 | mfg00 | 1.18401 | 0.30 | mfh00 | 1.20760 | 0.33 |
| 5 | mfa05 | 0.90838 | 0.24 | mfb05 | 0.97350 | 0.24 | mfc05 | 1.02828 | 0.24 | mfd05 | 1.07181 | 0.26 | mfe05 | 1.10839 | 0.28 | mff05 | 1.13810 | 0.30 | mfg05 | 1.16470 | 0.32 | mfh05 | 1.18669 | 0.34 |
| 10 | mfa10 | 0.89977 | 0.27 | mfb10 | 0.95809 | 0.26 | mfc10 | 1.00705 | 0.27 | mfd10 | 1.04838 | 0.28 | mfe10 | 1.08458 | 0.29 | mff10 | 1.11593 | 0.31 | mfg10 | 1.14232 | 0.33 | mfh10 | 1.16562 | 0.36 |
| 15 | mfa15 | 0.88635 | 0.29 | mfb15 | 0.93815 | 0.28 | mfc15 | 0.98439 | 0.28 | mfd15 | 1.02605 | 0.29 | mfe15 | 1.06148 | 0.30 | mff15 | 1.09348 | 0.32 | mfg15 | 1.11999 | 0.34 | mfh15 | 1.14338 | 0.36 |
| 20 | mfa20 | 0.87421 | 0.31 | mfb20 | 0.91872 | 0.30 | mfc20 | 0.96240 | 0.30 | mfd20 | 1.00288 | 0.30 | mfe20 | 1.03901 | 0.31 | mff20 | 1.07036 | 0.33 | mfg20 | 1.09821 | 0.35 | mfh20 | 1.12330 | 0.37 |
| 25 | mfa25 | 0.86520 | 0.33 | mfb25 | 0.90251 | 0.32 | mfc25 | 0.94300 | 0.31 | mfd25 | 0.98154 | 0.32 | mfe25 | 1.01715 | 0.32 | mff25 | 1.04916 | 0.33 | mfg25 | 1.07801 | 0.35 | mfh25 | 1.10296 | 0.37 |
| 30 | mfa30 | 0.85747 | 0.34 | mfb30 | 0.89069 | 0.33 | mfc30 | 0.92512 | 0.32 | mfd30 | 0.96208 | 0.32 | mfe30 | 0.99646 | 0.33 | mff30 | 1.02837 | 0.34 | mfg30 | 1.05680 | 0.35 | mfh30 | 1.08262 | 0.37 |
| 35 | mfa35 | 0.85241 | 0.35 | mfb35 | 0.87932 | 0.34 | mfc35 | 0.91057 | 0.34 | mfd35 | 0.94348 | 0.33 | mfe35 | 0.97695 | 0.34 | mff35 | 1.00788 | 0.35 | mfg35 | 1.03726 | 0.36 | mfh35 | 1.06280 | 0.37 |
| 40 | mfa40 | 0.85048 | 0.36 | mfb40 | 0.87090 | 0.35 | mfc40 | 0.89881 | 0.35 | mfd40 | 0.92823 | 0.34 | mfe40 | 0.95855 | 0.35 | mff40 | 0.98861 | 0.35 | mfg40 | 1.01736 | 0.36 | mfh40 | 1.04329 | 0.38 |
| 45 | mfa45 | 0.84817 | 0.37 | mfb45 | 0.86440 | 0.36 | mfc45 | 0.88814 | 0.36 | mfd45 | 0.91352 | 0.36 | mfe45 | 0.94167 | 0.35 | mff45 | 0.97133 | 0.36 | mfg45 | 0.99895 | 0.37 | mfh45 | 1.02429 | 0.38 |
| 50 | mfa50 | 0.84640 | 0.38 | mfb50 | 0.86122 | 0.37 | mfc50 | 0.87891 | 0.37 | mfd50 | 0.90308 | 0.37 | mfe50 | 0.92738 | 0.36 | mff50 | 0.95403 | 0.37 | mfg50 | 0.98139 | 0.37 | mfh50 | 1.00730 | 0.38 |

[1] EALF is the energy of the average neutron lethargy causing fission, in eV.

Source: Output DTN: MO0711LOADCURV.000, file: *LoadingCurve.xls*, worksheet: “Results.”

INTENTIONALLY LEFT BLANK

Table 6-40. Loading Curve Results for Various Burnup Credit Isotope Sets for Various Critical Limit Values

| Isotope Set | Enrichment [wt%] | Critical Limits | | | | | | | | | | | | | | | | | |
|---|---|---|---|---|---|---|---|---|---|---|---|---|---|---|---|---|---|---|---|
| | | Fresh Burned | 0.9905 0.9300 | Fresh Burned | 0.9905 0.9400 | Fresh Burned | 0.9905 0.9500 | Fresh Burned | 0.9905 0.9529 | Fresh Burned | 0.9905 0.9600 | Fresh Burned | 0.9905 0.9700 | Fresh Burned | 0.9905 0.9800 | Fresh Burned | 0.9905 0.9900 | Fresh Burned | 0.9905 1.0000 |
| | | Applied Limit | Required Burnup [gwd/mtu] | Applied Limit | Required Burnup [gwd/mtu] | Applied Limit | Required Burnup [gwd/mtu] | Applied Limit | Required Burnup [gwd/mtu] | Applied Limit | Required Burnup [gwd/mtu] | Applied Limit | Required Burnup [gwd/mtu] | Applied Limit | Required Burnup [gwd/mtu] | Applied Limit | Required Burnup [gwd/mtu] | Applied Limit | Required Burnup [gwd/mtu] |
| Principal | 1.5 | 0.9905 | 0.0 | 0.9905 | 0.0 | 0.9905 | 0.0 | 0.9905 | 0.0 | 0.9905 | 0.0 | 0.9905 | 0.0 | 0.9905 | 0.0 | 0.9905 | 0.0 | 0.9905 | 0.0 |
| Isotope | 2.0 | 0.9905 | 0.0 | 0.9905 | 0.0 | 0.9905 | 0.0 | 0.9905 | 0.0 | 0.9905 | 0.0 | 0.9905 | 0.0 | 0.9905 | 0.0 | 0.9905 | 0.0 | 0.9905 | 0.0 |
| | 2.5 | 0.9300 | 16.5 | 0.9400 | 14.8 | 0.9500 | 13.3 | 0.9529 | 12.8 | 0.9600 | 11.7 | 0.9700 | 10.2 | 0.9800 | 8.6 | 0.9900 | 7.0 | 1.0000 | 5.4 |
| | 3.0 | 0.9300 | 23.7 | 0.9400 | 21.7 | 0.9500 | 20.0 | 0.9529 | 19.5 | 0.9600 | 18.4 | 0.9700 | 16.7 | 0.9800 | 15.1 | 0.9900 | 13.6 | 1.0000 | 12.0 |
| | 3.5 | 0.9300 | 30.6 | 0.9400 | 28.7 | 0.9500 | 26.7 | 0.9529 | 26.2 | 0.9600 | 24.6 | 0.9700 | 22.8 | 0.9800 | 21.1 | 0.9900 | 19.4 | 1.0000 | 17.8 |
| | 4.0 | 0.9300 | 36.6 | 0.9400 | 34.7 | 0.9500 | 32.8 | 0.9529 | 32.2 | 0.9600 | 30.9 | 0.9700 | 29.0 | 0.9800 | 27.1 | 0.9900 | 25.1 | 1.0000 | 23.2 |
| | 4.5 | 0.9300 | 43.4 | 0.9400 | 41.3 | 0.9500 | 38.7 | 0.9529 | 37.9 | 0.9600 | 36.2 | 0.9700 | 34.3 | 0.9800 | 32.5 | 0.9900 | 30.6 | 1.0000 | 28.6 |
| | 5.0 | 0.9300 | 48.8 | 0.9400 | 46.5 | 0.9500 | 44.6 | 0.9529 | 44.1 | 0.9600 | 42.7 | 0.9700 | 40.3 | 0.9800 | 37.4 | 0.9900 | 35.3 | 1.0000 | 33.5 |
| PI-Metal | 1.5 | 0.9905 | 0.0 | 0.9905 | 0.0 | 0.9905 | 0.0 | 0.9905 | 0.0 | 0.9905 | 0.0 | 0.9905 | 0.0 | 0.9905 | 0.0 | 0.9905 | 0.0 | 0.9905 | 0.0 |
| | 2.0 | 0.9905 | 0.0 | 0.9905 | 0.0 | 0.9905 | 0.0 | 0.9905 | 0.0 | 0.9905 | 0.0 | 0.9905 | 0.0 | 0.9905 | 0.0 | 0.9905 | 0.0 | 0.9905 | 0.0 |
| | 2.5 | 0.9300 | 18.6 | 0.9400 | 16.8 | 0.9500 | 15.0 | 0.9529 | 14.5 | 0.9600 | 13.2 | 0.9700 | 11.5 | 0.9800 | 9.7 | 0.9900 | 7.9 | 1.0000 | 6.1 |
| | 3.0 | 0.9300 | 26.2 | 0.9400 | 24.2 | 0.9500 | 22.3 | 0.9529 | 21.8 | 0.9600 | 20.5 | 0.9700 | 18.7 | 0.9800 | 17.0 | 0.9900 | 15.3 | 1.0000 | 13.5 |
| | 3.5 | 0.9300 | 33.5 | 0.9400 | 31.5 | 0.9500 | 29.5 | 0.9529 | 28.9 | 0.9600 | 27.4 | 0.9700 | 25.4 | 0.9800 | 23.5 | 0.9900 | 21.6 | 1.0000 | 19.8 |
| | 4.0 | 0.9300 | 41.1 | 0.9400 | 38.2 | 0.9500 | 35.7 | 0.9529 | 35.1 | 0.9600 | 33.7 | 0.9700 | 31.7 | 0.9800 | 29.7 | 0.9900 | 27.7 | 1.0000 | 25.7 |
| | 4.5 | 0.9300 | 47.1 | 0.9400 | 45.0 | 0.9500 | 42.9 | 0.9529 | 42.3 | 0.9600 | 40.5 | 0.9700 | 37.7 | 0.9800 | 35.4 | 0.9900 | 33.4 | 1.0000 | 31.4 |
| | 5.0 | 0.9300 | 53.9 | 0.9400 | 51.2 | 0.9500 | 48.5 | 0.9529 | 47.7 | 0.9600 | 46.1 | 0.9700 | 44.0 | 0.9800 | 42.0 | 0.9900 | 39.2 | 1.0000 | 36.8 |
| PA+French | 1.5 | 0.9905 | 0.0 | 0.9905 | 0.0 | 0.9905 | 0.0 | 0.9905 | 0.0 | 0.9905 | 0.0 | 0.9905 | 0.0 | 0.9905 | 0.0 | 0.9905 | 0.0 | 0.9905 | 0.0 |
| | 2.0 | 0.9905 | 0.0 | 0.9905 | 0.0 | 0.9905 | 0.0 | 0.9905 | 0.0 | 0.9905 | 0.0 | 0.9905 | 0.0 | 0.9905 | 0.0 | 0.9905 | 0.0 | 0.9905 | 0.0 |
| | 2.5 | 0.9300 | 19.4 | 0.9400 | 17.5 | 0.9500 | 15.6 | 0.9529 | 15.1 | 0.9600 | 13.8 | 0.9700 | 12.1 | 0.9800 | 10.3 | 0.9900 | 8.5 | 1.0000 | 6.7 |
| | 3.0 | 0.9300 | 27.2 | 0.9400 | 25.3 | 0.9500 | 23.3 | 0.9529 | 22.7 | 0.9600 | 21.3 | 0.9700 | 19.5 | 0.9800 | 17.7 | 0.9900 | 15.9 | 1.0000 | 14.1 |
| | 3.5 | 0.9300 | 34.6 | 0.9400 | 32.6 | 0.9500 | 30.5 | 0.9529 | 29.9 | 0.9600 | 28.4 | 0.9700 | 26.3 | 0.9800 | 24.4 | 0.9900 | 22.5 | 1.0000 | 20.6 |
| | 4.0 | 0.9300 | 42.5 | 0.9400 | 39.9 | 0.9500 | 37.0 | 0.9529 | 36.4 | 0.9600 | 34.9 | 0.9700 | 32.9 | 0.9800 | 30.8 | 0.9900 | 28.8 | 1.0000 | 26.8 |
| | 4.5 | 0.9300 | 48.8 | 0.9400 | 46.3 | 0.9500 | 44.2 | 0.9529 | 43.6 | 0.9600 | 42.2 | 0.9700 | 39.5 | 0.9800 | 36.9 | 0.9900 | 34.8 | 1.0000 | 32.7 |
| | 5.0 | 0.9300 | 56.2 | 0.9400 | 53.4 | 0.9500 | 50.5 | 0.9529 | 49.7 | 0.9600 | 47.7 | 0.9700 | 45.5 | 0.9800 | 43.3 | 0.9900 | 40.9 | 1.0000 | 38.3 |

Source: Output DTN: MO0711LOADCURV.000, file: *LoadingCurve.xls*, worksheet: “LoadingCurve.”

INTENTIONALLY LEFT BLANK

Table 6-40. Loading Curve Results for Various Burnup Credit Isotope Sets for Various Critical Limit Values (Continued)

| Isotope Set | Enrichment [wt%] | Critical Limits: Fresh Burned | 0.9905 0.9300 | Fresh Burned | 0.9905 0.9400 | Fresh Burned | 0.9905 0.9500 | Fresh Burned | 0.9905 0.9529 | Fresh Burned | 0.9905 0.9600 | Fresh Burned | 0.9905 0.9700 | Fresh Burned | 0.9905 0.9800 | Fresh Burned | 0.9905 0.9900 | Fresh Burned | 0.9905 1.0000 |
|---|---|---|---|---|---|---|---|---|---|---|---|---|---|---|---|---|---|---|---|
| | | Applied Limit | Required Burnup [gwd/mtu] | Applied Limit | Required Burnup [gwd/mtu] | Applied Limit | Required Burnup [gwd/mtu] | Applied Limit | Required Burnup [gwd/mtu] | Applied Limit | Required Burnup [gwd/mtu] | Applied Limit | Required Burnup [gwd/mtu] | Applied Limit | Required Burnup [gwd/mtu] | Applied Limit | Required Burnup [gwd/mtu] | Applied Limit | Required Burnup [gwd/mtu] |
| PA+French –Metal | 1.5 | 0.9905 | 0.0 | 0.9905 | 0.0 | 0.9905 | 0.0 | 0.9905 | 0.0 | 0.9905 | 0.0 | 0.9905 | 0.0 | 0.9905 | 0.0 | 0.9905 | 0.0 | 0.9905 | 0.0 |
| | 2.0 | 0.9905 | 0.0 | 0.9905 | 0.0 | 0.9905 | 0.0 | 0.9905 | 0.0 | 0.9905 | 0.0 | 0.9905 | 0.0 | 0.9905 | 0.0 | 0.9905 | 0.0 | 0.9905 | 0.0 |
| | 2.5 | 0.9300 | 20.8 | 0.9400 | 18.8 | 0.9500 | 16.8 | 0.9529 | 16.3 | 0.9600 | 14.9 | 0.9700 | 13.0 | 0.9800 | 11.0 | 0.9900 | 9.1 | 1.0000 | 7.2 |
| | 3.0 | 0.9300 | 29.1 | 0.9400 | 27.0 | 0.9500 | 24.9 | 0.9529 | 24.3 | 0.9600 | 22.8 | 0.9700 | 20.8 | 0.9800 | 19.0 | 0.9900 | 17.1 | 1.0000 | 15.2 |
| | 3.5 | 0.9300 | 36.8 | 0.9400 | 34.6 | 0.9500 | 32.4 | 0.9529 | 31.8 | 0.9600 | 30.3 | 0.9700 | 28.2 | 0.9800 | 26.1 | 0.9900 | 24.1 | 1.0000 | 22.2 |
| | 4.0 | 0.9300 | 44.8 | 0.9400 | 42.6 | 0.9500 | 39.8 | 0.9529 | 39.0 | 0.9600 | 37.1 | 0.9700 | 34.9 | 0.9800 | 32.8 | 0.9900 | 30.7 | 1.0000 | 28.6 |
| | 4.5 | 0.9300 | 52.1 | 0.9400 | 49.2 | 0.9500 | 46.5 | 0.9529 | 45.9 | 0.9600 | 44.3 | 0.9700 | 42.0 | 0.9800 | 39.2 | 0.9900 | 36.9 | 1.0000 | 34.8 |
| | 5.0 | 0.9300 | 59.1 | 0.9400 | 56.3 | 0.9500 | 53.4 | 0.9529 | 52.6 | 0.9600 | 50.6 | 0.9700 | 47.8 | 0.9800 | 45.4 | 0.9900 | 43.1 | 1.0000 | 40.7 |
| Principal Actinide | 1.5 | 0.9905 | 0.0 | 0.9905 | 0.0 | 0.9905 | 0.0 | 0.9905 | 0.0 | 0.9905 | 0.0 | 0.9905 | 0.0 | 0.9905 | 0.0 | 0.9905 | 0.0 | 0.9905 | 0.0 |
| | 2.0 | 0.9905 | 0.0 | 0.9905 | 0.0 | 0.9905 | 0.0 | 0.9905 | 0.0 | 0.9905 | 0.0 | 0.9905 | 0.0 | 0.9905 | 0.0 | 0.9905 | 0.0 | 0.9905 | 0.0 |
| | 2.5 | 0.9300 | 28.6 | 0.9400 | 25.9 | 0.9500 | 23.4 | 0.9529 | 22.7 | 0.9600 | 21.0 | 0.9700 | 18.6 | 0.9800 | 16.2 | 0.9900 | 14.0 | 1.0000 | 11.8 |
| | 3.0 | 0.9300 | 38.7 | 0.9400 | 35.8 | 0.9500 | 33.1 | 0.9529 | 32.3 | 0.9600 | 30.5 | 0.9700 | 28.1 | 0.9800 | 25.7 | 0.9900 | 23.4 | 1.0000 | 21.0 |
| | 3.5 | 0.9300 | 47.8 | 0.9400 | 44.8 | 0.9500 | 41.9 | 0.9529 | 41.2 | 0.9600 | 39.3 | 0.9700 | 36.8 | 0.9800 | 34.3 | 0.9900 | 31.8 | 1.0000 | 29.4 |
| | 4.0 | 0.9300 | 56.4 | 0.9400 | 53.3 | 0.9500 | 50.5 | 0.9529 | 49.7 | 0.9600 | 47.7 | 0.9700 | 44.9 | 0.9800 | 42.1 | 0.9900 | 39.5 | 1.0000 | 36.9 |
| | 4.5 | 0.9300 | 65.0 | 0.9400 | 61.9 | 0.9500 | 58.7 | 0.9529 | 57.8 | 0.9600 | 55.5 | 0.9700 | 52.6 | 0.9800 | 49.8 | 0.9900 | 47.1 | 1.0000 | 44.5 |
| | 5.0 | 0.9300 | 71.5 | 0.9400 | 68.5 | 0.9500 | 65.5 | 0.9529 | 64.7 | 0.9600 | 62.6 | 0.9700 | 59.6 | 0.9800 | 56.7 | 0.9900 | 54.0 | 1.0000 | 51.3 |
| Actinide Only | 1.5 | 0.9905 | 0.0 | 0.9905 | 0.0 | 0.9905 | 0.0 | 0.9905 | 0.0 | 0.9905 | 0.0 | 0.9905 | 0.0 | 0.9905 | 0.0 | 0.9905 | 0.0 | 0.9905 | 0.0 |
| | 2.0 | 0.9905 | 0.0 | 0.9905 | 0.0 | 0.9905 | 0.0 | 0.9905 | 0.0 | 0.9905 | 0.0 | 0.9905 | 0.0 | 0.9905 | 0.0 | 0.9905 | 0.0 | 0.9905 | 0.0 |
| | 2.5 | 0.9300 | 30.1 | 0.9400 | 27.1 | 0.9500 | 24.4 | 0.9529 | 23.6 | 0.9600 | 21.6 | 0.9700 | 19.2 | 0.9800 | 16.8 | 0.9900 | 14.5 | 1.0000 | 12.1 |
| | 3.0 | 0.9300 | 41.4 | 0.9400 | 37.9 | 0.9500 | 34.9 | 0.9529 | 34.1 | 0.9600 | 32.1 | 0.9700 | 29.4 | 0.9800 | 26.7 | 0.9900 | 24.2 | 1.0000 | 21.7 |
| | 3.5 | 0.9300 | 51.5 | 0.9400 | 47.9 | 0.9500 | 44.7 | 0.9529 | 43.8 | 0.9600 | 41.6 | 0.9700 | 38.7 | 0.9800 | 35.9 | 0.9900 | 33.2 | 1.0000 | 30.6 |
| | 4.0 | 0.9300 | 60.5 | 0.9400 | 56.9 | 0.9500 | 53.7 | 0.9529 | 52.8 | 0.9600 | 50.7 | 0.9700 | 47.7 | 0.9800 | 44.6 | 0.9900 | 41.6 | 1.0000 | 38.9 |
| | 4.5 | 0.9300 | 67.9 | 0.9400 | 64.9 | 0.9500 | 61.9 | 0.9529 | 61.0 | 0.9600 | 58.9 | 0.9700 | 55.9 | 0.9800 | 52.9 | 0.9900 | 49.9 | 1.0000 | 47.0 |
| | 5.0 | 0.9300 | 76.5 | 0.9400 | 73.3 | 0.9500 | 70.2 | 0.9529 | 69.3 | 0.9600 | 67.1 | 0.9700 | 64.0 | 0.9800 | 60.9 | 0.9900 | 57.8 | 1.0000 | 54.8 |

Source: Output DTN: MO0711LOADCURV.000, file: *LoadingCurve.xls*, worksheet: "LoadingCurve."

INTENTIONALLY LEFT BLANK

## 6.4 MISLOAD ANALYSIS

The probability of exceeding the critical limit as a result of loading a *single* fuel assembly with insufficient burnup is evaluated. The resulting probability is intended for use in subsequent probabilistic analysis evaluating the overall risk associated with assembly misload events. Should additional analysis of multiple assembly misloads be required, the methodology presented here can be adapted easily to handle those cases. The analysis determines the likelihood that other assemblies within the waste package have sufficient excess burnup to compensate for the increased reactivity of a single misload assembly. Note that the analysis presumes a misload has occurred; the results do not include the probability of initially misloading an assembly.

The analysis is conducted with respect to the characterization of the projected fuel assembly waste stream presented in *Waste Packages and Source Terms for the Commercial 1999 Design Basis Waste Streams* (CRWMS M&O 2000 [DIRS 138239], Attachment III) using the “Case A” arrival forecast. This arrival forecast is selected based on Licensing Position LP-009, Waste Stream Parameters (Williams 2003 [DIRS 166132], Section 3.4).

A discretized representation of the PWR fuel inventory is shown in Figure 6-32. Here, the number of assemblies falling within 0.1 wt% enrichment and 1 GWd/MTU burnup bins are shown in a color-coded format. The color indicates the number of assemblies with burnup and enrichment falling within each bin, as indicated in the legend. The assemblies falling below the indicated PWR loading curve are potential misload assemblies and comprise the “misload inventory”. Those falling above the curve are acceptable assemblies, and are referred to as compensating assemblies and comprise the “compensating inventory”. Of the 93,770 assemblies in the inventory, a total of 1,990 (2.1%) are potential misload assemblies.

The corresponding BWR fuel inventory is represented in Figure 6-33 and shows that all assemblies in the arrival forecast meet the minimum burnup requirements. Hence, no BWR fuel misload analysis is performed.

The loading curve used to categorize assemblies as either misload or compensating assemblies did not include the step increase at the transition between fresh fuel and burnup fuel critical limits. Instead, the required minimum burnup for enrichments between 2.0 wt% and 2.5 wt% was obtained by linearly interpolating between 0.0 GWd/MTU at 2.0 wt% and 12.8 GWd/MTU at 2.5 wt%. That is, the step increase shown in Figure 6-32 at 2.0 wt% was removed. This discrepancy results in the mischaracterization of nine assemblies (out of 93,770) as compensating assemblies rather than misload assemblies.

This mischaracterization is insignificant because the required minimum burnup for these nine assemblies based on the step-wise loading curve is 11.02 GWd/MTU. The actual burnup of these assemblies shown in the inventory is 11.00 GWd/MTU. Hence, the assemblies are so close to the required minimum burnup that it is highly unlikely that a misload of any single one would exceed the critical limit.

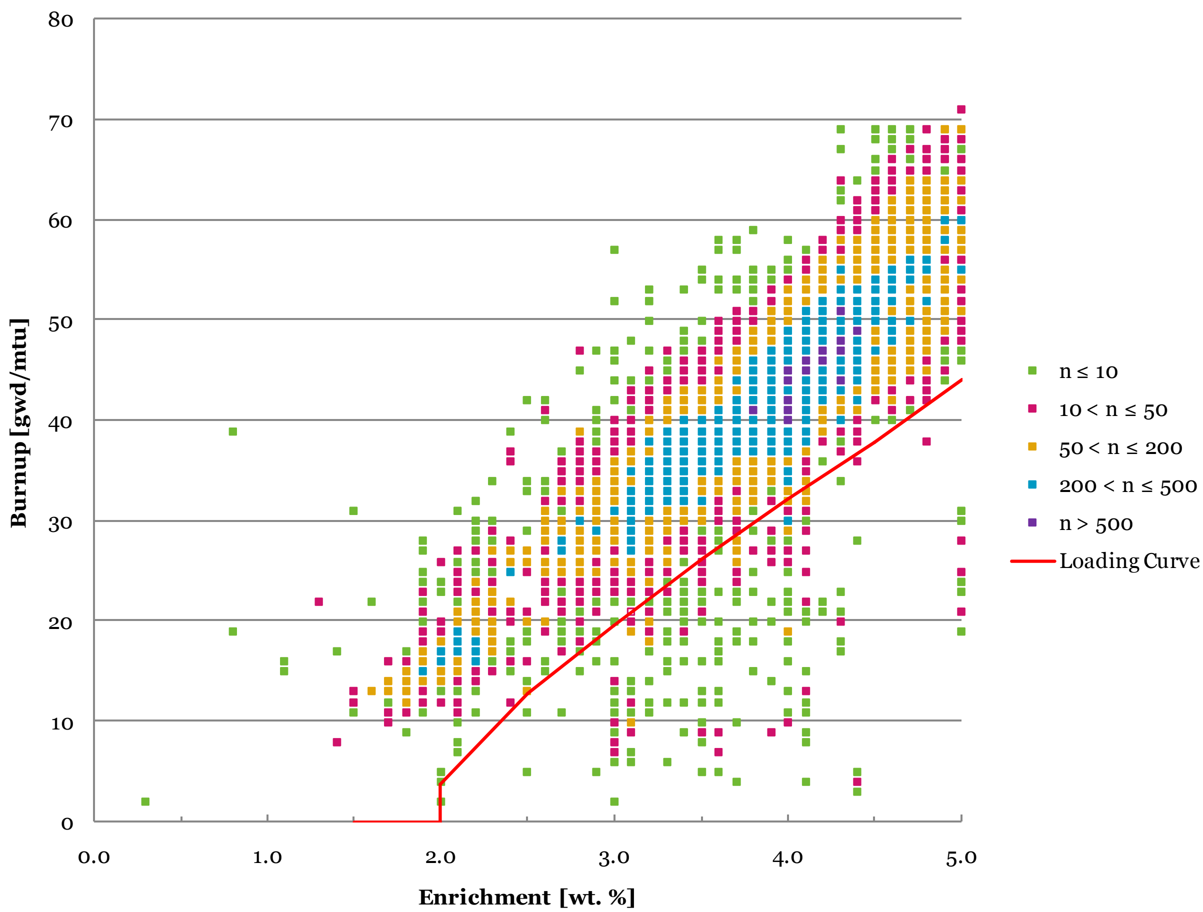


Source: Output DTN: MO0711LOADCURV.000, file: *LoadingCurve.xls*, worksheet: "Inventory."

NOTE: Parameter "n" is the number of assemblies within each burnup/enrichment bin.

Figure 6-32. Discretized Representation of PWR Fuel Inventory

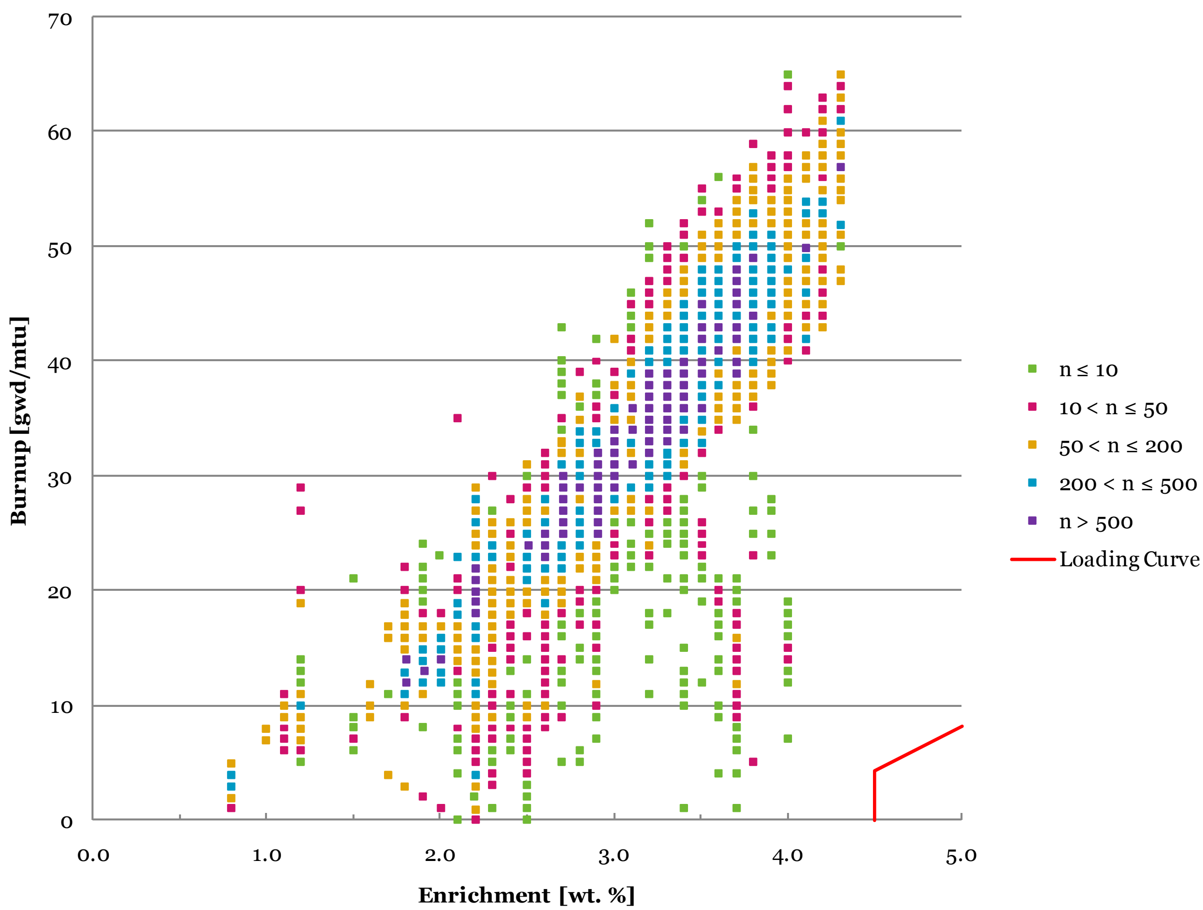


Source: Output DTN: MO0711LOADCURV.000, file: *LoadingCurve.xls*, worksheet: "InventoryBWR."

NOTE: Parameter "n" is the Number of Assemblies within Each Burnup/Enrichment bin.

Figure 6-33. Discretized Representation of BWR Fuel Inventory

### 6.4.1 Methodology

Due to symmetry, there are five unique basket positions in the 21PWR basket, labeled A through E as shown in Figure 6-34. A distinct misload analysis is performed for each position which evaluates the probability that a misload in that position leads to a $k_{eff}$ value exceeding the critical limit. The combined failure probability is then determined by combining the individual position results using the position multiplicities (the number of symmetrically identical positions of each type in the basket) as a weight function. If $P_{f,i}$ is the failure probability for a misload in position $i$ with multiplicity $M_i$, then the failure probability, $P_f$, is:

$$P_f = \frac{\sum_i M_i P_{f,i}}{\sum_i M_i}$$

The failure probabilities for each unique basket position, $P_{f,i}$ are determined by a stochastic analysis. In this analysis, waste packages are loaded based on random samples from the spent fuel inventory and the waste package reactivity is calculated and compared to the critical limit. For each misload position, a single assembly is uniformly sampled from the misload inventory. The remaining basket positions are filled by uniform sampling from the compensating assembly inventory. The samples with reactivities greater than the critical limit are tallied, and an estimate of the failure rate is obtained from the maximum likelihood estimator for a binomial distribution:

$$P = \frac{k}{n}$$

where $k$ is the number of failures in $n$ total trials.

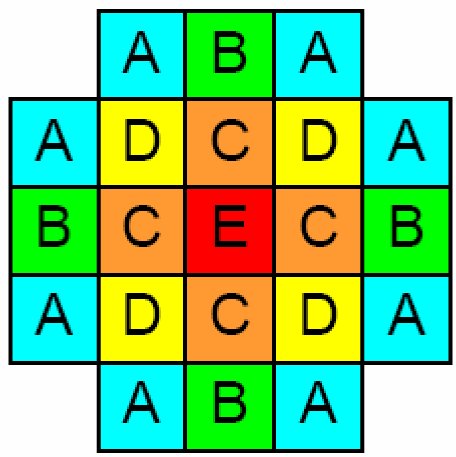


Source: For illustrative purposes.

Figure 6-34. Basket Position Identifiers

### 6.4.2 Analysis

For each trial, the sampled assemblies are conservatively represented with a burnup 5% less than the value provided in the spent fuel inventory database to account for uncertainty in indicated burnup values. In addition, although the spent fuel inventory contains assemblies with burnups in excess of 50 GWd/MTU, any sampled assembly with a burnup in excess of this value (after the 5% discount) is conservatively represented with a burnup of 50 GWd/MTU.

Reactivity calculations are performed using the base case configuration with a seven zone axial profile. The axial profile is employed in order to accentuate the potential effect of dissimilarities in axial burnup between neighboring assemblies.

A stratified sampling technique is employed in sampling the misload assembly for each trial. The stratification is based on the reactivity distribution of the misload assembly inventory. The reactivity for each misload assembly is determined by interpolating $k_{eff}$ on the assembly burnup and enrichment from the data in Table 6-8. The use of an approximate $k_{eff}$ value is of no consequence since the stratified sampling technique introduces no bias in the estimate. A histogram of the resulting $k_{eff}$ values for the misload inventory is shown in Figure 6-35. The stratified sampling parameters are shown in Table 6-41. The stratified sampling technique is equivalent to running a separate analysis for each strata and combining the results in proportion to the weight factor indicated in the table.

Analysis results are summarized in Table 6-42 based on the results for each misload position shown in Table 6-43 through Table 6-47. The results show that the assemblies in the highest $k_{eff}$ bin, comprising 36 assemblies in the entire inventory, are the only misload assemblies which violate the critical limit. Misload positions A and B, on the periphery of the basket, did not lead to any failures in the 1600 trials performed for each position.

The combined failure probability for all misload positions is 0.2%. By conservatively assuming that all misload positions have the same failure probability as the worst case E position, the resulting failure probability is 1.4%.

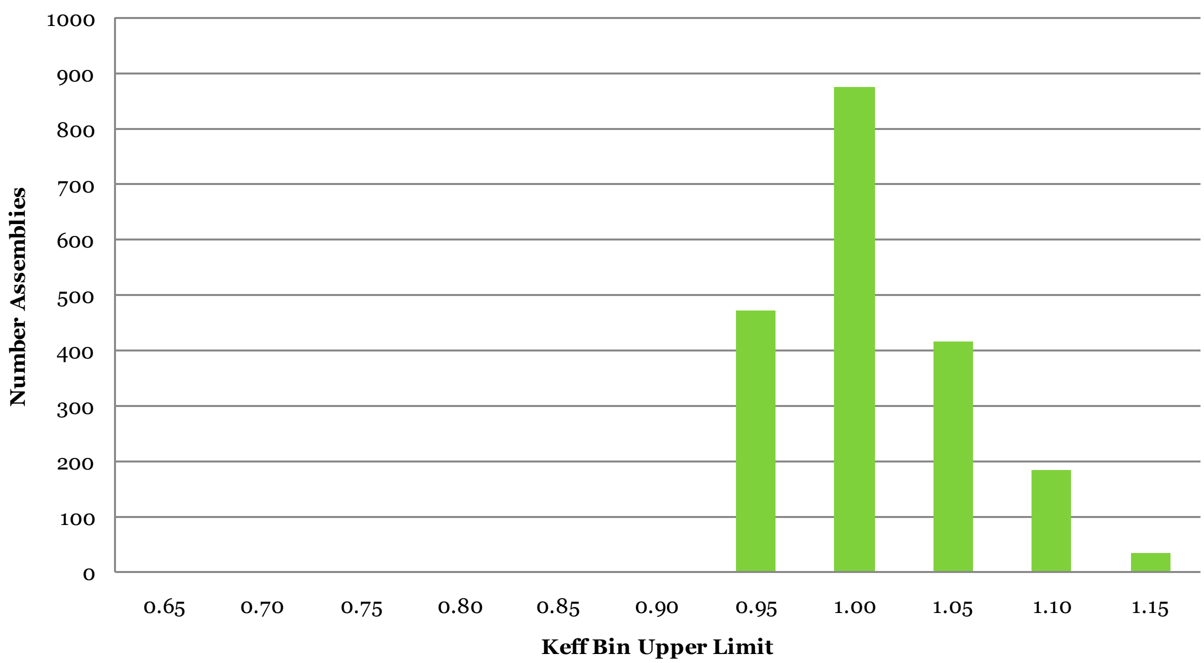


Source: Output DTN: MO0711LOADCURV.000, file: *LoadingCurve.xls*, worksheet: "Inventory."

Figure 6-35. Histogram of Misload Assembly $k_{eff}$ Values

Table 6-41. Misload Assembly Stratified Sampling Parameters

| Strata | Keff Bin Upper Limit | Num Assy | Weight |
|---|---|---|---|
| 0 | 0.95 | 474 | 0.238 |
| 1 | 1.00 | 877 | 0.441 |
| 2 | 1.05 | 417 | 0.210 |
| 3 | 1.10 | 186 | 0.093 |
| 4 | 1.15 | 36 | 0.018 |
| Total | | 1990 | 1.000 |

Source: Output DTN: MO0711LOADCURV.000, file: *LoadingCurve.xls*, worksheet: “ModelArb.”

Table 6-42. Combined Failure Probability for Each Misload Position

| Misload Type | Multiplicity | P fail | σ |
|---|---|---|---|
| A | 8 | 0.0% | 0.00% |
| B | 4 | 0.0% | 0.00% |
| C | 4 | 0.8% | 0.03% |
| D | 4 | 0.1% | 0.00% |
| E | 1 | 1.4% | 0.03% |
| Total | | 0.2% | 0.01% |

Source: Output DTN: MO0711LOADCURV.000, file: *LoadingCurve.xls*, worksheet: “Results.”

Table 6-43. Misload Type A Results

| Strata | $K_{eff}$ Bin Upper Limit | Num Assy | Weight | Cases | Series | Cases Run | k + 2σ > CL(0.9529) | | |
|---|---|---|---|---|---|---|---|---|---|
| | | | | | | | Failed | P fail | σ |
| 0 | 0.95 | 474 | 0.238 | 160 | fa0 | 160 | 0 | 0.0% | 0.0% |
| 1 | 1.00 | 877 | 0.441 | 160 | fa1 | 160 | 0 | 0.0% | 0.0% |
| 2 | 1.05 | 417 | 0.210 | 320 | fa2 | 320 | 0 | 0.0% | 0.0% |
| 3 | 1.10 | 186 | 0.093 | 320 | fa3 | 320 | 0 | 0.0% | 0.0% |
| 4 | 1.15 | 36 | 0.018 | 640 | fa4 | 640 | 0 | 0.0% | 0.0% |
| Total | | 1990 | 1.000 | 1600 | | 1600 | | 0.0% | 0.0% |

Source: Output DTN: MO0711LOADCURV.000, file: *LoadingCurve.xls*, worksheet: "Results."

Table 6-44. Misload Type B Results

| Strata | $K_{eff}$ Bin Upper Limit | Num Assy | Weight | Cases | Series | Cases Run | k + 2σ > CL(0.9529) | | |
|---|---|---|---|---|---|---|---|---|---|
| | | | | | | | Failed | P fail | σ |
| 0 | 0.95 | 474 | 0.238 | 160 | fb0 | 160 | 0 | 0.0% | 0.0% |
| 1 | 1.00 | 877 | 0.441 | 160 | fb1 | 160 | 0 | 0.0% | 0.0% |
| 2 | 1.05 | 417 | 0.210 | 320 | fb2 | 320 | 0 | 0.0% | 0.0% |
| 3 | 1.10 | 186 | 0.093 | 479 | fb3 | 479 | 0 | 0.0% | 0.0% |
| 4 | 1.15 | 36 | 0.018 | 479 | fb4 | 479 | 0 | 0.0% | 0.0% |
| Total | | 1990 | 1.000 | 1598 | | 1598 | | 0.0% | 0.0% |

Source: Output DTN: MO0711LOADCURV.000, file: *LoadingCurve.xls*, worksheet: "Results."

Table 6-45. Misload Type C Results

| Strata | $K_{eff}$ Bin Upper Limit | Num Assy | Weight | Cases | Series | Cases Run | k + 2σ > CL(0.9529) | | |
|---|---|---|---|---|---|---|---|---|---|
| | | | | | | | Failed | P fail | σ |
| 0 | 0.95 | 474 | 0.238 | 160 | fc0 | 160 | 0 | 0.0% | 0.0% |
| 1 | 1.00 | 877 | 0.441 | 320 | fc1 | 320 | 0 | 0.0% | 0.0% |
| 2 | 1.05 | 417 | 0.210 | 479 | fc2 | 479 | 0 | 0.0% | 0.0% |
| 3 | 1.10 | 186 | 0.093 | 479 | fc3 | 479 | 0 | 0.0% | 0.0% |
| 4 | 1.15 | 36 | 0.018 | 720 | fc4 | 720 | 312 | 43.3% | 1.8% |
| Total | | 1990 | 1.000 | 2158 | | 2158 | | 0.8% | 0.03% |

Source: Output DTN: MO0711LOADCURV.000, file: *LoadingCurve.xls*, worksheet: "Results."

Table 6-46. Misload Type D Results

| | $K_{eff}$ Bin | | | | | Cases | k + 2σ > CL(0.9529) | | |
|---|---|---|---|---|---|---|---|---|---|
| Strata | Upper Limit | Num Assy | Weight | Cases | Series | Run | Failed | P fail | σ |
| 0 | 0.95 | 474 | 0.238 | 160 | fd0 | 160 | 0 | 0.0% | 0.0% |
| 1 | 1.00 | 877 | 0.441 | 160 | fd1 | 160 | 0 | 0.0% | 0.0% |
| 2 | 1.05 | 417 | 0.210 | 320 | fd2 | 320 | 0 | 0.0% | 0.0% |
| 3 | 1.10 | 186 | 0.093 | 479 | fd3 | 479 | 0 | 0.0% | 0.0% |
| 4 | 1.15 | 36 | 0.018 | 479 | fd4 | 479 | 15 | 3.1% | 0.8% |
| Total | | 1990 | 1.000 | 1598 | | 1598 | | 0.1% | 0.0001% |

Source: Output DTN: MO0711LOADCURV.000, file: *LoadingCurve.xls*, worksheet: "Results."

Table 6-47. M Type E Results

| | $K_{eff}$ Bin | | | | | Cases | k + 2σ > CL(0.9529) | | |
|---|---|---|---|---|---|---|---|---|---|
| Strata | Upper Limit | Num Assy | Weight | Cases | Series | Run | Failed | P fail | σ |
| 0 | 0.95 | 474 | 0.238 | 160 | fe0 | 160 | 0 | 0.0% | 0.0% |
| 1 | 1.00 | 877 | 0.441 | 320 | fe1 | 320 | 0 | 0.0% | 0.0% |
| 2 | 1.05 | 417 | 0.210 | 479 | fe2 | 479 | 0 | 0.0% | 0.0% |
| 3 | 1.10 | 186 | 0.093 | 479 | fe3 | 479 | 0 | 0.0% | 0.0% |
| 4 | 1.15 | 36 | 0.018 | 720 | fe4 | 720 | 538 | 74.7% | 1.6% |
| Total | | 1990 | 1.000 | 2158 | | 2158 | | 1.4% | 0.03% |

Source: Output DTN: MO0711LOADCURV.000, file: *LoadingCurve.xls*, worksheet: "Results."

# 7. CONCLUSIONS

Loading curves for PWR and BWR fuel assemblies are developed. A sensitivity analysis shows that results are not highly sensitive to parameters used in the representation. An analysis of the potential for violating critical limits due to the misload of an underburned assembly shows that the overall probability of exceeding the critical limit due to misload is conservatively bounded by 1.4%.

Loading curves for PWR and BWR fuel are summarized in Table 7-1 and Table 7-2 and shown graphically in Figure 7-1 and Figure 7-2. Required minimum burnup values in GWd/MTU at intermediate enrichments are obtained using polynomial fits to the data as shown below:

For PWR fuel, the minimum required burnup in GWd/MTU is given by:

$$b = \begin{cases} 0 \text{ for } e < 2.0\,\text{wt.\%} \\ 0.4854\text{e}^5 - 8.6621e^4 + 60.9498e^3 - 211.9900e^2 + 378.3106e - 269.4040 \\ \text{for } 2.0\,\text{wt.\%} \le e \le 5.0\,\text{wt.\%} \end{cases}$$

Source: Output DTN: MO0711LOADCURV.000, file: *LoadingCurve.xls*, worksheet: “LoadingCurve.”
NOTE: Enrichment *e* has units weight *percent*, not weight *fraction*.

For BWR fuel, the minimum required burnup in GWd/MTU is given by:

$$b = \begin{cases} 0 \text{ for } e < 4.5\,\text{wt.\%} \\ 7.7911\text{e} - 30.7201 \text{ for } 4.5\,\text{wt.\%} \le e \le 5.0\,\text{wt.\%} \end{cases}$$

Source: Output DTN: MO0711LOADCURV.000, file: *LoadingCurve.xls*, worksheet: “LoadingCurve.”
NOTE: Enrichment *e* has units weight *percent*, not weight *fraction*.

Parameter sensitivity studies show that the base case representation provides a bounding description of the postclosure conditions of the waste package. The package is shown to be undermoderated, with full density pure water providing the maximum reactivity. The effect of a realistic representation of water based on the J13 well water composition shows an insignificant change in reactivity.

Table 7-3 summarizes the key parameters of the base case representation used to generate the loading curves.

Table 7-1. PWR Loading Curve

| **Enrichment [wt %]** | **Burnup Limit [GWd/MTU]** | **With 5% Margin [GWd/MTU]** |
|---|---|---|
| 1.5 | 0.0 | 0.0 |
| < 2.0 | 0.0 | 0.0 |
| ≥ 2.0 | 3.6 | 3.8 |
| 2.5 | 12.2 | 12.8 |
| 3.0 | 18.6 | 19.5 |
| 3.5 | 24.9 | 26.2 |
| 4.0 | 30.7 | 32.2 |
| 4.5 | 36.1 | 37.9 |
| 5.0 | 42.0 | 44.1 |

Source: Output DTN: MO0711LOADCURV.000, file: *LoadingCurve.xls*, worksheet: "Results."

Table 7-2. BWR Loading Curve

| **Enrichment [wt %]** | **Burnup Limit [GWd/MTU]** | **With 5% Margin [GWd/MTU]** |
|---|---|---|
| 1.5 | 0.0 | 0.0 |
| 2.0 | 0.0 | 0.0 |
| 2.5 | 0.0 | 0.0 |
| 3.0 | 0.0 | 0.0 |
| 3.5 | 0.0 | 0.0 |
| 4.0 | 0.0 | 0.0 |
| < 4.5 | 0.0 | 0.0 |
| ≥ 4.5 | 4.1 | 4.3 |
| 5.0 | 7.8 | 8.2 |

Source: Output DTN: MO0711LOADCURV.000, file: *LoadingCurve.xls*, worksheet: "Results."

Table 7-3. Base Case Representation Parameters

| **Parameter** | **Value** | **Basis** |
|---|---|---|
| Fuel Material | $UO_2$ Density 10.741 g/cm$^3$ | Sections 6.1.1.1.2 and 6.2.3.2 |
| Absorber | 6 mm thick borated stainless steel with 75% of the 1.12 wt. % boron loading credited | Sections 6.1.1.2.2, 6.2.3.1 and 6.2.4.3 |
| Moderator | Water at density of 1.0 g/cm$^3$ | Section 6.2.2 |
| Reflector | Dry tuff | Section 6.2.2 |
| Geometry | Tightly packed lattice array as shown in Figure 6-3 and Figure 6-4 for PWR and BWR baskets, respectively. | Sections 6.1.1.2 and 6.2.4 |

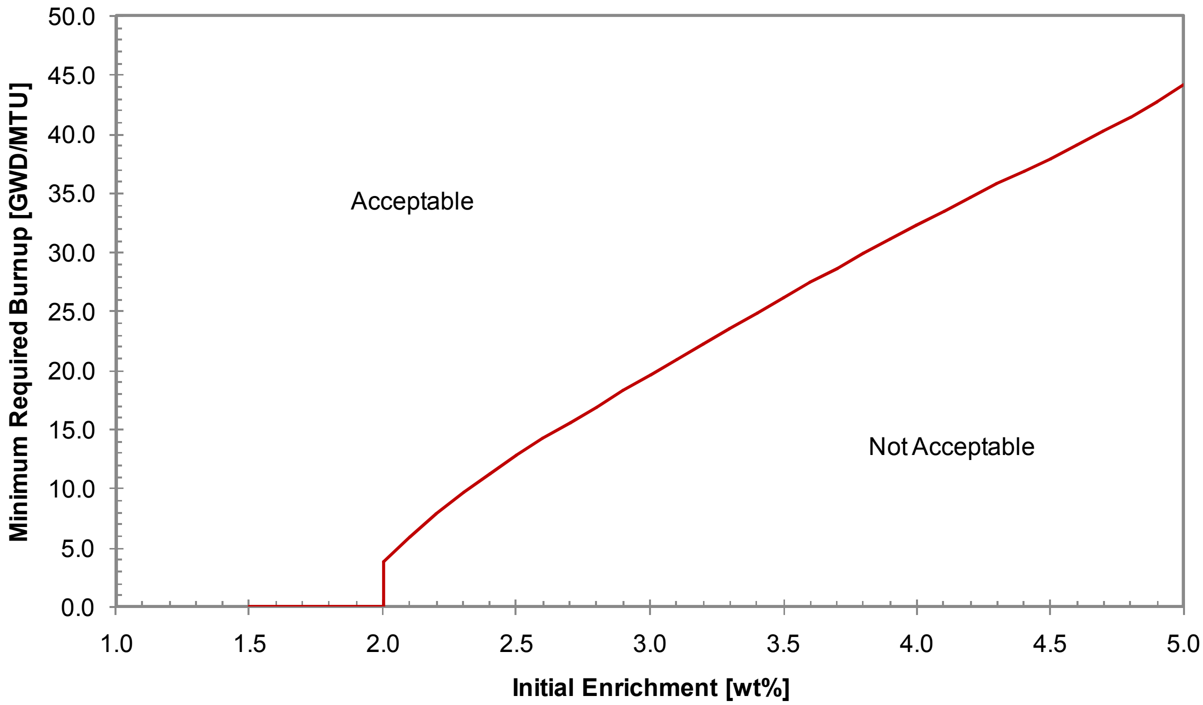


Source: Output DTN: MO0711LOADCURV.000, file: *LoadingCurve.xls*, worksheet: "Results."

Figure 7-1. PWR Loading Curve

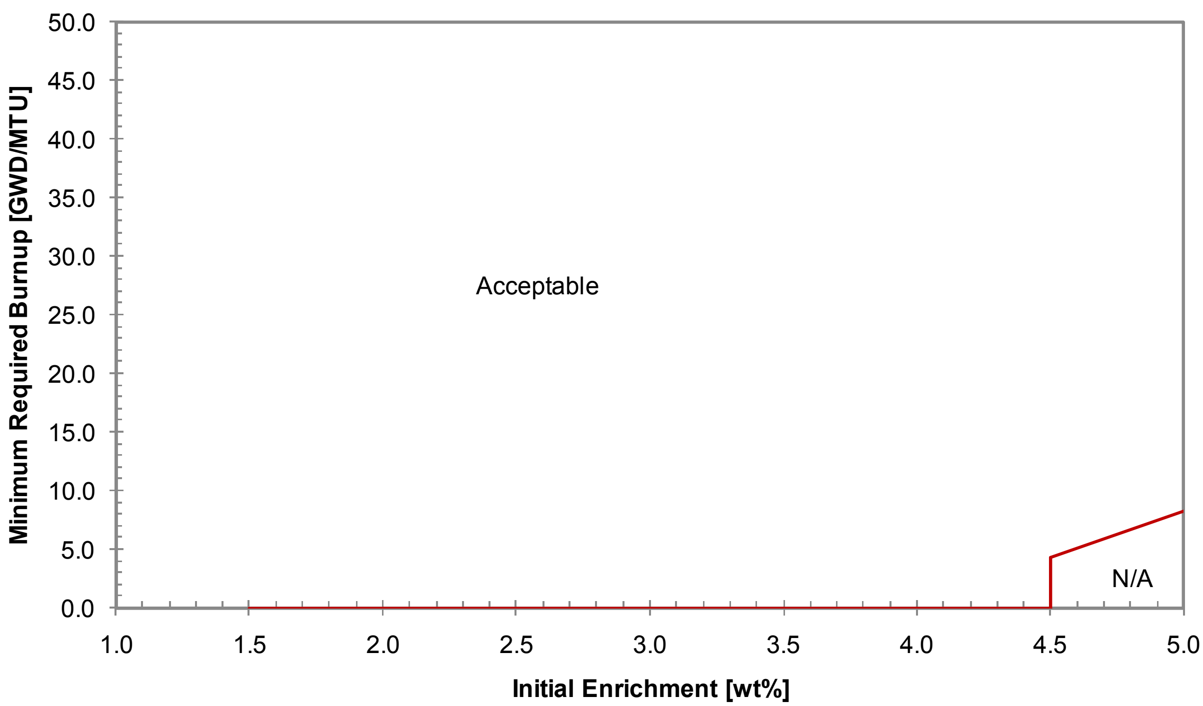


Source: Output DTN: MO0711LOADCURV.000, file: *LoadingCurve.xls*, worksheet: "Results."

Figure 7-2. BWR Loading Curve

INTENTIONALLY LEFT BLANK

# 8. INPUTS AND REFERENCES

## 8.1 DOCUMENTS CITED

168553 BSC (Bechtel SAIC Company) 2004. *Criticality Model.* CAL-DS0-NU-000003 REV 00A. Las Vegas, Nevada: Bechtel SAIC Company. ACC: DOC.20040913.0008; DOC.20050728.0007.

166142 BSC 2003. *Isotopic Generation and Confirmation of the PWR Application Model.* CAL-DSU-NU-000004 REV 00A. Las Vegas, Nevada: Bechtel SAIC Company. ACC: DOC.20031110.0003; DOC.20050523.0005; DOC.20050801.0005.

166138 BSC 2003. *PWR Axial Burnup Profile Analysis.* CAL-DSU-NU-000012 REV 00A. Las Vegas, Nevada: Bechtel SAIC Company. ACC: DOC.20031002.0002; DOC.20050727.0006.

169987 BSC 2004. *CSNF Waste Form Degradation: Summary Abstraction.* ANL-EBS-MD-000015 REV 02. Las Vegas, Nevada: Bechtel SAIC Company. ACC: DOC.20040908.0001; DOC.20050620.0004.

168554 BSC 2004. *Isotopic Model for Commercial SNF Burnup Credit.* CAL-DSU-NU-000007 REV 00B. Las Vegas, Nevada: Bechtel SAIC Company. ACC: DOC.20041122.0003; DOC.20050801.0003.

177193 BSC 2006. *Dimension and Material Specification Selection for Use in Criticality Analyses.* CAL-DSU-NU-000017 REV 0A. Las Vegas, Nevada: Bechtel SAIC Company. ACC: DOC.20060906.0004.

180664 BSC 2006. *Evaluation of Neutron Absorber Materials Used for Criticality Control in Waste Packages.* CAL-DS0-NU-000007 REV 0A. Las Vegas, Nevada: Bechtel SAIC Company. ACC: DOC.20061009.0003.

182214 BSC 2007. *Preclosure Criticality Analysis Process Report.* TDR-DS0-NU-000001 REV 02. Las Vegas, Nevada: Bechtel SAIC Company. ACC: DOC.20071023.0011.

137617 Cacciapouti, R.J. and Van Volkinburg, S. 1997. *Axial Burnup Profile Database for Pressurized Water Reactors.* YAEC-1937. Bolton, Massachusetts: Yankee Atomic Electric Company. ACC: MOL.19980209.0184.

138239 CRWMS M&O 2000. *Waste Packages and Source Terms for the Commercial 1999 Design Basis Waste Streams.* CAL-MGR-MD-000001 REV 00. Las Vegas, Nevada: CRWMS M&O. ACC: MOL.20000214.0479.

181316 DOE (U.S. Department of Energy) 1997. *Horizontal Burnup Gradient Datafile for PWR Assemblies.* DOE/RW-0496. Washington, D.C.: U.S. Department of Energy, Office of Civilian Radioactive Waste Management. ACC: MOV.19970625.0080.

180516 DOE 2007. *Software Validation Report for: MCNP5 v1.40.* Document ID: 11199-SVR-1.40-00-WINXP. Las Vegas, Nevada: U.S. Department of Energy, Office of Repository Development. ACC: MOL.20070228.0252.

181403 DOE 2007. *Transportation, Aging and Disposal Canister System Performance Specification.* WMO-TADCS-000001, Rev. 0. Washington, D.C.: U.S. Department of Energy, Office of Civilian Radioactive Waste Management. ACC: DOC.20070614.0007.

168494 Holtec International 2002. *Final Safety Analysis Report for the Holtec International Storage and Transfer Operation Reinforced Module Cask System (Hi-Storm 100 Cask System).* Holtec Report HI-2002444. Two volumes. NRC Docket No. 72-1014. Marlton, New Jersey: Holtec International. TIC: 255899.

146576 Larsen, N.H.; Parkos, G.R.; and Raza, O. 1976. *Core Design and Operating Data for Cycles 1 and 2 of Quad Cities 1.* EPRI NP-240. Palo Alto, California: Electric Power Research Institute. TIC: 237267.

173618 Massie, H.L., Jr. 2004. *Isotopic Generation and Confirmation of the BWR Application Model.* 32-5035847-02. Las Vegas, Nevada: Areva. ACC: DOC.20050125.0010.

170651 Massie, H.L., Jr. 2004. *Reactor Record Uncertainty Determination.* 32-5041666-02. Las Vegas, Nevada: Areva. ACC: DOC.20040623.0002; DOC.20050125.0013.

101903 NRC (U.S. Nuclear Regulatory Commission) 1997. *Standard Review Plan for Dry Cask Storage Systems*. NUREG-1536. Washington, D.C.: U.S. Nuclear Regulatory Commission. ACC: MOL.20010724.0307.

103896 Parrington, J.R.; Knox, H.D.; Breneman, S.L.; Baum, E.M.; and Feiner, F. 1996. *Nuclides and Isotopes, Chart of the Nuclides.* 15th Edition. San Jose, California: General Electric Company and KAPL, Inc. TIC: 233705.

178236 SNL (Sandia National Laboratories) 2007. *Criticality Input to Canister Based System Performance Specification for Disposal.* TDR-DS0-NU-000002 REV 01. Las Vegas, Nevada: Sandia National Laboratories. ACC: DOC.20070103.0002.

181165 SNL 2007. *Geochemistry Model Validation Report: Material Degradation and Release Model.* ANL-EBS-GS-000001 REV 02. Las Vegas, Nevada: Sandia National Laboratories. ACC: DOC.20070928.0010.

184433 SNL 2008. *Multiscale Thermohydrologic Model.* ANL-EBS-MD-000049 REV 03 AD 02. Las Vegas, Nevada: Sandia National Laboratories. ACC: DOC.20080201.0003.

182953 SNL 2007. *PWR Radial Burnup Gradient Reactivity Evaluation.* ANL-DSC-NU-000001 REV 000. Las Vegas, Nevada: Sandia National Laboratories. ACC: DOC.20071016.0002.

178869 SNL 2007. *Technical Work Plan for: Postclosure Criticality.* TWP-EBS-MD-000018 REV 01. Las Vegas, Nevada: Sandia National Laboratories. ACC: DOC.20070206.0003.

179394 SNL 2007. *Total System Performance Assessment Data Input Package for Requirements Analysis for Transportation Aging and Disposal Canister and Related Waste Package Physical Attributes Basis for Performance Assessment.* TDR-TDIP-ES-000006 REV 00. Las Vegas, Nevada: Sandia National Laboratories. ACC: DOC.20070918.0005.

107735 Todreas, N.E. and Kazimi, M.S. 1990. *Nuclear Systems I, Thermal Hydraulic Fundamentals.* New York, New York: Hemisphere Publishing. TIC: 226511.

166132 Williams, N.H. 2003. "Contract No. DE-AC28-01RW12101 - Licensing Position-009, Waste Stream Parameters." Letter from N.H. Williams (BSC) to J.D. Ziegler (DOE/ORD), November 13, 2003, 1105039412, with enclosure. ACC: MOL.20031215.0076.

169319 Wimmer, L.B. 2004. *Isotopic Generation and Confirmation of the BWR Appl. Model.* 32-5035847-01. Las Vegas, Nevada: Areva. ACC: DOC.20040630.0007.

165505 YMP (Yucca Mountain Site Characterization Project) 2003. *Disposal Criticality Analysis Methodology Topical Report.* YMP/TR-004Q, Rev. 02. Las Vegas, Nevada: Yucca Mountain Site Characterization Office. ACC: DOC.20031110.0005.

## 8.2 CODES, STANDARDS, REGULATIONS, AND PROCEDURES

180319 10 CFR 63. 2007. Energy: Disposal of High-Level Radioactive Wastes in a Geologic Repository at Yucca Mountain, Nevada. Internet Accessible.

178058 ASTM A 887-89 (Reapproved 2004). 2004. *Standard Specification for Borated Stainless Steel Plate, Sheet, and Strip for Nuclear Application.* West Conshohocken, Pennsylvania: American Society for Testing and Materials. TIC: 258746.

IM-PRO-003, *Software Management*

SCI-PRO-005, *Scientific Analyses and Calculations*

## 8.3 SOURCE DATA, LISTED BY DATA TRACKING NUMBER

178850 SN0612T0502404.014. Thermodynamic Database Input File for EQ3/6 - DATA0.YMP.R5. Submittal date: 12/15/2006.

151029 MO0006J13WTRCM.000. Recommended Mean Values of Major Constituents in J-13 Well Water. Submittal date: 06/07/2000.

184166 MO0711RABDPCSF.000. Range of Applicability and Bias Determination for Postclosure Criticality of Commercial Spent Nuclear Fuel. Submittal date: 11/01/2007..

163089 LL010902212241.026. CSNF Alteration Phase Porosity Estimates. Submittal date: 09/21/2001.

## 8.4 SOFTWARE CODES

180515 MCNP5 V. 1.40. 2007. Windows XP. STN: 11199-1.40-00.

## 8.5 OUTPUT DATA, LISTED BY DATA TRACKING NUMBER

MO0711LOADCURV.000. Electronic Files for CSNF Loading Curve Sensitivity Analysis. Submittal date: 09/21/2007.

# APPENDIX A
# INPUT FILE GENERATION

# A. INPUT FILE GENERATION

To facilitate the analysis, MCNP input descriptions are developed in Excel and written out to files using Excel macros. These routines are intended for the single purpose of copying data from Excel to text-format input files and have not been developed for routine use. The actual input files so generated are included in the scope of review of this analysis.

The key routine is “writeMCNPRangeToFile” which writes a selected Excel range to a text file making certain textual modifications as follows:

1. If the first cell in a row of the range starts with “n/u” or “not used”, the row is skipped.

2. If the first character in the first cell of a row is “#”, the following text is taken as the name of an Excel named range to include at that point. In that case, the named range is selected, and writeRangeToFile is called recursively to output that range.

3. If an output line would be longer than 80 characters (MCNP limit), an attempt is made to abbreviate the line if it is a comment card or contains a comment field at the end of the line. Otherwise, an error is signaled.

4. The routine supports an optional pattern substitution mechanism whereby strings of the form “%%TOKEN%%” in the Excel range are replaced by user-defined text.

A listing of the routine is shown below.

```
'
' writeMCNPRangeToFile
'
Public Sub writeMCNPRangeToFile(rng As Range, iFile As Integer, colPatSubst As Collection)
    Dim wkb As Workbook
    Dim sLine As String
    Dim iLen As Integer
    Dim lRow As Long
    Dim sToken As String
    Dim sDelim As String
    Dim iPos As Integer
    Dim rngInsert As Range
    Dim sInclude As String
    Dim colPatSubstInsert As Collection
    Dim wksThis As Worksheet
    Dim lcol As Long
    Dim nCol As Long
    Dim sOut As String

    Application.DisplayAlerts = False
    Set wksThis = rng.Worksheet
    sDelim = Chr(32)

    On Error Resume Next

    nCol = rng.Columns.Count
    For lRow = 1 To rng.Rows.Count

        sToken = Trim(rng.Cells(lRow, 1).Text)

        ' Check for not used
        If sToken = "n/u" Or sToken = "not used" Or sToken = "c not used" Then
            ' Skip this line

        ' Check for included range
        ElseIf Left(sToken, 1) = "#" Then
            ' Put the whole line together
            sLine = ""
            For lcol = 1 To nCol
                sLine = sLine & Trim(rng.Cells(lRow, lcol).Text)
                If lcol < nCol Then
                    sLine = sLine & sDelim
                End If
            Next lcol
            sLine = RTrim(sLine)
```

```
        parseInsert sLine, rngInsert, colPatSubstInsert, wksThis
        writeMCNPRangeToFile rngInsert, iFile, colPatSubstInsert

    ' Normal line
    Else
        ' Fix up first part of line
        If Left(sToken, 1) = "c" And Len(sToken) = 1 Then
            sToken = "c    "
        ElseIf Len(sToken) <> 0 Then
            iLen = Len(sToken)
            While iLen < 5
                sToken = sToken & " "
                iLen = Len(sToken)
            Wend
            ' if last char is not blank add a space
            If Right(sToken, 1) <> " " Then
                sToken = sToken & sDelim
            End If
        Else
            sToken = "     "
        End If

        ' Put the rest of the line together
        sLine = ""
        For lcol = 2 To nCol
            sLine = sLine & Trim(rng.Cells(lRow, lcol).Text)
            If lcol < nCol Then
                sLine = sLine & sDelim
            End If
        Next lcol
        sLine = RTrim(sLine)

        ' Prefix first part to line
        sLine = sToken & sLine

        doPatSubst sLine, sOut, colPatSubst

        ' If line too long, see if it can be shortened
        If Len(sOut) > 80 Then
            ' Check and see if a comment can be abbreviated
            If Left(sOut, 5) = "c    " Then
                sOut = Mid(sOut, 1, 80)
                ' Replace last char with a vertical bar to indicate abbreviation
                Mid(sOut, 80, 1) = "|"
            Else
```

```
                    ' Try to shorten inline comment
                    iPos = InStr(1, sOut, "$")
                    If iPos = 0 Or iPos > 80 Then
                        MsgBox "Error: Line longer than 80 cols" & Chr(10) & sOut, vbCritical
                        Exit Sub
                    Else
                        sOut = Mid(sOut, 1, 80)
                        ' Replace last char with a vertical bar to indicate abbreviation
                        Mid(sOut, 80, 1) = "|"
                    End If
                End If
            End If
            Print #iFile, sOut
        End If
    Next lRow

    Application.DisplayAlerts = True

End Sub
```

# APPENDIX B
# MISLOAD ANALYSIS MACRO

# B. MISLOAD ANALYSIS MACRO

Input files supporting the misload analysis are generated using the macro described in this appendix.

A listing of the routine is shown below.

```
Public Sub MakeArb()
    Dim wksModel As Worksheet
    Dim wksIso As Worksheet
    Dim rngTblInventoryM As Range
    Dim rngTblInventoryC As Range
    Dim rngTblArbPosition As Range
    Dim rngLnkCkbNeighborsOnly As Range
    Dim rngLnkCkbStratifiedMsl As Range
    Dim rngTblArbStratifiedMsl As Range
    Dim rngM As Range
    Dim rngC As Range
    '
    Dim caCAssy(MAXPOSITION) As clsAssembly
    Dim cMAssy As clsAssembly
    Dim cBAssy As clsAssembly
    Dim cBinM As clsBin
    '
    Dim lArbNumCase As Long
    Dim lArbSeed As Long
    Dim iCase As Long
    Dim nCase As Long
    Dim i As Long
    Dim j As Long
    Dim k As Long
    Dim numRecordM As Long
    Dim numRecordC As Long
    Dim nBinCountM As Long
    Dim laCDFM(MAXRECORD) As Long
    Dim laCDFC(MAXRECORD) As Long
    Dim lNumAssyM As Long
    Dim lNumAssyC As Long
    Dim lRnd As Long
    Dim lRndM As Long
    Dim laRndC(MAXPOSITION) As Long
    Dim laNeighbor(MAXPOSITION) As Long
    Dim nNeighbor As Long
    Dim nSamp As Long
    Dim nPosition As Long
    Dim lMisloadPosition As Long
    Dim lStartIndex As Long
    Dim nNumBatchCases As Long
    Dim nBatch As Long
    Dim nStrata As Long
    Dim iStrata As Long
    Dim iStrataBgn As Long
```

```
Dim iStrataEnd As Long
Dim lNumCaseStrata As Long
Dim lArbStrataIndexBgn As Long
Dim lArbStrataIndexEnd As Long
'
Dim sArbMisloadType As String
Dim sDirWork As String
Dim sVersion As String
Dim sDirCase As String
Dim sFile As String
Dim iFile As Integer
'
Dim dblArbDefaultEnr As Double
Dim dblArbDefaultBup As Double
Dim dblArbCompBupMax As Double
Dim dblArbBurnupDiscount As Double
Dim dblKeffBinUpper(MAXSTRATA) As Double
Dim dblCaseFraction(MAXSTRATA) As Double
Dim blnUnique As Boolean
Dim blnOldStatusBar As Boolean
Dim blnNeighborsOnly As Boolean
Dim blnStratifiedMsl As Boolean

Set wksModel = GetWorksheet("ModelArb")
Set wksIso = GetWorksheet("ArbIso")
Set rngTblInventoryM = ThisWorkbook.Names("tblInventoryM").RefersToRange
Set rngTblInventoryC = ThisWorkbook.Names("tblInventoryC").RefersToRange
Set rngTblArbPosition = wksIso.Names("tblArbPosition").RefersToRange
Set rngLnkCkbNeighborsOnly = ThisWorkbook.Names("lnkCkbNeighborsOnly").RefersToRange
Set rngLnkCkbStratifiedMsl = ThisWorkbook.Names("lnkCkbStratifiedMsl").RefersToRange
Set rngTblArbStratifiedMsl = wksModel.Names("tblArbStratifiedMsl").RefersToRange
Set rngM = rngTblInventoryM.Cells(1, 1)
Set rngC = rngTblInventoryC.Cells(1, 1)
numRecordM = rngTblInventoryM.Rows.Count
numRecordC = rngTblInventoryC.Rows.Count

lArbNumCase = wksModel.Names("arbNumCase").RefersToRange.value
lArbSeed = wksModel.Names("arbSeed").RefersToRange.value
lStartIndex = wksModel.Names("caseIndex").RefersToRange.value
sArbMisloadType = wksModel.Names("arbMisloadType").RefersToRange.value
dblArbDefaultEnr = wksModel.Names("arbDefaultEnr").RefersToRange.value
dblArbDefaultBup = wksModel.Names("arbDefaultBup").RefersToRange.value
dblArbCompBupMax = wksModel.Names("arbCompBupMax").RefersToRange.value
dblArbBurnupDiscount = wksModel.Names("arbBurnupDiscount").RefersToRange.value
lArbStrataIndexBgn = wksModel.Names("arbStrataIndexBgn").RefersToRange.value
```

```
lArbStrataIndexEnd = wksModel.Names("arbStrataIndexEnd").RefersToRange.value
nNumBatchCases = wksModel.Names("arbNumBatchCases").RefersToRange.value
blnNeighborsOnly = rngLnkCkbNeighborsOnly.value
blnStratifiedMsl = rngLnkCkbStratifiedMsl.value
nPosition = 21
sDirWork = ThisWorkbook.Names("dirWork").RefersToRange.value
sVersion = ThisWorkbook.Names("version").RefersToRange.Text
sDirCase = sDirWork & "\" & sVersion
SafeMkDir sDirCase
nBatch = 0

Select Case sArbMisloadType
    Case "A"
        lMisloadPosition = 1
        nNeighbor = 4
        laNeighbor(0) = 4
        laNeighbor(1) = 5
        laNeighbor(2) = 6
        laNeighbor(3) = 2
    Case "B"
        lMisloadPosition = 2
        nNeighbor = 5
        laNeighbor(0) = 1
        laNeighbor(1) = 5
        laNeighbor(2) = 6
        laNeighbor(3) = 7
        laNeighbor(4) = 3
    Case "C"
        lMisloadPosition = 6
        nNeighbor = 8
        laNeighbor(0) = 2
        laNeighbor(1) = 1
        laNeighbor(2) = 5
        laNeighbor(3) = 10
        laNeighbor(4) = 11
        laNeighbor(5) = 12
        laNeighbor(6) = 7
        laNeighbor(7) = 3
    Case "D"
        lMisloadPosition = 5
        nNeighbor = 7
        laNeighbor(0) = 1
        laNeighbor(1) = 4
        laNeighbor(2) = 9
        laNeighbor(3) = 10
```

```
        laNeighbor(4) = 11
        laNeighbor(5) = 6
        laNeighbor(6) = 2
    Case "E"
        lMisloadPosition = 11
        nNeighbor = 8
        laNeighbor(0) = 6
        laNeighbor(1) = 5
        laNeighbor(2) = 10
        laNeighbor(3) = 15
        laNeighbor(4) = 16
        laNeighbor(5) = 17
        laNeighbor(6) = 12
        laNeighbor(7) = 7
    Case Else
        MsgBox "Unrecognized misload type: " & sArbMisloadType, vbCritical
        End
End Select

' If stratified sampling, parse table
If blnStratifiedMsl Then
    nStrata = rngTblArbStratifiedMsl.Rows.Count - 2
    iStrataBgn = lArbStrataIndexBgn
    iStrataEnd = lArbStrataIndexEnd
    For iStrata = 0 To nStrata
        dblKeffBinUpper(iStrata) = rngTblArbStratifiedMsl.Cells(iStrata + 1, 2).value
        dblCaseFraction(iStrata) = rngTblArbStratifiedMsl.Cells(iStrata + 1, 5).value
    Next iStrata
Else
    dblKeffBinUpper(0) = 0#
    dblKeffBinUpper(1) = 2#
    dblCaseFraction(1) = 1#
    nStrata = 1
    iStrataBgn = 0
    iStrataEnd = 0
End If

' Bin up the misload assy
Set cBinM = New clsBin
cBinM.SetBinsbyBoundaries nStrata, dblKeffBinUpper
For j = 0 To numRecordM - 1
    cBinM.Bin rngM.Offset(j, omKEFF).value, rngM.Offset(j, omNUM).value, j + 1
Next j

' Init random number generator
```

```
If lArbSeed > 0 Then
    lArbSeed = -lArbSeed
End If
Randomize Rnd(lArbSeed)

' Generate CDF for comp assy
For j = 0 To numRecordC - 1
    If j = 0 Then
        laCDFC(0) = rngC.Offset(0, ocNUM).value
    Else
        laCDFC(j) = laCDFC(j - 1) + rngC.Offset(j, ocNUM).value
    End If
Next j
lNumAssyC = laCDFC(numRecordC - 1)

' Default assembly
Set cBAssy = New clsAssembly
With cBAssy
    .AssemblyID = 0
    .ActualEnrichment = dblArbDefaultEnr
    .ActualBurnup = dblArbDefaultBup
    .ActualBurnupRequired = dblArbDefaultBup
End With

blnOldStatusBar = Application.DisplayStatusBar
Application.DisplayStatusBar = True

CalcOff

' i is used as an index into the bin data, indexed from 0
' j is used as an index into the assembly tables, indexed from 0
' k is used as an index on position

nCase = 0
For iStrata = iStrataBgn To iStrataEnd

    nBinCountM = cBinM.BinCount(iStrata)

    If nBinCountM <> 0 Then

        lNumCaseStrata = Int(lArbNumCase * dblCaseFraction(iStrata))
        If lNumCaseStrata > 1000 Then
            MsgBox "Too many cases", vbCritical
            End
        End If
```

```
    ' Generate CDF for misload assy
    For i = 0 To nBinCountM - 1
        ' The ident is the assy record number, indexed from 1
        j = cBinM.BinIdent(iStrata, i) - 1
        If i = 0 Then
            laCDFM(0) = rngM.Offset(j, omNUM).value
        Else
            laCDFM(i) = laCDFM(i - 1) + rngM.Offset(j, omNUM).value
        End If
    Next i
    lNumAssyM = laCDFM(nBinCountM - 1)

    For iCase = 0 To lNumCaseStrata - 1

        If nCase Mod nNumBatchCases = 0 Then
            If nCase <> 0 Then
                Close #iFile
                nBatch = nBatch + 1
            End If

            ' Make a batch file
            sFile = sDirCase & "\" & wksModel.Names("caseSeries").RefersToRange.Text & Format(nBatch, "00") &
".bat"
            iFile = FreeFile
            Open sFile For Output As #iFile
        End If
        nCase = nCase + 1

        ' Sample for comp assy
        ' Get unique random numbers btw 0 and lNumAssyC-1
        nSamp = 0
        While nSamp < nPosition
            lRnd = Int(Rnd() * CDbl(lNumAssyC))
            blnUnique = True
            For k = 0 To nSamp - 1
                If lRnd = laRndC(k) Then
                    blnUnique = False
                End If
            Next k

            If blnUnique Then
                laRndC(nSamp) = lRnd
                nSamp = nSamp + 1
            End If
        Wend
```

```
' Get assy data
For k = 0 To nPosition - 1
    j = 0
    While laCDFC(j) <= laRndC(k)
        j = j + 1
    Wend

    Set caCAssy(k) = New clsAssembly
    caCAssy(k).AssemblyID = j + 1
    caCAssy(k).InitFromRange rngC.Offset(j, 0)

    ' Apply burnup discount
    caCAssy(k).ActualBurnup = caCAssy(k).ActualBurnup * (1# - dblArbBurnupDiscount)

    ' Limit comp burnup to specified max value
    ' The equiv parameters for this assy will be out of whack, but they
    ' are not used here
    If caCAssy(k).ActualBurnup > dblArbCompBupMax Then
        caCAssy(k).ActualBurnup = dblArbCompBupMax
    End If
Next k

' Sample for misload assy
lRndM = Int(Rnd() * CDbl(lNumAssyM))
i = 0
While laCDFM(i) <= lRndM
    i = i + 1
Wend

Set cMAssy = New clsAssembly
j = cBinM.BinIdent(iStrata, i) - 1
cMAssy.AssemblyID = j + 1
cMAssy.InitFromRange rngM.Offset(j, 0)

If blnNeighborsOnly Then
    ' Nearest neighbors only
    ' First fill with default assy
    For k = 0 To nPosition - 1
        rngTblArbPosition.Cells(k + 1, 3).value = cBAssy.AssemblyID
        rngTblArbPosition.Cells(k + 1, 4).value = cBAssy.ActualEnrichment
        rngTblArbPosition.Cells(k + 1, 5).value = cBAssy.ActualBurnup
        rngTblArbPosition.Cells(k + 1, 6).value = ""
    Next k
    ' Then overwrite neighbor assy
    For k = 0 To nNeighbor - 1
```

```
                        rngTblArbPosition.Cells(laNeighbor(k), 3).value = caCAssy(k).AssemblyID
                        rngTblArbPosition.Cells(laNeighbor(k), 4).value = caCAssy(k).ActualEnrichment
                        rngTblArbPosition.Cells(laNeighbor(k), 5).value = caCAssy(k).ActualBurnup
                        rngTblArbPosition.Cells(laNeighbor(k), 6).value = ""
                    Next k
                Else
                    ' Fill iso table first with comp assy
                    For k = 0 To nPosition - 1
                        rngTblArbPosition.Cells(k + 1, 3).value = caCAssy(k).AssemblyID
                        rngTblArbPosition.Cells(k + 1, 4).value = caCAssy(k).ActualEnrichment
                        rngTblArbPosition.Cells(k + 1, 5).value = caCAssy(k).ActualBurnup
                        rngTblArbPosition.Cells(k + 1, 6).value = ""
                    Next k
                End If

                ' Then overwrite the misload assy
                rngTblArbPosition.Cells(lMisloadPosition, 3).value = cMAssy.AssemblyID
                rngTblArbPosition.Cells(lMisloadPosition, 4).value = cMAssy.ActualEnrichment
                rngTblArbPosition.Cells(lMisloadPosition, 5).value = cMAssy.ActualBurnup
                rngTblArbPosition.Cells(lMisloadPosition, 6).value = True

                Application.StatusBar = "Processing Case " & iCase & " of " & lNumCaseStrata

                ' Set case parameters
                wksModel.Names("caseIndex").RefersToRange.value = iStrata * 1000 + lStartIndex + iCase
                MakeStudy
                Print #iFile, "call " & wksModel.Names("caseName").RefersToRange.Text & ".bat"

                DoEvents

                For k = 0 To nPosition - 1
                    Set caCAssy(k) = Nothing
                Next k
                Set cMAssy = Nothing
            Next iCase
        End If
    Next iStrata

    Close #iFile
    CalcOn
    Application.StatusBar = False
    Application.DisplayStatusBar = blnOldStatusBar

End Sub
```

## Listing of clsBin Class

```
Option Explicit
' Recall dim a(n) means n+1 values indexed from 0 to n

' mlNumBin is the number of "true" bins. There are two catchall bins on either
' end of the defined bin boundaries. They are indexed by 0 and mlNumBin+1.
' The "true" bins are indexed from 1 to mlNumBin

' The upper limit of bin i is x(i).
' Bin i contains all values x(i-1) < x <= x(i)
' Bin 0 contains all values x <= x(0)
' Bin mlNumBin+1 is all values x(mlNumBin) < x
' Only the counts (and a weight for each count) are maintained, not the actual values
' Could store the values in separate arrays for each bin, or store an array of identifiers (e.g., indices)

Private Const MAXBIN As Long = 100
Private Const MAXCOUNT As Long = 10000

Private mdblaBinUpper(MAXBIN) As Double
Private mlaBinCount(MAXBIN) As Long
Private mlaIdent(MAXBIN, MAXCOUNT) As Long
Private mdblaBinWeight(MAXBIN) As Double
Private mdblaBinMoment(MAXBIN) As Double
Private mlNumBin As Long
Private mblnHasCatchallData

Private Sub Class_Initialize()
    Dim i As Long
    Dim j As Long

    mlNumBin = 0
    mblnHasCatchallData = False
    For i = 0 To MAXBIN
        mdblaBinUpper(i) = 0#
        mlaBinCount(i) = 0
        mdblaBinWeight(i) = 0#
        mdblaBinMoment(i) = 0#
        For j = 0 To MAXCOUNT
            mlaIdent(i, j) = 0
        Next j
    Next i
End Sub
```

```
Property Get NumBin() As Long
    NumBin = mlNumBin
End Property

Property Get BinUpper(i As Long) As Double
    ' Bin mlNumBin+1 exists, but it has no upper limit
    If i > mlNumBin Then
        MsgBox "Invalid bin", vbCritical
        End
    ElseIf i < 0 Then
        MsgBox "Invalid bin", vbCritical
        End
    End If

    BinUpper = mdblaBinUpper(i)
End Property

Property Get BinCount(i As Long) As Long
    If i > mlNumBin + 1 Then
        MsgBox "Invalid bin", vbCritical
        End
    ElseIf i < 0 Then
        MsgBox "Invalid bin", vbCritical
        End
    End If

    BinCount = mlaBinCount(i)
End Property

Property Get BinWeight(i As Long) As Double
    If i > mlNumBin + 1 Then
        MsgBox "Invalid bin", vbCritical
        End
    ElseIf i < 0 Then
        MsgBox "Invalid bin", vbCritical
        End
    End If

    BinWeight = mdblaBinWeight(i)
End Property

Property Get BinWeightedAverage(i As Long) As Double
    If i > mlNumBin + 1 Then
        MsgBox "Invalid bin", vbCritical
        End
```

```
    ElseIf i < 0 Then
        MsgBox "Invalid bin", vbCritical
        End
    End If

    If mdblaBinWeight(i) = 0 Then
        BinWeightedAverage = 0
    Else
        BinWeightedAverage = mdblaBinMoment(i) / CDbl(mdblaBinWeight(i))
    End If

End Property

Property Get TotalWeight() As Double
    Dim i As Long

    TotalWeight = 0#
    For i = 0 To mlNumBin + 1
        TotalWeight = TotalWeight + mdblaBinWeight(i)
    Next i
End Property

Property Get TotalCount() As Long
    Dim i As Long

    TotalCount = 0#
    For i = 0 To mlNumBin + 1
        TotalCount = TotalCount + mlaBinCount(i)
    Next i
End Property

Property Get TotalWeightedAverage() As Double
    Dim i As Long
    Dim dblSumMoment As Double
    Dim dblSumWeight As Double

    dblSumMoment = 0#
    dblSumWeight = 0#
    For i = 0 To mlNumBin + 1
        dblSumMoment = dblSumMoment + mdblaBinMoment(i)
        dblSumWeight = dblSumWeight + mdblaBinWeight(i)
    Next i
    If dblSumWeight = 0 Then
        TotalWeightedAverage = 0
    Else
```

```
            TotalWeightedAverage = dblSumMoment / dblSumWeight
        End If
    End Property

    Property Get TotalWeightFraction() As Double
        Dim i As Long
        Dim dblSum As Double

        dblSum = 0#
        For i = 0 To mlNumBin + 1
            dblSum = dblSum + Me.WeightFraction(i)
        Next i
        TotalWeightFraction = dblSum
    End Property

    Property Get WeightFraction(i As Long) As Double

        If i > mlNumBin + 1 Then
            MsgBox "Invalid bin", vbCritical
            End
        ElseIf i < 0 Then
            MsgBox "Invalid bin", vbCritical
            End
        End If

        WeightFraction = Me.BinWeight(i) / Me.TotalWeight
    End Property

    Property Get BinIdent(i As Long, j As Long) As Long

        If i > mlNumBin + 1 Then
            MsgBox "Invalid bin", vbCritical
            End
        ElseIf i < 0 Then
            MsgBox "Invalid bin", vbCritical
            End
        End If
        If j < 0 Then
            MsgBox "Invalid index", vbCritical
            End
        End If
        If j > mlaBinCount(i) - 1 Then
            MsgBox "Invalid index", vbCritical
            End
        End If
```

```
    BinIdent = mlaIdent(i, j)
End Property

Public Sub SetBinsbyLimits(nBin As Long, dblLimitLo As Double, dblLimitHi As Double)
    Dim dblBinSize As Double
    Dim i As Long

    ' nBin is the number of "true" bins. They are indexed from 1 to nBin

    If dblLimitLo >= dblLimitHi Then
        MsgBox "Invalid bin structure", vbCritical
        End
    End If

    If nBin < 1 Then
        MsgBox "Invalid bin structure", vbCritical
        End
    End If

    If nBin + 1 > MAXBIN Then
        MsgBox "Too many bins", vbCritical
        End
    End If

    ' Recall there are two "catchall bins" one on either end of the upper and lower limits
    mdblaBinUpper(0) = dblLimitLo

    ' There is no upper index on the last bin
    mdblaBinUpper(nBin) = dblLimitHi

    ' Just define the interior bin limits, since the extremes are known
    ' There will be nBin-2 increments
    dblBinSize = (dblLimitHi - dblLimitLo) / CDbl(nBin)
    For i = 1 To nBin - 1
        mdblaBinUpper(i) = mdblaBinUpper(0) + CDbl(i) * dblBinSize
    Next i

    mlNumBin = nBin

End Sub

Public Sub SetBinsbySize(nBin As Long, dblBinSize As Double, dblLimitLo As Double)
    Dim i As Long
```

```
    If nBin < 1 Then
        MsgBox "Invalid bin structure", vbCritical
        End
    End If

    If nBin + 1 > MAXBIN Then
        MsgBox "Too many bins", vbCritical
        End
    End If

    ' Recall there are two "catchall bins" one on either end of the upper and lower limits
    mdblaBinUpper(0) = dblLimitLo

    For i = 1 To nBin
        mdblaBinUpper(i) = mdblaBinUpper(0) + CDbl(i) * dblBinSize
    Next i

    mlNumBin = nBin
End Sub

Public Sub SetBinsbyBoundaries(nBin As Long, dblBinLimit() As Double)
    Dim i As Long

    If nBin < 1 Then
        MsgBox "Invalid bin structure", vbCritical
        End
    End If

    If nBin + 1 > MAXBIN Then
        MsgBox "Too many bins", vbCritical
        End
    End If

    For i = 0 To nBin
        mdblaBinUpper(i) = dblBinLimit(i)
        If i > 0 Then
            If dblBinLimit(i) <= dblBinLimit(i - 1) Then
                MsgBox "Invalid bin structure", vbCritical
                End
            End If
        End If
    Next i

    mlNumBin = nBin
End Sub
```

```
Public Sub Bin(dblVal As Double, dblWgt As Double, lIdent As Long)
    Dim i As Long

    If dblVal > mdblaBinUpper(mlNumBin) Then
        addCount dblVal, dblWgt, lIdent, mlNumBin + 1
        mblnHasCatchallData = True
    ElseIf dblVal <= mdblaBinUpper(0) Then
        addCount dblVal, dblWgt, lIdent, 0
        mblnHasCatchallData = True
    Else
        For i = 1 To mlNumBin
            If dblVal <= mdblaBinUpper(i) Then
                addCount dblVal, dblWgt, lIdent, i
                Exit For
            End If
        Next i
    End If
End Sub

Public Sub DisplayExcel(rng As Range)
    Dim i As Long
    Dim iLast As Long

    CalcSave
    CalcOff

    rng.Offset(-1, 0).value = "Bin"
    rng.Offset(-1, 1).value = "Lower"
    rng.Offset(-1, 2).value = "Upper"
    rng.Offset(-1, 3).value = "Count"
    rng.Offset(-1, 4).value = "Weight"
    rng.Offset(-1, 5).value = "Wgt Avg"
    rng.Offset(-1, 6).value = "Wgt Frac"
    For i = 0 To mlNumBin + 1
        rng.Offset(i, 0).value = i
        If i = 0 Then
            rng.Offset(i, 1).value = "Lower"
        Else
            rng.Offset(i, 1).value = mdblaBinUpper(i - 1)
        End If
        If i = mlNumBin + 1 Then
            rng.Offset(i, 2).value = "Higher"
        Else
            rng.Offset(i, 2).value = mdblaBinUpper(i)
```

```
        End If
        rng.Offset(i, 3).value = mlaBinCount(i)
        rng.Offset(i, 4).value = mdblaBinWeight(i)
        rng.Offset(i, 5).value = Me.BinWeightedAverage(i)
        rng.Offset(i, 6).value = Me.WeightFraction(i)
    Next i
    iLast = mlNumBin + 2
    rng.Offset(iLast, 0).value = "Total"
    rng.Offset(iLast, 3).value = Me.TotalCount
    rng.Offset(iLast, 4).value = Me.TotalWeight
    rng.Offset(iLast, 5).value = Me.TotalWeightedAverage
    rng.Offset(iLast, 6).value = Me.TotalWeightFraction

    CalcRestore
End Sub

Private Sub addCount(dblVal As Double, dblWgt As Double, lIdent As Long, lBin As Long)

    mlaIdent(lBin, mlaBinCount(lBin)) = lIdent
    mdblaBinWeight(lBin) = mdblaBinWeight(lBin) + dblWgt
    mdblaBinMoment(lBin) = mdblaBinMoment(lBin) + dblVal * dblWgt
    mlaBinCount(lBin) = mlaBinCount(lBin) + 1

End Sub
```

## Listing of clsAssembly Class

```
Option Explicit

Dim mlAssyID As Long
Dim mlCount As Long
Dim mdblActEnr As Double
Dim mdblActBup As Double
Dim mdblActBupReq As Double
Dim mblnLoadable As Boolean
Dim mdblKeff As Double
Dim mdblEquEnr As Double
Dim mdblEquBup As Double
Dim mdblEquBupReq As Double

Property Get AssemblyID() As Long
    AssemblyID = mlAssyID
End Property

Property Let AssemblyID(lTemp As Long)
    mlAssyID = lTemp
End Property

Property Get Count() As Long
    Count = mlCount
End Property

Property Let Count(lTemp As Long)
    mlCount = lTemp
End Property

Property Get ActualEnrichment() As Double
    ActualEnrichment = mdblActEnr
End Property

Property Let ActualEnrichment(dblTemp As Double)
    mdblActEnr = dblTemp
End Property

Property Get ActualBurnup() As Double
    ActualBurnup = mdblActBup
End Property

Property Let ActualBurnup(dblTemp As Double)
```

```
    mdblActBup = dblTemp
End Property

Property Get ActualBurnupRequired() As Double
    ActualBurnupRequired = mdblActBupReq
End Property

Property Let ActualBurnupRequired(dblTemp As Double)
    mdblActBupReq = dblTemp
End Property

Property Get Loadable() As Boolean
    If mblnActBup > mblnActBupReq Then
        Loadable = True
    Else
        Loadable = False
    End If
End Property

Property Get ActualOverburn() As Double
    ActualOverburn = mdblActBup - mdblActBupReq
End Property

Property Get Keff() As Double
    Keff = mdblKeff
End Property

Property Let Keff(dblTemp As Double)
    mdblKeff = dblTemp
End Property

Property Get EquivalentEnrichment() As Double
    EquivalentEnrichment = mdblEquEnr
End Property

Property Let EquivalentEnrichment(dblTemp As Double)
    mdblEquEnr = dblTemp
End Property

Property Get EquivalentBurnup() As Double
    EquivalentBurnup = mdblEquBup
End Property

Property Let EquivalentBurnup(dblTemp As Double)
    mdblEquBup = dblTemp
```

```
End Property

Property Get EquivalentBurnupRequired() As Double
    EquivalentBurnupRequired = mdblEquBupReq
End Property

Property Let EquivalentBurnupRequired(dblTemp As Double)
    mdblEquBupReq = dblTemp
End Property

Property Get EquivalentOverburn() As Double
    EquivalentOverburn = mdblEquBup - mdblEquBupReq
End Property

Public Sub PrintExcelRange(rngStart As Range)
    With rngStart
        .Offset(0, 0).value = Me.ActualEnrichment
        .Offset(0, 1).value = Me.ActualBurnup
        .Offset(0, 2).value = Me.ActualBurnupRequired
        .Offset(0, 3).value = Me.Loadable
        .Offset(0, 4).value = Me.ActualOverburn
        .Offset(0, 5).value = Me.Keff
        .Offset(0, 6).value = Me.EquivalentEnrichment
        .Offset(0, 7).value = Me.EquivalentBurnup
        .Offset(0, 8).value = Me.EquivalentBurnupRequired
        .Offset(0, 9).value = Me.EquivalentOverburn
    End With

End Sub

Public Function Description() As String
    Dim sTemp As String
    sTemp = "id(" & Me.AssemblyID & ")"
    sTemp = sTemp & " m(" & Me.Count & ")"
    sTemp = sTemp & " ae(" & Format(Me.ActualEnrichment, "0.00") & ")"
    sTemp = sTemp & " ab(" & Format(Me.ActualBurnup, "0.00") & ")"
    sTemp = sTemp & " ao(" & Format(Me.ActualOverburn, "0.00") & ")"
    'sTemp = sTemp & " k(" & Format(Me.Keff, "0.0000") & ")"
    sTemp = sTemp & " ee(" & Format(Me.EquivalentEnrichment, "0.00") & ")"
    sTemp = sTemp & " eb(" & Format(Me.EquivalentBurnup, "0.00") & ")"
    sTemp = sTemp & " eo(" & Format(Me.EquivalentOverburn, "0.00") & ")"
    Description = sTemp
End Function

Public Sub InitFromRange(rng As Range)
```

```
    If rng.Rows.Count <> 1 Or rng.Columns.Count <> 1 Then
        MsgBox "Invalid range shape", vbCritical
        End
    End If

    ' Note: Misload and Comp inventory tables must be identical format
    With Me
        .Count = rng.Offset(0, ocNUM)
        .ActualEnrichment = rng.Offset(0, ocACTENR)
        .ActualBurnup = rng.Offset(0, ocACTBUP)
        .ActualBurnupRequired = rng.Offset(0, ocACTBUPREQ)
        .Keff = rng.Offset(0, ocKEFF)
        .EquivalentEnrichment = rng.Offset(0, ocEQUENR)
        .EquivalentBurnup = rng.Offset(0, ocEQUBUP)
        .EquivalentBurnupRequired = rng.Offset(0, ocEQUBUPREQ)
    End With

End Sub
```

INTENTIONALLY LEFT BLANK

## APPENDIX C
## OUTPUT DTN: MO0711LOADCURV.000 SPECIFICATIONS

# C. OUTPUT DTN: MO0711LOADCURV.000 FILE SPECIFICATIONS

This appendix contains a listing and description of the files contained in the Output DTN: MO0711LOADCURV.000 of this report. The zipped archive file within the DTN was created using standard Windows XP compression capabilities. The file attributes are as follows:

| Filename | File Size (bytes) | File Date | File Time | Description |
|---|---|---|---|---|
| *v3.4.zip* | 23,446,051 | 11/07/2007 | 02:57p | Archive containing MCNP files |
| *v3.5.zip* | 54,011,026 | 01/23/2008 | 02:40p | Archive containing MCNP files |
| *v3.6.zip* | 103,233,686 | 01/23/2008 | 05:01p | Archive containing MCNP files |
| *v3.6fa.zip* | 500,401,631 | 11/07/2007 | 12:12p | Archive containing MCNP files |
| *v3.6fb.zip* | 503,370,912 | 11/07/2007 | 12:27p | Archive containing MCNP files |
| *v3.6fc.zip* | 685,212,357 | 11/07/2007 | 12:56p | Archive containing MCNP files |
| *v3.6fd.zip* | 506,836,011 | 11/07/2007 | 01:12p | Archive containing MCNP files |
| *v3.6fe.zip* | 686,593,701 | 11/07/2007 | 01:35p | Archive containing MCNP files |
| *LoadingCurve.xls* | 24,934,400 | 02/06/2008 | 11:41a | Excel 2003 workbook |
| *LoadingCurve.xlsm* | 10,206,574 | 02/06/2008 | 11:39a | Excel 2007 workbook |

INTENTIONALLY LEFT BLANK